Investigating the Role of

Factor Inhibiting HIF (FIH) in Tumourigenesis

Jingyi Ma

Pembroke College

University of Oxford

A thesis submitted for the degree of

Doctor of Philosophy

Trinity 2017

Declaration

All of the work presented in this thesis is the result of my own work unless indicated here and in the corresponding sections. Histological examination of neoplasms was facilitated by pathologists Prof. Robert Goldin and Dr. Elizabeth Soilleux; and Mycobacterium bovis was provided by Dr. Paulo Bettencourt. The work described herein has not been accepted or submitted for any degree, diploma, or other qualification at the University of Oxford or any other institution. This thesis does not exceed 50,000 words, exclusive of bibliography, as required by the Nuffield Department of Medicine.

Investigating the Role of Factor Inhibiting HIF (FIH) in Tumourigenesis

Jingyi Ma, Pembroke College, DPhil in Clinical Medicine, Trinity 2017

The tumour microenvironment (TME) is frequently hypoxic and inflammatory, leading to the activation of the Hypoxia-Inducible Factor (HIF) family of transcription factors. HIF has been shown to exert broad, and sometimes controversial, effects on tumour progression through the induction of over 70 effector genes. Factor Inhibiting HIF (FIH), an oxygen-dependent hydroxylase of HIF, inhibits the transcription of selective HIF target genes, and is hence a potential therapeutic target to fine-tune HIF activity. However, how FIH may affect tumourigenesis has not been comprehensively investigated.

By monitoring the spontaneous tumour formation in mice, it was found that a lack of FIH expression does not profoundly affect the lifespan but accelerates the development of low-grade B cell lymphomas. To investigate whether FIH could suppress tumourigenesis via modulating the TME, syngeneic tumour models were employed on FIH-deficient animals. Reduced FIH expression in the host promotes tumour growth, which is recapitulated by FIH deletion only in the myeloid compartment. Tumours in mice deficient of myeloid FIH exhibit an altered immune profile, reflected by the increased expression of programmed death-ligand 1 (PD-L1) and Arginase 1 (ARG1) in tumour-associated macrophages (TAMs) and a reduced CD4 T cell population. *In vitro* characterisation of FIH-deficient macrophages reveals that FIH suppresses cell migration to C5a and CCL5, and affects the expression of several inflammatory mediators including PD-L1 and ARG1. Importantly, the transcription of FIH is upregulated in macrophages by tumour cell-conditioned media as well as bacterial infection. Altogether, this study provides the genetic evidence for the role of FIH in tumour suppression, which may result from its influence on the myeloid-mediated immune response. Therefore, FIH represents a new candidate regulator of the TME and can be implicated in other inflammatory conditions such as infection.

Acknowledgements

I would like to express my gratitude to my supervisors Prof. Xin Lu and Prof. Sir. Peter J. Ratcliffe for their guidance and inspiration throughout my DPhil. I am also grateful for financial support from the Ludwig Institute for Cancer Research, the Nuffield Department of Medicine, and Pembroke College.

The work presented in this thesis could not have been achieved without help from the following people. Prof. Robert Goldin, Dr. Elizabeth Soilleux, and Ms. Indrika Ratnayaka provided massive support on the histological studies. I would also like to thank Lewis Taylor, Theodoros Kapellos, Asif Iqbal, and Paulo Bettencourt, who showed me macrophage-based assays and provided feedback on my project. Acknowledgements also go to Matous Hrdinka, Erica De Zan, Carol Leung, Julia Colston, Consuelo Anzilotti, Xijin Xu, and Hanlin Zhang for their help on flow cytometry techniques. I would also like to thank Thomas Lessing and James Chan for discussion regarding FIH.

Although not presented in this thesis, some of my work could not have been achieved without help from the following colleagues. Mark Shipman and Dennis Sangberg provided instrumental support regarding image analysis. I would like to thank Paul Miller for his guidance on the acute pancreatitis model. Thanks also go to Richard Owen, Andrew Roth, Felix Zhou, and Pakavarin Louphrasitthiphol for their help on the analysis of RNA sequencing data.

This thesis could not have been completed without critical reading by Dr. Elizabeth Slee, Dr. Elizabeth Soilleux, Dr. Imogen Roth, and Dr. Ludovico Buti, who all made invaluable comments, and Dr. Claire Beveridge who provided editorial support. I am also grateful for social support from my writing buddies: Min Sun, Martin Cusack, Xiao Qin, and Felix Zhou.

I am blessed to have received immense support from past and present members of the institute. I would like to thank Dr. Yihua Wang for his mentorship during the first year of my DPhil. Special thanks also go to Xiao Qin, who has always been a reassuring presence as a colleague and friend. I would also like to express my gratitude to everyone in the institute, especially Gopinath Sutendra, Min Lu, Jennifer Lim, Zinaida Dedeic, Veronica Counsell, Shan Zhong, Shuo Chen, Mike White, Stefanie Zentelis, Carlos Ruiz Puig, Khatoun Al Moussawi, Kundan Sharma, Ping Zhang, Chen-Yi Wang, Emma Fenech, and Kira Chouliaras. It has been my privilege to know you and work with you.

Abbreviations

2-OG	2-Oxoglutarate
ADM	Adrenomedullin
ALL	Acute Lymphocytic Leukaemia
AML	Acute Myeloid Leukaemia
ANG	Angiogenin
APC	Allophycocyanin
APC	Antigen-Presenting Cell
APS	Ammonium Persulfate
ARD	Ankyrin Repeat Domain
ARG	Arginase
ASPP2	Apoptosis-Stimulating P53-binding Protein 2
AUC	Area Under Curve
BCG	Bacillus Calmette-Guérin
BMDMs	Bone Marrow-Derived Macrophages
BNIP	BCL2 Interacting Protein 3
BSA	Bovin Serum Albumin
BV	Brilliant Violet
C-TAD	C-terminal Transactivation Domain
C5a	Complement component 5a
C5AR	Complement component 5a Receptor 1
CAC	Colitis-Associated Cancer
CBP	CREB-Binding Protein
CCL	Chemokine (C-C motif) Ligand
CCR	C-C Chemokine Receptor
ccRCC	clear cell Renal Cell Carcinoma
CD	Cluster of Differentiation
cDMEM	complete Dulbecco Modified Eagle Medium
CIM plate	Cell Invasion and Migration plate
CSF	Colony Stimulating Factor
CTLA-4	Cytotoxic T Lymphocyte-Associated protein 4
Ctrl	Control
CXCL	C-X-C motif Chemokine Ligand
DAPI	4',6-Diamidino-2-Phenylindole, Dihydrochloride
DFS	Disease-Free Survival
DLBCL	Diffused Large B Cell Lymphoma
DMOG	Dimethyloxallyl Glycine
DMSO	Dimethyl Sulfoxide
DNA	Deoxyribonucleic Acid
e.g.	For Example
ECM	Extracellular Matrix
EDTA	Ethylenediaminetetraacetic Acid
EGF	Epidermal Growth Factor
EGFR	Epidermal Growth Factor Receptor
EMT	Epithelial-Mesenchymal Transition
EPO	Erythropoietin
FACS	Fluorescence-Activated Cell Sorting
FBS	Foetal Bovine Serum

FDCS	Follicular Dendritic Cell Sarcoma
FFPE	Formalin-Fixed Paraffin-Embedded
FIH	Factor Inhibiting Hypoxia-inducible factor
FITC	Fluorescein Isothiocyanate
Foxp3	Forkhead box, p3
FSC	Forward Scatter
G-MDSC	Granulocytic-Myeloid Derived Suppressor Cell
GFP	Green Fluorescent Protein
gMFI	geometric Mean Fluorescence Intensity
GNT buffer	Genotyping buffer
H&E staining	Haematoxylin and Eosin staining
HCC	Hepatocellular Carcinoma
HCl	Hydrochloric acid
Hi	High
HIF	Hypoxia-Inducible Factor
HN	Haematopoietic Neoplasm
Hr	Hour
HRE	Hypoxia Response Element
HRP	Horseradish Peroxidase
HSC	Haematopoietic Stem Cell
HUVEC	Human Umbilical Vein Endothelial Cells
ICC	Immunocytochemistry
IFN	Interferon
IHC staining	Immunohistochemistry staining
IHC:	Immunohistochemistry
IL-4R	Interleukin-4 Receptor
IL	Interleukin
Inflammatory Mo	Inflammatory Monocyte
Int	Intermediate
iR	Inhibitory Receptor
IκBα	Nuclear Factor κB Inhibitor α
KO	Knockout
LCM	L929-Conditioned Medium
LLC	Lewis Lung Carcinoma
Lo	Low
LOX	Lysyl Oxidase
LPS	Lipopolysaccharide
LysM	Lysozyme 2
M-CSF	Macrophage Colony-Stimulating Factor
M-MDSC	Monocytic-Myeloid Derived Suppressor Cell
MAb	Monoclonal Antibodies
MACS	Magnetic-Activated Cell Sorting
MALT	Mucosa-Associated Lymphoid Tissue
MAPK	p42/p44 Mitogen-Activated Protein Kinase
Max	Maximum
MDSC	Myeloid-Derived Suppressor Cell
MEF	Mouse Embryonic Fibroblast
MFI	Mean Fluorescence Intensity
MHC	Major Histocompatibility Complex
Min	Minimum

Mint 3	Munc18-1-interacting protein 3
miR	microRNA
MKO	Myeloid Knockout
MMP	Matrix Metalloproteinase
MMTV/PyMT	Mouse Mammary Tumour Virus/Polyomavirus Middle T Antigen
MOI	Multiplicity of Infection
Mrc1	Mannose receptor C type 1
mRNA	messenger Ribonucleic Acid
MSC	Myeloid Suppressor Cell
MT1	Membrane Type 1
Mtb	Mycobacterium tuberculosis
mTOR	Mammalian Target of Rapamycin
MZL	Marginal Zone Lymphoma
N-TAD	N-terminal Transactivation Domain
NFκB	Nuclear Factor κB
NGS	Normal Goat Serum
NHL	Non-Hodgkin Lymphoma
NICD	Notch Intracellular Domain
NK cell	Natural Killer cell
NO	Nitric Oxide
NOS	Nitric Oxide Synthase
NSCLC	Non-Small Cell Lung Cancer
ODC	Ornithine Decarboxylase
OS	Overall Survival
PAGE	Polyacrylamide Gel Electrophoresis
Par-3	Partitioning-defective homologue 3
PBS	Phosphate-Buffered Saline
PD-1	Programmed Death-1
PD-L1	Programmed Death-Ligand 1
PD-L2	Programmed Death-Ligand 2
PDGF	Platelet-Derived Growth Factor
PE/Cy7	Phycoerythrin/Cyanine5.5
PerCP/Cy5.5	Peridinin-Chlorophyll Protein/Cyanine5.5
PET	Pancreatic Endocrine Tumour
PFA	Paraformaldehyde
PGK	Phosphoglyceratekinase
PHD	Prolyl Hydroxylases
PI3K	Phosphatidylinositol 3-Kinase
PLOD	Procollagen-Lysine, 2-Oxoglutarate 5-Dioxygenase
RBC	Red Blood Cell
RCC	Renal Cell Carcinoma
RNA	Ribonucleic Acid
ROS	Reactive Oxygen Species
RT-qPCR	Real Time-quantitative Polymerase Chain Reaction
RT	Room Temperature
RTCA-DP	Real Time Cell Analyser-Dual Purpose model
SD	Standard Deviation
SDS	Sodium Dodecyl Sulphate
SSC	Side Scatter

STAT3	Signal Transducer and Activator of Transcription 3
TAM	Tumour-Associated Macrophage
TB	Tuberculosis
TBS	Tris-buffered Saline
TBST	Tris Buffered Saline with Tween 20
TCA	Tricarboxylic Acid Cycle
TCM	Tumour-Conditioned Medium
TCR	T Cell Receptor
TDLN	Tumour-Draining Lymph Node
TEMED	Tetramethylethylenediamine
TGF-α	Transforming Growth Factor-α
TGF-β	Transforming Growth Factor-β
Th	T helper cells
TIL	Tumour-Infiltrating Lymphocyte
TME	Tumour Microenvironment
TNFα	Tumour Necrosis Factorα
Treg cell	Regulatory T cells
TRP	Transient Receptor Potential
U/ml	Unit/millilitre
UD	Undetectable
UT	Untreated
V/V	Volume/Volume
VEGF	Vascular Endothelial Growth Factor
VHL	von Hippel-Lindau
W/V	Weight/Volume
WB	Western Blotting
WT	Wild Type

List of Figures

Figure 1.1 HSC-derived cell lineages 6
Figure 1.2 The two-signal model of T cell activation 8
Figure 1.3 L-arginine metabolism in myeloid cells 13
Figure 1.4 Crosstalk between tumour cells, MSCs, and T cells in the TME 16
Figure 1.5 Mechanism of HIF activation 20
Figure 1.6 Hypoxia co-opts immune cells to promote tumour development 28
Figure 1.7 Cross-cancer alteration of *HIF1AN* 37
Figure 3.1 FIH is expressed in various murine tissues 75
Figure 3.2 Mice with reduced FIH expression show enhanced spontaneous tumourigenesis 77
Figure 3.3 Reduced FIH expression promotes the incidence of B cell lymphomas 80
Figure 3.4 Loss of FIH confers susceptibility to pulmonary low-grade B cell lymphomas 84
Figure 3.5 Reduced ASPP2 expression accelerates oncogenesis in FIH$^{-/-}$ mice at week 88 88
Figure 3.6 ASPP2 does not profoundly alter the tumour spectrum of FIH-null mice 89
Figure 3.7 Mice with reduced ASPP2 expression do not show enhanced B cell lymphomagenesis in the lung 91
Figure 3.8 Nuclear HIF-α expression is not strongly detected in malignant B cells 95
Figure 4.1 Adult WT and FIH$^{-/-}$ mice show a similar profile of immune cells in various tissues 104
Figure 4.2 Mice with reduced FIH expression show enhanced growth of B16 and LLC tumours 106
Figure 4.3 Reduced FIH expression leads to altered quantity of CD4 TILs in B16 and LLC tumours 109
Figure 4.4 Mice lacking FIH expression display an increased myeloid population in LLC tumours 111
Figure 4.5 TAMs of FIH$^{-/-}$ LLC tumour-bearing mice show increased expression of *Arg1* and *Nos2*, and reduced expression of *Il-6* 114
Figure 4.6 FIH does not profoundly affect the immune response in the spleen of B16 tumour-bearing mice 117
Figure 4.7 FIH MKO animals show enhanced tumour growth 120
Figure 4.8 Myeloid deletion of FIH results in a reduced population of CD4 TILs 122
Figure 4.9 FIH expression in myeloid cells affects the population of T_{CM} and naive Treg cells in B16 tumours 124
Figure 4.10 B16 tumours grown in FIH MKO mice show an increased fraction of TAMs 126
Figure 4.11 FIH deficiency in myeloid cells results in an increased fraction of PD-L1^{+} TAMs 129
Figure 4.12 FIH MKO animals show an increased proportion of ARG1^{+} TAMs 130
Figure 4.13 Myeloid FIH expression affects tumour immune response in the spleen 133
Figure 5.1 Generation of BMDMs 143
Figure 5.2 The transcription of FIH is induced by LLC TCM, LPS/IFNγ, and BCG infection in BMDMs 144
Figure 5.3 FIH$^{-/-}$ BMDMs show increased PD-L1 expression on unpolarised and M1 BMDMs 146
Figure 5.4 *Cd274* expression is elevated in FIH-null BMDMs 148

Figure 5.5 FIH$^{-/-}$ BMDMs exhibit enhanced ARG induction by LPS/IFNγ and LLC TCM 150
Figure 5.6 *Arg1* induction is augmented in FIH-null macrophages in response to M1 polarising reagents and LLC TCM.....151
Figure 5.7 FIH-null macrophages show enhanced migration towards CCL5 and C5a ...155
Figure 5.8 FIH$^{-/-}$ BMDMs show increased expression of receptors for CCL5 and C5a on the cell surface.....156
Figure 5.9 FIH is dispensable for macrophage phagocytosis 158
Figure 5.10 FIH-deficient M1 macrophages display altered expression of *Egln3*, *Sell*, and *Cxcl1*.....161
Figure 5.11 Expression of *Mrc1* and *Retnla* is aberrant in FIH$^{-/-}$ M2 BMDMs.....162

List of Tables

Table 1.1 FIH-sensitive HIF target genes 32
Table 2.1 List of primers used to genotype mouse colonies.....48
Table 2.2 List of primers for qPCR 48
Table 2.3 List of antibodies used for IHC/ICC/WB 49
Table 2.4 List of antibodies used for flow cytometry.....50
Table 2.5 List of cell lines.....51
Table 2.6 PCR protocols for genotyping 53
Table 2.7 Antibody panels used for flow cytometry.....61

Table of Contents

Chapter 1 Introduction 1

1.1 Tumourigenesis in brief 1
1.1.1 Types of cancer 1
1.1.1 Cancer as a genetic disease 2
1.1.2 Cancer as an immune disorder 3
1.2 The TME 4
1.2.1 A glimpse of the host immune system 5
1.2.2 CD4 and CD8 T cells 10
1.2.3 Regulatory T cells (Treg cells) 10
1.2.4 TAMs 11
1.2.5 MDSCs 14
1.2.6 Immunosuppression by myeloid suppressor cells (MSCs) 14
1.2.7 Summary 16
1.3 The hypoxia-inducible factor (HIF) 17
1.3.1 Activation and regulation of HIF 17
1.3.2 The role of HIF in tumour cells 22
1.3.3 The role of HIF in tumour-infiltrating MSCs 24
1.3.4 The role of HIF in tumour-infiltrating T cells 27
1.3.5 Summary 27
1.4 FIH 29
1.4.1 Overview 29
1.4.2 FIH and ankyrin repeat domain (ARD)-containing proteins 33
1.4.3 FIH expression in human cancer 36
1.4.4 FIH in tumour biology 39
1.4.5 The role of FIH beyond cancer 40
1.5 Aim of the study 43

Chapter 2 Materials and Methods 44

2.1 Materials 44
2.1.1 Reagents 44
2.1.2 Mouse colonies 47
2.1.3 Primers 48
2.1.4 Antibodies 49
2.1.5 Cell lines 51
2.2 Methods 52
2.2.1 Mouse studies 52
2.2.1.1 Colony maintenance 52
2.2.1.2 Mouse genotyping and agarose gel electrophoresis 52
2.2.1.3 Spontaneous tumour analysis 54
2.2.1.4 Syngeneic tumour model 54
2.2.2 Histology techniques 55
2.2.2.1 Preparing for formalin-fixed paraffin-embedded (FFPE) tissues 55
2.2.2.2 Haematoxylin and Eosin (H&E) staining 55
2.2.2.3 Immunohistochemistry (IHC) staining on FFPE sections 55
2.2.3 Flow cytometry 56
2.2.3.1 Sample preparation 56
2.2.3.2 Immunostaining 59
2.2.3.3 FACS sorting 62

2.2.3.4 MACS 63
2.2.4 Tissue culture 63
2.2.4.1 Maintenance of cell lines 63
2.2.4.2 Freezing/thawing of cells 63
2.2.4.3 Preparation of L929-conditioned medium (LCM) 64
2.2.4.4 Preparation of bone marrow-derived macrophages (BMDMs) 64
2.2.4.5 Tumour cell-conditioned media (TCM) 65
2.2.5 Cell-based assays 65
2.2.5.1 Lentiviral transduction of B16 cells 65
2.2.5.2 Immunocytochemistry (ICC) 66
2.2.5.3 *In vitro* stimulation 66
2.2.5.4 RNA extraction, reverse transcription, and real time-quantitative PCR (RT-qPCR) 66
2.2.5.5 Chemotaxis assay 67
2.2.5.6 Phagocytosis assay 68
2.2.5.7 Infection of BMDMs with Bacillus Calmette-Guérin (BCG) 68
2.2.5.8 Protein analysis 69
2.2.6 Data analysis 71

Chapter 3 FIH deficiency promotes spontaneous tumourigenesis *in vivo* 73

3.1 Introduction 73
3.2 Results 74
3.2.1 FIH is expressed in various tissues 74
3.2.2 Mice with reduced FIH expression show enhanced tumour susceptibility ... 76
3.2.3 Mice with reduced FIH expression are more vulnerable to B cell lymphomas 78
3.2.4 Mice lacking FIH expression show increased incidence of low-grade B cell lymphomas in the lung 81
3.2.5 The genetic interaction of FIH and ASPP2 in tumour suppression 85
3.2.5.1 ASPP2 heterozygosity accelerates oncogenesis in FIH-null mice at an early stage 85
3.2.5.2 The tumour spectrum of FIH-null animals is not profoundly affected by ASPP2 expression 88
3.2.5.3 Mice with partial deficiency of ASPP2 do not show enhanced pulmonary B cell lymphomagenesis 90
3.2.6 Nuclear HIF-α expression is not strongly detected in B cell lymphoma tissues 92
3.3 Discussion 95

Chapter 4 Host expression of FIH suppresses tumour growth *in vivo* ... 100

4.1 Introduction 100
4.2 Results 101
4.2.1 FIH-deficient mice show a similar lymphoid and myeloid profile to WT animals 101
4.2.2 Loss of FIH leads to increased tumour burden 105
4.2.2.1 Mice with reduced FIH expression show enhanced tumour growth 105
4.2.2.2 Tumours from FIH-deficient animals show altered quantity of CD4 T cells 107
4.2.2.3 Mice lacking FIH show an increased population of myeloid cells in LLC tumours 110
4.2.2.4 TAMs from FIH-deficient LLC tumour-bearing mice show altered expression of *Arg1*, *Nos2*, and *Il-6* 112

4.2.2.5 FIH does not profoundly affect the immune response in the spleens of B16 tumour-bearing mice 115
4.2.3 Mice deficient of myeloid FIH show enhanced tumour growth 118
4.2.3.1 Mice lacking FIH in myeloid cells exhibit enhanced tumour growth 118
4.2.3.2 Mice lacking FIH in myeloid cells show a reduced population of CD4 TILs 120
4.2.3.3 Mice deficient of myeloid FIH show an increased population of TAMs in B16 tumours 125
4.2.3.4 TAMs in mice deficient of myeloid FIH exhibit increased PD-L1 and ARG1 expression 127
4.2.3.5 Myeloid expression of FIH affects tumour immune response in the spleen of B16 tumour-bearing mice 131
4.3 Discussion 133

Chapter 5 The role of FIH in macrophage function 141

5.1 Introduction 141
5.2 Results 142
5.2.1 FIH is induced in BMDMs transcriptionally by inflammatory stimuli 142
5.2.2 FIH-null BMDMs show increased *Cd274* (PD-L1) expression 145
5.2.3 FIH-deficient macrophages show augmented *Arg1* induction in M1 and LLC TCM-treated BMDMs 149
5.2.4 BMDMs deficient of FIH show improved migration towards CCL5 and C5a 152
5.2.5 FIH may not be required for macrophage phagocytosis 157
5.2.6 FIH-null M1 macrophages show aberrant expression of *Egln3*, *Sell* and *Cxcl1* 159
5.2.7 FIH is required for the expression of *Mrc1* and *Retnla* in M2 macrophages 161
5.3 Discussion 163

Chapter 6 Final discussion and perspectives 168

6.1 Overview 168
6.2 FIH status in tumours and the tumour stroma 169
6.3 FIH in tumour suppression: mechanism of action 170
6.4 The role of FIH as a HIF regulator 172
6.5 The potential role of FIH in the host response to infection 174
6.6 Conclusion 175

Supplementary tables 177

Bibliography 182

Chapter 1 Introduction

1.1 Tumourigenesis in brief

Cancer is one of the leading causes of morbidity and mortality worldwide. According to the World Health Organization (WHO), cancer accounted for 8.8 million deaths in 2015, almost one-sixth of all deaths worldwide. Cancer, as described by the American oncologist Siddhartha Mukherjee, is indeed 'the emperor of all maladies'.

1.1.1 Types of cancer

There are four major types of cancer based on the tissue of origin: carcinoma, sarcoma, lymphoma, and leukaemia (G. M. Cooper 2000). Carcinomas originate from epithelial cells and are the most commonly diagnosed type of human cancer. Carcinomas that develop in glands are called adenocarcinomas. Sarcomas, which are rare in humans, are tumours of connective tissues. Lymphomas and leukaemias account for about 8% of human malignancies. Lymphomas are a malignancy of the lymphocytes, which usually develop in the lymph nodes but can occur in almost any tissue (Shankland, Armitage, and Hancock 2012). Leukaemia, on the other hand, is caused by the uncontrolled proliferation of haematopoietic precursors (Izraeli 2004).

Cancer involves both primary and metastatic disease. Tumours derived from one tissue (the primary site) can spread to distant organs via a complex succession of events that are collectively termed the invasion–metastasis cascade (Valastyan and Weinberg 2011). Cancer cells of epithelial origin first go into 'ready-to-go' mode through epithelial–mesenchymal transition (EMT), a process by which epithelial cells lose tight junctions and cell polarity, and dissociate into individual cells with mesenchymal characteristics (Thiery 2002). The cells then locally invade the surrounding extracellular matrix (ECM) and stromal cells, followed by their entry into the lymphatic or blood vessels via a process called intravasation. Once cancer cells intravasate successfully, they travel around the body via the circulatory system until they get arrested at a distant organ site, where they extravasate and colonise a new territory (Valastyan and Weinberg 2011); a process termed metastasis. The ability of cancer cells to disseminate throughout the body underlines why it is so challenging to eradicate cancer. As a matter of fact, metastasis causes more than 90% of human cancer deaths (Gupta and Massagu 2006).

1.1.1 Cancer as a genetic disease

The transformation of normal cells to cancerous ones goes hand-in-hand with the acquisition of multiple hallmarks, including sustained proliferative signalling, evasion of growth suppression, the activation of invasion and metastasis, resistance to cell death, enabling of replicative immortality, induction of angiogenesis, reprogramming of energy metabolism, and the evasion of immune surveillance. Underlying these hallmarks are two driving forces: genome instability and inflammation (Hanahan and Weinberg 2011).

Cancer has long been considered as a genetic disease caused by gain-of-function mutations in proto-oncogenes and loss-of-function mutations in tumour suppressor genes (Lodish et al. 2008). Normally, proteins encoded by proto-oncogenes are necessary to maintain cell growth and division. Mutated proto-oncogenes may be constantly active, leading to excessive cell proliferation. In contrast, tumour suppressor genes encode proteins that limit cell proliferation or survival. Transcription factor p53, for instance, induces a variety of genes involved in apoptosis and cell cycle regulation. Inactivating mutations of TP53, the gene encoding p53, are observed in about half of all human cancers (Green and Kroemer 2009). Cells acquire mutations in a more-or-less random manner, and those with survival-favouring mutations will be selected for and will undergo expansion, a process similar to Darwinian evolution (Stratton, Campbell, and Futreal 2009).

1.1.2 Cancer as an immune disorder

Inflammation is an umbrella term that describes how the immune system counteracts noxious stimuli such as tissue injury or infection. Innate immune cells can detect damage-associated molecular patterns (DAMPs) or pathogen-associated molecular patterns (PAMPs) released from injured cells and initiate signalling cascades that recruit and activate other immune cells, thereby amplifying immune responses (Newton and Dixit 2012).

Inflammation is essential for host defence. However, excessive inflammation is closely related to the development of neoplasms. Inflammation can drive tumourigenesis through the generation of DNA-damaging reagents such as reactive oxygen species (ROS) or by compromising the barrier function to allow the entrance of genotoxic bacteria (Noy and Pollard 2014). Indeed, many

malignancies have been shown to be fostered by chronic inflammation. For example, inflammatory bowel disease (IBD) is associated with an increased risk of colorectal cancer (Dyson 2012), *Helicobacter pylori* infection is associated with gastric cancer (Wroblewski, Peek, and Wilson 2010), and chronic hepatitis B and C infection is associated with hepatocellular carcinoma (HCC) (Wroblewski, Peek, and Wilson 2010).

In addition to cancer initiation, inflammation also sustains established neoplastic tissues. In fact, a tumour is not merely a collection of malignant cells, but is also heavily populated by leukocytes, first noticed in 1863 by German physician and pathologist Rudolf Virchow (Balkwill and Mantovani 2001). Collectively, these cells, together with the bioactive molecules they produce, make up the tumour microenvironment (TME), which affects virtually every step of tumourigenesis (Grivennikov, Greten, and Karin 2010).

1.2 The TME

Tumours are heavily infiltrated by non-malignant cells including immune cells, fibroblasts, endothelial cells, pericytes, and mesenchymal cells, as well as non-cellular components such as the ECM. These components create a complex ecosystem termed the TME. Unfortunately, the overall effect of the TME is often immunosuppressive and tumour-promoting (Pattabiraman and Weinberg 2014). In this study, the contribution of immune cells to the TME will be elaborated upon and explored experimentally.

1.2.1 A glimpse of the host immune system

- **Innate and adaptive immunity**

Two different defence mechanisms are utilised by our immune system: innate immunity and adaptive immunity. Innate immunity provides immediate, on-site protection against pathogenic microbes and toxins by mounting inflammatory responses. Cells from the innate immune system include leukocytes such as monocytes, macrophages, granulocytes, natural killer cells (NK cells), and dendritic cells, as well as epithelial cells that form physical barriers (Beutler 2004). In contrast, the adaptive immune system takes longer to respond, but provides antigen-specific defence mechanisms. The adaptive immune system can be divided into humoural and cell-mediated immunity. Humoural immunity is governed by B cells, which produce antibodies that recognise specific antigens. Cell-mediated immunity does not rely on antibodies; rather, it requires the participation of T cells and antigen-presenting cells (APCs) (Chaplin 2010). Adaptive immunity can form memory cells that are able to respond to the same antigen more swiftly upon the second exposure (Murphy 2011).

Developmentally, immune cells originate from haematopoietic stem cells (HSCs) in the bone marrow through haematopoiesis (Figure 1.1). HSCs differentiate into two lineages: the myeloid lineage, which gives rise to erythrocytes, megakaryocytes, monocytes, granulocytes; and the lymphoid lineage, which differentiates into B and T lymphocytes. Leukocytes not only function in lymphoid organs like the spleen and lymph nodes, but also play an active role in maintaining homeostasis in non-lymphoid organs including the skin, lung, and liver (Murphy 2011).

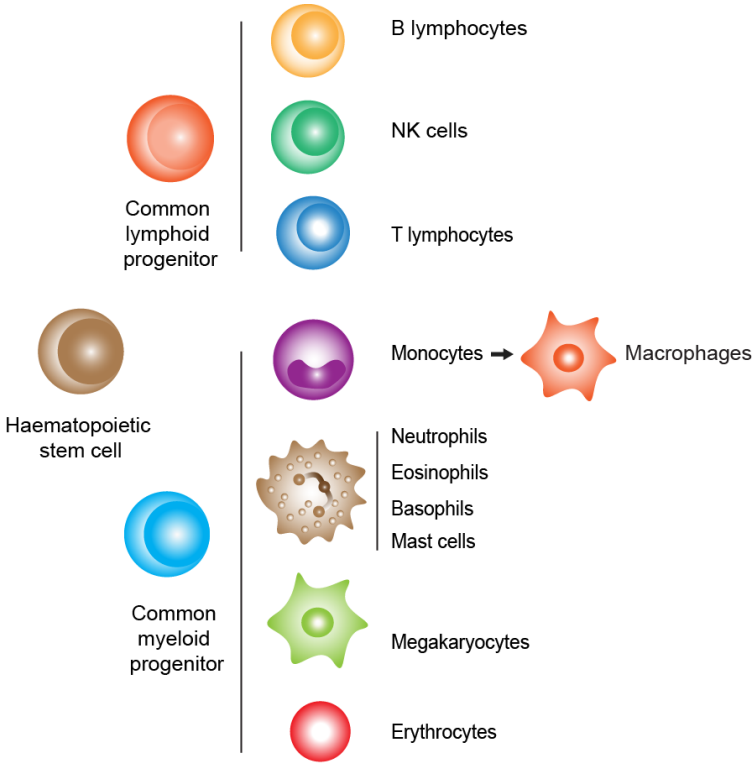

Figure 1.1 HSC-derived cell lineages
Pluripotent HSCs in the bone marrow give rise to common lymphoid and myeloid progenitor cells. Lymphoid progenitor cells differentiate into B cells, T cells, and NK cells. Myeloid progenitor cells differentiate into granulocytes (neutrophils, eosinophils, basophils, and mast cells), monocytes, megakaryocytes, and erythrocytes. Monocytes differentiate into macrophages in the peripheral tissues.

- **T cells**

T cells arise from committed progenitors in the bone marrow and migrate to the thymus, where they undergo negative and positive selection to acquire appropriate levels of reaction towards self-antigens recognised by T cell receptors (TCRs). Those with TCRs that bind self-antigen-major histocompatibility (MHC) class I complexes become cytotoxic CD8 T cells, whereas thymocytes with TCRs that bind self-antigen-MHC class II complexes become CD4 T helper (Th) cells

(Germain 2002). Accordingly, a major role of T cells is to identify foreign antigens and destroy infected cells.

To be functional effector cells, naive T cells require two activation signals: the first one is the engagement of TCRs by MHC-bound antigen on APCs, and the second, also known as the 'co-stimulatory signal', comes from the binding of CD80/86 on APCs and co-stimulatory receptor CD28 on T cells (Figure 1.2). Once activated, CD8 T cells acquire strong cytotoxicity by upregulating the expression of tumour necrosis factorα (TNFα), perforin, granzymes, and Fas ligand (Reiser and Banerjee 2016), while CD4 Th cells differentiate into several lineages according to the type of cytokines in the environment and provide essential help to other cells including CD8 T cells and B cells (Wan 2010). For example, Th1 cells secrete interferon gamma (IFNγ) and interleukin (IL)-2, which are important for the activation of CD8 T cells and the formation of memory T cells, while Th2 cells secrete IL-4, which is essential for isotype switching of B cells (Ekkens et al. 2007; J. Zhu and Paul 2008; Crotty 2015) . T cells that are only activated by the first signal will undergo anergy, represented by reduced proliferation and diminished effector function (Schwartz 2003).

Apart from the co-stimulatory receptor CD28, T cells also express a set of inhibitory receptors (iRs) including programmed death-1 (PD-1), cytotoxic T lymphocyte-associated protein 4 (CTLA-4), and lymphocyte-activated gene-3 (LAG-3). Engagement of iRs as the second signal will suppress T cell effector function (L. Chen and Flies 2013).

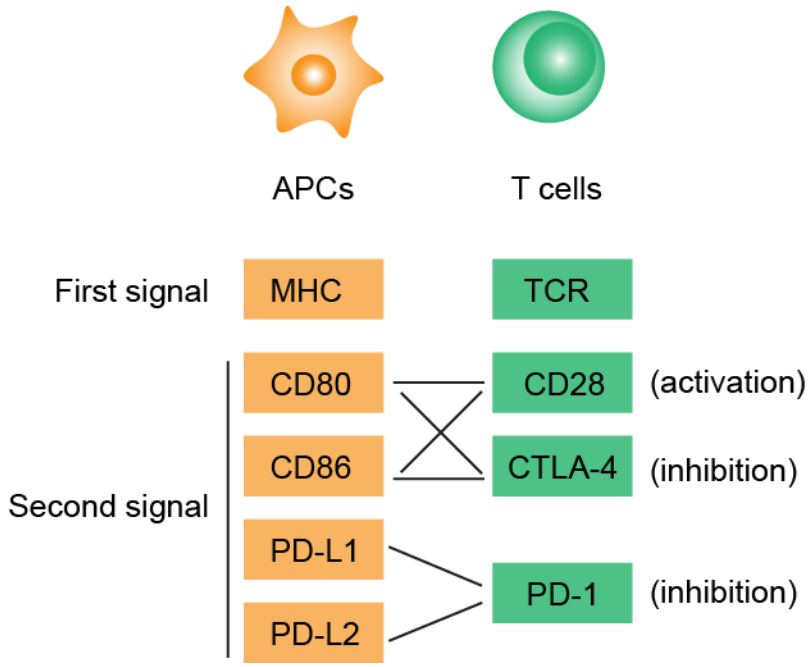

Figure 1.2 The two-signal model of T cell activation
T cells require two signals to be fully activated. The first signal is provided by the interaction between the TCR and peptide-MHC from APCs. The second signal, also known as the co-stimulatory signal, originates from the engagement of T cell co-stimulatory receptor CD28 by co-stimulatory molecules CD80 and CD86 on APCs. APCs can also send inhibitory signals to T cells by interacting with inhibitory receptors expressed on T cells, including PD-1 and CTLA-4. Note that T cells express a wide range of receptors that are not shown here. For a comprehensive understanding of T cell co-stimulatory and co-inhibitory mechanisms, please refer to the review indicated (L. Chen and Flies 2013). PD-L1: programmed death-ligand 1.

- **Macrophages**

Macrophages are mononuclear phagocytes that derive from blood monocytes. They are distributed throughout the body and reside within the parenchyma of major organs (e.g., the heart, brain, lung, and liver), and therefore readily react to tissue injury and infection (Beutler 2004). As professional phagocytes, they are efficient in removing dead cells and damaged tissues. Moreover, they act as

sentinels and respond to assault by secreting a plethora of mediators to recruit other immune cells and modulate inflammatory responses. Macrophages can also function like dendritic cells by presenting antigens to CD4 T cells via MHC class II (Mosser and Edwards 2008; Dunster 2015).

Macrophages also display extensive plasticity. Depending on the environmental cues, macrophages acquire a spectrum of phenotypes, a process referred to as macrophage polarisation. Two ends of polarised macrophages are represented by M1 (classical activated) and M2 (alternative activated) macrophages. M1 macrophages are induced by Th1 cell-derived cytokine IFNγ and Toll-like receptor ligands such as lipopolysaccharide (LPS), and they are characterised by robust production of pro-inflammatory cytokines (e.g., IL-6 and IL-12), chemokines, and enhanced pathogen killing activity. M2 macrophages, on the other hand, are polarised by Th2-derived cytokines IL-4 or IL-13. M2 macrophages exhibit reduced expression of pro-inflammatory mediators but increased production of immunoregulatory factors, and are important for immune responses to allergy, parasitic infection, and tissue repair (Martinez and Gordon 2014).

- **Other cells in the immune system**

Neutrophils are short-lived (~6 hr in circulation) phagocytes and act as potent bacterial killers by producing a large amount of cytotoxic ROS. NK cells eliminate cells that show reduced MHC class I molecule expression, e.g., virus-infected cells and cancer cells. Dendritic cells are professional APCs and express both MHC class I and class II molecules to permit antigen recognition by TCRs. B cells are antigen-producing cells from the adaptive immune system. Like APCs, B cells also capture their cognate antigens and process them for presentation to T cells. The T

cell–B cell interaction also induces B cells to undergo isotope switching, which is strongly associated with the development of B cell memory. Comprehensive reviews about the function of these immune cells are available for reference (Chaplin 2010; Eibel et al. 2014).

1.2.2 CD4 and CD8 T cells

Mutations in the tumour genome can produce mutant proteins that serve as neoantigens to adaptive immune responses (Yarchoan et al. 2017). However, in the TME, the activity of both CD4 and CD8 T cells is suppressed. For example, due to their prolonged exposure to tumour-derived antigens, T cells frequently undergo exhaustion, which is reflected by reduced proliferation, diminished cytokine production, and increased expression of iRs (Y. Jiang, Li, and Zhu 2015). T cell activity is further limited due to the binding of iRs by ligands expressed on tumour cells and other cells, including tumour-associated macrophages (TAMs) and myeloid-derived suppressor cells (MDSCs) (see below). Lastly, environmental factors (e.g., the abundance of inhibitory cytokines such as IL-10 and transforming growth factor (TGF)-β, and the depletion of essential amino acids) may also contribute to T cell inactivation (Wherry and Kurachi 2015; Noy and Pollard 2014).

1.2.3 Regulatory T cells (Treg cells)

A major source of inhibitory cytokines in the TME are Treg cells, an immunosuppressive subtype of CD4 T cells characterised by the expression of transcriptional factor forkhead box p3 (Foxp3). Treg cells are essential for the maintenance of immunological unresponsiveness to self-antigens and suppressing excessive immune responses: mutation of *FOXP3* causes IPEX (immune dysregulation, polyendocrinopathy, enteropathy, X-linked syndrome), a disease

manifesting multiple autoimmune disorders (Sakaguchi et al. 2008). Not surprisingly, Treg cells usually favour tumour progression. The prevalence of Treg cells in the tumour tissue has been shown to be associated with poor clinical prognosis in various types of cancer, including renal cell carcinoma, lung carcinoma, HCC, and pancreatic cancer (Fridman et al. 2012; Tanaka and Sakaguchi 2016).

Treg cells can dampen anti-tumour immunity in various ways. Firstly, Treg cells produce TGF-β and IL-10, which inhibit the activation, survival, and proliferation of effector T cells, and polarise macrophages towards a more tumour-permissive phenotype (Vignali, Collison, and Workman 2008; Facciabene, Motz, and Coukos 2012). Secondly, Treg cells do not produce but consume IL-2, an essential cytokine for T cell survival, which may cause the apoptosis of effector T cells (Pandiyan et al. 2007). Thirdly, Treg cells constitutively express inhibitory receptor CTLA4, which engages with CD80/86 on APCs with higher affinity than co-stimulatory molecule CD28 (Takahashi et al. 2000). This suggests that CTLA4-expressing Treg cells could outcompete the conventional CD28-expressing T cells for binding to CD80/86, thereby blocking the co-stimulation of the latter (Tanaka and Sakaguchi 2016).

1.2.4 TAMs

The majority of TAMs arise from bone marrow-derived monocytes that are recruited to the tumour site by a wide range of factors, such as chemokine C-C motif ligand 2 (CCL2), CCL3, CCL4, CCL5, and C-X-C motif chemokine ligand 12 (CXCL12), as well as growth factors including M-CSF, vascular endothelial growth factor (VEGF), and TGF-α (Richards, Hettinger, and Feuerer 2012).

Once recruited, the phenotype of TAMs is shaped by a plethora of molecules in the TME, including lactic acid, M-CSF, IL-10, IL-4, IL-13, and oxygen deficiency (hypoxia) (L. Yang and Zhang 2017; Colegio et al. 2015; Egners, Erdem, and Cramer 2016). These tumour-educated macrophages, in return, are able to affect virtually every step of tumourigenesis, mainly in a tumour-favouring manner.

- **TAMs and tumour cell survival**

TAMs can directly fuel tumour cell proliferation by supplying pro-proliferating molecules such as polyamines. TAMs express high levels of Arginase 1 (ARG1), an enzyme that converts $_{L}$-arginine to urea and $_{L}$-ornithine, the latter of which is metabolised to polyamines (putrescine, spermidine, and spermine) by ornithine decarboxylase (ODC) (Z. Yang and Ming 2013; Munder 2009).

TAMs also express nitric oxide synthase 2 (NOS2), which shares the same substrate with ARG1 and converts $_{L}$-arginine to nitric oxide (NO), a cytotoxic agent. It has been shown that increased ARG1 activity attenuates NO production and thus dampens the tumouricidal activity of macrophages (C. I. Chang, Liao, and Kuo 2001). Of note, neither ARG1 nor NOS2 is constitutively expressed, but they are inducible in macrophages upon stimulation (Bronte et al. 2003). The metabolic reactions of $_{L}$-arginine in macrophages are shown in Figure 1.3.

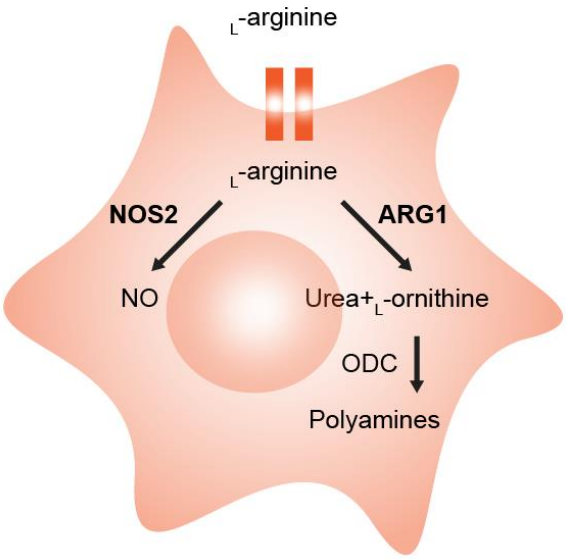

Figure 1.3 L-arginine metabolism in myeloid cells
L-arginine is taken up by myeloid cells via cationic amino acid transporters and is metabolised by NOS2 and ARG1. L-ornithine is further converted to putrescine, spermidine, and spermine by ODC.

- **TAMs and tumour progression**

As the size of a tumour increases, it has to develop a vascular system that can supply oxygen and nutrients, referred to as the 'angiogenic switch' (Hanahan and Weinberg 2011). TAMs can facilitate vascular formation by the production of angiogenic factors, including VEGF and platelet-derived growth factor (PDGF) (Y. Liu and Cao 2015).

TAMs also prepare tumour cells for invasion and metastasis. For example, macrophages have been shown to coordinate with tumour cells during their migration towards blood vessels in a lock-step manner, a process driven by the tumour-derived M-CSF and macrophage-derived epidermal growth factor (EGF) (Wyckoff et al. 2004). TAMs also assist tumour progression by secreting bioactive molecules such as TGF-β, which drives EMT (Bonde et al. 2012), osteonectin,

which mediates the adhesion of tumour cells to the ECM (Sangaletti et al. 2008), and various proteases that break down the ECM (Qian and Pollard 2010).

1.2.5 MDSCs

MDSCs represent a heterogeneous population of bone marrow-derived immature myeloid cells. Most MDSCs are mononuclear cells (M-MDSCs), which are phenotypically similar to monocytes, while others are granulocytic cells (G-MDSCs), which resemble neutrophils (Youn and Gabrilovich 2010). Expansion of MDSCs in the peripheral blood and in tumour tissues is frequently observed in cancer patients (Messmer et al. 2014; Diaz-Montero, Finke, and Montero 2014). MDSCs from the circulation are recruited to tumour sites by a range of chemokines including CCL2, CCL5, and CXCL1 (Umansky et al. 2016). Upon entering the tumour site, MDSCs upregulate the expression of ARG1, NOS2, TGF-β, and PD-L1, thereby promoting the immunosuppressive microenvironment (see below).

1.2.6 Immunosuppression by myeloid suppressor cells (MSCs)

TAMs and MDSCs are considered as myeloid suppressor cells (MSCs) for their similarly inhibitory effects on effector T cells via the various mechanisms described below.

- **ARG1/NOS2-dependent T cell suppression**

As mentioned earlier, MSCs express high levels of ARG1 (Munder 2009). On one hand, ARG1 is secreted and can break down $_{L}$-arginine locally; on the other, MSCs rapidly uptake $_{L}$-arginine by upregulating the cationic amino acid transporter 2B (CAT-2B) (Doedens et al. 2010; Sharda et al. 2011; Rath et al. 2014; Rodriguez, Ochoa, and Al-Khami 2017). Together, these mechanisms result in the depletion of $_{L}$-arginine in the TME, which consequently suppresses T cell proliferation by

inhibiting the re-expression of the TCR ζ chain (Rodriguez et al. 2003; Rodriguez et al. 2004).

NOS2 expression in MSCs also mediates T cell suppression. NOS2 metabolises $_L$-arginine to generate NO, which interferes with IL-2R signalling in the T cells, thereby preventing T cell proliferation. Additionally, with a suboptimal amount of $_L$-arginine in the local environment, the function of NOS2 can be shifted to predominantly produce O_2^-, which reacts with other molecules and generates a series of ROS that can induce T cell apoptosis (Bronte et al. 2003).

- **iR-dependent T cell suppression**

MSCs express ligands that bind to iRs on T cells, thus triggering inhibitory pathways in T cells. Both TAMs and MDSCs have been shown to express PD-L1 and PD-L2, ligands of PD-1 receptor expressed on T cells (Nguyen and Ohashi 2015).

Furthermore, co-stimulatory molecules CD80 and CD86 can not only bind to the co-stimulatory receptor CD28, but also to the inhibitory CTLA-4 receptor on T cells. Moreover, CD80/86 binds to CTLA-4 with higher affinity than CD28 (Greenwald, Latchman, and Sharpe 2002). Given that CTLA-4 is highly expressed in exhausted T cells in the TME (Y. Jiang, Li, and Zhu 2015), the expression of co-stimulatory molecules CD80/86 on MSCs may actually confer an inhibitory effect on T cell function.

- **Promotion of Treg cells in the TME**

MSCs have been shown to promote the recruitment of Treg cells through the secretion of CCL4, CCL5, CCL20, and CCL22 (Curiel et al. 2004; J. Liu et al. 2011; Kumar et al. 2016). Moreover, MSC-derived IL-10 and TGF-β can induce the

differentiation of Treg cells from CD4 T cells (J. W. Pollard 2004; Ostrand-Rosenberg and Sinha 2009).

1.2.7 Summary

Although tumour cells can be immunogenic, the ability of the host immune system to reject a tumour is largely compromised in the TME. Often, immune cells not only fail to exercise immune surveillance, but facilitate tumour progression. The tumour–immune cell interaction described in this section is summarised in Figure 1.4.

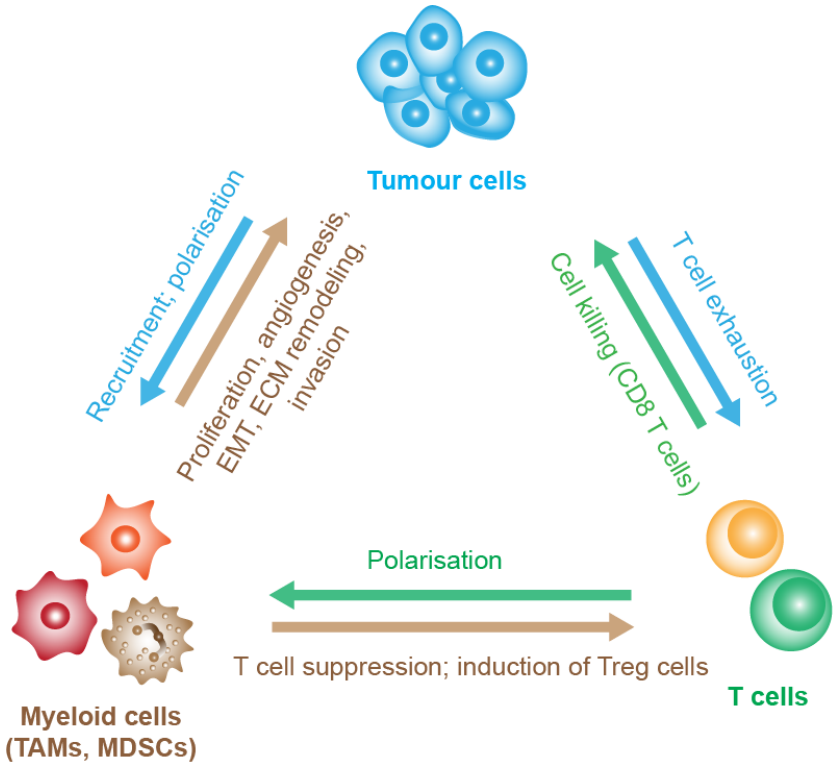

Figure 1.4 Crosstalk between tumour cells, MSCs, and T cells in the TME

Tumour cells recruit myeloid cells through the secretion of chemoattractants including chemokines, M-CSF, VEGF, and TGF-α. In response to the molecules produced by tumour cells (e.g., lactic acid and M-CSF) and T cells (e.g., IFNγ, IL-4, and IL-13), myeloid cells acquire multiple tumour-promoting properties: they may enhance tumour growth by supplying polyamines; they

facilitate tumour progression by promoting angiogenesis, EMT, migration to the blood vessels, and ECM remodelling; they can suppress the effector function of T cells through L-arginine depletion and NO production mediated by ARG1 and NOS2, as well as the engagement of iRs on T cells; and they are also involved in the recruitment and induction of Treg cells.

1.3 The hypoxia-inducible factor (HIF)

Low oxygen tension (hypoxia) is another important feature of the TME. Fast proliferating cells in solid tumours require oxygen, which can outweigh the limited supply partly due to the insufficient vascularisation. This may result in the development of tissue areas with lower O_2 tensions than the corresponding normal tissue. For example, the median oxygen partial pressure (pO_2 values) in the advanced primary breast cancer is 10 mmHg (1.3 %), whereas 65 mmHg (8.6%) in the normal breast tissue; in the brain, oxygenation has been measured at 13 mmHg (1.7%) in primary brain tumours and 35 mmHg (4.6%) in the normal brain tissue. Accumulating evidence shows that hypoxic tissue areas are prevalent in a wide range of human malignancies, although the oxygen levels may vary (Höckel and Vaupel 2001; Vaupel, Mayer, and Höckel 2004; Carreau et al. 2011).

Cellular adaptation to hypoxia is mostly mediated by the HIF family of transcription factors (LaGory and Giaccia 2016).

1.3.1 Activation and regulation of HIF

HIF is an αβ-heterodimer that was first identified as a nuclear factor that binds to the enhancer of the gene encoding erythropoietin (EPO) and mediates its transcription upon hypoxia (Semenza and Wang 1992; G. L. Wang et al. 1995). While the HIF-β subunit is constitutively expressed in the nucleus, HIF-α subunits are inducible by hypoxia. Three HIF-α isoforms have been identified in humans

and mammals: HIF-1α, HIF-2α, and HIF-3α (Semenza and Wang 1992; H. Tian, McKnight, and Russell 1997; Makino et al. 2001). Among the three isoforms, HIF-1α and HIF-2α are each able to bind hypoxia response elements (HREs) to induce transcriptional activity (Wiesener et al. 1998), while HIF-3α exercises dominant negative regulation of HIF-mediated control of gene expression (Makino et al. 2001).

- **O_2-dependent HIF activation**

The oxygen-sensitivity of HIF activity is conferred by post-translational modification by a series of O_2-dependent hydroxylases, namely prolyl hydroxylases (PHDs) and asparaginyl hydroxylase factor inhibiting HIF (FIH). Under normoxia, both PHDs and FIH are enzymatically active. PHDs hydroxylate HIF-α at two prolyl residues (Pro402 and Pro564 in human HIF-1α), thereby tagging HIF for proteasomal degradation via von Hippel–Lindau tumour suppressor protein (VHL)-dependent polyubiquitination (Huang et al. 1998; Maxwell et al. 1999; Jaakkola et al. 2001; Masson et al. 2001; Epstein et al. 2001). On the other hand, FIH hydroxylates an asparaginyl residue in the C-terminal transactivation domain (C-TAD) of HIF-α, preventing the interaction between HIF-α C-TAD and transcription co-activator p300/CREB-binding protein (CBP) to form an effective transcriptional complex (Mahon, Hirota, and Semenza 2001; Lando, Peet, Whelan, et al. 2002; Lando, Peet, Gorman, et al. 2002). Therefore, under normoxia, PHDs suppress HIF-α by promoting its degradation while FIH inhibits the transcriptional activity of HIF-α.

During hypoxia, however, the activities of both PHDs and FIH are inhibited, resulting in reduced hydroxylation of HIF-α at the prolyl and asparaginyl residues and the stabilisation of HIF-α. HIF-α then translocates into the nucleus, where it

forms a complex with the HIF-β subunit and p300/CBP, and binds to gene promoters that contain HREs (Schofield and Ratcliffe 2004a) (the working mechanism of HIF is illustrated in Figure 1.5). In this way, HIF coordinates a transcriptional programme that helps cells adapt to oxygen deficiency. More than 70 genes have been identified as transcriptional targets of HIF-α to date, and the list of genes is still growing (Dengler, Galbraith, and Espinosa 2013).

What is the oxygen threshold for HIF activation? Culture cells show an exponential induction of HIF-1α protein and its DNA-binding activity as oxygen level is reduced over the range 10.0%–0.6%, with maximal induction being observed at ~1% oxygen (Schofield and Ratcliffe 2004a). This response range overlaps that of physiological oxygen partial pressure *in vivo* (kidney: 9.5 ± 2.6%, intestinal tissue: 7.6 ± 0.3%, bone marrow: 6.4 ± 0.6%, muscle: 3.8 ± 0.2%, brain: 4.4 ± 0.3%, lung: 5.6%, venous blood: 5.3%, arterial blood: 13.2%, air in the alveoli: 14.5%) (Carreau et al. 2011). HIF-1α protein level is generally low in human and rodent tissues at basal state, but is robustly increased in pathological conditions such as cancer and tissue ischaemia. Unlike cultured cells, the activation of HIF *in vivo* seems to be set with different thresholds in different tissues for appropriate control of oxygen homeostasis. For example, HIF-1α can be induced in proximal nephron segments by systemic hypoxia, but not in the adjacent distal nephron segments that presumably experience a similar oxygen tension (Rosenberger et al. 2002; Schofield and Ratcliffe 2004a).

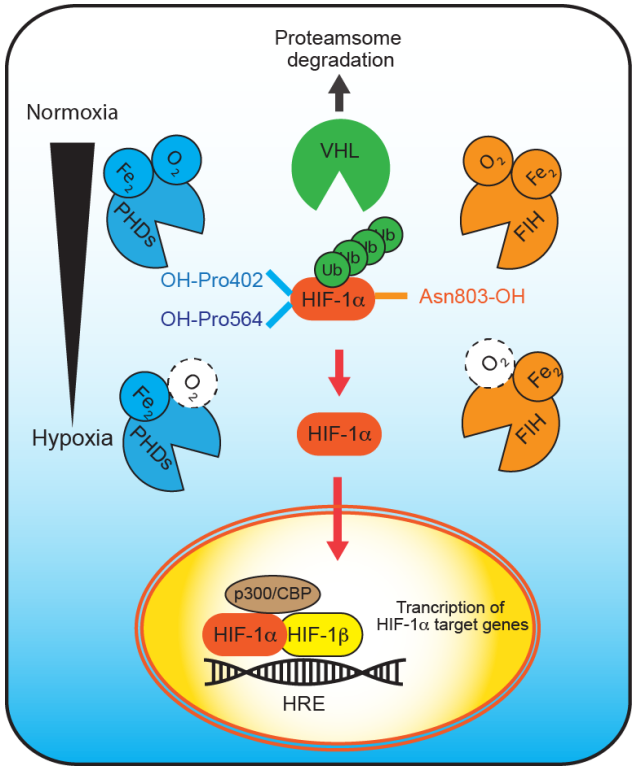

Figure 1.5 Mechanism of HIF activation
Under normoxia, HIF-α is hydroxylated by PHDs and FIH in an oxygen-dependent manner. PHDs hydroxylate HIF-α at two prolyl residues, causing HIF-α to be polyubiquitinated and sent for proteasome degradation. FIH hydroxylates HIF-α at an asparaginyl residue, which does not result in polyubiquitination but prevents the interaction with transcriptional co-activators p300/CBP, thereby inhibiting the transcriptional activity of HIF-α. Under hypoxia, the activity of PHDs and FIH is inhibited. HIF-α is accumulated and it translocates into the nucleus, where it dimerises with the β subunit, recruits p300/CBP, and binds to HREs to induce the expression of target genes. This figure is adapted from a published review (Palazon et al. 2014).

- **O_2-independent HIF activation**

In addition to the oxygen-dependent regulation of HIF signalling, oxygen-independent activation of HIF activation has been demonstrated in many cell types, including tumour and immune cells. In clear cell Renal Cell Carcinoma (ccRCC), loss-of-function mutation of the gene that encodes VHL prevents HIF degradation,

thereby inducing HIF activity (Cowey and Rathmell 2009). Genetic mutations of metabolic enzymes have also been reported to stabilise HIF protein, as the resulting accumulation of metabolic intermediates (e.g., succinate, fumarate, pyruvate, and oxaloacetate) can inhibit the activity of PHDs (Lu et al. 2005; P. J. Pollard 2005). Additionally, aberrant activation of phosphatidylinositol 3-kinase (PI3K)/AKT/mammalian target of rapamycin (mTOR) pathway may trigger HIF signalling (B. H. Jiang et al. 2001; Mayerhofer 2002; Brugarolas et al. 2003). ROS has also been implicated as a mediator of mitochondrial HIF stability by inhibiting HIF hydroxylase function (Mansfield et al. 2005; Niecknig et al. 2012; Masson et al. 2012), however the mechanism remains debatable due to the coupling between ROS production and oxygen consumption (Hagen 2012).

In macrophages, HIF has been reported to be activated by inflammatory stimulants such as IL-1β (Y.-J. Jung et al. 2003), TNFα (Y. Jung et al. 2003; Zhou, Schmid, and Brüne 2003), TGF-β (McMahon et al. 2006) and LPS (Frede et al. 2006; Rius et al. 2008; Nishi et al. 2008; Peyssonnaux et al. 2007; Fang et al. 2009). Mechanistically, these stimulants induce HIF-1α transcription via activating Nuclear Factor κB (NFκB), a master transcription factor mediating inflammatory responses (Rius et al. 2008), although other mechanisms involving ROS production (Nishi et al. 2008), PHD inhibition (Peyssonnaux et al. 2007), and p42/p44 mitogen-activated protein kinases (MAPKs) (Frede et al. 2006) may also exist. Interestingly, HIF isoforms are differentially regulated in macrophages by environmental cues: HIF-1α is induced in M1 macrophages stimulated by Th1 cytokines while HIF-2α is induced in M2 macrophages stimulated by Th2 cytokines (Takeda, O'Dea, Doedens, and Kim 2010).

In T cells, engagement of TCR has been shown to stimulate the protein synthesis of HIF-1α, probably via PI3K/mTOR pathway (Nakamura et al. 2005). Additionally, IL-6, and TGF-β have both been shown to induce HIF-1α at the messenger ribonucleic acid (mRNA) level in a signal transducer and activator of transcription 3 (STAT3)-dependent manner (Dang et al. 2011; Kojima et al. 2002; Shi et al. 2011).

1.3.2 The role of HIF in tumour cells

Increased expression of HIF-1α and HIF-2α has been observed in many types of human cancer (H. Zhong et al. 1999; Talks et al. 2000). HIF-α expression is associated with poor prognosis in various malignancies including brain, breast, colon, head and neck, liver, lung, skin, and pancreatic cancers, as well as certain types of leukaemias (Bertout, Patel, and Simon 2008; Deeb et al. 2011; Frolova et al. 2014). Functionally, HIF has been shown to influence tumour cell survival, invasion, and escape of immune surveillance.

- **HIF and tumour cell survival**

Cancer cells switch their glucose metabolism from oxidative phosphorylation to glycolysis (the Warburg effect (Vander Heiden, Cantley, and Thompson 2009). HIF facilitates this metabolic reprogramming by promoting glycolysis while inhibiting oxidative phosphorylation. To be more specific, HIF enhances glycolytic flux by upregulating the expression of glucose transporters (GLUT1 and GLUT3) and glycolytic enzymes (e.g., phosphofructokinase-1 and phosphoglycerate kinase) (Masson and Ratcliffe 2014). Meanwhile, HIF blocks the flow of pyruvate into the tricarboxylic acid (TCA) cycle by inducing pyruvate dehydrogenase kinase 1, hence suppressing oxidative phosphorylation (Kim et al. 2006; Papandreou et al. 2006).

The enhanced glycolysis generates large amounts of metabolic intermediates as building blocks to assemble new cells, which may in consequence facilitate the rapid growth of cancer cells (Hanahan and Weinberg 2011). Moreover, tuning down mitochondrial functions to reduce oxygen consumption may ameliorate intracellular hypoxia, therefore conferring tumour cells with a growth advantage (Denko 2008).

- **HIF and tumour progression**

HIF-1α and HIF-2α have been shown to stimulate blood vessel development by inducing the production of pro-angiogenic factors, including VEGF, angiopoietin 1 (ANG-1), angiopoietin 2 (ANG-2), PDGF and others. In addition, hypoxia signalling has also been shown to affect vessel patterning, maturation, and function (Krock, Skuli, and Simon 2012).

HIF also promotes tumour invasiveness by facilitating EMT. HIF-1α has been shown to induce the expression of EMT regulators SNAIL, Zinc Finger E-Box Binding Homeobox 1 (ZEB1), and TWIST (Evans et al. 2006; W. Zhang et al. 2015; M.-H. Yang et al. 2008). Additionally, HIF-1α can suppress the expression of E-cadherin, an epithelial cadherin that maintains tissue integrity and architecture (Imai et al. 2003; Esteban et al. 2006).

Another way that HIF promotes tumour invasion is through remodelling the ECM. For instance, HIFs regulate the production of collagen-modifying enzymes (e.g., lysyl oxidase (LOX) and procollagen-lysine 2-oxoglutarate 5-dioxygenase 2 (PLOD2)) that promote the formation of dense, aligned collagen fibres, which increases the ability of tumour cells to invade blood vessels. HIF-1α and HIF-2α also regulate ECM degradation by increasing the expression of matrix metalloproteinases (MMPs) (Gilkes, Semenza, and Wirtz 2014).

- **HIF and immune evasion**

Hypoxia or HIF signalling has been shown to help tumour cells evade immune surveillance. Firstly, hypoxic tumour cells promote the recruitment of Treg cells and macrophages from the circulation by upregulating the relevant chemokines (Murdoch 2004; Facciabene et al. 2011), some of which have been demonstrated to be HIF-dependent (e.g., VEGF, endothelin-1, endothelin-2, CCL2, CCL5, CXCL12, CXCR4, CXCR7, and CXCL8) (Leek et al. 2002; Grimshaw 2007; Du et al. 2008; Krock, Skuli, and Simon 2012; Nagarsheth, Wicha, and Zou 2017).

Once recruited, hypoxic tumour cells may further promote the immunosuppressive phenotype of the immune cells. For example, lactic acid, a metabolic by-product of hypoxic tumour cells, polarises TAMs to express increased levels of ARG1 and VEGF (Colegio et al. 2015). The fast-dividing tumour cells may also suppress T cell expansion by depleting glucose, a process that can be augmented by hypoxia (Ho et al. 2015; C.-H. Chang et al. 2015). Hypoxic tumour cells also execute direct T cell inhibition via their expression of PD-L1 (Barsoum et al. 2014; Ruf, Moch, and Schraml 2016).

1.3.3 The role of HIF in tumour-infiltrating MSCs

A rapidly increasing body of evidence has shown the significance of HIF in the biology of tumour stroma. Due to the pace and breadth of this research, a truly comprehensive review is probably impossible and beyond the scope of this thesis. Therefore, this section aims to focus on how hypoxia or HIF signalling influences tumour-infiltrating myeloid cells and T cells. For more information, please refer to the indicated review (LaGory and Giaccia 2016).

Both HIF-1α and HIF-2α are expressed in TAMs (Burke et al. 2002; Talks et al. 2000). In addition, increased expression of HIF-2α has been shown to be

correlated with poorer prognosis in a variety of human cancers (Leek et al. 2002; Kawanaka et al. 2008).

In line with human data, studies using myeloid-specific HIF knockout mice have demonstrated that both HIF-1α and HIF-2α expression in the myeloid compartment contributes to tumour progression. As shown in the MMTV-PyMT (Mouse Mammary Tumour Virus/Polyomavirus Middle T Antigen) model of mammary carcinogenesis, myeloid HIF-1α expression increases tumour burden and promotes tumour progression without altering vascularisation (Doedens et al. 2010). In a colitis-associated cancer (CAC) model, HIF-2α expression in the myeloid compartment favours tumour progression accompanied by increased infiltration of myeloid cells (Imtiyaz et al. 2010). Characterisation of HIF-deficient macrophages (and neutrophils) provides several pointers on how myeloid-derived HIF fuels tumour development.

- **Macrophage migration**

Cramer and colleagues were the first to demonstrate the function of HIF-1α in macrophages. Using primary murine macrophages and neutrophils, they showed that HIF-1α is essential for the regulation of glycolysis; loss of HIF-1α results in a reduced cellular ATP pool, which consequently impairs energy-requiring activities including cell aggregation, invasion, motility, and bacterial killing under normoxia *in vitro* (Cramer et al. 2003). However, this may not be directly linked to the infiltration of macrophages in tumour *in vivo*. As demonstrated in the MMTV/PyMT model, tumours established in myeloid-specific HIF-1α-null animals show a similar extent of macrophage infiltration when compared with wild-type (WT) counterparts (Doedens et al. 2010).

HIF-2α is also required for macrophage migration, but through regulating the expression of chemoattractant receptors including M-CSF-receptor (M-CSF-R) and C-X-C motif chemokine receptor 4 (CXCR4), as well as fibronectin, an important mediator of cellular interactions with the ECM. Unlike HIF-1 α, HIF-2α does not affect ATP production (Pankov and Yamada 2002; Imtiyaz et al. 2010).

- **MSC-mediated T cell suppression**

As discussed earlier, $_{L}$-arginine-metabolising enzymes NOS2 and ARG1 are able to suppress T cell function. Hypoxia has been shown to promote the expression of both enzymes in macrophages in a HIF-dependent manner (Corzo et al. 2010; Takeda, O'Dea, Doedens, Kim, et al. 2010). By co-culturing macrophages with T cells under hypoxia, Doedens et al found that macrophages inhibit T cell proliferation in a HIF-1α/NOS2-dependent manner. This observation is also in concert with the *in vivo* observation of a higher percentage of IFNγ-producing T cells in mammary tumours from macrophage-HIF-1α-null animals (Doedens et al. 2010).

Additionally, HIF-1α has been shown to directly induce PD-L1 expression in MDSCs and macrophages (Noman et al. 2014), which potentiates the immunosuppression of MSCs on T cells. Furthermore, HIF-1α has been found to mediate the differentiation of MDSCs to TAMs (Corzo et al. 2010).

- **Macrophage-regulated tumour angiogenesis**

Hypoxic TAMs regulate tumour angiogenesis by upregulating the expression of pro-angiogenic factors including receptor tyrosine kinase Tie2, VEGF, and MMP-9. While the upregulation of Tie2 (Lewis, De Palma, and Naldini 2007) and MMP-9 (Du et al. 2008) by hypoxia has been shown to promote angiogenesis, the effect of macrophage-derived VEGF seems to be controversial (E. Y. Lin et al. 2007;

Stockmann et al. 2008). Furthermore, HIF-2α induces a soluble VEGF receptor in hypoxic macrophages that neutralises VEGF (Roda et al. 2011), adding another layer of regulation of angiogenesis by macrophages in control of HIF.

1.3.4 The role of HIF in tumour-infiltrating T cells

HIF-1α seems to play contrasting roles in balancing the differentiation of Treg cells and Th17 cells from the common ancestor CD4 T cells. HIF-1α has been shown to favour the Th17 development while suppress Treg cell differentiation via the regulation of glycolysis (Shi et al. 2011) or the induction of RORγt (retinoid acid receptor-related orphan receptor), a master transcription factor directing the differentiation of Th17 cells (Dang et al. 2011). On the contrary, hypoxia has also been demonstrated to induce Foxp3 expression, therefore enhancing the differentiation of CD4 T cells to Treg cells (Clambey and McNamee 2012).

The activity of CD8 T cells is generally suppressed by low O_2 tensions, although the contribution of HIF activity and hypoxia has not been clearly uncoupled (de Silly, Dietrich, and Walker 2016). In another study, however, both HIF-1α and HIF-2α are shown to enhance the effector function of CD8 T cells, which could be associated with the role of HIF on glycolysis in cooperation with mTOR pathway (Finlay et al. 2012; Doedens et al. 2013).

1.3.5 Summary

The hypoxic TME has a broad influence on both tumour cells and stromal cells. Although introduced separately, one should be aware that hypoxia not only alters the biology of individual cells, but orchestrates interactions between each cellular component. Figure 1.6 summarises how tumour hypoxia co-opts immune cells to promote tumourigenesis.

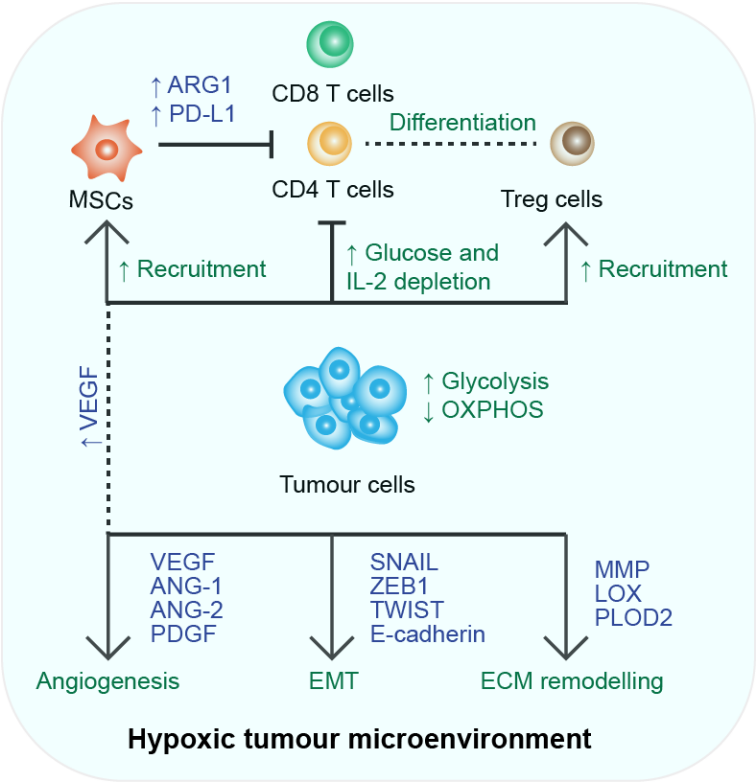

Figure 1.6 Hypoxia co-opts immune cells to promote tumour development

Hypoxia promotes tumour angiogenesis, EMT, and ECM remodelling by inducing the expression of relevant genes. Hypoxia also enhances the immunosuppressive environment through the recruitment of MSCs (mainly TAMs and MDSCs) and Treg cells by inducing the secretion of a range of chemokines. Hypoxic tumour cells inhibit T cell survival by depleting local sources of glucose and IL-2. Hypoxia also potentiates T cell suppression via inducing the inhibitory molecules in MSCs and regulates the differentiation of CD4 T cells to Treg cells. OXPHOS: oxidative phosphorylation.

1.4 FIH

1.4.1 Overview

- **Discovery of FIH**

FIH was first identified as an interacting partner of HIF-1α in a two-hybrid assay; it got its name because of the ability to inhibit HIF-1α transcriptional activity, as demonstrated by luciferase reporter assays (Mahon, Hirota, and Semenza 2001). Later, it was found that the transcriptional activities of both HIF-1α and HIF-2α are inhibited by the hydroxylation of an asparagine residue within their C-TAD, which blocks the recruitment of the p300/CBP co-activator (Lando, Peet, Whelan, et al. 2002). Soon after, FIH was identified to be the protein hydroxylating both HIF-1α and HIF-2α, at N803 and N851, respectively (Lando, Peet, Gorman, et al. 2002).

- **Regulation of FIH activity**

Like PHDs, FIH utilises molecular oxygen to couple the oxidative decarboxylation of 2-oxoglutarate (2-OG) to the hydroxylation of HIF-α subunit in a reaction that requires Fe(II) and ascorbate as cofactors (Lando, Peet, Gorman, et al. 2002; Cockman, Webb, and Ratcliffe 2009). Compared with PHDs, FIH shows higher affinity with O_2 (Koivunen et al. 2004). In line with this notion, several studies have reported that FIH can still inhibit HIF transcriptional activity at low oxygen tensions (0.2–1%) in several cell lines, whereas the PHDs are inactive under the same condition (Lando, Peet, Gorman, et al. 2002; Stolze, Tian, Appelhoff, Turley, Wykoff, Gleadle, and Ratcliffe 2004a). While FIH is less sensitive to decreasing oxygen tensions than PHDs in some cell lines, it appears to be more sensitive in some others (Bracken et al. 2006). This context-dependent

characteristic suggests that the activity of FIH should be assessed experimentally in different systems.

Another interesting feature of FIH is that, despite its reduced sensitivity to oxygen, FIH is substantially more sensitive to peroxide compared to PHDs, which may account for the activation of HIF by ROS (Masson et al. 2012).

As mentioned, FIH requires 2-OG to catalyse the hydroxylation reaction. While PHDs are negatively regulated by the TCA cycle intermediates fumarate, succinate, and oxaloacetate, FIH activity is not affected by any of these compounds at physiological concentrations, suggesting a unique chemical nature of FIH compared with other HIF hydroxylases (Hewitson et al. 2007; Lisy and Peet 2008).

- **Expression of FIH**

Although FIH protein has been detected across different cell lines at similar levels (Lisy and Peet 2008), a few mechanisms have been identified that regulate the transcription of FIH. In renal cell carcinoma (RCC) cells, FIH transcription is repressed by protein kinase Cζ (PKCζ). Li and colleagues discovered a specific region of the FIH promoter containing the consensus sequence for CDP/Cut (cut-like homeodomain protein), a protein that usually suppresses gene transcription. PKCζ has been shown to facilitate the binding of CDP/Cut to FIH promoter, thereby inhibiting the transcription of FIH (J. Li et al. 2007).

FIH expression can also be regulated by a series of microRNAs. FIH has been shown to be suppressed by microRNA (miR)-31 in corneal epithelia, head and neck carcinoma cells, and hepatic stellate cells (C. J. Liu et al. 2010; Peng, Hamanaka, et al. 2012; Hu et al. 2015), exosome-derived miR-135b in endothelial cells (Umezu et al. 2014), miR-182 in prostate cancer cells (Y. Li et al. 2015), and miR-184 in glioma cells (Yuan et al. 2014). The frequent upregulation of the indicated

microRNAs and the resulting downregulation of FIH in pathological conditions including cancer suggest a biological function of FIH in this context.

- **Localisation of FIH**

FIH protein is mostly reported to be in the cytoplasm, and its localisation is not subjected to hypoxia or hypoxia mimetic (Depping, Jelkmann, and Kosyna 2015). Interestingly, treating human umbilical vein endothelial cells (HUVECs) with dimethyloxallyl glycine (DMOG) at 100 μM for 4 hr significantly increases FIH protein in the nucleus in a HIF-1α-dependent manner (Liang et al. 2015). FIH also shows distinct subcellular localisation in human cancer tissues, as will be discussed shortly.

- **Effects of FIH on the expression of HIF target genes**

While compelling results of luciferase assays show that FIH suppresses HIF-1α-mediated gene transcription (Mahon, Hirota, and Semenza 2001; Lando, Peet, Gorman, et al. 2002), FIH does not overly inhibit the transcription of HIF target genes, but instead acts like a discriminator between C-TAD and N-TAD-sensitive genes (Dayan et al. 2006). Also, the modification of HIF-2α by FIH is less efficient than that of HIF-1α, (Park et al. 2003; Koivunen et al. 2004), which may limit the effect of FIH on HIF pathway. To date, a handful of HIF target genes have been identified as being FIH-sensitive. This set of gene is highly subjective to the type of tissue investigated. FIH-dependent HIF target genes are summarised in Table 1.1

Table 1.1 FIH-sensitive HIF target genes

Reference	Cell line	Treatment	Method	Genes
Chan et al, 2016	MCF-7 (human breast cancer)	FIH inhibitor	Microarray RNA sequencing RT-qPCR	*CA9, ADM, EGLN3, HK2, ANKRD37*
	U2OS (human osteosarcoma)			*CA9, EGLN3*
	Hep3B (human hepatocellular carcinoma)			*CA9, EGLN3, ANKRD37*
	Hela (human cervical adenocarcinoma)			*CA9, EGLN3, SOX9, ANKRD37*
Dayan et al, 2007	Hela (human cervical adenocarcinoma)	FIH silencing by siRNA; FIH overexpression	RT-qPCR	*EGLN3, CA9, GLUT1, BNIP3L, RTP801, HK2, KRT19, VEGF, CYCLIN G2, LDHA, ADM, PPARG, TFF3, CITED2, PLAUR, CDKN1A*
Khan et al, 2011	RCC10 (human renal cell carcinoma)	FIH silencing by siRNA	RT-qPCR	*GLUT1, EGLN3, VEGF, BNIP3*
	RCC4 (human renal cell carcinoma)	FIH silencing by siRNA	RT-qPCR	*GLUT1, EGLN3, VEGF*
	786-O (human renal cell carcinoma)	FIH silencing by siRNA+HIF-1α stabilisation	RT-qPCR	*EGLN3, VEGF, BNIP3*
Chen et al, 2015	LOVO and SW116 (human colorectal carcinoma)	FIH overexpression	RT-qPCR	*GLUT1, VEGF*
Pelletier et al, 2011	LS174 (human colorectal carcinoma)	FIH silencing by shRNA	Microarray RT-qPCR	*ANGPT1, TGFB1, VEGFA, BAD, CASP8, CFLAR, MET, MMP1, SERPINB5, BRCA1, TP53, ITGA2, ITGB1*

RT-qPCR: Real time-quantitave polymerase chain reaction; siRNA: small interfering RNA; shRNA: short hairpin RNA; ADM: Adrenomedullin; ANGPT1: Angiopoietin 1; ANKRD37: Ankyrin repeat domain 37; BAD: BCL2 associated agonist of cell death; BNIP3: BCL2 interacting protein 3; BNIP3L: BCL2 interacting protein 3 like; CA9: Carbonic Anhydrase 9; CASP8: Caspase 8; CDKN1A: Cyclin dependent kinase inhibitor 1A; CFLAR: CASP8 and FADD like apoptosis regulator; CITED2: Cbp/p300 interacting transactivator with Glu/Asp rich carboxy-terminal domain 2; EGLN3: Egl-9 family hypoxia inducible factor 3 (PHD3); GLUT1: Glucose transporter 1; HK2: Hexokinase 2; ITGA2: Integrin subunit alpha 2; ITGB1: Integrin subunit beta 1; MET: MET proto-oncogene receptor tyrosine kinase; MMP1: Matrix metallopeptidase 1; PLAUR: Plasminogen activator, urokinase receptor; PPARG: Peroxisome proliferator activated receptor gamma; SERPINB5: Serpin family B member 5; SOX9: Sex determining region Y-box 9; TFF3: Trefoil factor 3; TGFB1: Transforming growth factor beta 1; VEGFA: Vascular endothelial growth factor A.

1.4.2 FIH and ankyrin repeat domain (ARD)-containing proteins

FIH does not only target HIF, but also a collection of proteins containing a ubiquitous protein–protein interaction motif called an ARD. To date, more than 20 ARD-containing proteins have been identified as FIH-interacting partners, 11 of which have been confirmed as *bona fide* FIH substrates (Cockman, Webb, and Ratcliffe 2009), including components in NFκB signalling pathways (NFκB inhibitor alpha (IκBα) and p105) (Cockman et al. 2006), Notch signalling (Notch 1-3) (Coleman et al. 2007), and apoptosis-stimulating p53-binding protein (ASPP) 2 (Janke et al. 2013). The list of FIH substrates will probably keep growing, as proteomic studies indicate that ~300 ARD-containing species in the human proteome are likely to be subjected to asparaginyl hydroxylation (Cockman et al. 2009).

Interestingly, compared with HIF-α, ARD-containing proteins may be more favoured by FIH as substrates. Analyses of Notch family substrates show that FIH has a higher affinity for Notch1 ARD compared to HIF C-TAD (K_M values being 0.2 and 50 μM, respectively) (Wilkins et al. 2009). The abundance of ARD-containing proteins and their high affinity to FIH indicates that ARD-containing proteins may compete with HIF-α for FIH-mediated hydroxylation. Indeed, several ARD-containing proteins, including Notch1 (Coleman et al. 2007; Zheng et al. 2008), myosin phosphatase target subunit 1(MYPT1), Tankyrase1, and IκBα (Webb et al. 2009; Shin et al. 2009), have been shown to increase HIF activity through competition for FIH interaction.

In addition, hydroxylation modification by FIH can also affect ARD-containing proteins directly. FIH-dependent hydroxylation has been shown to increase the thermal stability of the ARD fold (L. Kelly et al. 2009; Hardy et al. 2009). Other functional consequences of FIH-mediated hydroxylation have been reported (see below).

- **The ASPP2/p53 pathway**

ASPP2 belongs to the family of ASPP proteins, characterised by a common C-terminal sequence: ankyrin repeats, an SH3 domain, and a protein-rich region. The best-known function of the ASPP family proteins is their ability to regulate the apoptotic function of p53 family members. The ASPP2/p53 interaction has been shown to specifically stimulate the pro-apoptotic activity of p53 (Samuels-Lev et al. 2001) and other p53 family members p63 and p73 (Bergamaschi et al. 2004). Apart from p53, ASPP2 also binds the tight junction scaffolding protein partitioning-defective homologue 3 (Par-3), and this interaction is critical for maintaining cell

polarity of neural progenitors during central nervous system (CNS) development (Sottocomola et al. 2010).

ASPP2 is hydroxylated by FIH at N986 within its ARD. While FIH depletion does not affect the interaction between ASPP2 and p53, it impairs the binding between ASPP2 and Par-3 and results in the relocation of ASPP2 from cell–cell junctions to the cytosol in HCT116 and H441 cells, suggesting that FIH may influence cell polarity via ASPP2 (Janke et al. 2013).

- **The NFκB pathway**

NFκB signalling is a central player in mediating inflammatory responses (Lawrence 2009). NFκB is composed of three core elements: IκB kinase (IKK), IκB, and NFκB transcription factors. In the resting state, NFκB is sequestered in the cytosol by IκB proteins. Upon stimuli, IKK is activated, leading to the phosphorylation and degradation of IκB proteins. NFκB is therefore liberated, and it translocates to the nucleus and initiates the induction of target genes. The NFκB family of transcription factors consists of five members: NFκB1 (p105), NFκB2 (p100), RelA (p65), RelB, and c-Rel. NFκB1 (p105) and NFκB2 (p100) are precursors that give rise to subunits p50 and p52, respectively. Unlike RelA, RelB, and c-Rel, p50 and p52 do not have DNA-binding ability and have to heterodimerise with the DNA-binding NFκB members to induce the expression of target genes. Alternatively, they can also negatively regulate the transcriptional activity of NFκB (Hayden and Ghosh 2012).

FIH hydroxylates p105 at N678, and IκBα at N210 and N244; however, how these modifications influence the transcriptional activity of NFκB remains unclear (Cockman et al. 2006). *In vitro* biophysical characterisation suggests that hydroxylation of IκBα by FIH does not alter the NFκB binding kinetics and

thermodynamics, nor the stability of IκBα (Devries et al. 2010). However, it can enhance HIF-1α activity due to the sequester of FIH by IκBα (Shin et al. 2009).

- **The Notch pathway**

Notch signalling regulates cell fate decisions, differentiation, and proliferation (Artavanis-Tsakonas, Rand, and Lake 1999). Deregulation of the Notch pathway is linked to a range of diseases including cancer (Louvi and Artavanis-Tsakonas 2012). There are four Notch transmembrane receptors (Notch 1–4) in mammalian cells. Upon receiving extracellular signals, the Notch intracellular domain (NICD) is cleaved from the plasma membrane. The NICD then enters the nucleus, where it interacts with CSL (CBF-1/Suppressor of hairless/Lag-1) and recruits the nuclear transcriptional activation complex. The ARD within NICD is essential for its interaction with CSL (Bray 2016).

FIH hydroxylates NICD at N1945 and N2012. This hydroxylation modification has been shown to inhibit Notch activity and promote myogenic differentiation, as well as alleviate the inhibitory effect of FIH on HIF (Coleman et al. 2007; Zheng et al. 2008).

1.4.3 FIH expression in human cancer

Chromosomal region 10q24, which contains *HIF1AN* (the gene that encodes FIH) has been reported to be deleted in glioblastoma multiforme cases (Albarosa et al. 1996), prostate cancers (Matsuyama et al. 2002), and a small set of paediatric T cell acute lymphoblastic leukaemias (Kees et al. 2003). Overall, *HIF1AN* is not frequently mutated in the cancer genome (information resource: cBioPortal http://bit.ly/2yzL1m2, Figure 1.7).

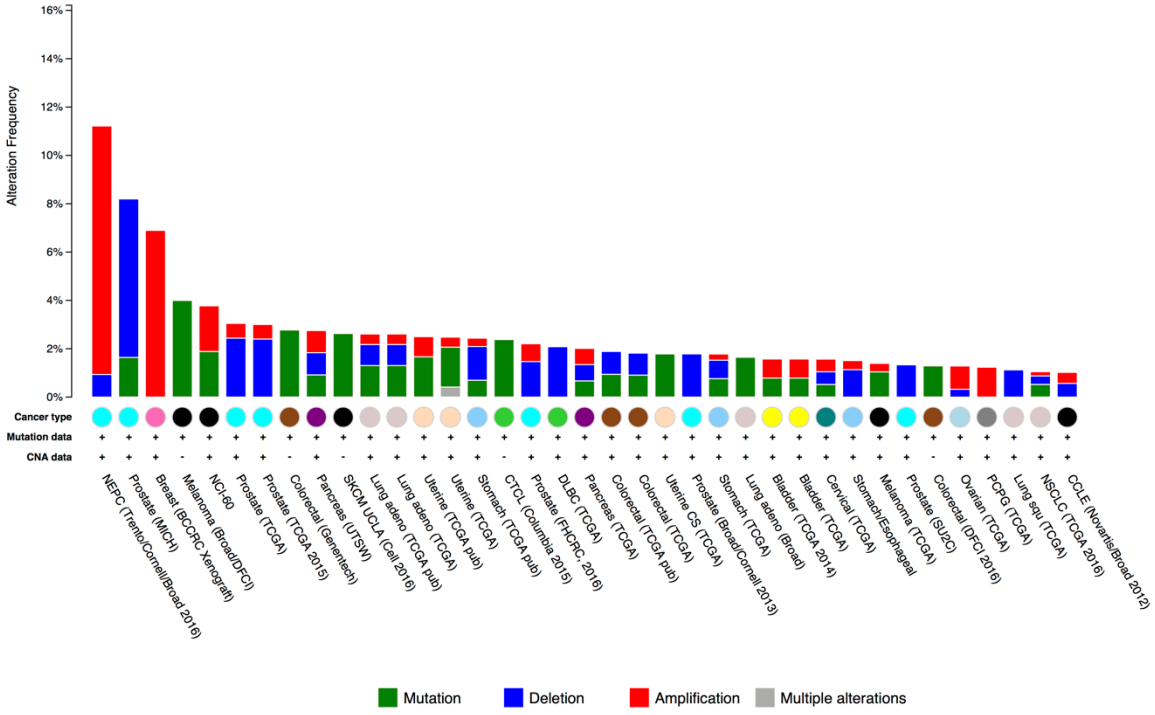

Figure 1.7 Cross-cancer alteration of *HIF1AN*
One-hundred and sixty-four studies from cBioPortal database are curated. Cancer types bearing a minimum of 1% alteration frequency of *HIF1AN* are shown.

In normal human biopsies, FIH protein is detected in a wide range of tissues at a similar level, and the localisation of FIH is predominantly cytoplasmic (Soilleux et al. 2005). However, in tumour tissues, the abundance and localisation of FIH can be altered, which may have prognostic value for diseases of various types and stages.

In colorectal tumour tissues, FIH has been detected in both tumour cells and tumour stromal cells. One study reports that most tumour cells show nuclear FIH expression, but the level does not associate with clinical pathological parameters (Vakil et al. 2016). In another study, FIH is detected in both the nucleus and the cytoplasm of tumour cells. The protein level of FIH in the tumour is lower than normal tissue, and patients with reduced FIH expression show poorer prognosis (T. Chen et al. 2015).

In HCC, FIH is predominantly observed in the nucleus. Protein level of FIH is significantly reduced in tumour tissues compared with adjacent non-tumour liver tissues. Lower expression of FIH in tumour tissues is correlated with more aggressive behaviours of HCCs. In terms of the prognostic, patients with reduced FIH expression show remarkably shortened disease-free survival (DFS), lower overall survival (OS), and higher recurrence (Ma et al. 2017).

Analyses of pancreatic endocrine tumours (PETs) show that FIH is expressed in both the cytoplasm and nucleus, with cytoplasmic FIH level being associated with more malignant PETs. FIH expression in the stromal compartment is detected in 23% of tumour samples and is correlated with poorer DFS (Couvelard et al. 2008).

In non-small cell lung cancer (NSCLC), FIH is predominantly in the cytoplasm of the tumour cell (Giatromanolaki et al. 2008). High expression of FIH is an unfavourable prognostic indicator for disease-specific survival (Andersen et al. 2011). FIH protein is not detected in the tumour stroma of NSCLCs (Giatromanolaki et al. 2008; Andersen et al. 2011).

In two studies of invasive breast carcinomas, FIH shows exclusive nuclear or cytoplasmic expression patterns. Exclusive nuclear FIH expression is inversely associated with tumour grade, whereas exclusive cytoplasmic FIH expression is positively associated with tumour grade (Tan et al. 2007; Hyseni et al. 2011).

Although primarily localised in the cytoplasm in normal kidney tissues, FIH is predominantly localised in the nucleus of ccRCC cells. Low level of nuclear FIH is a significant independent predictor for worse OS (Kroeze et al. 2010).

In prostate cancer tissues, in contrast, FIH is mainly detected in the cytoplasm. Additionally, nuclear FIH is associated with poor prognosis and a higher chance of recurrence of patients (Shaida et al. 2011).

In summary, FIH is detectable in a wide range of tumour tissues. The expression level and the localisation of FIH vary with the type of malignancy and may have differing association with clinical parameters. The expression of FIH in stromal cells has not been examined in detail.

1.4.4 FIH in tumour biology

FIH can affect tumour development through both HIF-dependent and -independent mechanisms.

Some studies demonstrate FIH to be tumour-promoting. For example, FIH has been shown to suppress the p53/p21 axis and promote the proliferation of LS174 (colon adenocarcinoma) and A375 (melanoma) cells (Pelletier et al. 2011). In ccRCC cells, FIH was shown to inhibit HIF-1α-dependent apoptosis. FIH has also been implicated in promoting tumour vessel development via the upregulation of PDGF-c, as shown by overexpressing FIH in LM8 cells (osteosarcoma) in a syngeneic tumour model (Kuzmanov et al. 2012).

Some other studies have identified FIH to be able to inhibit tumour development. It has been shown that FIH inhibits the proliferation, migration, invasion, and colony formation of LOVO and SW116 (both human colon carcinoma) cells *in vitro* and the growth of LOVO xenografts *in vivo*, accompanied by the downregulated expression of the HIF target genes GLUT1 and VEGF (T. Chen et al. 2015). In human tongue squamous cell carcinoma cells (SAS), FIH suppresses the oncogenic phenotype and VEGF production of the cancer cells (C. J. Liu et al. 2010). FIH and PHD2 expression is suppressed by miR-182 in prostate cancer cells, which results in the

sustained activation of HIF-1α and accelerated tumour progression (Y. Li et al. 2015). The tumour suppressing effect of FIH with similar mechanisms discussed above has also been uncovered in colorectal cancer cells and glioma cells (T. Chen et al. 2014; Yuan et al. 2014).

1.4.5 The role of FIH beyond cancer

FIH is also involved in other biological processes, including metabolism, the differentiation and migration of keratinocytes, endothelial cell development, and stimulus sensing.

- **Metabolism**

The first evidence for a role of FIH in metabolic regulation came from the characterisation of FIH homozygous knockout mice. FIH-null mice exhibit no discernible phenotypes relevant to classical HIF functions, such as angiogenesis, erythropoiesis, or development; instead, they show reduced body weight, increased metabolic rate, hyperventilation, and increased insulin sensitivity. Some of the major metabolic defects are recapitulated in neuron-specific FIH-deficient mice, indicating the significance of neural expression of FIH in metabolic regulation (N. Zhang et al. 2010).

The role of FIH in metabolism has been corroborated by other studies. For example, it has been found that FIH negatively regulates glycogen deposition in HCEKs (human corneal epithelial keratinocytes) *in vitro* and murine limbal epithelial tissue *in vivo*. The action of FIH is HIF-1α-independent but associated with the c-Kit/AKT/glycogen synthase kinase (GSK)-3β signalling pathway (Peng, Hamanaka, et al. 2012). In another study using HEK293 cells (human embryonic kidney cells), FIH was shown to hydroxylate the deubiquitinase ovarian tumour domain-containing aldehyde-binding protein 1 (OTUB1). Mutation of the FIH-

targeting residue N22A of OTUB1 profoundly alters its interaction with metabolism-associated proteins, suggesting the importance of asparagine hydroxylation by FIH in regulating metabolic processes (Scholz et al. 2016).

- **Keratinocyte differentiation and migration**

Elevated FIH expression is observed in epithelial tissues with abnormal differentiation such as psoriasis and diabetic keratopathies. Functionally, FIH has been shown to suppress keratinocyte differentiation via a coordinate suppression of Notch signalling (Peng, Kaplan, et al. 2012).

In normal epithelial cells, FIH enhances cell migration *in vitro* and wound healing *in vivo.* Mechanistically, FIH binds leucine-rich repeat kinase 1 (LRRK1) and disrupts the formation of the EGF receptor (EGFR)/LRRK1 complex, resulting in enhanced EGFR signalling (Peng et al. 2014).

- **Endothelial cell development**

FIH has been shown to affect vascular development through various mechanisms. In HUVECs, reduced expression of FIH leads to enhanced apoptosis and growth arrest, accompanied by increased expression of Hey 1 (hairy/enhancer-of-split related with YRPW motif protein 1) and reduced expression of survivin (an inhibitor of apoptosis) in a Notch-dependent manner, suggesting that FIH is essential for the survival of HUVECs (Kiriakidis et al. 2015). In contrast, in a zebrafish model, FIH has been demonstrated to suppress ectopic angiogenic sprouts by downregulating VEGF (So et al. 2014). The anti-angiogenic effect of FIH was also observed in a system mimicking the hypoxic bone marrow microenvironment, where exosomal miR-135b derived from hypoxic multiple myeloma cells downregulates FIH expression, enhances the transcriptional activity

of HIF-1α, and promotes endothelial tube formation of HUVECs (Umezu et al. 2014).

- **Stimulus sensing**

Transient receptor potential (TRP) channels function as cellular sensors to a diverse range of stimuli (Venkatachalam and Montell 2007). FIH has been shown to hydroxylate TRP vanilloid 3 (TRPV3), a member of the TRP family that mediates thermosensing and nociception in the skin (Broad et al. 2016), at N242. Furthermore, mutation of N242 potentiates TRPV3-mediated current, implying the functional significance of FIH-dependent hydroxylation modification (Karttunen et al. 2015). Another TRP family member, TRP vanilloid 4 (TRPV4), is also hydroxylated by FIH; however, the functional consequence has not yet been investigated (M. Yang et al. 2011).

1.5 Aim of the study

Our current knowledge about the role of FIH in tumourigenesis is still limited, with most of the studies based on *in vitro* assays using cancer cell lines. While these approaches may provide a solid biochemical foundation, there is a lack of physiological relevance. Furthermore, the role of FIH in the other compartment of tumours, the TME, is almost unexplored. Therefore, the aim of this study is to demonstrate the influence of FIH on tumour development in a physiological setting by taking advantage of *in vivo* tumour models.

This study develops from the observation that loss of FIH promotes the spontaneous formation of low-grade B cell lymphomas (Chapter 3), which is closely associated with chronic inflammation in human. Therefore, to test whether FIH could affect tumourigenesis by modulating the immune environment, syngeneic tumour models were applied on mice lacking FIH expression globally or in the myeloid compartment (Chapter 4). The tumour suppressive effect of FIH in myeloid cells then prompted the *in vitro* functional characterisation of $FIH^{-/-}$ macrophages (Chapter 5).

Chapter 2 Materials and Methods

2.1 Materials

2.1.1 Reagents

All chemicals were purchased from Sigma unless otherwise stated. The source of other reagents is mentioned in the *Methods* if not listed here.

Genotyping (GNT) buffer

GNT buffer was prepared in distilled water with the following compounds: 50 mM KCl, 1.5 mM $MgCl_2$, 10 mM Tris HCl (pH 8.5), 0.01% gelatin, 0.45% NP-40, and 0.45% Tween-20. GNT buffer was autoclaved and stored at 4°C.

Ethidium bromide (EtBr)

A 10 mg/ml stock solution was prepared by dissolving EtBr in distilled water. Stock solution was stored at room temperature (RT) in the dark.

EDTA (ethylenediaminetetraacetic acid) solution

1 L of 0.5 M EDTA stock solution was prepared by dissolving 186 g of EDTA in distilled water. The pH was adjusted to 8.0 with NaOH.

50× Tris-acetate EDTA (TAE) solution

1 L of 50× TAE solution was prepared in distilled water with the following compounds: 242 g Tris base, 57.1 ml glacial acetic acid, and 100 ml 0.5 M EDTA

(pH 8.0). pH of the solution was adjusted to 8.5. 1× TAE was prepared by diluting the 50× stock with distilled water.

10× Sodium citrate buffer

1 L of 10× sodium citrate buffer (100 mM) was prepared by dissolving 29.4 g tri-sodium citrate (dihydrate) in distilled water with the pH adjusted to 6.0. A 1× working solution was made by diluting 100 mM solution with distilled water.

Lung digestion buffer

An appropriate amount of collagenase D (final concentration 2 mg/ml) and DNaseI (final concentration 40 U/ml) was dissolved in phosphate-buffered saline (PBS). Digestion buffer was freshly prepared for each use.

Fluorescence-activated cell sorting (FACS) buffer

1 L of FACS buffer was prepared in 1× PBS with 0.5 g sodium azide, 20 ml 0.5 M EDTA, and 20 ml heat-inactivated foetal bovine serum (FBS).

Magnetic-activated cell sorting (MACS) buffer

MACS buffer was prepared in 1× PBS with 0.5% bovine serum albumin (BSA) and 2 mM EDTA.

4% Paraformaldehyde (PFA) solution

4 g PFA was dissolved in 100 ml PBS facilitated by gentle heating to 40°C. The solution was aliquoted and stored at -20°C.

DAPI (4',6-diamidino-2-phenylindole, dihydrochloride) staining solution

DAPI powder was dissolved in distilled water at 1 mg/ml and stored in aliquots at -20°C.

Chemotaxis buffer

Chemotaxis buffer was prepared in Dulbecco's Modified Eagle's Medium (DMEM) with 0.5% w/v BSA and 25 mM 4-(2-hydroxyethyl)-1-

piperazineethanesulfonic acid (HEPES)

Urea buffer

Urea buffer was prepared by dissolving the following compounds in distilled water with gentle heating: 8 M urea, 1 M thiourea, 0.5% (w/v) 3-[(3-cholamidopropyl) dimethylammonio]-1-propanesulfonate hydrate (CHAPS), 50 mM dithiothreitol (DTT), and 24 mM spermine. The resulting solution was aliquoted and stored at -20°C.

6× Laemmli buffer

10 ml of 6× Laemmli buffer was prepared in distilled water with the following compounds: 1.2 g sodium dodecyl sulphate (SDS), 0.93 g DTT, 6 mg bromophenol blue, 4.7 ml glycerol, and 1.2 ml Tris 0.5 M (pH 6.8). The resulting solution was aliquoted for storing at -20°C.

Ammonium persulfate (APS)

An appropriate amount of APS was dissolved in distilled water to make a 10% (w/v) APS solution.

Resolving gel solution (8% acrylamide)

10 ml of 8% resolving gel solution was prepared with the following components: 4.6 ml distilled water, 2.7 ml acrylamide/bis-acrylamide, 2.5 ml 1.5 M Tris-HCl (pH 8.8), 100 µl 10% (w/v) SDS, 100 µl 10% (w/v) APS, and 8 µl tetramethylethylenediamine (TEMED) (added right before casting the gel).

Stacking gel solution

10 ml of stacking gel solution was prepared with the following components: 6.1 ml distilled water, 1.3 ml acrylamide/bis-acrylamide, 2.5 ml 1.0 M Tris-HCl (pH 6.8), 100 µl 10% (w/v) SDS, 100 µl 10% (w/v) APS, and 10 µl TEMED (added right before casting the gel).

10× SDS-polyacrylamide gel electrophoresis (SDS-PAGE) running buffer

5 L of 10× SDS-PAGE running buffer was prepared by dissolving 720 g glycine, 150 g Tris, and 50 g SDS in distilled water.

10× SDS-PAGE transfer buffer

5 L of 10× SDS-PAGE transfer buffer was prepared by dissolving 725 g glycine and 145 g Tris in distilled water. 1× buffer was prepared in 20% ethanol.

Stripping buffer

Stripping buffer was prepared in distilled water containing 62.5 mM Tris HCl (pH 6.7), 100 mM β-mercaptoethanol, and 2% (w/v) SDS.

10× Tris-buffered saline (TBS)

1 L of 10× TBS solution was prepared by dissolving 24.2 g Tris base and 80 g NaCl in distilled water. pH was adjusted to pH 7.6 with HCl. To prepare 1× TBST buffer, 1 L of 1× TBS buffer was supplemented with 1 ml of Tween-20.

2.1.2 Mouse colonies

FIH transgenic mice were generated on a mixed C57BL/6 × 129SvJ background in Prof. Peter Ratcliffe's lab. Exon 1 and 2 of the FIH gene was flanked by two loxP sites (FIH floxed allele). The FIH knockout allele was generated by Cre-mediated excision of exon 1 and 2.

In the spontaneous tumourigenesis study, mice carrying the FIH knockout allele were crossed with mice deficient of the exon 3 of ASPP2 gene, which were generated on a mixed C57BL/6J × 129SvJ background in Prof. Xin Lu's lab (Vives et al. 2006), to produce animals of the following genotypes: $FIH^{+/+}$ $ASPP2^{+/+}$, $FIH^{+/-}$ $ASPP2^{+/+}$, $FIH^{-/-}$ $ASPP2^{+/+}$, $FIH^{+/+}$ $ASPP2^{+/-}$, and $FIH^{-/-}$ $ASPP2^{+/-}$.

For syngeneic tumour studies, mice with the FIH knockout allele were backcrossed in a C57BL/6 background for 8 generations before the administration of tumour cells of C57BL/6 origin. Mice harbouring the FIH floxed alleles ($FIH^{fl/fl}$) were crossed with Lysozyme 2 (LysM)-Cre animals on a C57BL/6 background (obtained from Dr. Eileen McNeil, University of Oxford) to generate myeloid-specific FIH knockout mice (FIH MKO). The LysM driver leads to the excision of the FIH floxed alleles in macrophages and neutrophils (Clausen et al. 1999). Mice that did not have the LysM-cre transgene or a floxed FIH gene were referred to as 'wild-type (WT)' mice, whereas $FIH^{fl/fl}$ LysM-cre-positive mice were referred to as FIH MKO mice.

2.1.3 Primers

Table 2.1 List of primers used to genotype mouse colonies

Target gene	Primers (5'-3')	Expected bands
FIH	LOX1: GACTGCTGCCAAACCCCTTC SDL2: GGTTTCACACTGGTGAGACCCTG 3'NEO_2: CCAAACAGAACCGCACAATG	WT: 225 bp Floxed: 259 bp Knockout: 430 bp
ASPP2	F4: CGGTTTGGAAGTCAAAGGAA B3: TCAATGTGTCCAGCACCCTA PGK2: TACCCGCTTCCATTGCTCAG	WT: 597 bp Knockout: 800 bp
LysM-cre	oIMR3066: CCCAGAAATGCCAGATTACG oIMR3067: CTTGGGCTGCCAGAATTTCTC oIMR3068: TTACAGTCGGCCAGGCTGAC	WT: 350 bp LysM-cre: 700 bp

Table 2.2 List of primers for qPCR

Target gene		Designed primers (5'-3')
Actg	F	CCAACAGCAGACTTCCAGGATT
	R	CTGGCAAGAAGGAGTGGTAACTG
Chil3	F	AAGCTCTCCAGAAGCAATCCTG
	R	TAGGAAGATCCCAGCTGTACG
Cxcl1	F	TCTCCGTTACTTGGGGACAC
	R	CCAGAGCTTGAAGGTGTTGC
Mrc1	F	CTGCAGATGGGTGGGTTATT

Target gene		Designed primers (5'-3')
Mrc1	R	GGCATTGATGCTGCTGTTATG
Nos2	F	TGGTGAAGGGACTGAGCTGT
	R	CTGAGAACAGCACAAGGGGT
Retnla	F	CAGCTGATGGTCCCAGTGAAT
	R	AGTGGAGGGATAGTTAGCTGG
Sell	F	AATGGAACGATGACGCCTGT
	R	CTGGACCACTGTGTAGCAGA
Tnfa	F	GGCAGGTCTACTTTGGAGTCATTGC
	R	ACATTCGAGGCTCCAGTGAATTCGG

Target gene	Primers purchased from Qiagen
Adm	QT00249676
Arg1	QT00134288
Ccl2	QT00167832
Cd274	QT00148617
Cxcl2	QT00113253
Egln3	QT00135436
Glut1	QT01044953
Hif-1a	QT01039542
Hif-2a	QT00106197
Hif1an	QT00133035
Il-10	QT00106169
Il-12b	QT00153643
Il-6	QT00098875
Tnfa	QT00104006
Vegf	QT00160769

2.1.4 Antibodies

Table 2.3 List of antibodies used for IHC/ICC/WB

Primary antibodies

Antigen	Clone	Host	Dilution	Source	Application
Arginase	-	Rabbit	1 in 2000	abcam (ab91279)	WB
B220	RA3-6B2	Rat	1 in 300	BD 550286	IHC
CD11b	EPR1344	Rabbit	1 in 2000	abcam (ab133357)	IHC
CD3	-	Rabbit	1 in 300	abcam (ab5690)	IHC
CD8	-	Rabbit	1 in 200	Bioss (bs-0648R)	IHC
F4/80	CI: A3-1	Rat	1 in 500	Bio-Rad MCA487G	IHC/ICC
FIH	3F9	Mouse	1 in 25	Moravian Biotech	WB
Foxp3	FJK-16s	Rat	1 in 50	Thermo Fisher (11-5773-82)	IHC

Antigen	Clone	Host	Dilution	Source	Application
HIF-1α	-	Rabbit	1 in 200	Novus Biologicals (NB100-449)	IHC
HIF-2α	-	Rabbit	1 in 3000	Ratcliffe Lab	IHC
NOS2	-	Rabbit	1 in 2000	Millipore (06-573)	WB
p65	-	Rabbit	1 in 1000	Millipore (06-418)	WB
p-p65 (Ser536)	-	Rabbit	1 in 1000	CST (#3031)	WB
p-STAT3 (Ser727)	-	Rabbit	1 in 1000	CST (#9134)	WB
STAT3	124H6	Mouse	1 in 1000	CST (#9139)	WB
β-actin	C4	Mouse	1 in 2000	Santa Cruz (sc-47778)	WB
β-tubulin	-	Rabbit	1 in 4000	abcam (ab6046)	WB

Secondary antibodies

Name	Host	Dilution	Source	Application
Alexa Fluor 488 anti-rat IgG (H+L)	Goat	1 in 400	Thermo Fisher (A-11006)	ICC
Anti-mouse immunoglobulins/HRP	Rabbit	1 in 2000	Dako (P0161)	WB
Anti-rabbit immunoglobulins/HRP	Swine	1 in 2000	Dako (P0399)	WB
Biotinylated anti-rabbit	Goat	1 in 250	Vector Labs (BA-1000)	IHC
Biotinylated anti-rat	Goat	1 in 250	Vector Labs (BA-9400)	IHC

IHC: immunohistochemistry; ICC: immunocytochemistry; WB: Western blotting; p-p65: phosphorylated p65; p-STAT3: phosphorylated STAT3; CST: Cell Signaling Technology; HRP: horseradish peroxidase.

Table 2.4 List of antibodies used for flow cytometry

Antigen	Clone	Fluorochrome	Usage/ test (µl)	Source
Arginase 1	-	FITC	1.0	R&D Systems (IC5868F)
B220	RA3-6B2	PB	0.5	BioLegend (103230)
B220	RA3-6B2	PE/Cy7	0.25	BioLegend (103221)
C5AR	20/70	APC	0.5	BioLegend (135807)
CC5R	HM-CCR5	PE	0.5	BioLegend (107005)
CD11b	M1/70	FITC	0.25	Thermo Fisher (11-0112-82)
CD11b	M1/70	PerCP/Cy5.5	0.25	BD (561114)
CD11c	HL3	PE/Cy7	0.25	BD (561022)
CD25	PC61	PB	0.5	BioLegend (102021)

Antigen	Clone	Fluorochrome	Usage/ test (µl)	Source
CD4	GK1.5	BV421	0.25	BioLegend (100437)
CD4	RM4-4	FITC	0.5	Thermo Fisher (11-0043-82)
CD44	IM7	PE/Cy7	0.25	BioLegend (103029)
CD62L	MEL-14	PerCP/Cy5.5	0.25	BioLegend (104431)
CD86	GL-1	APC	0.25	BioLegend (105011)
CD8a	53-6.7	BV510	0.5	BioLegend (100751)
CD8a	53-6.7	APC	0.5	Thermo Fisher (17-0081-81)
F4/80	BM8	Pacific Blue	0.25	BioLegend (123123)
F4/80	BM8	PerCP/Cy5.5	0.25	BioLegend (123127)
Foxp3	150D	PE	0.25	BioLegend (320007)
IFNγ	XMG1.2	APC	2.0	BioLegend (505810)
IFNγ	XMG1.2	FITC	2.5	BioLegend (505806)
IL-10	JES-16E3	PE	1.0	BioLegend (505008)
IL-2	JES6-5H4	APC	2.5	BioLegend (503809)
IL-4	11B11	PE/Cy7	2.0	BioLegend (504117)
IL-4R	I015F8	PE/Cy7	0.5	BioLegend (144805)
Ly-6C	HK1.4	APC	0.25	BioLegend (128015)
Ly-6G	1A8	PE	0.25	BD (561104)
MHC class II	M5/114.15.2	PE	0.25	Thermo Fisher (12-5321-81)
NK1.1	PK136	FITC	0.25	Thermo Fisher (11-5941-81)
PD-L1 (CD274)	MIH5	PE/Cy7	0.25	Thermo Fisher (25-5982-80)
PD-L2 (CD273)	122	FITC	0.25	Thermo Fisher (11-9972-81)

FITC: Fluorescein Isothiocyanate; PE: Phycoerythrin; APC: Allophycocyanin; PerCP/Cy5.5: Peridinin-chlorophyll protein/Cyanine5.5; PE/Cy7: Phycoerythrin/Cyanine7; BV421: Brilliant Violet 421; BV510: Brilliant Violet 510; BD: BD Biosciences.

2.1.5 Cell lines

Table 2.5 List of cell lines

Cell line	Host	Source
L929	Mus musculus, fibroblast	Prof. N Hoggs, The Francis Crick Institute, UK
B16F10	Mus musculus, melanoma	ATCC
LLC	Mus musculus, lung carcinoma	Dr. C Beisswenger, Universitätsklinikum des Saarlandes, Germany

LLC: Lewis Lung Carcinoma; GFP: Green Fluorescent Protein.

2.2 Methods

2.2.1 Mouse studies

2.2.1.1 Colony maintenance

All animal breeding, maintenance, and procedures were approved by the University of Oxford's ethical review committee and licensed by the UK Home Office (PPL 30/3451; PIL IE0450E9C). Mice were kept in individually-ventilated cages (IVCs) at the Functional Genomics Facility, University of Oxford.

2.2.1.2 Mouse genotyping and agarose gel electrophoresis

Ear biopsies were obtained with an ear punch for identification and genotyping. Ear tissues were incubated in 100 µl of GNT buffer containing 7.8 mg/ml Proteinase K (QIAGEN) at 55℃ overnight. Digestion was terminated by boiling the samples at 95℃ for 15 min and 0.5 µl of the resulting solution was used for polymerase chain reaction (PCR) analysis. PCR programmes used for the indicated genes are listed in Table 2.6.

Table 2.6 PCR protocols for genotyping

Target gene	Reaction component (µl)		PCR programme		
FIH	Template	0.5	Step 1	94℃ 5 min	Steps 2-4 were repeated for 35 cycles.
	LOX1	0.1	Step 2	95℃ 1 min	
	SDL2	0.1	Step 3	56℃ 30 s	
	3'NEO_2	0.1	Step 4	72℃ 1 min	
	Water	9.2	Step 5	72℃ 3 min	
	Master Mix	10.0	Step 6	4℃	
ASPP2	Template	0.5	Step 1	94℃ 3 min	Steps 2-4 were repeated for 29 cycles.
	F4	0.1	Step 2	94℃ 40 s	
	B3	0.1	Step 3	60℃ 40 s	
	PGK2	0.1	Step 4	72℃ 40 s	
	Water	9.2	Step 5	72℃ 3 min	
	Master Mix	10.0	Step 6	4℃	
LysM-cre	Template	0.5	Step 1	95℃ 10 min	Steps 2-4 were repeated for 29 cycles with temperature decreasing 0.5℃ every cycle.
	oIMR3066	0.2	Step 2	94℃ 30 s	
	oIMR3067	0.2	Step 3	62℃ 30 s	
	oIMR3068	0.1	Step 4	72℃ 1 min	
	Water	9.0	Step 5	72℃ 10 min	
	Master Mix	10.0	Step 6	4℃	

Double-distilled water was used. Master Mix (GoTaq Green) was purchased from Promega. All PCR primers were prepared at a concentration of 1 µM.

Agarose gels were prepared at concentrations of 1.0–1.5% depending on the size of the DNA fragments that needed to be resolved. An appropriate amount of agarose powder was measured and mixed with 1× TAE solution in a microwavable flask. The solution was then heated in a microwave oven until the agarose was completely dissolved. EtBr was added at a final concentration of 20 µg/ml to the dissolved gel solution before it was poured into a gel tray with the well comb in place. Newly-poured gel was placed in a fume hood for 20 min at RT for complete solidification. A 1 kilobase ladder (New England Biolabs) was loaded into the first

lane of the gel and 10 µl of each PCR product was loaded into the following wells. DNA samples were electrophoresed in 1× TAE buffer at 80 V for approximately 30 min. DNA samples were visualised using a BioDoc-It benchtop trans-illuminator (UVP).

2.2.1.3 Spontaneous tumour analysis

Mice that showed signs of illness or visible tumours were culled and subjected to necropsy. Heart, lung, thymus, liver, pancreas, stomach, intestine, and lymph nodes were collected and tissue histopathology was analysed in collaboration with pathologists Prof. Robert Goldin (Imperial College London) and Dr. Elizabeth Soilleux (University of Cambridge).

2.2.1.4 Syngeneic tumour model

Tumour cell suspension was prepared in a tissue culture hood. Tumour cells were maintained in T-75 flasks to 50% confluence on the day of harvest. Cells were detached after trypsinisation and passed through a 70 µm cell strainer twice. Cells were washed with PBS twice before counting with trypan blue discrimination. Only cell samples free of clumps and with high viability (above 90%) were qualified for injection.

Only 8–12-week-old mice with matched sex and age were selected as experimental animals. For subcutaneous injection, mice were shaved on the back and flanks and received 1×10^5 B16F10 (referred to as B16 hereafter) or 4×10^5 LLC cells suspended in 100 µl of PBS. The cell suspension was sufficiently mixed before withdrawing for each injection. The length and width of the tumour mass was measured with a caliper during the course of tumour growth. Tumour volume (V) was calculated using the formula $V=(\text{Length} \times \text{Width}^2) \div 2$ (J. Wang et al. 2017).

Animals were monitored until the endpoint (described in Protocol 19, 30/3451) was met, when mice were sacrificed by cervical dislocation. Tumours were removed with a scalpel, weighed, and divided into portions for protein/RNA, histology, and flow cytometry analysis. Samples were preserved in liquid nitrogen, 10% neutral buffered formalin, and PBS, respectively.

2.2.2 Histology techniques

2.2.2.1 Preparing for formalin-fixed paraffin-embedded (FFPE) tissues

Tissues were collected and fixed in 10% neutral buffered formalin solution at 4℃ for 24 hr. Fixed tissues were processed in an Excelsior AS tissue processor (Thermo Fisher) using the routine overnight programme. Processed tissues were embedded into paraffin blocks and sectioned at 4 μm-thick by Ms Indrika Ratnayaka.

2.2.2.2 Haematoxylin and Eosin (H&E) staining

FFPE tissue sections were deparaffinised in two changes of histoclear (National diagnostics), and rehydrated in a gradient of ethanol solution (100, 90, and 70%). Slides were sequentially incubated in Harris haematoxylin for 3 min, acid alcohol (1% v/v) for 2 s, Scott's water for 30 s, and eosin for 3 min, with washes in tap water between each step. Sections were then dehydrated in a gradient of ethanol (70, 90, 100%) and two changes of histoclear before being mounted with mounting medium (Vectamount, Vector Labs).

2.2.2.3 Immunohistochemistry (IHC) staining on FFPE sections

FFPE tissue sections were deparaffinised and hydrated by serial incubation with histoclear, 100% ethanol, 90% ethanol, and 70% ethanol. Sections were

incubated in 3% (v/v) H_2O_2 in methanol for 10 min at RT to inactivate endogenous peroxidase. Antigenic epitopes were retrieved by incubating the slides in boiling sodium citrate buffer (pH 6.0) for 10 min. Slides were left in the buffer to cool for 20 min at RT. Samples were blocked with 10% (v/v) normal goat serum (NGS)/PBS for 2 hr at RT. Sections were then incubated with primary antibodies diluted in 5% (v/v) NGS/PBS overnight at 4℃ in a humidified chamber, followed by incubation with biotinylated secondary antibodies diluted in 5% (v/v) NGS/PBS for 1 hr at RT. Slides were washed with PBS for 15 min after each incubation with antibodies. Sections were then incubated in Avidin-Biotin Complexes (ABC Reagent, Vector Labs) for 20 min at RT, washed in PBS, and applied with HRP substrate solution (DAB substrate kit, Vector Labs) till a dark brown colour was visualised. Slides were counterstained with haematoxylin, dehydrated by immersion in increasing gradients of ethanol solution, and mounted with mounting medium (Vectamount, Vector Labs).

2.2.3 Flow cytometry

2.2.3.1 Sample preparation

The processing methods for samples from mouse tissues and primary cells are described in this section. Samples were kept cold on ice during processing. All centrifugations were performed at 350×*g* for 5 min at 4°C unless specified.

- **Spleen**

Murine spleen tissue was cut into small pieces before being crushed with the end of a 1 ml syringe against a 70 μm cell strainer (Falcon) placed on a 50 ml Falcon tube. The filtrate was centrifuged and the resulting pellet was resuspended in 5 ml of 1× red blood cell (RBC) lysis buffer (BioLegend). Samples were incubated

on ice for 5 min with occasional shaking. Next, 30 ml of PBS was added to stop the lysis. Cell suspensions were filtered with 70 µm cell strainers to remove any clumps.

- **Lung**

Lung tissue was cut into pieces and incubated with 5 ml of lung digestion buffer for 30 min at 37°C with shaking at 150 rpm. Samples were further dissociated by a gentleMACS Dissociator using the programme m_lung_02. Tissues were then meshed and passed through a 70 µm cell strainer. Single cell suspensions were subjected to incubation with 1 ml of 1× RBC lysis buffer for 2 min on ice. Cell suspensions were further washed with and kept in PBS.

- **Thymus**

Thymus tissue was crushed with the end of a 1 ml syringe against a 70 µm cell strainer placed on top of a 50 ml Falcon tube. Filtrate was collected and washed with PBS.

- **Blood**

Blood withdrawal from the left ventricle was performed shortly after the mouse was sacrificed by cervical dislocation. Equal amounts of blood (~500 µl) and 0.5 M EDTA solution were mixed in a 1.5 ml eppendorf tube to prevent clotting. After centrifugation, blood samples were lysed with 500 µl 1× RBC lysis buffer (BioLegend) for 5 min with occasional shaking. This step was repeated until desirable red blood cell lysis was achieved. Samples were resuspended in PBS for further analysis.

- **Bone marrow**

Mice were sacrificed, and tibias and femurs of both legs were dissected and kept in ice-cold PBS. In a tissue culture hood, muscles and epiphyses of both ends

of the bones were removed with a scalpel. Bone marrow was flushed out with ice-cold PBS using a 10 ml syringe loaded with a 25G needle. Cell clumps were disrupted by pipetting the suspension up and down gently with a P1000 pipetman. Any remaining clumps were removed by passing the cell suspension through a 70 µm cell strainer. Bone marrow cells were incubated with 2 ml of 1× RBC lysis buffer for 1 min and washed with 20 ml of PBS.

- **Bone marrow-derived macrophages (BMDMs)**

BMDMs were cultured in non-tissue culture-treated plates for easier detachment. Cells were washed with PBS and incubated with 10 mM EDTA/PBS for 5 min at RT. Cells were lifted by gentle pipetting. Cell suspension was collected and washed with PBS.

- **Tumours**

LLC tumours were collected and cut into small pieces of 2–4 mm. Single cell suspensions for each sample were prepared with the Tumour Dissociation Kit (130-096-730, Miltenyi Biotec) following the manufacturer's instructions. Briefly, tumour samples were dissociated with a GentleMacs instrument (Miltenyi Biotec) using program m_impTumor_02. Disrupted tumour samples were incubated in the tumour digestion buffer (prepared according to the manufacturer's instructions) for 40 min at 37℃, before being ground again with GentleMacs using program m_impTumor_03. Dissociated tumour samples were then passed through a 70 µm cell strainer and washed with PBS. Samples were incubated with 3 ml of 1× RBC lysis buffer (BioLegend) for 2 min on ice with constant shaking.

B16 tumours were disrupted mechanically and passed through a 70 µm cell strainer. Single cell suspensions of B16 tumour samples were incubated with 3 ml of 1× RBC lysis buffer and washed with PBS.

2.2.3.2 Immunostaining

Single cell suspensions were washed and resuspended in FACS buffer. Cells were counted with trypan blue discrimination. 5×10^5 live cells were used for each test. Immunostaining was performed in a 96-well V-bottom plate (Corning). Splenocytes were used for single-colour staining for fluorescence compensation during data analysis.

Cells were washed with FACS buffer twice and blocked with 50 µl of FACS buffer containing 1 µl of anti-CD16/32 antibody (BioLegend) for 10 min at RT. When staining cell surface antigens, samples were incubated with a master mix of fluorophore-conjugated antibodies for 30 min at 4℃. After one wash with FACS buffer, samples were fixed by incubation with fixation buffer (BioLegend) for 20 min at RT. After that, cells were washed with and stored in FACS buffer for future analysis.

When intracellular staining (ICS) was also required, cells that were already stained with required cell surface antigens were fixed as described above, washed twice with 1× Permeabilisation Wash Buffer (BioLegend), and incubated with fluorophore-conjugated antibodies diluted in 1× Permeablisation Wash Buffer for 20 min in the dark at RT. Stained cells were washed and resuspended in FACS buffer for analysis.

To detect nuclear Foxp3, samples that were already stained with required surface antigens were incubated with Fixation Permeabilisation Buffer (Thermo Fisher) for 30 min at RT. Samples were then washed with Permeabilisation Buffer (Thermo Fisher) twice followed by incubation with anti-Foxp3 antibody diluted in Permeabilisation Buffer for 30 min in the dark at RT. Next, cells were washed and resuspended in FACS buffer.

A live cell fixable dye (L10119, Thermo Fisher) was used in all staining reactions to exclude dead cells. All of the centrifugation steps were performed at 350×*g* at 4℃. Samples were analysed using an LSRFortessa X-20 cell analyser (BD Biosciences). FACS data were analysed using FlowJo v10.

7 panels of antibodies were used in this study (Table 2.7).

Table 2.7 Antibody panels used for flow cytometry

Panel 1		
Laser and filter	**Fluorochrome**	**Antigen**
B 710/50	PerCP-5.5	CD11b
B 530/30	FITC	CD4
R 780/60	APC/Cy7	Viability dye
R 670/30	APC	CD8
V 450/40	PB	CD25
YG 586/15	PE	Foxp3
YG 780/60	PE/Cy7	B220
Panel 2		
Laser and filter	**Fluorochrome**	**Antigen**
B 710/50	PerCP-5.5	CD11b
B 530/30	FITC	NK1.1
R 780/60	APC/Cy7	Viability dye
R 670/30	APC	Ly-6C
V 450/40	PB	F4/80
YG 586/15	PE	Ly-6G
YG 780/60	PE/Cy7	CD11c
Panel 3		
Laser and filter	**Fluorochrome**	**Antigen**
B 710/50	PerCP-5.5	CD11b
B 530/30	FITC	IFNγ
R 780/60	APC/Cy7	Viability dye
R 670/30	APC	IL-2
V 450/40	BV421	CD4
V 529/24	BV510	CD8
YG 586/15	PE	IL-10
YG 780/60	PE/Cy7	IL-4
Panel 4		
Laser and filter	**Fluorochrome**	**Antigen**
B 710/50	PerCP-5.5	CD62L
B 530/30	FITC	CD4
R 780/60	APC/Cy7	Viability dye
R 670/30	APC	CD8
V 450/40	PB	B220
YG 586/15	PE	Foxp3
YG 780/60	PE/Cy7	CD44
Panel 5		
Laser and filter	**Fluorochrome**	**Antigen**
B 710/50	PerCP-5.5	F4/80
B 530/30	FITC	ARG1
R 780/60	APC/Cy7	Viability dye

Laser and filter	Fluorochrome	Antigen
R 670/30	APC	IFNγ
V 450/40	BV421	CD4
YG 586/15	PE	IL-10
YG 780/60	PE/Cy7	IL-4
Panel 6		
Laser and filter	**Fluorochrome**	**Antigen**
B 710/50	PerCP-5.5	CD11b
B 530/30	FITC	PD-L2
R 780/60	APC/Cy7	Viability dye
R 670/30	APC	CD86
V 450/40	BV421	F4/80
YG 586/15	PE	MHC class II
YG 780/60	PE/Cy7	PD-L1
Panel 7		
Laser and filter	**Fluorochrome**	**Antigen**
B 710/50	PerCP-5.5	CD11b
B 530/30	FITC	ARG1
R 780/60	APC/Cy7	Viability dye
R 670/30	APC	Ly-6C
V 450/40	PB	F4/80
YG 586/15	PE	Ly-6G
YG 780/60	PE/Cy7	CD11c

B: blue; R: red; V: violet; YG: yellow green; PB: pacific blue.

2.2.3.3 FACS sorting

To prepare for cell sorting, samples were stained as required and resuspended in the sorting buffer (2% (v/v) FBS/PBS) to reach a final concentration of about 2×10^7 cells/ml. Unstained and single colour-stained samples were also prepared. Cell sorting services were provided by Mr Andrew Worth (Jenner Institute, University of Oxford) using a Beckman Coulter Legacy MoFlo MLS High Speed Cell Sorter.

2.2.3.4 MACS

Primary mouse tumours were enriched for macrophages with an Anti-F4/80 MicroBeads UltraPure kit (130-110-443, Miltenyi Biotec) according to the manufacturer's protocol. Briefly, 5×10^6 tumour cells were resuspended in 50 µl of MACS buffer containing 5 µl of Anti-F4/80 MicroBeads UltraPure for 15 min in the dark at 4℃. Cells were then subjected to magnetic separation with MACS LS columns. Unlabelled cells were removed by washing the columns with MACS buffer. The magnetically-retained $F4/80^+$ cells were eluted after removing the column from the magnetic field. Eluted samples were then stained with anti-F4/80 antibody and checked for enrichment efficiency with flow cytometry.

2.2.4 Tissue culture

2.2.4.1 Maintenance of cell lines

All cell lines were cultured in complete DMEM (cDMEM), which is DMEM supplemented with penicillin/streptomycin (100 U/ml), $_L$-glutamine (2 mM), and 10% (v/v) FBS in flasks (Falcon). Cell cultures were maintained in a Heraeus incubator at 37℃ with 5% CO_2.

Once reaching confluence, cells were washed with PBS and incubated with 0.05% Trypsin-EDTA for 3 min at 37℃. Trypsinisation was terminated by adding an appropriate volume of cDMEM. Cells were detached from the flasks and seeded in fresh flasks at the desired density.

2.2.4.2 Freezing/thawing of cells

Freezing medium was prepared by adding 1 volume of dimethyl sulfoxide (DMSO) to 9 volumes of FBS. Cells that detached from the flasks after

trypsinisation were centrifuged and the resulting cell pellet was resuspended in an appropriate volume of freezing medium. The cell suspension was then aliquoted in cryogenic vials (Corning) and kept in a Nalgen Cryo 1℃ freezing jar in a -80℃ freezer (New Brunswick Scientific) overnight before being transferred to the liquid nitrogen tank.

To thaw cells, one cryogenic vial was removed from liquid nitrogen storage and immediately placed in a 37℃ water bath. The vial was gently swirled until there was just a small piece of ice left. The cell suspension was then transferred to 40 ml pre-warmed DMEM. The freezing medium-containing supernatant was discarded after centrifugation and the cell pellet was resuspended in cDMEM for culture.

2.2.4.3 Preparation of L929-conditioned medium (LCM)

1×10^6 L929 cells were plated in a T175 flask and cultured until confluent. Cell culture medium was replaced with fresh cDMEM and cells were left growing for another 7 days. Cell medium was then collected, filtered through a 0.45 μm filter, aliquoted, and stored at -20℃.

2.2.4.4 Preparation of bone marrow-derived macrophages (BMDMs)

Bone marrow cells were prepared as described in section 2.2.3.1. Cells were counted using a haemocytometer after trypan blue staining. 4×10^6 cells were placed in a 10 cm petri dish containing 10 ml of macrophage growth medium, which was 15% (v/v) LCM in cDMEM. Cells were kept in a humidified incubator with 5% CO_2 at 37℃. Another 5 ml of macrophage growth medium was added after 3 days of culture.

BMDMs were fully differentiated after 7 days of culture. To harvest the cells, culture medium was removed and cells were incubated with 5 ml of 10 mM EDTA in PBS for 5 min at RT. Next, 10 ml of PBS was added and cells were detached by pipetting. Cells were counted and re-plated at an appropriate density in cDMEM without LCM and incubated overnight before experiments were performed.

2.2.4.5 Tumour cell-conditioned media (TCM)

B16 and LLC cells were maintained in cDMEM in T175 flasks. Once they reached confluence, cell culture media were replaced with fresh cDMEM and cells were allowed to grow for another 7 days. Culture media were then collected, filtered through a 0.45 μm filter, aliquoted, and stored at -20℃.

2.2.5 Cell-based assays

2.2.5.1 Lentiviral transduction of B16 cells

Venus-expressing lentivirus was kindly provided by Dr. Rasmas Freter.

B16 cells were seeded in a 6-well plate and allowed to grow until 30% confluence for transduction. A frozen vial of lentivirus was thawed at RT and resuspended in 1 ml of calcium-containing Hank's Balanced Salt Solution (HBSS). B16 culture medium was aspirated and replaced with 500 μl lentivirus-containing HBSS. The tissue culture plate was centrifuged at 600×*g* for 1 hr at RT before being kept in an incubator for 4 hr. HBSS was then removed and 2 ml of cDMEM was added. Venus fluorescence was detectable 24 hr post-transduction. Cells were expanded with two passages and those with high expression levels of venus were sorted by FACS.

2.2.5.2 Immunocytochemistry (ICC)

ICC staining was performed at RT. BMDMs that were cultured on coverslips or optical 96-well reaction plates (Thermo Fisher) were fixed in 4% PFA. After three washes with PBS, cells were permeabilised through the incubation in 0.25% Triton X-100/PBS solution for 5 min. Samples were rinsed with PBS and incubated in blocking buffer (5% BSA/PBS) for 30 min, after which samples were incubated with primary antibody diluted in blocking buffer for 1 hr. Cells were washed with PBS, and incubated with secondary antibody and DAPI diluted in blocking buffer for 45 min. Finally, cells were rinsed with PBS and mounted with Fluoromount-G (SouthernBiotech).

2.2.5.3 *In vitro* stimulation

BMDMs were harvested, counted, and re-plated in 24-well plates with 5×10^5 cells per well in cDMEM without LCM. Cells were left quiescent overnight and stimulated the next day. BMDMs were polarised to M1 macrophages by stimulation with 5 ng/ml LPS plus 1 ng/ml IFNγ (PeproTech) for 24 hours, and to M2 macrophages by stimulation with 10 ng/ml IL-4 (PeproTech) for 24 hours. For cells stimulated with B16- or LLC- derived TCM, 1 volume of TCM was mixed with 1 volume of cDMEM before application on to cells.

2.2.5.4 RNA extraction, reverse transcription, and real time-quantitative PCR (RT-qPCR)

RNA was extracted from cells using an RNeasy Mini Kit (QIAGEN) following the manufacturer's instructions. First, 200 ng of total RNA was used to prepare cDNA with the SuperScript III First-Strand Synthesis System (Thermo Fisher), according to the manufacturer's protocol.

Next, 1 unit volume of cDNA sample obtained from reverse transcription was diluted by 4 unit volumes of RNase-free water. Each qPCR reaction was performed in duplicate using 2 µl of cDNA template, 2 µl of RNase-free water, 1 µl of primer mix at a final concentration of 100 nM, and 5 µl of SYBR green (QIAGEN). Quantitative PCR was performed using the gene-specific primers listed in Table 2.2. StepOnePlus Real-Time PCR System was used to conduct the following thermal cycles: 95℃ (10 min); 40 cycles of 94℃ (15 s), -55 ℃ (30 s), and -72 ℃ (1 min); followed by the melting curve run. Data were collected at the elongation phase of each cycle. All the primers used were tested for amplification efficiency. The expression level of each target gene was presented as relative expression normalised by γ-actin.

2.2.5.5 Chemotaxis assay

Chemotaxis assay of BMDMs was performed according to a previously published protocol (Iqbal et al. 2013). Chemokine was added to pre-warmed chemotaxis buffer to the desired concentration. Next, 160 µl of chemokine- or vehicle-containing chemotaxis buffer was added to each well of the bottom chamber of a 16-well xCELLigence CIM-plate (ACEA Biosciences). After assembling the top plate with the bottom chamber, 50 µl of chemotaxis buffer was added to each well of the top plate. The assembled plate was placed in an incubator at 37℃ for 30 min for pre-equilibrium. Meanwhile, BMDMs were harvested, counted, and resuspended in chemotaxis buffer to a final concentration of 2×10^5 cells/ml. Next, 50 µl of cell suspension was added to each well in the top chamber of the CIM-plate. The loaded CIM-plate was then placed in the

xCELLigence RTCA-DP machine (ACEA Biosciences) and data were collected every 5 s for up to 6 hr using the RTCA software (ACEA Biosciences).

2.2.5.6 Phagocytosis assay

First, 1×10^5 BMDMs were plated in a 96-well optical plate with black walls (Thermo Fisher) one day before the experiment. The next day, one vial of pHrodo™ Green Zymosan Bioparticles (Thermo Fisher) was thawed in 4 ml of Live Cell Imaging Solution (Thermo Fisher), and sonicated for 5 min on ice. The culture medium of the BMDMs was removed and replaced with 100 µl of bioparticle suspension. BMDMs in the control wells were incubated with bioparticle-free Live Cell Imaging Solution. The plate was transferred to an incubator at 37℃. At each time point, cells were washed with PBS twice to remove extracellular bioparticles before fluorescence intensity was read using a Clariostar Microplate Reader (BMG LABTECH). Phagocytic activity was indicated by relative fluorescence activity, which was calculated by subtracting the fluorescence intensity of the particle-free control well from value of the corresponding experimental well.

2.2.5.7 Infection of BMDMs with Bacillus Calmette-Guérin (BCG)

Mycobacterium bovis BCG was kindly cultured by Dr. Paulo Bettencourt (Jenner Institute, University of Oxford). On the day of infection, the bacterial culture showed an OD_{600} (optical density value at 600 nm) within the range of 0.6–1.0. 10 ml of bacterial culture was transferred to a 15 ml Falcon tube for brief centrifugation (~1200 rpm, 30 s). Culture supernatant was transferred to a fresh tube and sonicated in an ultrasonic bath for 5 min. The OD_{600} of the sonicated bacterial culture was measured, and the number of bacteria was calculated using the following conversion: an OD value of $1=3\times10^8$ colony forming units (cfu)/ml

(established by Dr. Bettencourt experimentally). The desired volume of bacterial culture was washed with and resuspended in antibiotic-free cDMEM of an appropriate volume.

BMDMs were seeded in 24-well plates the day before infection. Before infection, BMDMs were washed twice with antibiotic-free cDMEM. Next, 500 µl of bacteria-containing medium was added to each well of BMDMs. Tissue culture plates were swirled gently before being placed into an incubator. After 4 hr of incubation, BMDMs were washed with PBS to remove extracellular bacteria, and 1 ml of antibiotic-containing cDMEM was added to each well for prolonged incubation until samples were harvested at the indicated time points.

2.2.5.8 Protein analysis

- **Sample preparation**

Adherent cells were washed with PBS and 200 µl urea buffer was applied per well of a 24-well plate. Cells were scraped off the plates using sterile cell scrapers (Greiner) and lysates were transferred to 1.5 ml eppendorf tubes. Cells underwent lysis in the eppendorf tubes on ice for 20 min with occasional agitation. Lysates were centrifuged at 15,000×*g* for 15 min at 4℃ and supernatants were collected into fresh tubes.

To extract protein samples from frozen mouse tissues, a piece of tissue was transferred to a pre-chilled mortar placed on dry ice. An appropriate volume of liquid nitrogen was added into the mortar and the tissue sample was quickly ground by a pestle once the liquid nitrogen had nearly evaporated. The ground sample was then collected into a 1.5 ml eppendorf tube, and 200 µl urea buffer was added into the tube followed by agitation on a vortex mixer (Stuart) for 5 s. Samples were centrifuged at 15,000×*g* for 15 min at 4℃, and supernatants were collected**.**

- **Protein concentration determination**

Protein concentration was determined using the Bio-Rad Bradford protein assay (Bio-Rad). 1 µl of cell lysate was mixed with 200 µl of 1× Bio-Rad protein assay dye reagent in a well of a 96-well plate. BSA was used to establish the standard curve. The absorbance at 595 nm was measured with a spectrophotometer (Anthos Labtech).

- **Preparation of protein samples for electrophoresis**

Cell lysate of known volume was mixed with an appropriate volume of 6× Laemmli buffer. Samples were boiled for 10 min at 95℃ and were then ready for gel electrophoresis.

- **Preparation of SDS-PAGE gels**

SDS-PAGE gels were prepared with a Mini-PROTEAN® Tetra Cell system (Bio-Rad). Resolving gel solution containing 8% acrylamide was poured in the assembled plates, overlaid with isopropanol, and left for polymerisation for 45 min at RT. Once polymerised, isopropanol was replaced with stacking gel solution and a 15-well comb was inserted immediately. Gels were allowed to polymerise for 20 min at RT.

For experiments involving a large number of samples, pre-cast 26-well Midi Protein Gels (Thermo Fisher) were used.

- **SDS-PAGE**

Prepared samples of equal amounts of protein and a pre-stained protein marker (New England Biolabs) were loaded into SDS-PAGE gels. When using home-made gels, the gel tank (Bio-Rad) was filled with 1× SDS-PAGE running buffer to the indicated level. Protein samples underwent electrophoresis for 20 min at a constant voltage of 80 V followed by 90 min at a constant voltage of 120 V. When using pre-

cast gels, 2-(N-morpholino) ethanesulfonic acid (MES) buffer (Thermo Fisher) was loaded in the gel running tank. Protein samples underwent electrophoresis for 40 min at a constant voltage of 180 V.

- **Western blotting**

Protein samples separated by SDS-PAGE were transferred onto a nitrocellulose membrane (Whatman) using a wet transfer system (Hoefer) loaded with 1× transfer buffer. The transfer was performed at a constant voltage of 80 V at 4℃ for 3 hr. The nitrocellulose membrane was briefly stained with Ponceau S solution to check for transfer efficacy. The membrane was then blocked with 5% (w/v) milk (Marvel) in 1× TBST solution for 1 hr at RT before being incubated with primary antibody diluted in 5% (w/v) milk or 5% (w/v) BSA overnight at 4℃. The membrane was washed with 1× TBST for 20 min and incubated with HRP-conjugated secondary antibody at RT for 1 hr. Next, the membrane was washed with 1× TBST for 20 min followed by the application of enhanced chemiluminescence (ECL) Western blotting detection reagent (GE Healthcare). The result was visualised with X-ray film (Fujifilm) using a film developer in the dark. If another antibody was required for immunoblotting, the membrane was incubated with stripping buffer for 20 min at 55℃ and blocked again before application of the new primary antibody.

When required, gel bands were quantified using ImageJ following the user's guide (https://imagej.nih.gov/ij/docs/menus/analyze.html#gels).

2.2.6 Data analysis

Statistical analysis was performed in GraphPad. Differences were considered significant at $p<0.05$. The Mantel–Cox test was conducted to determine the

statistical significance of difference in spontaneous tumourigenesis between indicated mouse strains. The χ^2 test was used to compare the tumour incidence of mice of different genotypes. A two-tailed, unpaired *t*-test was used to compare sizes of tumours at each time point, and data analysis of flow cytometry and some RT-qPCR experiments, before which sample data were checked for normal distribution. A two-tailed, paired *t*-test was used to compare *Hif1an* expression level acquired by RT-qPCR before and after the indicated treatment. The statistical test used in each experiment is described within the relevant section of text.

Chapter 3 FIH deficiency promotes spontaneous tumourigenesis *in vivo*

3.1 Introduction

The HIF family of transcription factors are widely expressed in many human cancers, and their expression is frequently correlated with poor patient prognosis (Bertout, Patel, and Simon 2008; Deeb et al. 2011; Frolova et al. 2014). On the other hand, a tumour suppressive role of HIF has also been reported. For example, in RCC cells, HIF-1α positively regulates the expression of the pro-apoptotic gene BNIP3 and retards the growth of RCC xenografts (Raval et al. 2005), whereas HIF-2α suppresses the tumour development in a rat glioma xenograft model (Acker et al. 2005) and a $KRAS^{G12D}$-driven lung cancer model (Mazumdar, Hickey, and Pant 2010). Given the multifaceted roles of HIF in tumour biology, one needs to be cautious when considering pan-HIF inhibition strategies for therapeutic application.

FIH emerges as a promising therapeutic target in this context due to its fine-tuning effect on HIF activity. Unlike PHDs, which switch HIF signalling on and off by controlling the protein degradation of HIF, FIH appears to selectively affect only a subset of HIF target genes (Lisy and Peet 2008). Moreover, the frequent downregulation of FIH by miRs in several types of cancer suggests that FIH may be actively involved in the regulation of tumour development (for review, refer to

section 1.4). To better understand the biological role of FIH in this context, FIH-null mice were created and monitored for spontaneous tumourigenesis.

3.2 Results

3.2.1 FIH is expressed in various tissues

FIH-null mice lacking exons 1 and 2 of the *Hif1an* gene (the gene that encodes FIH) on a mixed B6; 129 (C57BL/6 × 129SvJ) background were generated in Prof. Peter Ratcliffe's lab. To examine the expression of FIH in mice, protein samples from different tissues were obtained from adult WT and FIH knockout (KO) animals and analysed by Western blotting. FIH band for each sample was normalised against the corresponding β-tubulin band using densitometric analysis in ImageJ (lower panel). As shown in Figure 3.1, FIH protein was detected in all samples collected from the WT animal, with higher levels of protein being detected in the spleen and skeletal muscle (lower panel). FIH protein was not detected in the samples from the KO animal (Figure 3.1).

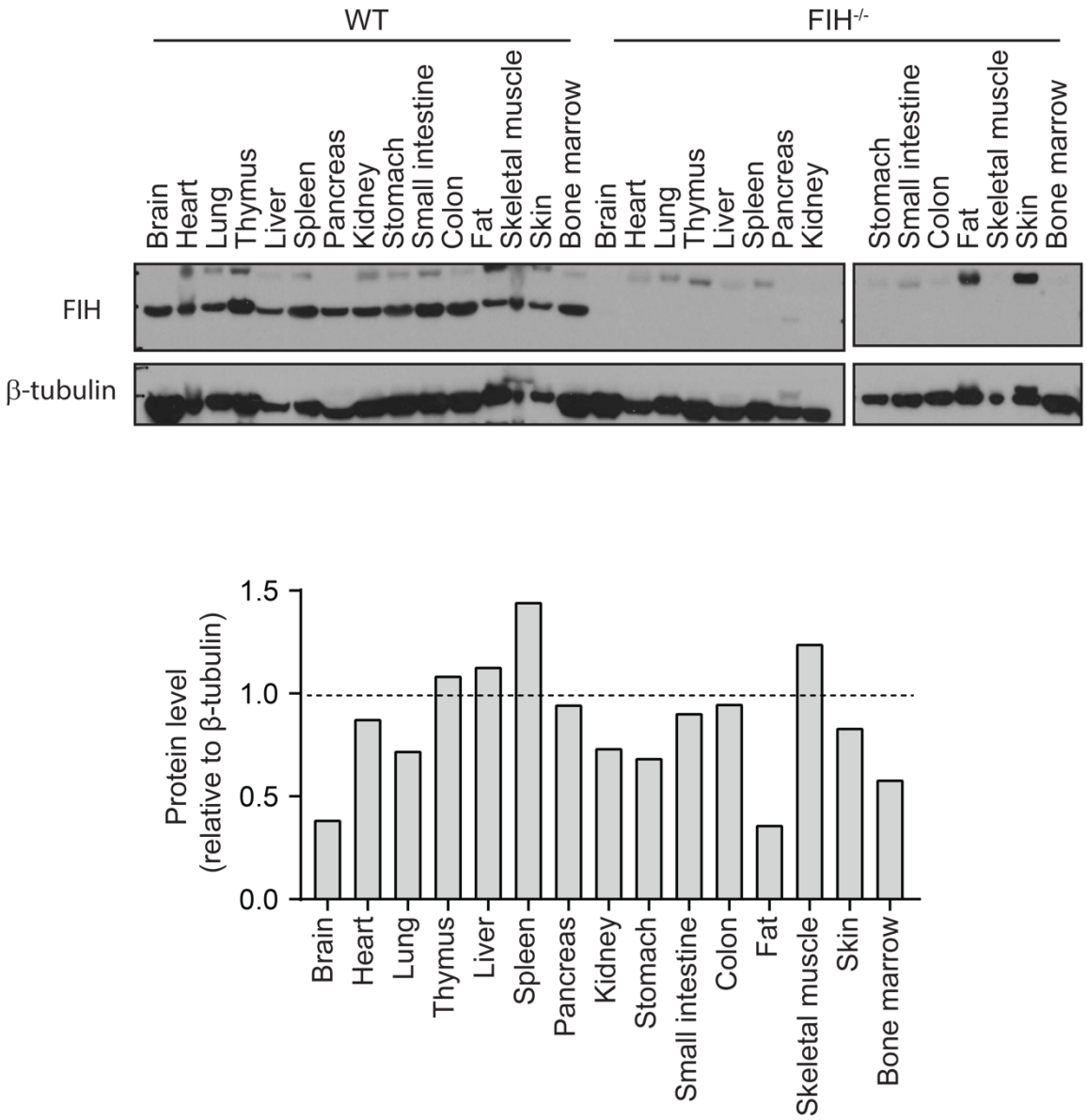

Figure 3.1 FIH is expressed in various murine tissues

The indicated tissues were harvested from WT and FIH$^{-/-}$ mice. Whole-tissue lysates were prepared and blotted with anti-FIH antibody (upper panel). β-tubulin was used as a loading control. Protein bands were quantified using densitometric analysis in ImageJ and the expression levels of FIH relative to β-tubulin are shown in the lower panel.

3.2.2 Mice with reduced FIH expression show enhanced tumour susceptibility

To characterise the phenotype of FIH-deficient mice, a cohort of WT (n=14), $FIH^{+/-}$ (n=21), and $FIH^{-/-}$ (n=22) mice was generated by setting up heterozygous breeders. Mice were monitored closely during a period of 125 weeks. Loss of FIH did not significantly change the life expectancy (Figure 3.2A), but accelerated the onset of spontaneous tumours (WT vs $FIH^{+/-}$ p=0.0351, WT vs $FIH^{-/-}$ p=0.0358; Mantel–Cox test; Figure 3.2B).

Some mice that were culled due to sickness were found not to have tumours (confirmed by pathologists Prof. R. Goldin and Dr. E. Soilleux), which accounted for the discrepancy between the total survival (Figure 3.2A) and tumour-free survival curves (Figure 3.2B). A range of histological observations were made in these mice, including inflammatory lymphocyte infiltration in the kidney (Figure 3.2C), lung (D), and liver (E), where a mixed population of $CD3^+$ T cells, $B220^+$ B cells, and $F4/80^+$ phagocytes could be observed (Figure 3.2 H–J). Liver fibrosis (F) and necrosis (G) were also observed in some animals.

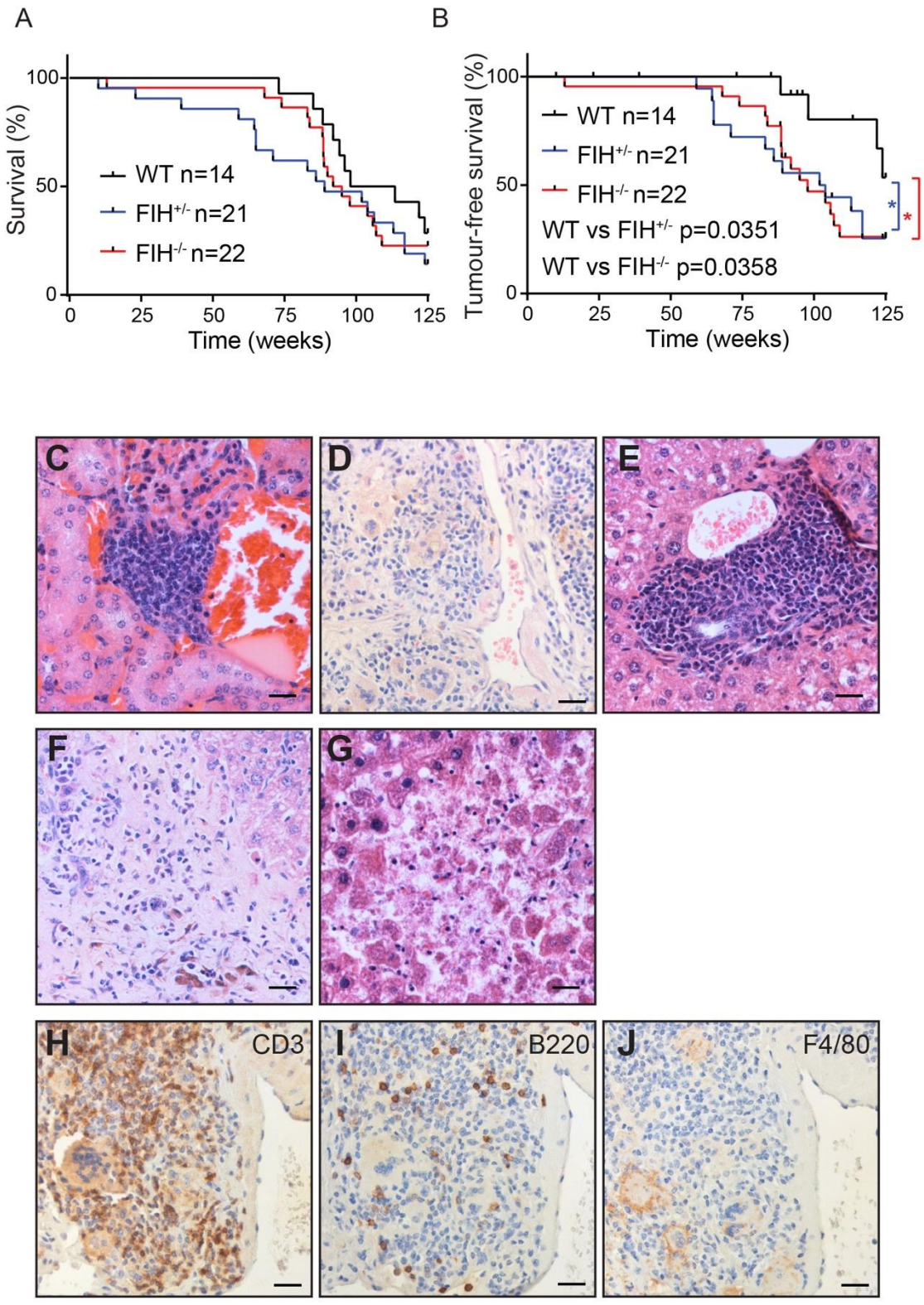

Figure 3.2 Mice with reduced FIH expression show enhanced spontaneous tumourigenesis

Mice were monitored for a total of 125 weeks. (A) Survival curve is shown, where each step of the curve represents an animal that had died or required euthanasia due to ill health. (B) Tumour-free survival curve is shown, in which each step of the curve indicates the death of a tumour-bearing animal over the course of the study. * indicates $p<0.05$ by Mantel–Cox test. Blue asterisk represents the comparison between WT and $FIH^{+/-}$ groups, while red indicates the comparison between WT and $FIH^{-/-}$ groups. (C–G) Some mice that died or that had to be culled showed no tumour formation, but a range of non-neoplastic changes including lymphocyte infiltration in the kidney (C), lung (D), and liver (E), as well as liver fibrosis (F) and necrosis (G). (H–J) IHC staining shows the presence of cells that are positive for CD3 (H), B220 (I), and F4/80 (J). Scale bar, 25 μm.

3.2.3 Mice with reduced FIH expression are more vulnerable to B cell lymphomas

In addition to differing kinetics of oncogenesis, $FIH^{-/-}$ mice showed heightened overall tumour incidence compared with WT mice (WT vs $FIH^{+/-}$ p=0.0532, WT vs $FIH^{-/-}$ p=0.0203; χ^2 test; Figure 3.3A).

Histopathological analysis facilitated by pathologists revealed that most of the malignancies developed across the three groups of animals were lymphomas or leukaemias, which were initially categorised as haematopoietic neoplasms (HNs) (Figure 3.3A). HNs were found in 4 out of 14 WT animals, 13 out of 21 $FIH^{+/-}$ animals, and 14 out of 22 $FIH^{-/-}$ animals (Figure 3.3A). Some mice suffered more than one type of cancer in addition to HNs, which was morphologically diagnosed as follicular dendritic cell sarcoma (FDCS) (in a WT mouse; Figure 3.3C), colon adenocarcinoma (in an $FIH^{+/-}$ mouse, Figure 3.3B), and HCC (in an $FIH^{-/-}$ mouse) by pathologists (Figure 3.3A). Among all the mice examined, one mouse was diagnosed with lung adenocarcinoma without HN (Figure 3.3A).

To determine the origin of the malignant haematopoietic cells, IHC staining was performed to identify B cells, T cells, and cells of myeloid origin (Figure 3.3E). B cell lymphomas were found to be the predominant type of neoplasms in all three groups of mice (Figure 3.3D). $FIH^{-/-}$ mice showed increased incidence of B cell lymphomas compared with WT animals (WT: 28.6%, $FIH^{-/-}$: 63.6%, p=0.0402; χ^2 test; Figure 3.3D). Less frequently, 3 out of 21 (14.3%) $FIH^{+/-}$ mice were found with neoplasms of myeloid origin, and 1 out of 21 (4.76%) $FIH^{+/-}$ mouse developed T cell lymphomas in the thymus, spleen, liver, and lung (Figure 3.3D).

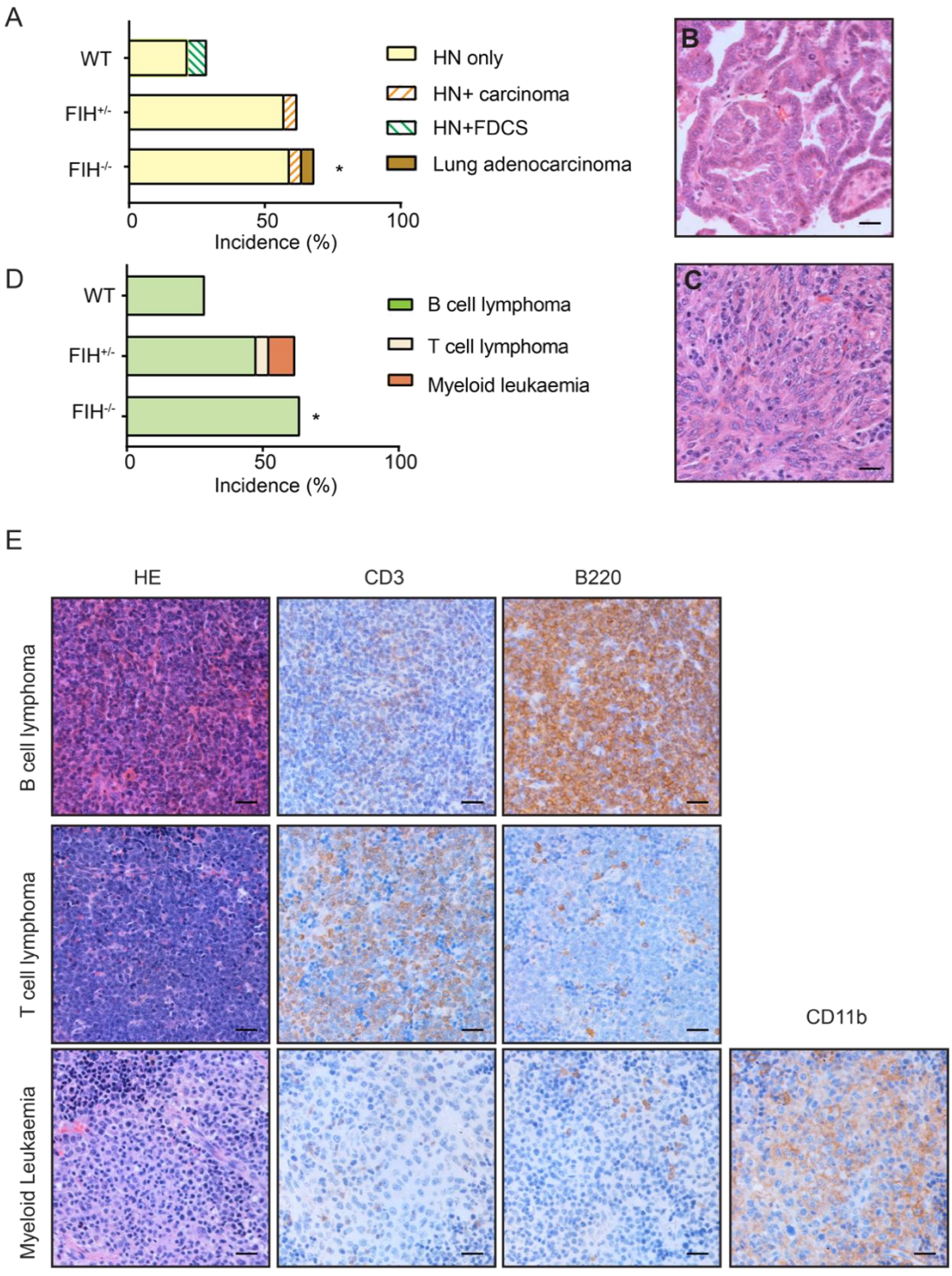

Figure 3.3 Reduced FIH expression promotes the incidence of B cell lymphomas

(A) Tumours were categorised as carcinoma, sarcoma, or HN based on their morphology. The percentage of mice with the indicated types of cancer in each genotype group is shown. 4 out of 14 (28.6%) WT, 13 out of 21 (61.9%) FIH$^{+/-}$, and 14 out of 22 (63.6%)

FIH$^{-/-}$ mice developed HNs. Among the tumour-bearing mice, one WT mouse was found with both HN and FDCS; one FIH$^{+/-}$ mouse had HN and colon adenocarcinoma; one FIH$^{-/-}$ mouse developed HN and HCC; and one FIH$^{-/-}$ mouse had lung carcinoma with no other malignancy. FIH$^{-/-}$ mice showed increased tumour incidence compared with WT mice during the course of the study (p=0.0203, χ^2 test). Examples of a case of colon carcinoma (B) and FDCS in the spleen (C) histologically diagnosed by pathologists are shown. (D) Subtypes of HNs were determined by the IHC staining of markers of B cells, T cells, and myeloid cells with antibodies against B220, CD3, and F4/80/CD11b, respectively. The percentage of mice with the indicated types of HN in each genotype group is shown. FIH$^{-/-}$ mice showed increased incidence of B cell lymphomas than the WT mice (WT: 4 out of 14 (28.6%); FIH$^{-/-}$: 14 out of 22 (63.6%), p=0.0402, χ^2 test). Representative images of tumour samples analysed by H&E and IHC staining are shown in (E). Scale bar, 25 μm.

3.2.4 Mice lacking FIH expression show increased incidence of low-grade B cell lymphomas in the lung

Two prominent features of the B cell lymphoma cases were noticed during the study: malignant B cells were detected in a wide range of tissues, and they were of different grades (Figure 3.4, A and B).

Spatially, B cell lymphomas were frequently observed in lymphoid tissues such as the spleen, lymph nodes, and thymus (Figure 3.4A). Among the lymphoid tissues, the spleen appeared to be the most common site for the colonisation of tumour cells for all three groups of mice studied (Figure 3.4A). Compared with WT mice, FIH-null animals showed significantly increased incidence of splenic B cell lymphomas (Figure 3.4A: WT vs FIH$^{-/-}$ p=0.0266, χ^2 test). Lymph nodes were also frequently invaded by neoplastic cells, yet the incidence was not affected by FIH status (Figure 3.4A). Less frequently, two FIH heterozygous mice were found with

B cell lymphomas in the thymus, one of which had concurrent B cell neoplasm in the pericardial fat (Figure 3.4A).

In WT animals, B cell lymphomas were found in non-lymphoid tissues such as the lung, liver, kidney, and fat at a lower frequency (Figure 3.4A). Tumour cells within these tissues exhibited some consistent histological patterns. For example, pulmonary lymphomas frequently resided around the airway (Figure 3.4C), hepatic lymphomas usually surrounded central veins and portal triads (Figure 3.4D), and renal lymphomas were found in the medullary region and fat surrounding the ureter (Figure 3.4, E and F). Remarkably, loss of FIH significantly increased the incidence of pulmonary B cell lymphomas (WT vs $FIH^{+/-}$ p=0.0157, WT vs $FIH^{-/-}$ p=0.0015; χ^2 test; Figure 3.4A). WT, $FIH^{+/-}$, and $FIH^{-/-}$ animals showed similar tumour incidence in other tissues examined (Figure 3.4A).

B cell lymphomas found in this cohort of mice were of different grades, which were categorised as low-grade, low-grade with high-grade components, and high-grade, as determined by the pathologist based on the morphology (Dr. E. Soilleux). High-grade tumours mostly resembled diffused large B cell lymphomas (DLBCLs) in human patients, featuring large-sized cells with prominent nuclei. Low-grade B cell lymphomas mostly presented as marginal zone lymphomas (frequently observed in the lung and spleen), where small, mildly pleomorphic, malignant cells were observed. Some cases displayed an intermediate grade, with mixed features of both low- and high-grade B cell lymphomas (Figure 3.4G). As shown in Figure 3.4B, compared with the composition of B cell lymphomas in WT mice, B cell malignancies in the $FIH^{-/-}$ mice showed a significantly enlarged fraction of low-grade B cell lymphomas (WT vs $FIH^{-/-}$ p=0.0043; χ^2 test; Figure 3.4B) and a

reduced fraction of high-grade lymphomas (WT vs FIH$^{-/-}$ $p<0.0001$; χ^2 test; Figure 3.4B).

To sum up the data shown so far, both FIH$^{+/-}$ and FIH$^{-/-}$ mice show accelerated onset of spontaneous tumours compared with WT animals. B cell lymphomas are the predominant type of malignancy regardless of the genotype of the animal. While FIH expression does not affect the tumour spectrum, FIH deficiency promotes the incidence of B cell lymphomas, especially in the lung. In addition, B cell lymphomas that are developed in FIH$^{-/-}$ animals show an increased fraction of low-grade tumours and a decreased proportion of high-grade tumours compared with those developed in WT animals.

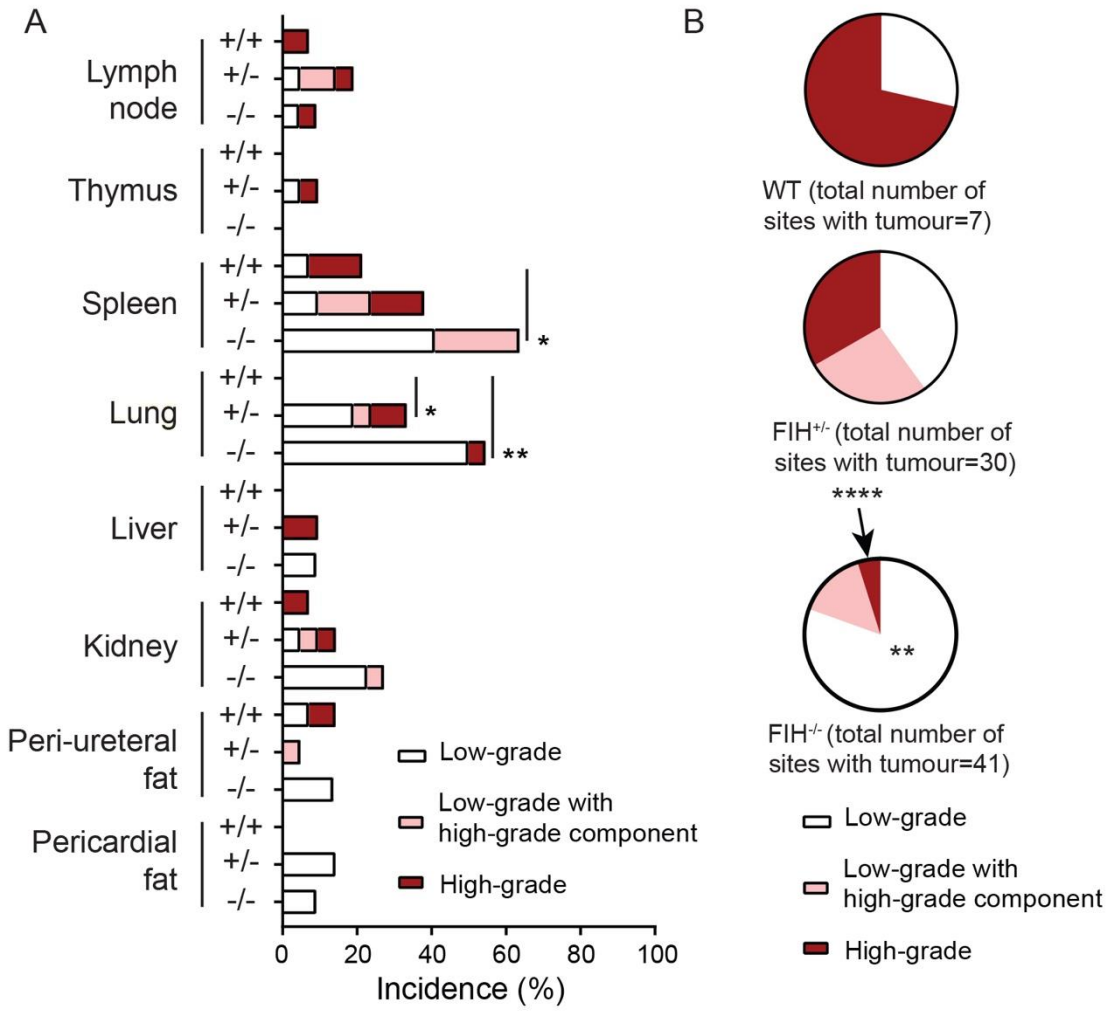

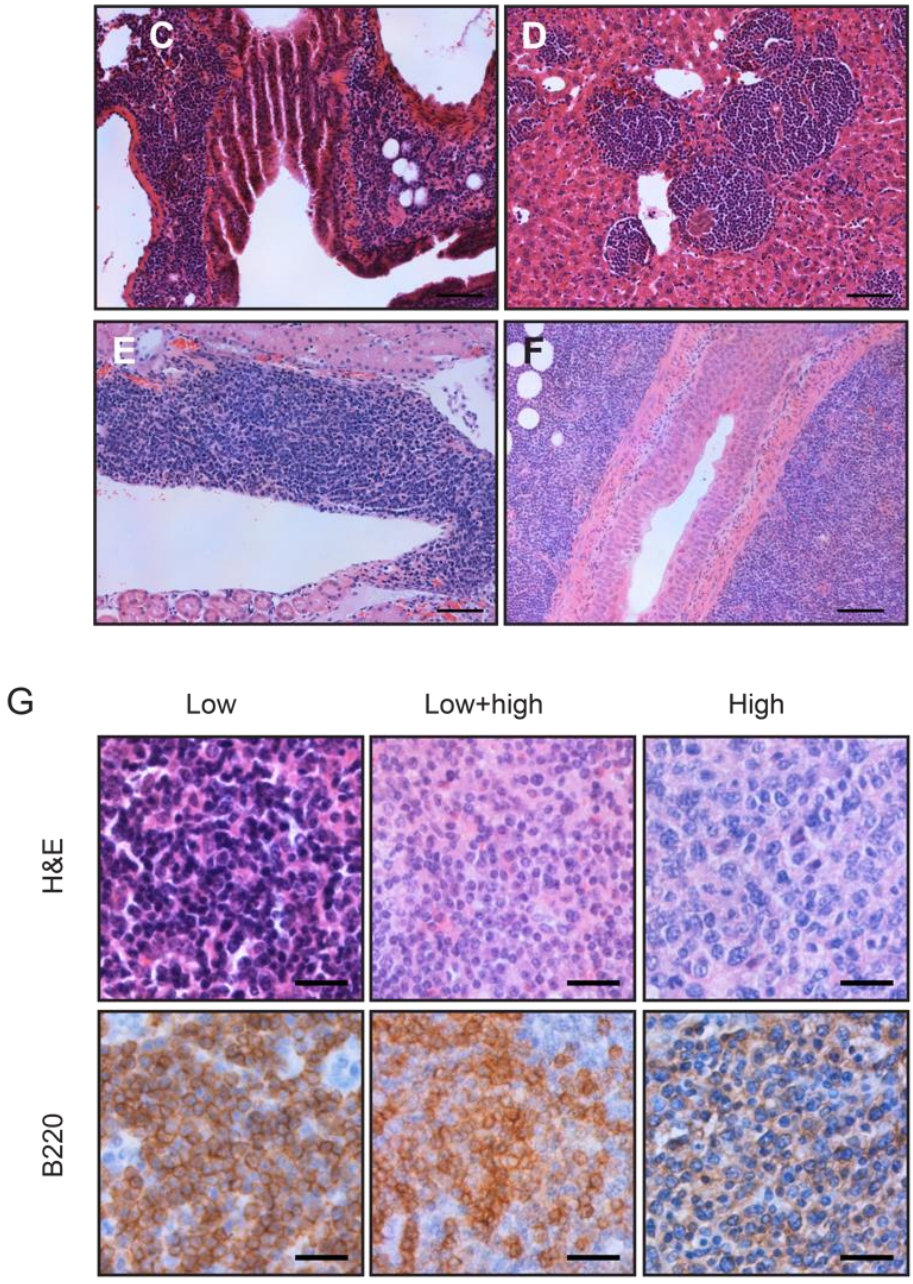

Figure 3.4 Loss of FIH confers susceptibility to pulmonary low-grade B cell lymphomas

(A) B cell lymphomas were observed in various tissues (for details, please refer to Table S1). The percentage of mice with neoplasms at the indicated site in each genotype group is shown. Increased tumour incidence in the spleen and lung was observed in mice with reduced FIH expression (spleen: WT vs $FIH^{-/-}$: 3 out of 14 (21.4%) vs 14 out of 22 (63.6%), p=0.0266; lung: WT vs $FIH^{+/-}$: 0 out of 14 (0) vs 7 out of 21 (33.3%), p=0.0157, WT vs $FIH^{-/-}$: 0 out of 14 (0) vs 12 out of 22 (54.5%), p=0.0015, χ^2 test). Tumours were

categorised as low-grade, low-grade with high-grade components, and high-grade lymphomas based on morphological features identified by the pathologist. (B) The number of neoplastic sites of certain grade was normalised by the total number of sites with tumours found within each group, reflected as proportions in the pie chart. Compared with the WT, FIH-null mice showed an increased percentage of low-grade B cell lymphomas (WT vs $FIH^{-/-}$: 2 out of 7 (28.6%) vs 33 out of 41 (80.5%), p=0.0043, χ^2 test) and a decreased fraction of high-grade B cell lymphomas (WT vs $FIH^{-/-}$: 5 out of 7 (71.4%) vs 2 out of 41 (4.9%), p<0.0001, χ^2 test). (C–F) Representative H&E images show the location of malignant cells in non-lymphoid tissues, including the lung (C), liver (D), kidney (E), and adipose tissue surrounding the ureter (F). (G) Representative micrographs of lymph node-residing B cell lymphomas of different grades are shown. B cells were identified by B220 staining shown in the lower panel. Scale bar, 25 μm.

3.2.5 The genetic interaction of FIH and ASPP2 in tumour suppression

3.2.5.1 ASPP2 heterozygosity accelerates oncogenesis in FIH-null mice at an early stage

ASPP2 is a haploinsufficient tumour suppressor; reduced ASPP2 expression has been shown to confer B6; 129 mice with susceptibility to lymphomas and sarcomas (Vives et al. 2006). FIH has been reported to hydroxylate ASPP2 (Janke et al. 2013). To determine the effect of genetic interaction between FIH and ASPP2 on tumourigenesis, $FIH^{+/+}$ $ASPP2^{+/-}$ (n=11) and $FIH^{-/-}$ $ASPP2^{+/-}$ (n=13) animals were included in the cohort described previously (made up of $FIH^{+/+}$, $FIH^{+/-}$, and $FIH^{-/-}$ animals). ASPP2 homozygosity in B6; 129 mice are embryonically lethal (Vives et al. 2006), therefore only $ASPP2^{+/-}$ mice were obtained for this study.

During the course of the study, a single deletion of FIH or ASPP2 ($FIH^{-/-}$ $ASPP2^{+/+}$ or $FIH^{+/+}$ $ASPP2^{+/-}$) did not profoundly affect the lifespan of the animals

(Figure 3.5A). However, a concomitant lack of FIH and ASPP2 ($FIH^{-/-}$ $ASPP2^{+/-}$) appeared to cause earlier deaths, and this was statistically significant at week 88, as indicated by the dashed line ($FIH^{+/+}$ $ASPP2^{+/+}$ vs $FIH^{-/-}$ $ASPP2^{+/-}$ p=0.0013; Mantel–Cox test; Figure 3.5A). Additionally, at week 88, ASPP2 heterozygosity further shortened the lifespan of FIH KO animals ($FIH^{-/-}$ $ASPP2^{+/+}$ vs $FIH^{-/-}$ $ASPP2^{+/-}$ p=0.0017; Mantel–Cox test; Figure 3.5A), yet the effect was not observed at the later stage as the animals aged (Figure 3.5A).

As expected, partial deficiency of ASPP2 promoted tumourigenesis ($FIH^{+/+}$ $ASPP2^{+/+}$ vs $FIH^{+/+}$ $ASPP2^{+/-}$ p=0.0172; Mantel–Cox test; Figure 3.5B), and the effect was already observed at week 88 ($FIH^{+/+}$ $ASPP2^{+/+}$ vs $FIH^{+/+}$ $ASPP2^{+/-}$ p=0.0179; Mantel–Cox test; Figure 3.5E, dashed line). Although a single deletion of FIH did not significantly affect tumourigenesis at this stage (week 88, Figure 3.5C), reduced expression of ASPP2 in FIH-deficient mice accelerated oncogenesis ($FIH^{-/-}$ $ASPP2^{+/+}$ vs $FIH^{-/-}$ $ASPP2^{+/-}$ p=0.0421; Mantel–Cox test; Figure 3.5F), indicating an additive effect of the two molecules in tumour suppression at this time point.

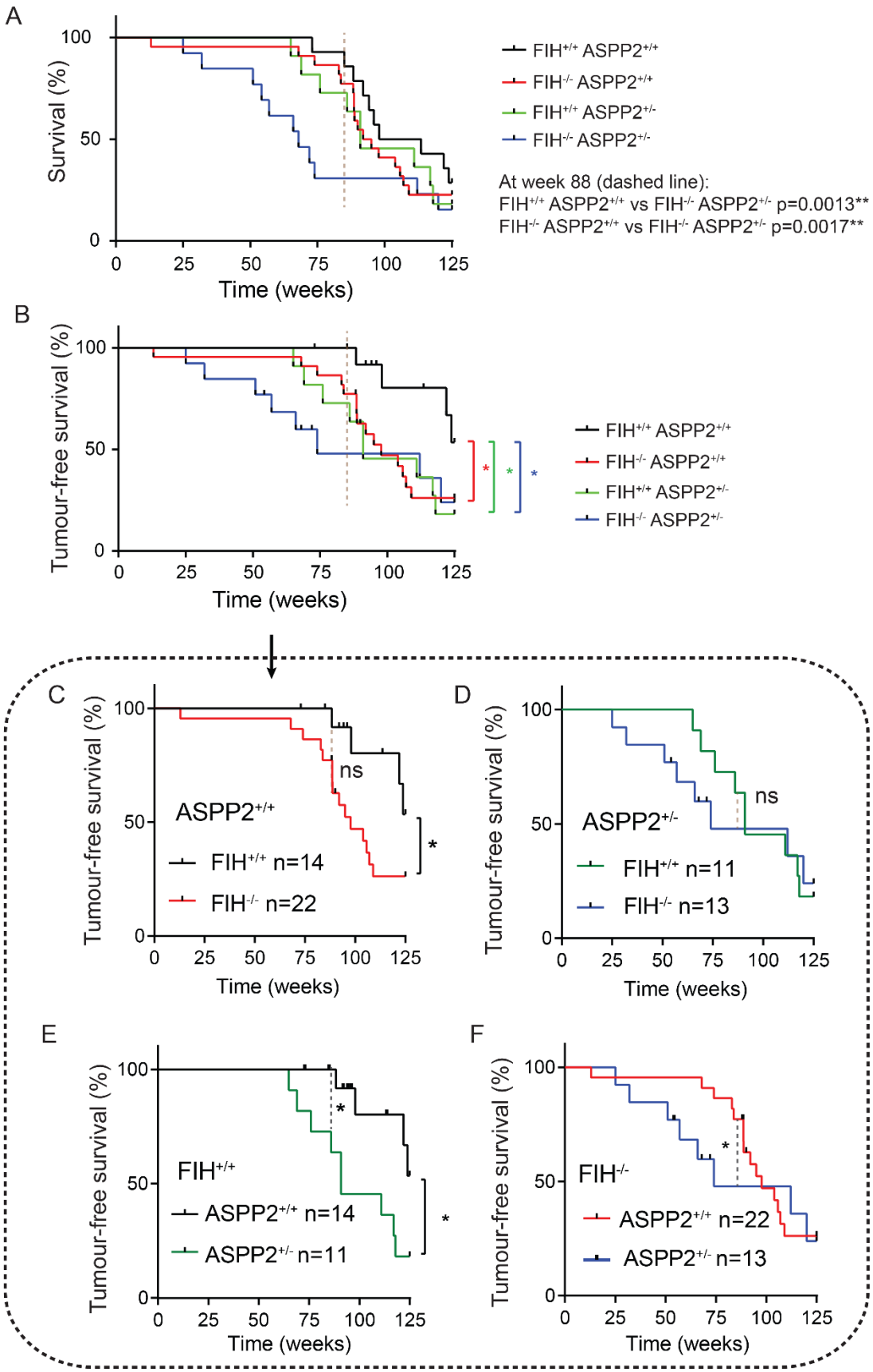
A
Survival (%)
Time (weeks)
FIH+/+ ASPP2+/+
FIH-/- ASPP2+/+
FIH+/+ ASPP2+/-
FIH-/- ASPP2+/-
At week 88 (dashed line):
FIH+/+ ASPP2+/+ vs FIH-/- ASPP2+/- p=0.0013**
FIH-/- ASPP2+/+ vs FIH-/- ASPP2+/- p=0.0017**
B
Tumour-free survival (%)
Time (weeks)
C
ASPP2+/+
ns
FIH+/+ n=14
FIH-/- n=22
D
ASPP2+/-
ns
FIH+/+ n=11
FIH-/- n=13
E
FIH+/+
ASPP2+/+ n=14
ASPP2+/- n=11
F
FIH-/-
ASPP2+/+ n=22
ASPP2+/- n=13

Figure 3.5 Reduced ASPP2 expression accelerates oncogenesis in FIH$^{-/-}$ mice at week 88

Mice were monitored over a period of 125 weeks. (A) Survival curve is shown. At week 88 (indicated by the dashed line), double mutant mice (FIH$^{-/-}$ ASPP2$^{+/-}$) showed a reduced survival rate compared with the WT (FIH$^{+/+}$ ASPP2$^{+/+}$) and the FIH$^{-/-}$ ASPP2$^{+/+}$ animals. (B) Tumour-free survival curve is shown. Mice with reduced expression of ASPP2, FIH, or both, all exhibited increased tumourigenesis compared with WT animals. (C–F) Data from (B) were divided into separate graphs to show the dosage effect of FIH and ASPP2 on tumour-free survival. Mantel–Cox test was performed at week 88 and week 125. * indicates $p<0.05$ by Mantel–Cox test. ns, not significant.

3.2.5.2 The tumour spectrum of FIH-null animals is not profoundly affected by ASPP2 expression

In an agreement with the role of ASPP2 as a tumour suppressor (Vives et al. 2006), partial deficiency of ASPP2 promoted tumour incidence in mice with wild-type FIH (FIH$^{+/+}$ ASPP2$^{+/+}$ vs FIH$^{+/+}$ ASPP2$^{+/-}$ $p=0.0082$; χ^2 test; Figure 3.6A. Interestingly, concomitant reduction of FIH and ASPP2 expression did not significantly promote tumour incidence by the end of the study (Figure 3.6A), although double mutant mice (FIH$^{-/-}$ ASPP2$^{+/-}$) experienced the lowest tumour-free survival rate among the groups of mice analysed at the early stage of the study (Figure 3.5B).

Within each group of mice, the predominant type of tumours was HNs (Figure 3.6A). In comparison with the other groups of mice, FIH$^{+/+}$ ASPP2$^{+/-}$ mice appeared to develop more tumours of non-haematopoietic origin (two cases of HCC and one case of neuroendocrine tumour (NET) in the small intestine) (Figure 3.6A).

B cell lymphomas remained the major type of HNs in each group of mice examined (Figure 3.6B). Although some cases of T cell and myeloid malignancies

were observed in ASPP2 heterozygous mice (both FIH$^{+/+}$ ASPP2$^{+/-}$ and FIH$^{-/-}$ ASPP2$^{+/-}$), the incidence was not significantly different from that of FIH$^{+/+}$ ASPP2$^{+/+}$ or FIH$^{-/-}$ ASPP2$^{+/+}$ animals (χ^2 test).

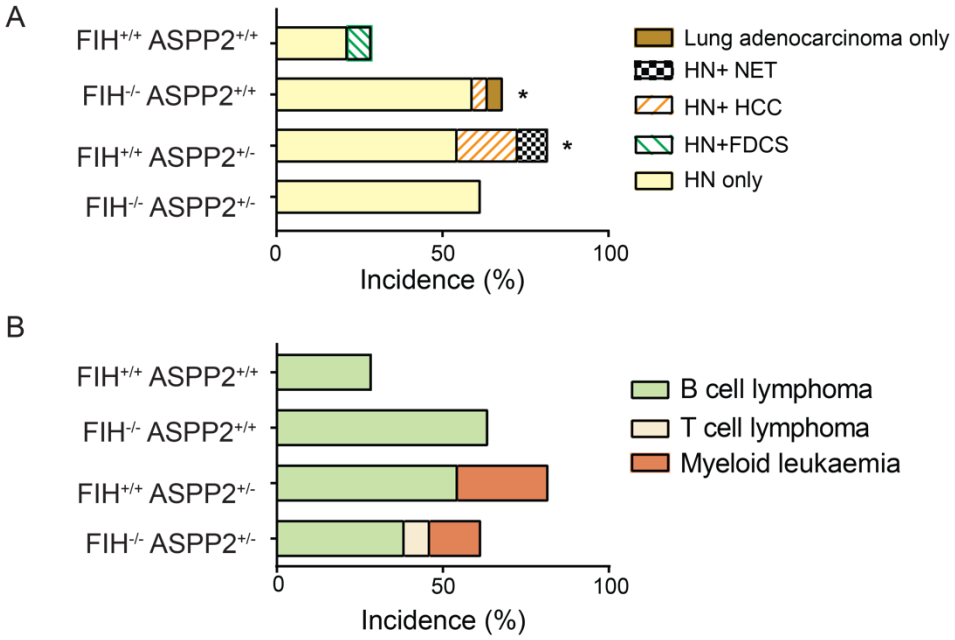

Figure 3.6 ASPP2 does not profoundly alter the tumour spectrum of FIH-null mice

(A) Histopathological examination was performed to identify cancer types. The percentage of mice with the indicated types of cancer in each genotype group is shown. 4 out of 14 (28.6%) FIH$^{+/+}$ ASPP2$^{+/+}$ mice, 15 out of 22 (68.2%) FIH$^{-/-}$ ASPP2$^{+/+}$ mice, 9 out of 11 (82.8%) FIH$^{+/+}$ ASPP2$^{+/-}$ mice, and 8 out of 13 (61.5%) FIH$^{-/-}$ ASPP2$^{+/-}$ mice were diagnosed with tumours. While most of the malignancies arose from haematological cells, tumours of other origins were also found. Both FIH$^{-/-}$ ASPP2$^{+/+}$ and FIH$^{+/+}$ ASPP2$^{+/-}$ mice showed increased tumour incidence compared with WT (FIH$^{+/+}$ ASPP2$^{+/+}$) animals. * indicates $p<0.05$ by χ^2 test. (B) Subtypes of HN cases were determined by IHC staining using antibodies against CD3, B220, F4/80, and CD11b to identify T cells, B cells, and myeloid cells. The percentage of mice with the indicated types of HN in each genotype group is shown.

3.2.5.3 Mice with partial deficiency of ASPP2 do not show enhanced pulmonary B cell lymphomagenesis

B cell lymphoma cases were further analysed regarding their sites. ASPP2-deficient animals ($FIH^{+/+}$ $ASPP2^{+/-}$ and $FIH^{-/-}$ $ASPP2^{+/-}$) showed a similar distribution of B cell lymphomas compared with $FIH^{+/+}$ $ASPP2^{+/+}$ mice, except for moderately elevated incidence of tumour in the spleen (Figure 3.7A). Interestingly, the high incidence of pulmonary B cell lymphomas observed in $ASPP2^{+/+}$ $FIH^{-/-}$ animals was substantially mitigated in $ASPP2^{+/-}$ $FIH^{-/-}$ mice (Figure 3.7A), indicating the interplay between FIH and ASPP2 in mediating lung pathology.

Regarding the tumour grade, B cell lymphomas developed in all mutant mice showed increased proportions of low-grade tumours compared with the WT counterpart ($FIH^{+/+}$ $ASPP2^{+/+}$ vs $FIH^{-/-}$ $ASPP2^{+/+}$ p=0.0043, $FIH^{+/+}$ $ASPP2^{+/+}$ vs $FIH^{+/+}$ $ASPP2^{+/-}$ p=0.0043, $FIH^{+/+}$ $ASPP2^{+/+}$ vs $FIH^{-/-}$ $ASPP2^{+/-}$ p=0.0006; χ^2 test; Figure 3.7B).

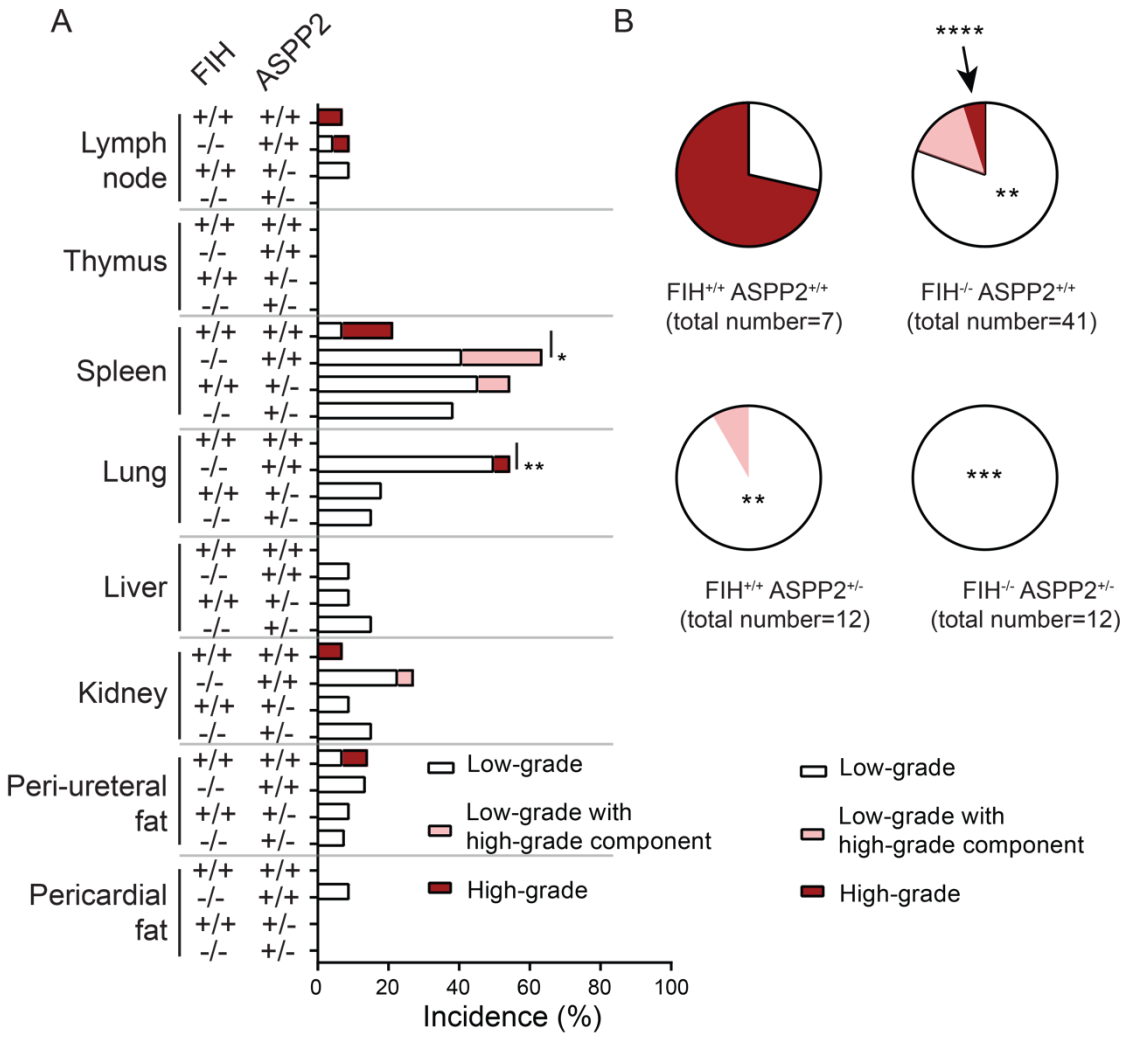

Figure 3.7 Mice with reduced ASPP2 expression do not show enhanced B cell lymphomagenesis in the lung

(A) The percentage of mice with B cell lymphoma at the indicated site in each genotype group is shown (for details, please refer to Supplementary Figure S1). FIH$^{-/-}$ ASPP2$^{+/+}$ animals showed increased incidence of B cell lymphomas in the spleen and lung compared with FIH$^{+/+}$ ASPP2$^{+/+}$ animals (spleen: FIH$^{+/+}$ ASPP2$^{+/+}$ vs FIH$^{-/-}$ ASPP2$^{+/+}$: 3 out of 14 (21.4%) vs 14 out of 22 (63.6%), p=0.0266; lung: FIH$^{+/+}$ ASPP2$^{+/+}$ vs FIH$^{-/-}$ ASPP2$^{+/+}$: 0 out of 14 (0) vs 12 out of 22 (54.5%), p=0.0015, χ^2 test). (B) Grades of B cell lymphomas were determined by histological examination. The number of neoplastic sites of certain grade was normalised by the total number of sites with tumours found within each genotype group, reflected as proportions in the pie chart. B cell lymphomas developed in all mutant mice showed increased proportions of low-grade tumours compared with the WT counterpart (FIH$^{+/+}$ ASPP2$^{+/+}$

vs $FIH^{-/-}$ $ASPP2^{+/+}$: 2 out of 7 (28.6%) vs 33 out of 41 (80.5%), p=0.0043; $FIH^{+/+}$ $ASPP2^{+/+}$ vs $FIH^{+/+}$ $ASPP2^{+/-}$: 2 out of 7 (28.6%) vs 11 out of 12 (91.7%), p=0.0043; $FIH^{+/+}$ $ASPP2^{+/+}$ vs $FIH^{-/-}$ $ASPP2^{+/-}$: 2 out of 7 (28.6%) vs 12 out of 12 (100%), p=0.0006). The frequencies of indicated group were compared using χ^2 test (*p<0.05, **p<0.01, ***p<0.001, and ****p<0.0001).

Collectively, these data show that reduced ASPP2 expression further accelerates tumour formation in FIH-null animals at an early stage (week 88). Mice lacking FIH, ASPP2, or both genes, show a similar tumour spectrum compared with the WT counterpart, with low-grade B cell lymphomas being the dominant type of malignancy. B cell lymphomas are similarly distributed in mice with various dosages of FIH and ASPP2 genes in non-lymphoid tissues, except that the high incidence of pulmonary B cell lymphomas observed in $ASPP2^{+/+}$ $FIH^{-/-}$ mice is largely attenuated by partial deficiency of ASPP2.

3.2.6 Nuclear HIF-α expression is not strongly detected in B cell lymphoma tissues

Both HIF-1α and HIF-2α have been detected in human B cell lymphomas (Evens et al. 2008; Stewart et al. 2002; Argyriou et al. 2010). To examine whether this could also apply to B cell lymphomas of mice, sections of tumours at the same site and of the same grade were selected and stained with anti-HIF-1α and anti HIF-2α antibodies (Figure 3.8A). Overall, both HIF-1α and HIF-2α expression was detectable at the protein level, yet the percentage of cells with nuclear HIF was generally low (Figure 3.8A). WT and FIH-deficient mice showed similar HIF expression qualitatively (Figure 3.8A). Morphologically, HIF-α-positive cells showed smaller nuclei compared to the malignant cells. Spatially, they did not aggregate, but spread sparsely across the tumour tissue (Figure 3.8A). Given that

HIF isoforms have been reported to be expressed in various immune cells, including Treg cells, CD8 T cells, and macrophages (Palazon et al. 2014), the presence of these cells were detected by IHC staining. Due to the working limitations of the antibodies, double staining could not be conducted to simultaneously examine HIF expression in these cells. Nonetheless, B cell lymphomas of different grades were found with immune cells scattering within the tumour tissues (Figure 3.8B).

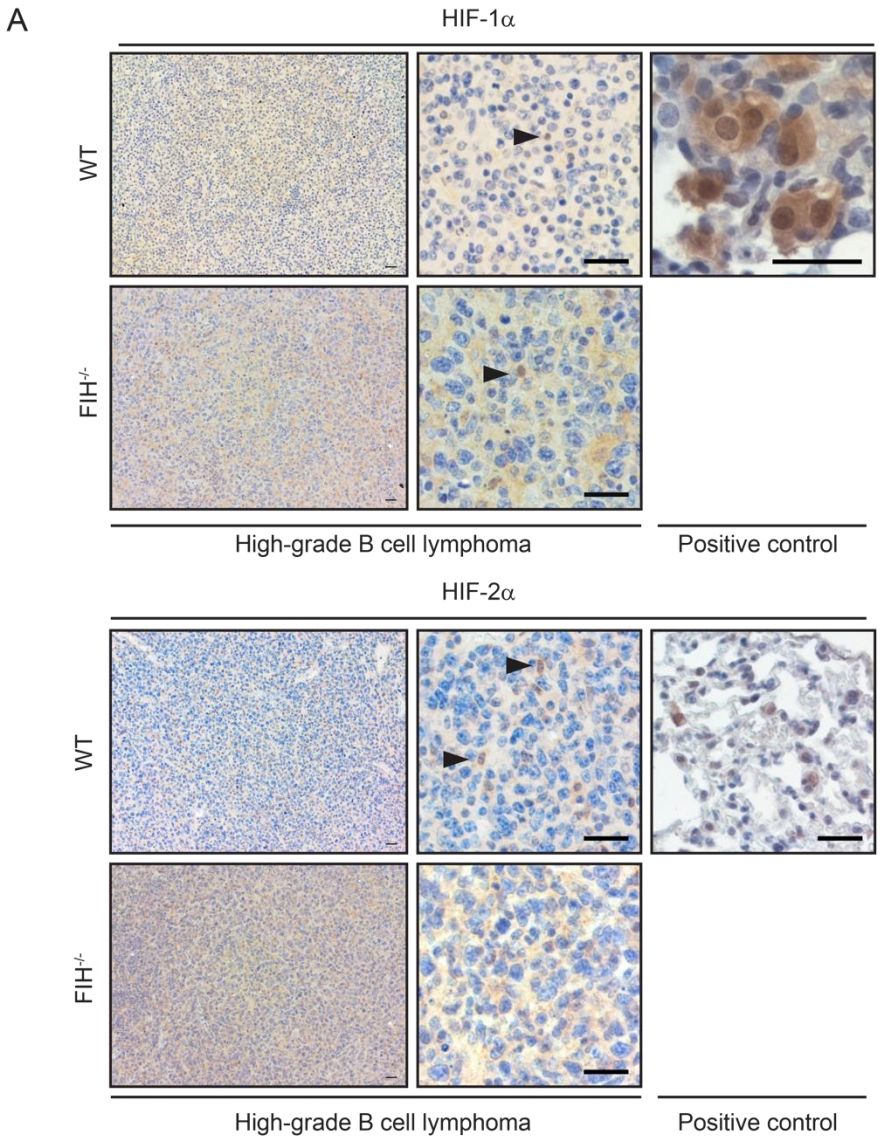
A
HIF-1α
WT
FIH-/-
High-grade B cell lymphoma
Positive control
HIF-2α
WT
FIH-/-
High-grade B cell lymphoma
Positive control

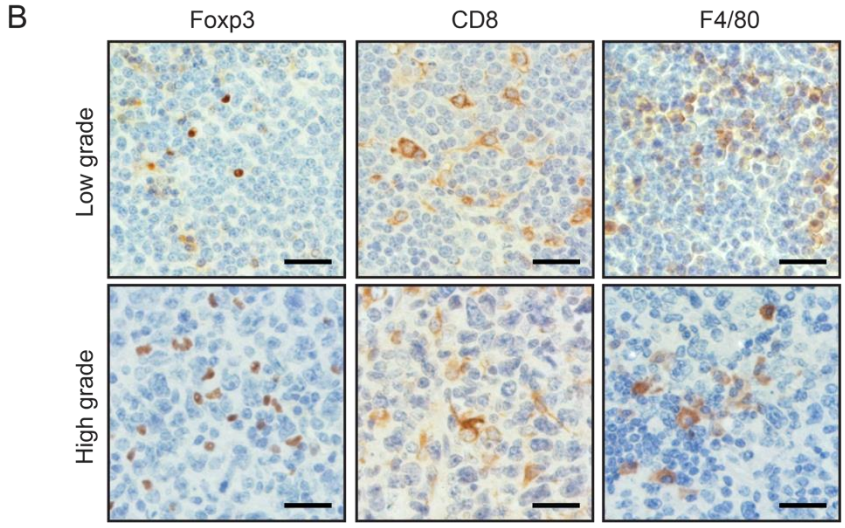
B
Foxp3
CD8
F4/80
Low grade
High grade

Figure 3.8 Nuclear HIF-α expression is not strongly detected in malignant B cells

(A) B cell lymphoma samples obtained from WT and FIH-null mice were stained with antibodies detecting HIF-1α (upper panel) and HIF-2α (lower panel). Representative images of two cases of high-grade splenic B cell lymphomas are shown. Lung biopsies obtained from BCG-infected or DMOG-treated mice were used as positive controls for HIF-1α and HIF-2α staining, respectively. Black arrows indicate cells with positive nuclear staining. (B) B cell lymphoma sections were stained with antibodies against Foxp3, CD8, and F4/80 to identify Treg cells, CD8 T cells, and macrophages, respectively. Representative images of one case of low-grade B cell lymphoma and one case of high-grade lymphoma are shown. Scale bar, 25 μm.

Collectively, these data show that HIF-α protein is not strongly detected in the B cell lymphomas developed in this cohort of mice. Some cells are positive for nuclear HIF-α, which might be tumour-infiltrating immune cells.

3.3 Discussion

In line with the study by Zhang and colleagues (N. Zhang et al. 2010), FIH was found to be expressed in a variety of tissues in mice. Reduced expression of FIH does not profoundly affect the lifespan of mice, but confers tumour susceptibility. Loss of FIH increases the incidence of B cell lymphomas, and this effect is most strikingly observed in the lung. Additionally, B cell lymphomas developed in $FIH^{-/-}$ animals show an increased fraction of low-grade lymphomas and a decreased fraction of high-grade lymphomas in comparison with the profile of WT animals. Partial deficiency of ASPP2 further accelerates the oncogenesis of FIH-null mice at week 88, yet the effect is abolished at a later stage of the study. Nonetheless, the tumour spectrum of FIH-null animals is not profoundly changed by ASPP2 gene

dosage. Collectively, these data provide genetic evidence for the role of FIH in suppressing tumourigenesis.

Mice used in this study are on a B6;129 background, in which the incidence of spontaneous development of lymphomas has been reported to be 15–67% in WT animals. The wide range is probably due to the fact that B6;129 stock is not a defined strain and is produced by different laboratories (Haines, Chattopadhyay, and Ward 2001). Nonetheless, in the present study, the rate of lymphomas in WT animals (28.6%) falls in the range above (Figure 3.3A), and is in line with data published by our group that 22.2% of WT mice on the same background develop lymphomas (Vives et al. 2006). One caveat of this study is the lack of molecular genetic evidence to prove the clonal expansion of neoplastic lymphocytes. While the similar morphological characteristics might blur the boundary between hyperplastic and low-grade malignant B cells, a consistent guideline was kept during the examination of all histology sections by an experienced pathologist (Dr. E. Soilleux) to maximise the accuracy of the diagnosis. Molecular diagnosis of the low-grade B cell lymphoma samples should be performed for confirmation.

The tumour suppressive effect of FIH and the interaction between FIH and ASPP2 raises the question that whether ASPP2 mediates the effect of FIH. At week 88, reduced expression of ASPP2 further accelerates oncogenesis in FIH-null animals (Figure 3.5F), and FIH deficiency seems to promote tumourigenesis in $ASPP2^{+/-}$ mice (Figure 3.5D), indicating an additive effect of the two molecules at this stage. In agreement with above, mice with reduced expression of FIH and ASPP2 also show worse survival compared with $FIH^{-/-}$ $ASPP2^{+/+}$ and $FIH^{+/+}$ $ASPP2^{+/-}$ animals at week 88 (Figure 3.5A). Of note, some $FIH^{-/-}$ $ASPP2^{+/-}$ mice that were culled due to sickness by this time point did not develop malignancy in

the tissues examined (Table S1), indicating the existence of other causes of death apart from cancer. Nonetheless, the shortened life span of $FIH^{-/-}$ $ASPP2^{+/-}$ due to non-cancer pathologies could prevent the spontaneous tumourigenesis that is likely to occur in aged animals.

Expression of both HIF-1α and HIF-2α has been detected in subsets of human B cell lymphomas with various abundance in different studies (Evens et al. 2008; Stewart et al. 2002; Argyriou et al. 2010). Mechanistically, HIF-1α has been reported to promote haematological cancers by maintaining cancer stem cells (CSCs) (Y. Wang et al. 2011), and HIF-2α has been shown to enhance the proliferation of haematopoietic malignant cells (Forristal et al. 2015). In this study, however, neither HIF-1α nor HIF-2α protein is prevalent in the nuclei of tumour cells. This may indicate that these tumour tissues are neither hypoxic nor under the influence of the regulatory pathways involved in oxygen-independent HIF activation. Nonetheless, FIH may regulate the transcriptional activity of HIF-α at the basal level. Examination of the expression of HIF target genes in FIH-deficient tumour samples will help evaluate the effects of FIH on HIF pathway.

Interestingly, a substantial number of FIH-null mice developed pulmonary B cell lymphoma during the course of the study. One question is whether these malignancies are primary or secondary diseases. In human, the lung is often a secondary locus in lymphoma cases (William et al. 2013), which seems to be reminiscent of the observations in mice that all of the $FIH^{-/-}$ mice with pulmonary lymphomas also had neoplasms in the spleen. This implies that cancer cells present in the lung might be disseminated from other tissues such as the spleen. If so, FIH expression may affect lymphocyte homing to the lung tissue, which is guided by lymphocyte–endothelial interactions mediated by adhesion molecules

(e.g., L-selectin, integrins, and CD44) and certain chemokines (Gallatin et al. 1986; Pals, de Gorter, and Spaargaren 2007). Interestingly, the development of pulmonary B cell lymphomas caused by FIH deficiency is largely attenuated in mice with an $ASPP2^{+/-}$ background, indicating the involvement of ASPP2 in this process. Given that ASPP2 plays a pivotal role in maintaining epithelial cell polarity by binding to Par-3 (Sottocomola et al. 2010; Cong et al. 2010), and that FIH regulates ASPP2/Par-3 interaction (Janke et al. 2013), FIH might affect endothelial polarity and consequently the leukocyte–endothelial cell interaction through an ASPP2-dependent mechanism.

Existing as a rare entity, primary pulmonary B cell lymphoma accounts for 0.4% of all lymphoma cases in humans (Parissis 2011). Most primary pulmonary lymphomas are low-grade and are frequently observed around bronchi or bronchioles (Cadranel, Wislez, and Antoine 2002), which matches the histological features of the murine counterparts observed in $FIH^{-/-}$ animals (Figure 3.4C). Approximately 80% of pulmonary lymphomas are developed in mucosa-associated lymphoid tissue (MALT) that is scattered along mucosal linings in the body. MALT lymphoma is mostly induced by chronic inflammation. For example, the occurrence of gastric MALT lymphoma, the most common type of MALT lymphoma, is strongly associated with gastroduodenitis induced by *H. pylori* infection. Prolonged proliferation of B cells during chronic inflammation, together with the ROS produced by other inflammatory cells, increase the risk of genetic mutations in B cells (Sagaert et al. 2010).

Remarkably, some mutations in B cells result in the constitutive activation of NFκB, which induces the expression of genes favouring B cell proliferation (Jost and Ruland 2007). This raises the possibility that FIH may affect B cell survival via

the NFκB pathway. Although *in vitro* biophysical assays have failed to demonstrate the functional consequences of FIH hydroxylation on IκBα (Devries et al. 2010), a more physiological context may be required to demonstrate its biological relevance.

On the other hand, given that MALT lymphomas are deeply rooted in chronic inflammation, FIH may facilitate their development by acting in the inflammatory cells. In this study, inflammatory loci are frequently observed in various organs of aged mice regardless of the genotype (Figure 3.2, C-E). Potentially, these inflammatory B cells may develop into hyperplasias and eventually neoplasms. Loss of FIH may speed up the transition by promoting the inflammatory microenvironment. This is in line with the observation that the best-known substrates of FIH, HIF-1α and HIF-2α, are not strongly detected in the nuclei of malignant cells, but potentially in the tumour-infiltrating cells, which could be immune cells (Figure 3.8). Considering the substantial effects of HIF on orchestrating the TME (Palazon et al. 2014), it is plausible that FIH may suppress tumourigenesis by regulating the tumour stroma, which is explored in the next chapter.

Chapter 4 Host expression of FIH suppresses tumour growth *in vivo*

4.1 Introduction

Tumour hypoxia and tumour-induced inflammation can activate the HIF signalling pathway, which in turn exerts a broad range of effects on the tumour immune response (Kumar and Gabrilovich 2014; Palazon et al. 2014). For example, HIF-1α expression in TAMs and MDSCs has been shown to potentiate T cell suppression by upregulating the expression of immunosuppressive molecules, such as PD-L1 and ARG1 (Corzo et al. 2010; Noman et al. 2014; Colegio et al. 2015). HIF-1α also plays an important role in regulating the lineage differentiation of CD4 T cells (Dang et al. 2011) and the effector function of CD8 T cells (Doedens et al. 2013) (for review, please refer to section 1.3). Despite the prominent roles of HIF in modulating the TME, the function of FIH, a negative regulator of HIF transcriptional activity, has not been investigated in this context.

To assess the influence of FIH in the TME, FIH-deficient mice were characterised in syngeneic tumour models. Given the well-characterised roles of HIF in TAMs and MDSCs, myeloid-specific FIH knockout (FIH MKO) mice were also characterised in these models.

4.2 Results

4.2.1 FIH-deficient mice show a similar lymphoid and myeloid profile to WT animals

Given that HIF-1α is implicated in lymphocyte development and function, (Kojima et al. 2002; Goda et al. 2003; Biju et al. 2004), the immune system of FIH-deficient mice was profiled in the present study. Lymphoid and myeloid constituents of primary lymphoid organs (bone marrow and thymus), a secondary lymphoid organ (spleen), peripheral blood, and lung tissues of FIH-deficient adult mice were analysed by flow cytometry.

To identify the lymphoid populations, samples were stained with antibodies detecting lymphocyte markers (Panel 1, Table 2.7) and analysed as illustrated in Figure 4.1A. WT and $FIH^{-/-}$ mice showed similar numbers of CD4 T cells, Treg cells, CD8 T cells, and B cells in tissues examined (Figure 4.1, B–F).

To identify the myeloid populations, samples were stained with antibodies against myeloid markers (Panel 2, Table 2.7). $CD11b^{+}$ $CD11c^{-}$ myeloid cells and myeloid subsets (inflammatory monocytes, neutrophils, and macrophages) were identified as shown in Figure 4.1G. Thymus tissues were not analysed by this panel due to the scarcity of myeloid cells. No profound difference in the numbers of $CD11b^{+}$ $CD11c^{-}$ myeloid cells as well as myeloid cell subsets was detected between WT and FIH-null animals (Figure 4.1, H–K).

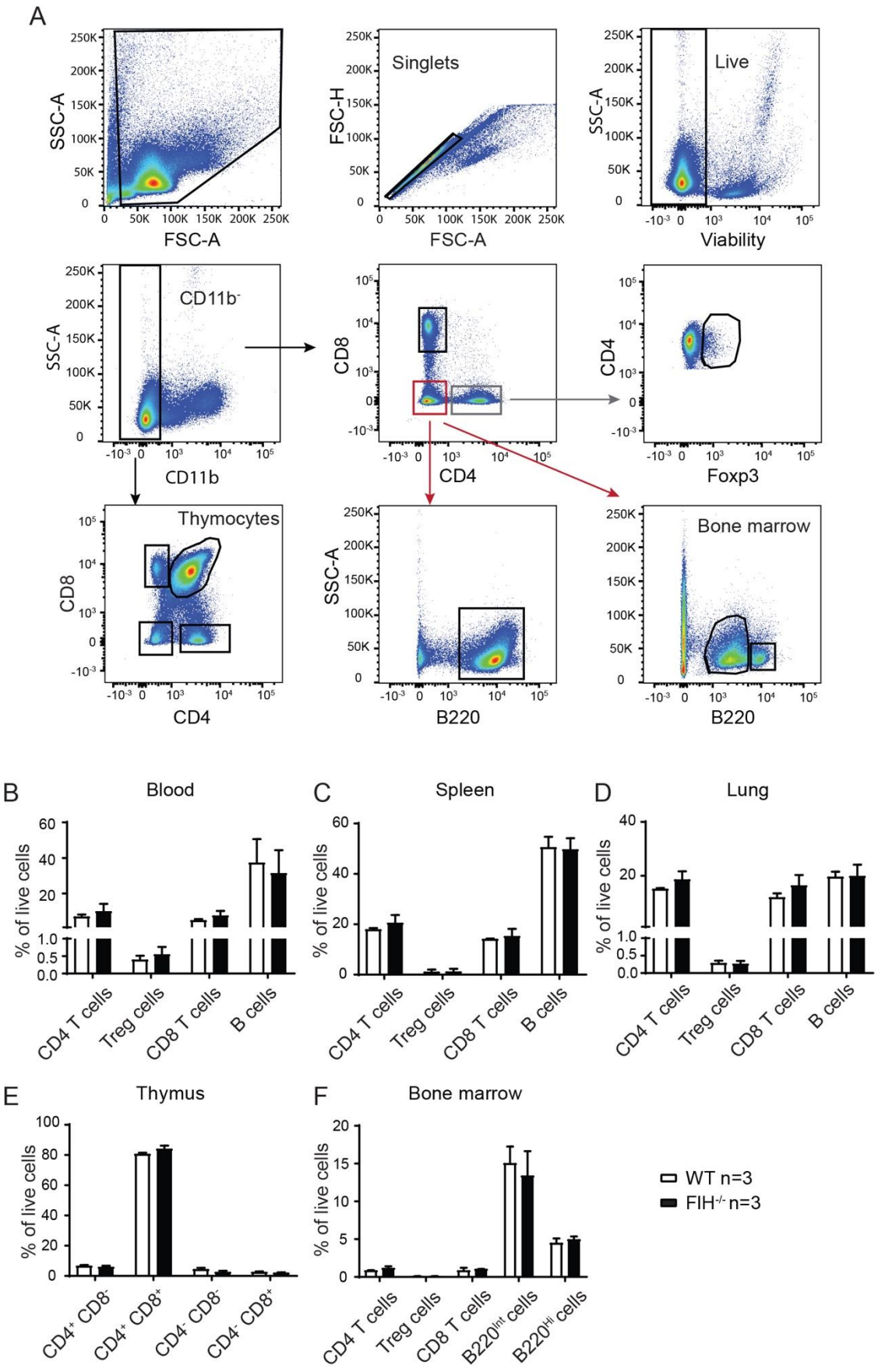
A
SSC-A
FSC-A
Singlets
FSC-H
Live
Viability
CD11b-
CD11b
CD8
CD4
Foxp3
Thymocytes
Bone marrow
B220
B Blood
C Spleen
D Lung
% of live cells
CD4 T cells
Treg cells
CD8 T cells
B cells
E Thymus
F Bone marrow
CD4+ CD8-
CD4+ CD8+
CD4- CD8-
CD4- CD8+
B220int cells
B220Hi cells
WT n=3
FIH-/- n=3

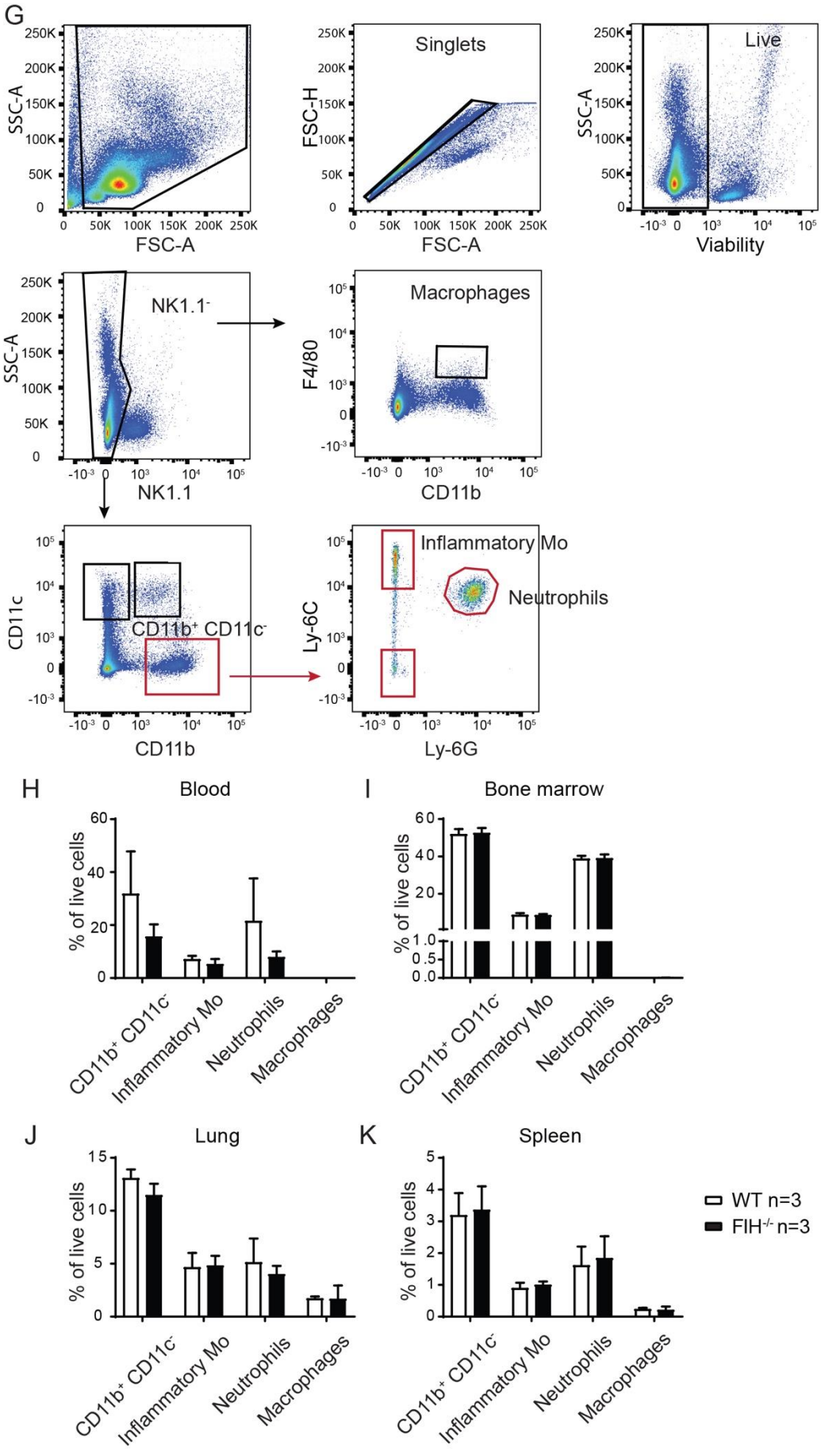
G
SSC-A
FSC-A
Singlets
FSC-H
Live
Viability
NK1.1⁻
NK1.1
Macrophages
F4/80
CD11b
CD11c
CD11b⁺ CD11c⁻
Inflammatory Mo
Neutrophils
Ly-6C
Ly-6G
H
Blood
I
Bone marrow
% of live cells
CD11b⁺ CD11c⁻
Inflammatory Mo
Neutrophils
Macrophages
J
Lung
K
Spleen
WT n=3
FIH-/- n=3

Figure 4.1 Adult WT and FIH$^{-/-}$ mice show a similar profile of immune cells in various tissues

Peripheral blood, spleen, lung, thymus, and bone marrow samples were collected from WT and FIH$^{-/-}$ animals and analysed by flow cytometry. All samples were gated according to the forward scatter/side scatter (FSC/SSC) profile first and doublets were excluded in the FSC-Area (FSC-A)/FSC-Height(FSC-H) plot. Live cells were distinguished by a fixable fluorescent dye (these steps were used in all the flow cytometry analysis shown in this thesis). (A) Samples were stained with antibodies shown in Panel 1, Table 2.7. CD11b^{-} live cells were further gated to identify CD4 T cells (CD4^{+} CD8^{-}), Treg cells (CD4^{+} Foxp3^{+}), CD8 T (CD4^{-} CD8^{+}) cells, and B cells (CD4^{-} CD8^{-} B220^{+}). Bone marrow cells show two B220^{+} populations, with B220^{lo} cells being pro-, pre-, and immature B cells and B220^{hi} being mature B cells (Murphy 2011). (B–F) Percentages of CD4 T cells, Tregs, CD8 T cells, and B cells out of live cells in the indicated tissue are shown. (G) Samples were stained with antibodies in Panel 2, Table 2.7. NK1.1^{-} live cells were gated to distinguish inflammatory monocytes (CD11b^{+} CD11c^{-} Ly-6G^{-} Ly-6C^{hi}), neutrophils (CD11b^{+} CD11c^{-} Ly-6G^{+} Ly-6C^{int}) (Rose, Misharin, and Perlman 2011), and macrophages (CD11b^{+} F4/80^{+}). (H–K) Percentages of CD11b^{+} CD11c^{-} cells, inflammatory monocytes, neutrophils, and macrophages out of live cells in the indicated tissue are shown. An unpaired, two-tailed *t*-test was performed and no significant difference between the WT and FIH$^{-/-}$ samples was detected. Error bars indicate standard deviation (SD). Inflammatory Mo, inflammatory monocytes; lo, low; int: intermediate; hi: high.

Collectively, these data demonstrate that loss of FIH does not change the major lymphoid and myeloid populations in the bone marrow, thymus, spleen, peripheral blood, or lung.

4.2.2 Loss of FIH leads to increased tumour burden

4.2.2.1 Mice with reduced FIH expression show enhanced tumour growth

To test the hypothesis that FIH suppresses tumour development through modifying the TME, WT, $FIH^{+/-}$, and $FIH^{-/-}$ animals were injected with B16 or LLC cells subcutaneously and monitored for tumour growth. Figure 4.2, A and C show the growth curve of individual tumours over the course of study. Once the tumours showed signs of ulceration, animals were required to be culled, causing the termination of the growth curve before the end of the study. Figure 4.2, B and D present the average sizes of tumours, including ulcerated ones, at the indicated time points.

In the B16 model, partial deficiency of FIH resulted in an increased tumour volume at multiple time points during the study (WT vs $FIH^{+/-}$ day 10: 43.3 mm^3 vs 100.5 mm^3, p=0.0441; day 12: 97.8 mm^3 vs 204.7 mm^3, p=0.0043; day 14: 182.0 mm^3 vs 281.4 mm^3, p=0.0459; *t*-test; Figure 4.2B). FIH-null animals also showed enhanced tumour growth, and their average tumour volume was significantly higher than that of the WT counterpart at days 12 and 14 post-injection (WT vs $FIH^{-/-}$ day 12: 97.8 mm^3 vs 245.2 mm^3, p=0.0128; day 14: 182.0 mm^3 vs 391.8 mm^3, p=0.0134; *t*-test; Figure 4.2B).

In the LLC model, compared with the WT, $FIH^{+/-}$ animals showed an increased tumour volume at multiple days post-injection (WT vs $FIH^{+/-}$ day 10: 93.3 mm^3 vs 135.6 mm^3, p=0.0124; day 12: 134.5 mm^3 vs 196.6 mm^3, p=0.0020; day 13: 184.4 mm^3 vs 289.0 mm^3, p=0.0030, day 14: 206.0 mm^3 vs 350.7 mm^3, p=0.0101; *t*-test; Figure 4.2D). $FIH^{-/-}$ animals also exhibited a trend of an increased tumour volume compared with WT mice; however, the difference was only significant on day 14 post-injection (WT vs $FIH^{-/-}$ 206.0 mm^3 vs 388.7 mm^3, p=0.0011; *t*-test; Figure 4.2D).

Additionally, LLC tumours grown in FIH$^{+/-}$ and FIH$^{-/-}$ mice showed increased weights on day 14 in comparison with those from WT animals (WT vs FIH$^{+/-}$ 0.10 g vs 0.23 g, p<0.0001, WT vs FIH$^{-/-}$ 0.10 g vs 0.19 g, p=0.0073; *t*-test; Figure 4.2E). The weights of B16 tumours were not measured due to the severe necrosis of the tumours (data not shown).

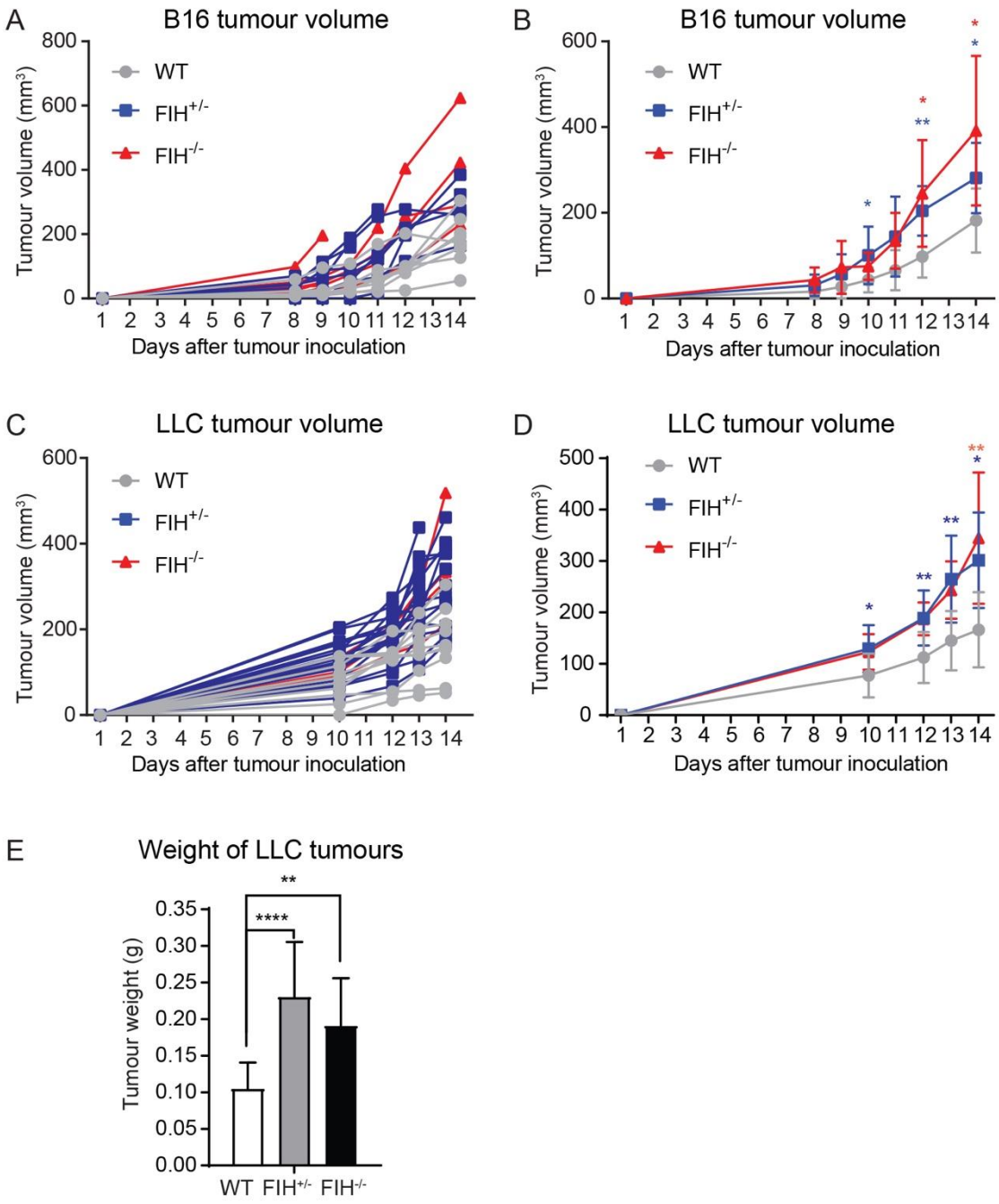

Figure 4.2 Mice with reduced FIH expression show enhanced growth of B16 and LLC tumours

B16 or LLC cells were injected into WT and FIH-mutant animals subcutaneously. (A and B) A total of 2×10^5 B16 cells were injected into five WT, seven $FIH^{+/-}$, and four $FIH^{-/-}$ mice in both flanks. Volumes of individual tumours are shown in A, and averaged volumes are shown in B. The number of mice and tumours at indicated time points is shown in Figure S2. (C and D) A total of 4×10^5 LLC cells were injected into seven WT, eleven $FIH^{+/-}$, and two $FIH^{-/-}$ mice in both flanks. Volumes of individual tumours are shown in C, and averaged volumes are shown in D. The number of mice and tumours at indicated time points in shown in Figure S3. Tumour sizes follow a normal distribution, and an *F* test revealed no significant difference in variance of tumour volumes between the compared groups. (E) Average weights of LLC tumours resected on day 14 from WT (tumour number=10), $FIH^{+/-}$ (tumour number=14), and $FIH^{-/-}$ (tumour number=4) animals are shown. A two-tailed, unpaired *t*-test was performed to test the difference between WT and $FIH^{+/-}$, $FIH^{-/-}$ groups, respectively. * indicates $p<0.05$, ** indicates $p<0.01$, and **** indicates $p<0.0001$. Asterisks in blue refer to comparison between WT and $FIH^{+/-}$ animals, whereas asterisks in red indicate comparison between WT and $FIH^{-/-}$ animals. Data are presented as mean ± SD.

4.2.2.2 Tumours from FIH-deficient animals show altered quantity of CD4 T cells

To characterise the immune components of the tumour, B16 and LLC tumours were resected at the end of the experiments and analysed by flow cytometry techniques. To examine the number and cytokine production of tumour-infiltrating lymphocytes (TILs), tumour samples were stained with antibodies against lymphocyte markers (CD4 and CD8) as well as their signature cytokines (IFNγ, IL-4, and IL-10) (Panel 3, Table 2.7).

B16 tumours showed a high prevalence of CD4 TILs out of live cells (Figure 4.3A), probably due to the fact that most of the tumour cells were dead, and hence were excluded from the analysis (Figure 4.4A). Tumours developed in mice with reduced FIH expression showed an increased proportion of CD4 TILs compared

with that of WT animals (WT vs $FIH^{+/-}$ 39.6% vs 53.3%, p=0.0354; WT vs $FIH^{-/-}$ 39.6% vs 70.0%, p=0.0012; *t*-test; Figure 4.3A), while the fraction of CD8 TILs remained unchanged regardless of genotype of the host (Figure 4.3B). Cells producing IFNγ, IL-4, or IL-10 were detectable in both CD4 and CD8 TILs, and their relative numbers were not profoundly affected by host expression of FIH (Figure 4.3, C and D).

The percentage of CD4 TILs in LLC tumours was substantially lower compared with that in B16 tumours (Figure 4.3, A and E). Partial deficiency of FIH gave rise to a reduced fraction of both CD4 and CD8 TILs compared with the WT (CD4 T cells: WT vs $FIH^{+/-}$ 6.89% vs 1.95%, p=0.0062; CD8 T cells: WT vs $FIH^{+/-}$ 2.70% vs 1.15%, p=0.0012; *t*-test; Figure 4.3, E and F). Tumour-infiltrating T cells of $FIH^{-/-}$ animals followed the same trend, although the difference from WT was not statistically significant (Figure 4.3, E and F). In addition to the quantity of TILs, FIH expression in the host also affected their cytokine production (Figure 4.3, G and H). Both CD4 and CD8 TILs from $FIH^{-/-}$ animals exhibited a reduced proportion of cells producing IFNγ (WT vs $FIH^{-/-}$ $CD4^+$ $IFN\gamma^+$: 2.08% vs 0.82%, p=0.0105; $CD8^+$ $IFN\gamma^+$: 1.99% VS 1.00%, p=0.0412; *t*-test; Figure 4.3, G and H) or IL-4 in comparison with their WT counterparts (WT vs $FIH^{-/-}$ $CD4^+$ $IL\text{-}4^+$: 2.93% vs 1.54%, p=0.0388; $CD8^+$ $IL\text{-}4^+$: 1.70% vs 0.92%, p=0.0300; *t*-test; Figure 4.3, G and H). Interestingly, CD4 TILs from $FIH^{+/-}$ animals displayed an increased fraction of $IL\text{-}4^+$ cells compared with those isolated from WT animals (WT vs $FIH^{+/-}$ 2.93% vs 3.82%, p=0.0273; *t*-test; Figure 4.3G). Additionally, CD8 TILs from FIH-null animals showed a diminished $IL\text{-}10^+$ population compared with the WT (WT vs $FIH^{-/-}$ 0.13% vs 0, p=0.0300; *t*-test; Figure 4.3H).

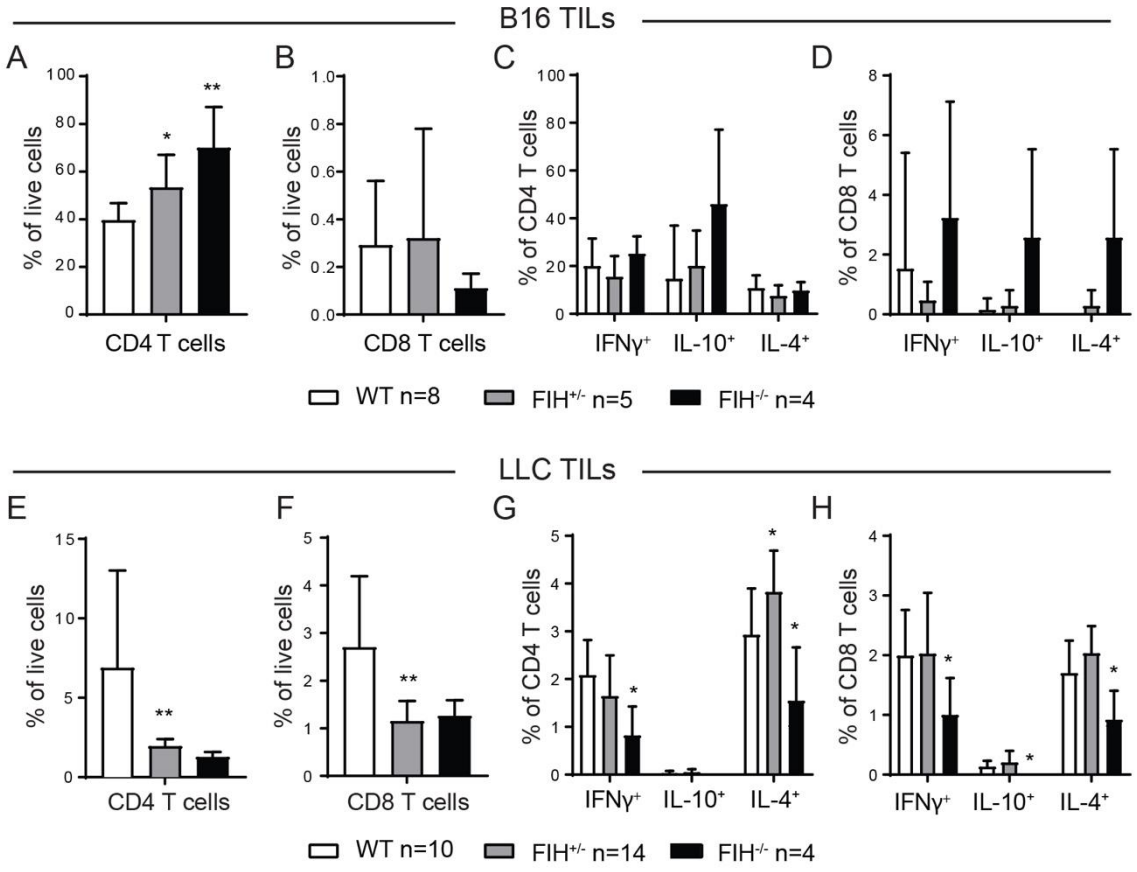

Figure 4.3 Reduced FIH expression leads to altered quantity of CD4 TILs in B16 and LLC tumours

B16 and LLC tumours were harvested on day 14. Samples were stained with antibodies against CD4, CD8, IFNγ, IL-10, and IL-4 (Panel 3, Table 2.7) followed by flow cytometry analysis. CD4 and CD8 T cells were identified, and the percentage of cells expressing the indicated cytokines out of the parental population was analysed. (A–D) Lymphoid profiles of B16 tumours are shown. (E–H) Lymphoid profiles of LLC tumours are shown. n represents the number of tumours. A two-tailed, unpaired *t*-test was performed to test the difference between the WT and two mutant groups, respectively. * indicates $p<0.05$, and ** indicates $p<0.01$. Data are presented as mean ± SD.

Taken together, these data demonstrate that a lack of FIH expression in the host results in an enlarged CD4 TIL population in B16 tumours, but a diminished

CD4 T cell population in LLC tumours. Loss of FIH also suppresses the production of IFNγ and IL-10 by CD4 and CD8 TILs of LLC tumours.

4.2.2.3 Mice lacking FIH show an increased population of myeloid cells in LLC tumours

The intra-tumoural myeloid cells were also profiled by flow cytometry. A panel of surface markers (Panel 2, Table 2.7) was used to distinguish TAMs, G-MDSCs, and M-MDSCs (Talmadge and Gabrilovich 2013) (Figure 4.4A). G-MDSCs were identified in the same way as neutrophils (described in section 4.2.1), given the high similarity of the two populations, both functionally and phenotypically (Zilio and Serafini 2016).

$CD11b^+$ myeloid cells were detected in both types of tumour samples with abundance (Figure 4.4, B and D). In the B16 model, mice lacking FIH tended to have an increased percentage of $CD11b^+$ cells (Figure 4.4B), which was also reflected in the myeloid subsets G-MDSCs and M-MDSCs (Figure 4.4C). Similarly, in LLC tumours, reduced expression of FIH marginally augmented the percentage of intra-tumoural myeloid cells (WT vs $FIH^{+/-}$ 43.6% vs 49.3%, p=0.0114; WT vs $FIH^{-/-}$ 43.6% vs 51.8%, p=0.0128; *t*-test; Figure 4.4D). However, no significant difference was detected between WT and FIH mutant animals in the number of myeloid subsets (Figure 4.4E).

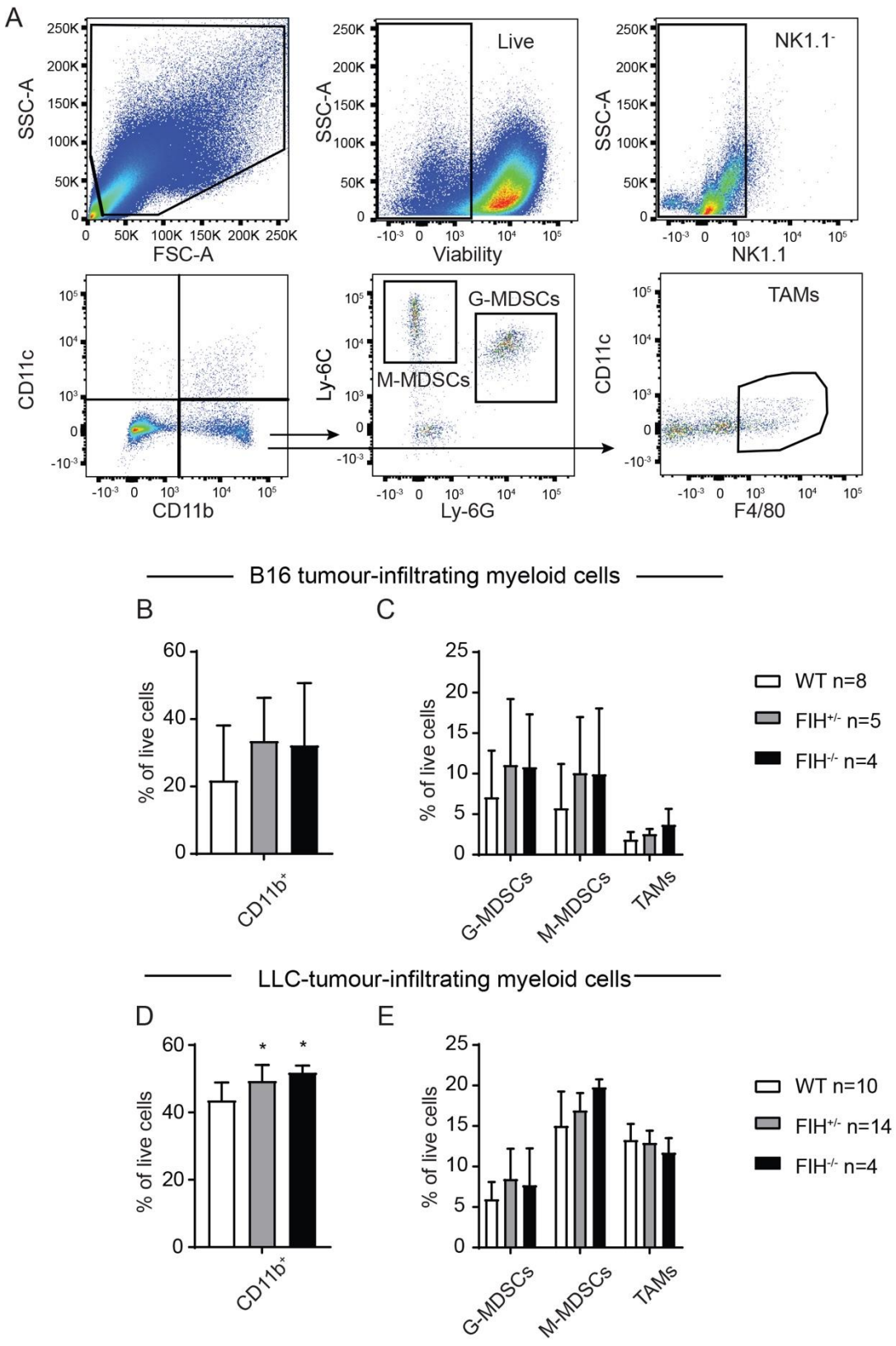

Figure 4.4 Mice lacking FIH expression display an increased myeloid population in LLC tumours

B16 and LLC tumours were resected on day 14. Samples were stained with antibodies shown in Panel 2, Table 2.7 and analysed by flow cytometry. (A) The gating strategy for distinguishing myeloid cells ($NK1.1^-$ $CD11b^+$), G-MDSCs ($NK1.1^-$ $CD11b^+$ $CD11c^-$ $Ly\text{-}6G^+$ $Ly\text{-}6C^{int}$), M-MDSCs ($NK1.1^-$ $CD11b^+$ $CD11c^-$ $Ly\text{-}6G^-$ $Ly\text{-}6C^{hi}$), and TAMs ($NK1.1^-$ $CD11b^+$ $CD11c^-$ $F4/80^+$) of a B16 tumour sample is shown. (B and C) Myeloid cell subsets of B16 tumours were analysed. (D and E) Myeloid cell subsets of LLC tumours were analysed. n equals the number of tumours. * indicates $p<0.05$ using a two-tailed, unpaired *t*-test. Data are presented as mean ± SD.

Together, these data show that FIH-deficient animals tend to show an increased percentage of tumour-infiltrating myeloid cells.

4.2.2.4 TAMs from FIH-deficient LLC tumour-bearing mice show altered expression of *Arg1*, *Nos2*, and *Il-6*

To assess the expression of inflammatory mediators by myeloid cells, TAMs were isolated from primary tumours (Figure 4.5, A and C) and gene expression was examined by RT-qPCR (Figure 4.5, B and D). The panel of genes of interest includes *Arg1*, *Vegf*, *Il-10*, *Il-6*, and *Nos2*, which are known to be induced or upregulated in TAMs (Williams, Yeh, and Soloff 2016).

For B16 tumour-bearing mice, macrophages from B16 tumour and spleen samples were sorted by FACS (Figure 4.5A). Compared with the spleen macrophages, mRNA levels of all the mediators appeared to be upregulated in TAMs (Figure 4.5B). FIH heterozygosity tended to promote the induction of *Arg1* and *Nos2* in TAMs, yet the effect was not statistically significant (Figure 4.5B).

TAMs of LLC tumour samples were isolated by MACS technique. Flow cytometry analysis of the purified sample confirmed that TAMs were significantly enriched (sample purity before vs after enrichment: 13.6 vs 78.3%, $p<0.0001$; Figure 4.5C). TAMs from FIH-null mice showed increased expression of *Arg1* (fold

change 1.85, p=0.0366; *t*-test), *Nos2* (fold change 3.13, p=0.0034; *t*-test), and a reduced level of *Il-6* (fold change 0.37, p=0.0287; *t*-test) than the WT counterparts (Figure 4.5D).

Among the targets examined, *Arg1* was the most abundantly expressed gene in TAMs isolated from both types of tumours, followed by *Il-10*, *Il-6*, and *Nos2* (Figure 4.5, B and D). The expression of *Vegf*, a well-defined HIF target gene (Forsythe et al. 1996), was not affected by FIH status in TAMs from either type of tumours (Figure 4.5, B and D).

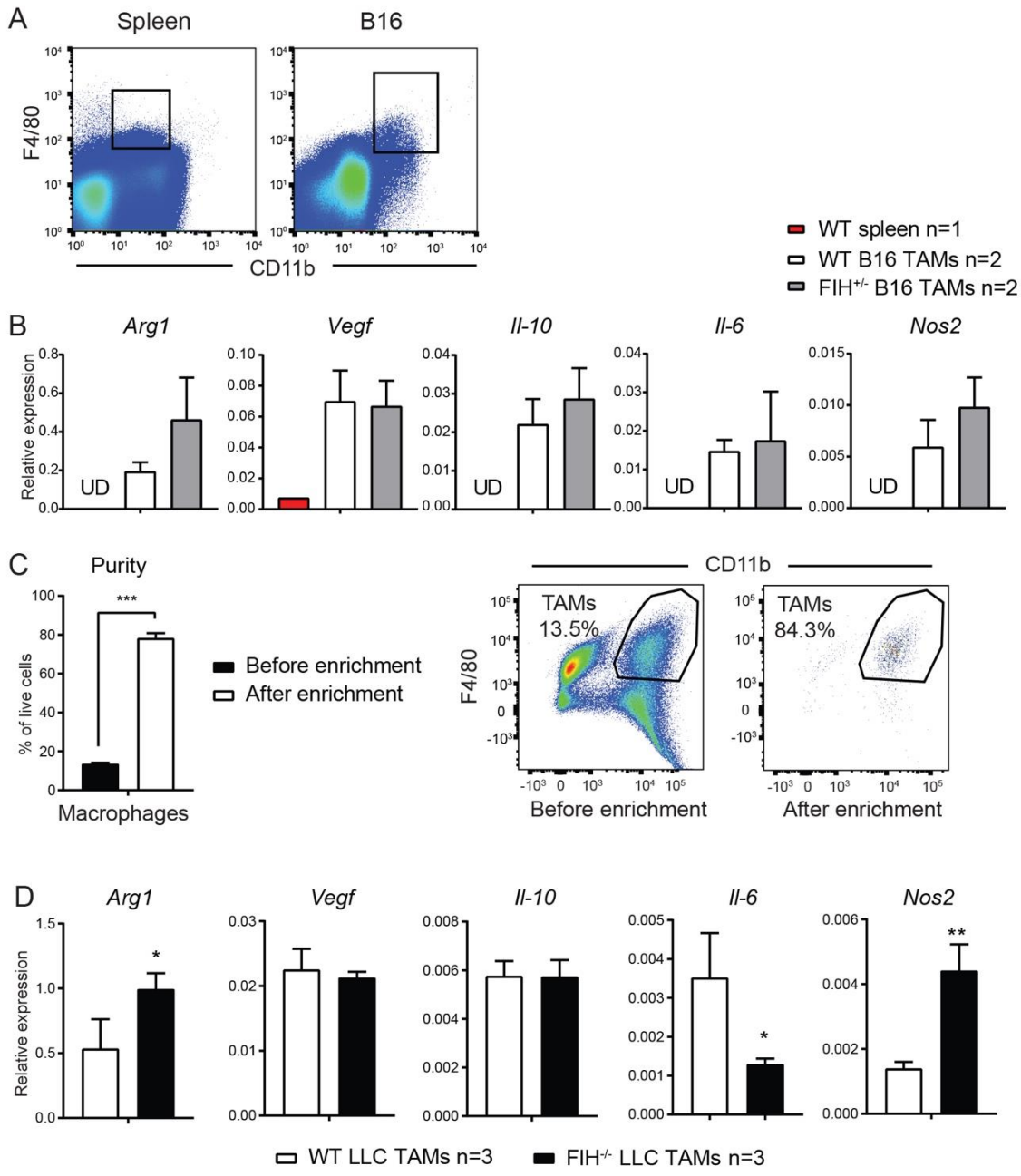

Figure 4.5 TAMs of FIH$^{-/-}$ LLC tumour-bearing mice show increased expression of *Arg1* and *Nos2*, and reduced expression of *Il-6*

(A) B16 tumour samples from WT and FIH$^{+/-}$ animals, as well as the spleen of a WT B16-bearing mouse, were stained with anti-CD11b and anti-F4/80 antibodies. Macrophages (CD11b^{+} F4/80^{+}, as gated) were sorted by FACS. (B) Expression of the indicated genes normalised by γ-actin level was evaluated by RT-qPCR. (C) LLC tumour samples from WT and FIH$^{-/-}$ animals were isolated by MACS using anti-F4/80 magnetic beads. Isolated cells were stained with

anti-CD11b and anti-F4/80 antibodies and the purity of macrophages was examined by flow cytometry. (D) Expression of the indicated genes normalised by γ-actin level was analysed by RT-qPCR. * indicates $p<0.05$ and ** indicates $p<0.01$ using a two-tailed, unpaired *t*-test. n represents the number of tumour/spleen samples. The histogram bars are displayed as mean ± SD. UD, undetectable.

Together, these data show that LLC tumours established in FIH-deficient animals display differing expression of *Arg1*, *Nos2*, and *Il-6* in TAMs.

4.2.2.5 FIH does not profoundly affect the immune response in the spleens of B16 tumour-bearing mice

To test whether host expression of FIH could also affect tumour-induced inflammation in the secondary lymphoid tissue, spleens of B16 tumour-bearing mice were collected and analysed by flow cytometry. FIH deficiency did not profoundly change the number of CD4 T cells, CD8 T cells, B cells, or Treg cells in the spleen (Figure 4.6, A and B). Cytokine production by CD4 T cells and CD8 T cells was not affected by FIH status (Figure 4.6, C and D). WT and FIH-mutant animals also showed similar constituents of myeloid subsets in the spleen (Figure 4.6E).

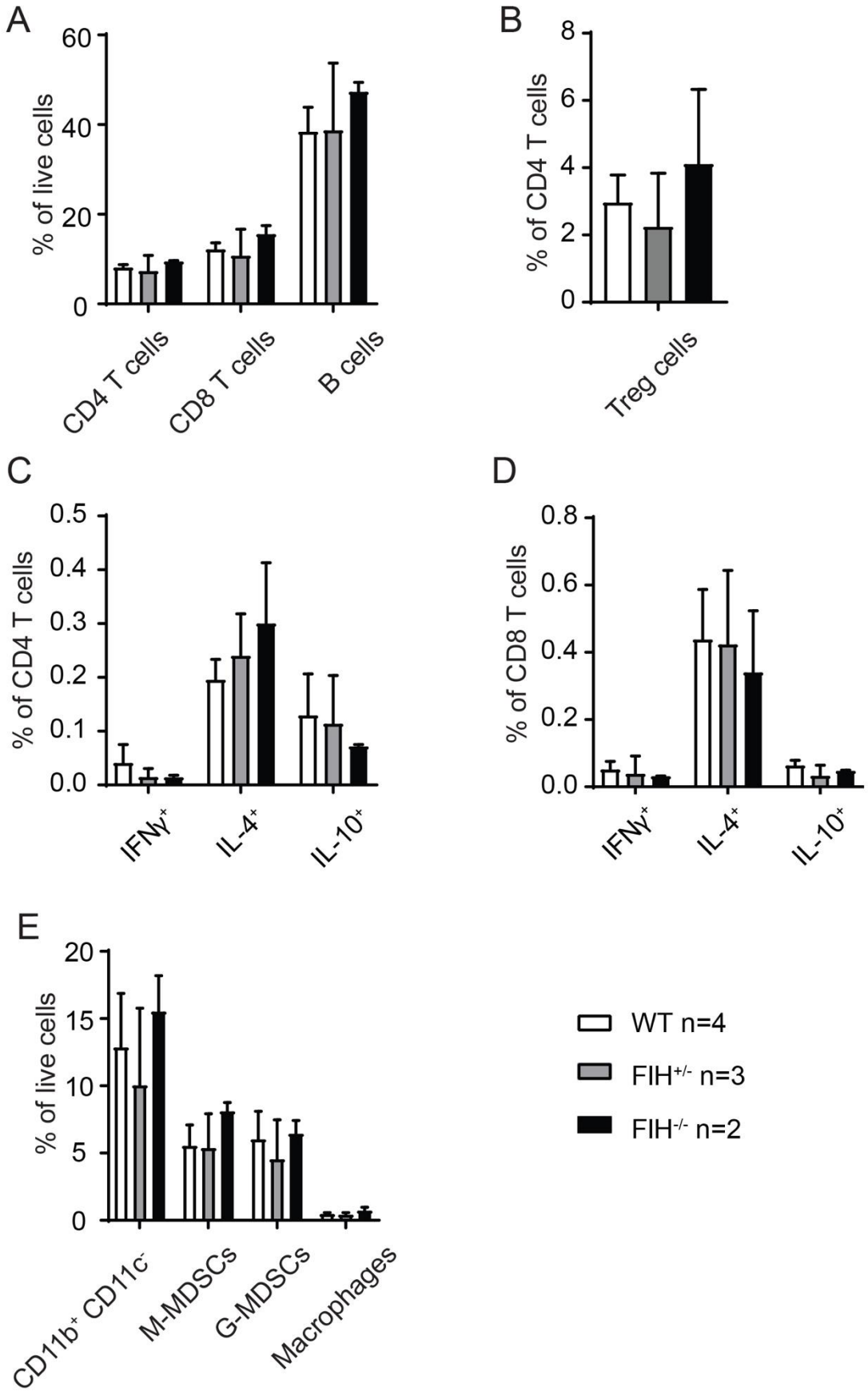
A
% of live cells
60
40
20
0
CD4 T cells
CD8 T cells
B cells
B
% of CD4 T cells
8
6
4
2
0
Treg cells
C
% of CD4 T cells
0.5
0.4
0.3
0.2
0.1
0.0
IFNγ+
IL-4+
IL-10+
D
% of CD8 T cells
0.8
0.6
0.4
0.2
0.0
IFNγ+
IL-4+
IL-10+
E
% of live cells
20
15
10
5
0
CD11b+ CD11c-
M-MDSCs
G-MDSCs
Macrophages
WT n=4
FIH+/- n=3
FIH-/- n=2

Figure 4.6 FIH does not profoundly affect the immune response in the spleen of B16 tumour-bearing mice
Immune responses in the spleens of B16 tumour-bearing animals were characterised by flow cytometry. CD4 T cells, CD8 T cells, B cells, and Treg cells were identified using antibodies in Panel 1, Table 2.7; CD4 T cells and CD8 T cells that produced IFNγ, IL-4, or IL-10 were distinguished using antibodies in Panel 3, Table 2.7; and $CD11b^+$ $CD11c^-$, M-MDSCs, G-MDSCs, and macrophages were identified by antibodies in Panel 2, Table 2.7. (A) Percentages of CD4 T cells, CD8 T cells, and B cells out of live cells are shown. (B) Percentage of Treg cells out of CD4 T cells is shown. (C) Percentages of CD4 T cells producing indicated cytokines are shown. (D) Percentages of CD8 T cells producing indicated cytokines are shown. (E) Fractions of myeloid subsets are shown. A two-tailed, unpaired *t*-test was performed and revealed no significant difference between samples from WT and FIH-mutant animals. n represents the number of experimental animals. The histogram bars are displayed as mean ± SD.

So far, I have shown that FIH deficiency does not affect the immune cell components in major lymphoid organs (Figure 4.1). When inoculated with syngeneic tumour cells, both $FIH^{+/-}$ and $FIH^{-/-}$ animals show enhanced tumour growth compared with WT mice (Figure 4.2). Host expression of FIH does not have a pronounced impact on the immune response in the spleen (Figure 4.6). However, it does affect the intra-tumoural immune profile. In terms of TILs, reduced FIH expression results in an increased CD4 TIL population in B16 tumours (Figure 4.3A), but a decreased CD4 TIL fraction in LLC tumours (Figure 4.3E); with respect to myeloid cells, FIH deficiency in the host leads to an increased population of $CD11b^+$ cells (Figure 4.4D) and the aberrant expression of *Il-6*, *Arg1* and *Nos2* in TAMs in LLC tumours (Figure 4.5D).

4.2.3 Mice deficient of myeloid FIH show enhanced tumour growth

In light of the enhanced tumour growth in $FIH^{-/-}$ animals, one question that arose was in which type(s) of cells does FIH expression mediate tumour suppression. Given that myeloid cells remained a large constituent of tumour-infiltrating immune cells (Figure 4.4, B–E) and a lack of FIH expression might alter the expression of certain inflammatory mediators in TAMs in both tumour models (Figure 4.5, B and D), one plausible hypothesis was that myeloid expression of FIH could play a critical role in modulating the tumour immune response. To test this, $FIH^{fl/fl}$ mice were crossed to a LysM-Cre-carrying strain on a C57BL/6 background to generate FIH MKO mice.

In the following sets of experiments, B16 or LLC tumour cells were administered subcutaneously in WT and FIH MKO mice, and immune responses in their tumours and spleens were characterised by flow cytometry.

4.2.3.1 Mice lacking FIH in myeloid cells exhibit enhanced tumour growth

WT and FIH MKO animals were injected with B16 or LLC tumour cells subcutaneously and monitored on a daily basis. The growth curve of individual tumours is shown in Figure 4.7, A and C, whereas the average size of tumours at the indicated time point is shown in Figure 4.7, B and D.

On day 13 post-injection, FIH MKO mice showed an increased volume of B16 tumours compared with WT animals (WT vs FIH MKO: 202.4 mm^3 vs 337.1 mm^3, p=0.0348; *t*-test; Figure 4.7B). For mice receiving LLC cells, FIH MKO mice showed significantly increased tumour volumes at day 13 (WT vs MKO: 104.5 mm^3 vs 161.5 mm^3, p=0.0464; *t*-test) and day 14 (WT vs MKO: 121.1 mm^3 vs 187.3

mm^3, p=0.0429; *t*-test; Figure 4.7D) post-injection. LLC tumours from FIH MKO animals also tended to show increased weights compared with the tumours established in WT animals, although the difference was not significant (Figure 4.7E).

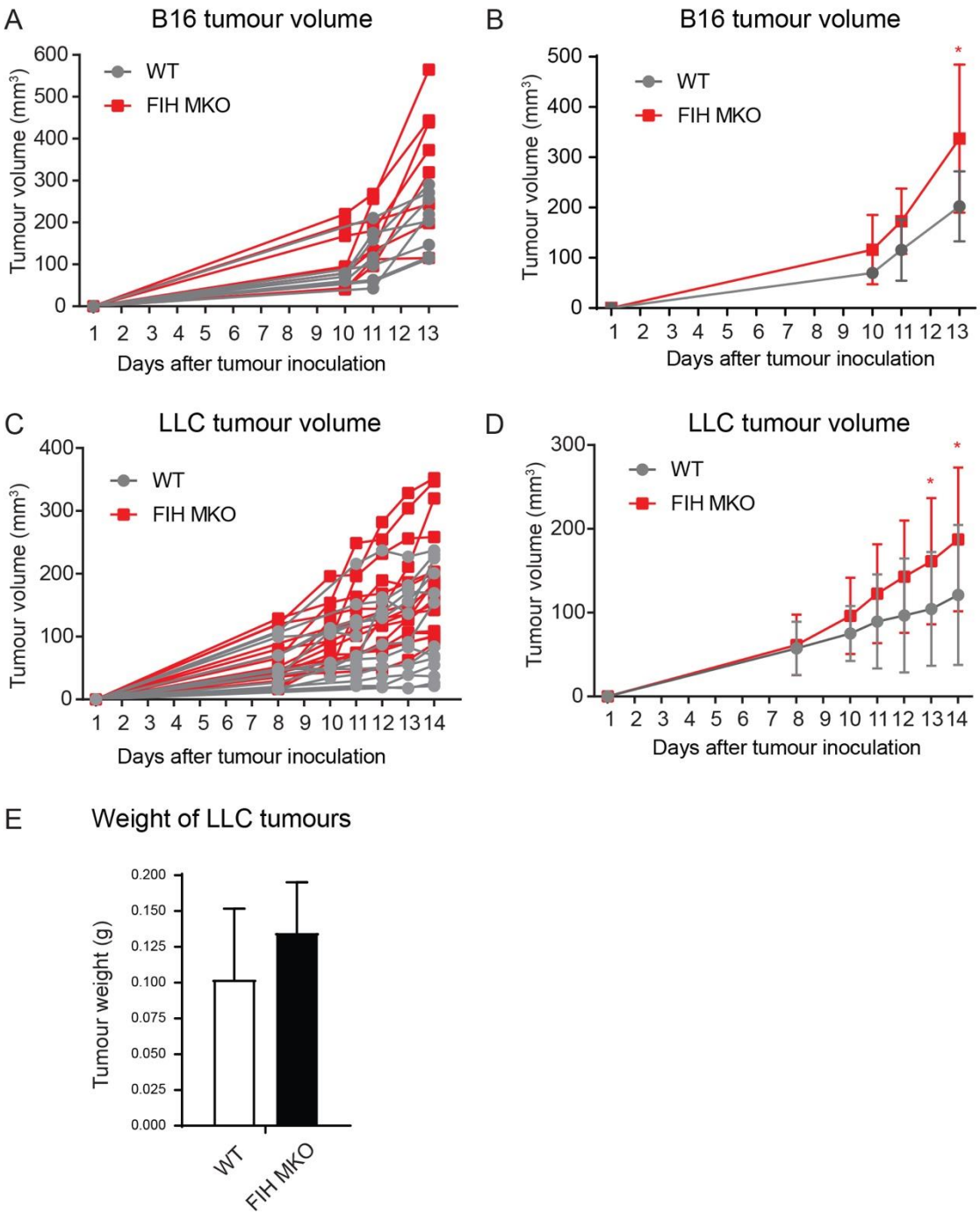

Figure 4.7 FIH MKO animals show enhanced tumour growth
B16 or LLC cells were subcutaneously injected into WT and FIH MKO mice. (A and B) A total of 2×10^5 B16 cells were injected into five WT and four FIH MKO animals at both flanks. Volumes of individual tumours are shown in A and averaged tumour volumes are shown in B. The number of tumours and mice measured at indicated time points is shown in Table S4. (C and D) A total of 4×10^5 LLC cells were injected into nine WT and nine FIH MKO mice at both flanks. Volumes of individual tumours are shown in C, and averaged volumes are shown in D. The number of tumours and mice measured at indicated time points is shown in Table S5. Tumour sizes follow a normal distribution, and an *F* test revealed no significant difference in variance of tumour volumes between the compared groups. (E) Average weights of LLC tumours resected on day 14 from WT (tumour number=13) and FIH MKO (tumour number=17) animals are shown. An unpaired *t*-test was performed to compare the mean value between WT and FIH MKO animals at each time point. * indicates $p<0.05$. The bars are displayed as mean ± SD.

Collectively, these data show that FIH deficiency in myeloid cells promotes the growth of B16 and LLC cells.

4.2.3.2 Mice lacking FIH in myeloid cells show a reduced population of CD4 TILs

At the conclusion of the tumour study, tumours were collected and their immune cell composition was analysed by flow cytometry.

In the B16 model, intra-tumoural immune profile resembled that of the total knockout colony (Figure 4.3, A and B): CD4 T cells made up the majority of the live cells in the tumour samples (Figure 4.8A); the proportion of CD8 T cells was substantially smaller than that of CD4 T cells (Figure 4.8, A and B). Compared with the WT, tumours from FIH MKO animals showed a reduced population of CD4 T cells (WT vs FIH MKO 73.4% vs 57.6%, p=0.0138; *t*-test; Figure 4.8A), although

the percentage of CD4 T cells producing IFNγ, IL-4, or IL-10 remained unchanged (Figure 4.8D). The number of CD8 T cells and Treg cells in B16 tumour samples was not affected by FIH status in the myeloid cells (Figure 4.8, B and C).

LLC tumours established in FIH MKO mice also showed similar TIL components to those of $FIH^{-/-}$ mice (Figure 4.3, E–G and Figure 4.8, E, F, and H) in that both CD4 and CD8 TIL populations were detected at similarly low level. FIH deficiency in myeloid cells led to a reduced percentage of CD4 TILs (WT vs FIH MKO 1.34% vs 0.72%, p=0.0013; *t*-test; Figure 4.8E) without affecting the number of CD8 or Treg cells (Figure 4.8, F and G). Production of IFNγ, IL-4, and IL-10 by CD4 was not affected by FIH status (Figure 4.8H), similar to what was observed in the B16 tumours (Figure 4.8D).

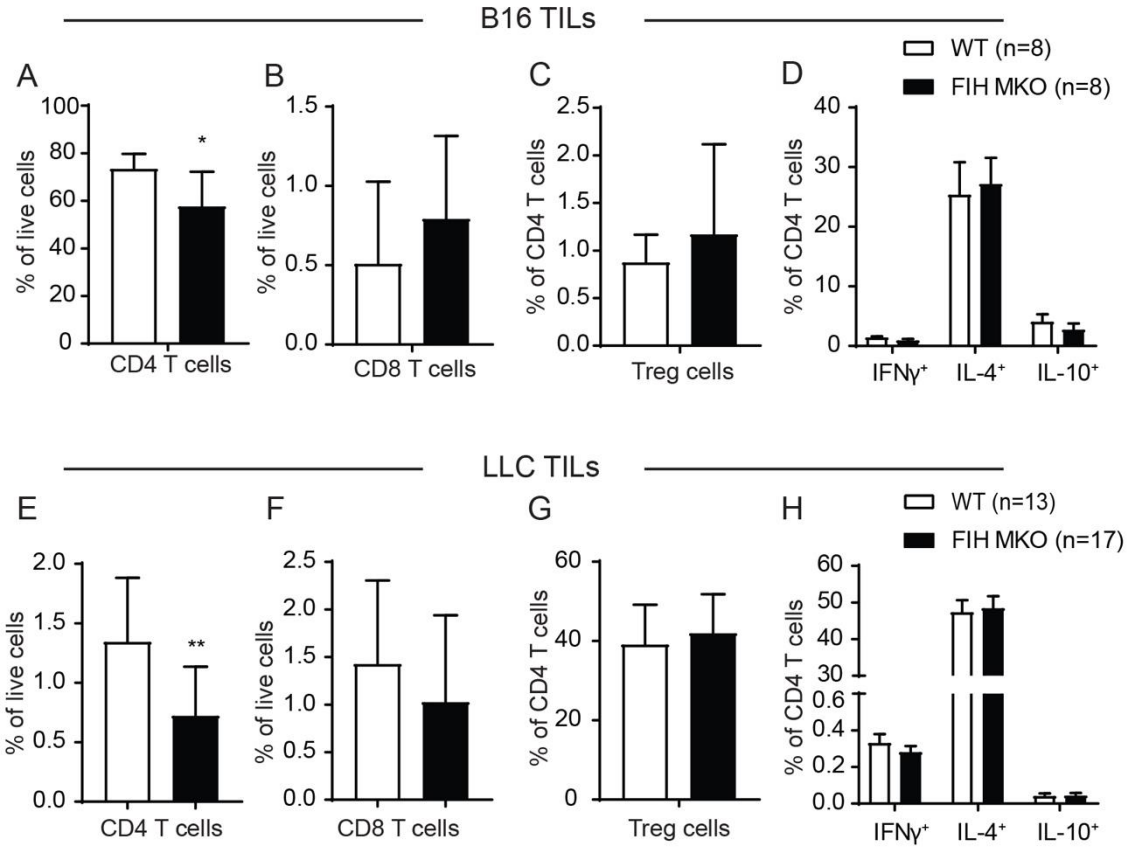

Figure 4.8 Myeloid deletion of FIH results in a reduced population of CD4 TILs

B16 and LLC samples were collected on days 13 and 14, respectively, and analysed by flow cytometry. To determine the number of CD4 T cells, CD8 T cells, and Treg cells, samples were stained with antibodies in Panel 4, Table 2.7. To analyse the production of IFNγ, IL-4, and IL-10 by CD4 T cells, samples were stained with antibodies in Panel 5, Table 2.7. (A–D) The lymphoid subsets in B16 tumours were analysed. (E–H) The lymphoid subsets in LLC tumours were analysed. n indicates number of tumours. * indicates $p<0.05$ and ** indicates $p<0.01$ using a two-tailed, unpaired *t*-test. Data are presented as mean ± SD.

To further characterise the activation states of TILs, tumour samples were stained with antibodies shown in Panel 4 of Table 2.7 to identify naive T cells, central memory T (T_{CM}) cells, and effector memory T (T_{EM}) cells (Dillon et al. 2004), as demonstrated in Figure 4.9, A (for B16 TILs) and K (for LLC TILs).

In B16 tumours, the majority of CD4 and CD8 T cells were T_{EM} (Figure 4.9, B and E), with a small fraction of T_{CM} and naive cells being present (Figure 4.9, C, D, F, and G). No overt change in the quantity of T_{EM} and T_{CM} cells was observed in the tumours of FIH MKO mice (Figure 4.9, B–G). Treg cells, in contrast, were predominantly naive (Figure 4.9J). Treg cells from FIH MKO animals showed a marginally decreased proportion of naive cells (fold change=0.88, p=0.0124; *t*-test; Figure 4.9J) and an increased fraction of T_{CM} (fold change=3.33, p=0.0333; *t*-test; Figure 4.9I).

T cells in LLC tumours were mostly T_{EM} (Figure 4.9 L, O, and R). Loss of FIH did not change the T_{EM}, T_{CM}, and naive T cell compositions (Figure 4.9, L–T).

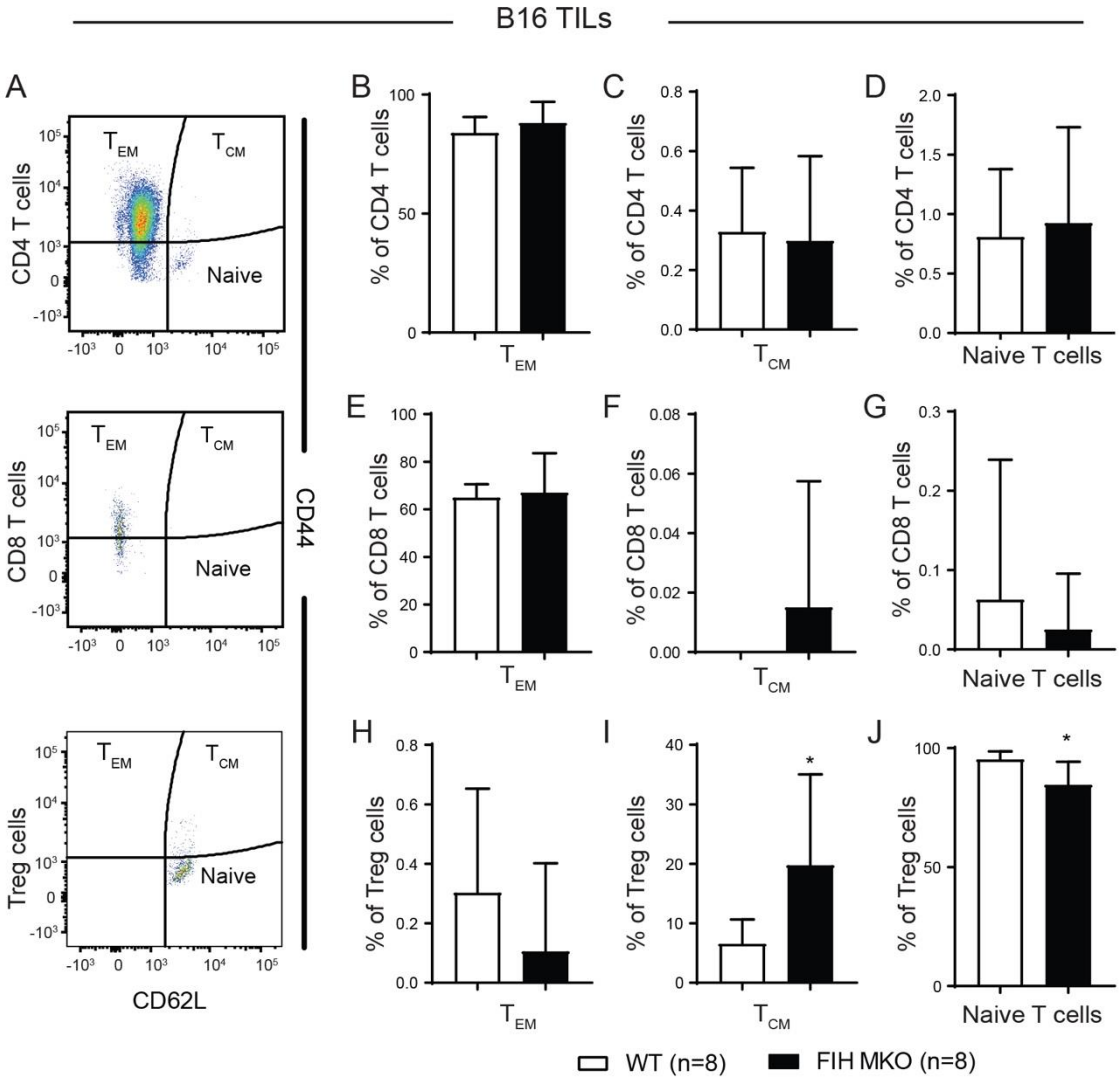
B16 TILs
A
CD4 T cells
CD8 T cells
Treg cells
T EM
T CM
Naive
CD44
CD62L
B
C
D
E
F
G
H
I
J
% of CD4 T cells
% of CD8 T cells
% of Treg cells
T EM
T CM
Naive T cells
*
WT (n=8)
FIH MKO (n=8)

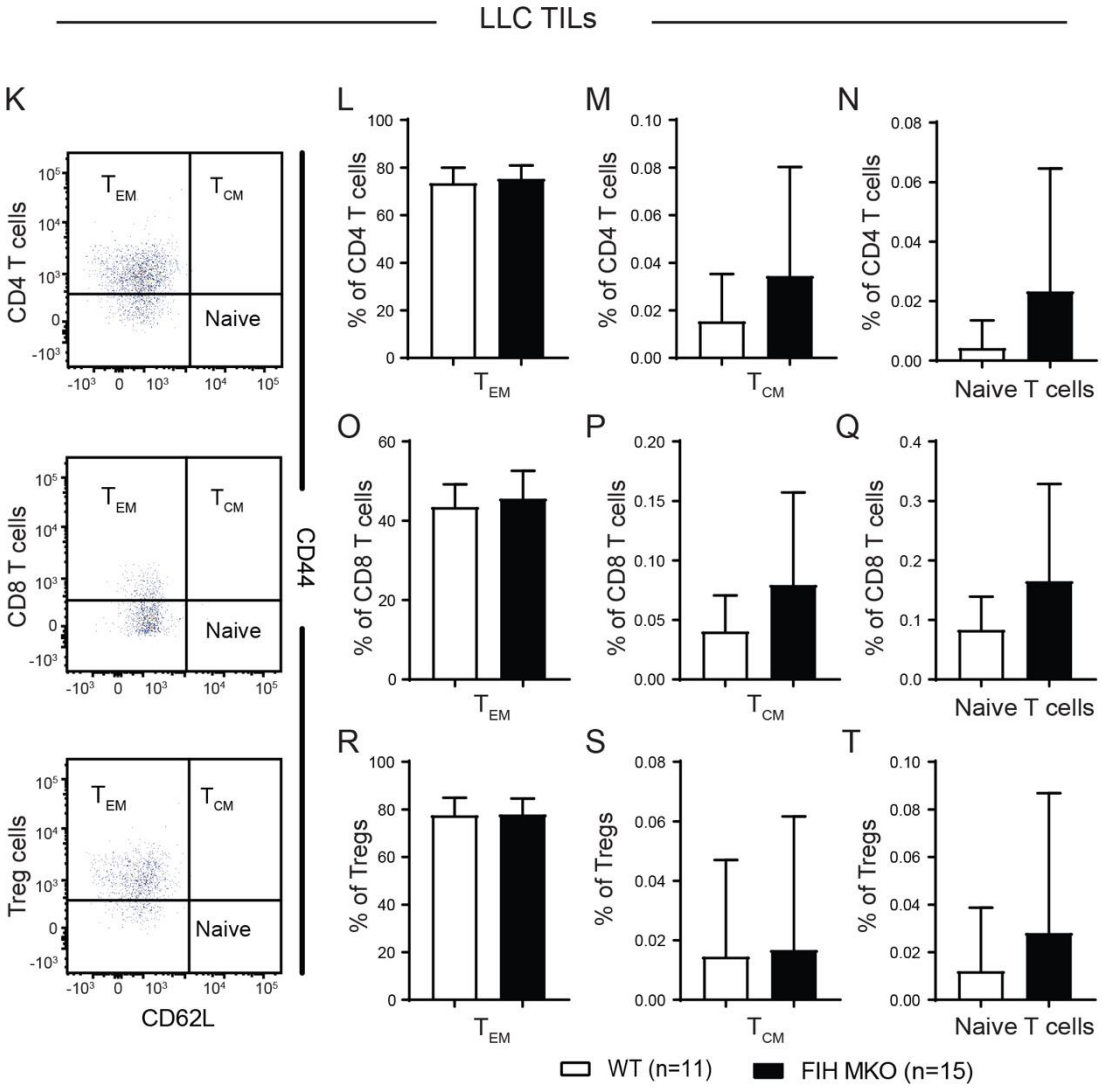

Figure 4.9 FIH expression in myeloid cells affects the population of T_{CM} and naive Treg cells in B16 tumours

B16 and LLC tumour samples were stained with antibodies against lymphocyte markers together with CD44 and CD62L (Panel 4 in Table 2.7) and analysed by flow cytometry. CD4, CD8, and Treg cells were further characterised based on CD44/CD62L expression as T_{EM} cells ($CD62L^{-}$ $CD44^{int\text{-}hi}$), T_{CM} cells ($CD62L^{+}$ $CD44^{int\text{-}hi}$), and naive T cells ($CD62L^{+}$ $CD44^{lo}$). (A) Gating strategy used in analysing B16 samples is shown. (B–J) B16 TILs were analysed. B–D: CD4 T cells; E–G: CD8 T cells; H–J: Treg cells. (K) Gating strategy used in analysing LLC samples is shown. (L–T) LLC TILs were analysed. L-N: CD4 T cells; O-Q: CD8 T cells; R-T: Treg cells. * indicates $p<0.05$ using a two-tailed, unpaired *t*-test. n indicates number of tumours. Data are shown as mean ± SD.

Together, these data suggest that FIH expression in myeloid cells does not overly change T_{EM}, T_{CM}, and naive T cell compositions of TILs, except for the T_{CM} and naive Treg cell subsets in B16 tumours.

4.2.3.3 Mice deficient of myeloid FIH show an increased population of TAMs in B16 tumours

To characterise the tumour-infiltrating myeloid cells, myeloid cells ($CD11b^+$) and myeloid subsets (G-MDSCs, M-MDSCs, and TAMs) were identified in the tumour samples.

The prevalence of myeloid cells in B16 and LLC tumours remained similar across the two mouse colonies tested (FIH total knockout and FIH myeloid-specific knockout animals; Figure 4.4, B and D and Figure 4.10, A and C). B16 tumours derived from FIH MKO mice showed an increased population of $CD11b^+$ myeloid cells in comparison with their WT counterparts (fold change=1.52, p=0.0334; *t*-test; Figure 4.10A), which could be attributed by the increased fraction of TAMs (fold change=1.61, p=0.0253; *t*-test; Figure 4.10B). However, this was not reproduced in LLC tumours, where WT and FIH MKO animals displayed a similar composition of tumour-infiltrating myeloid cells (Figure 4.10, C and D).

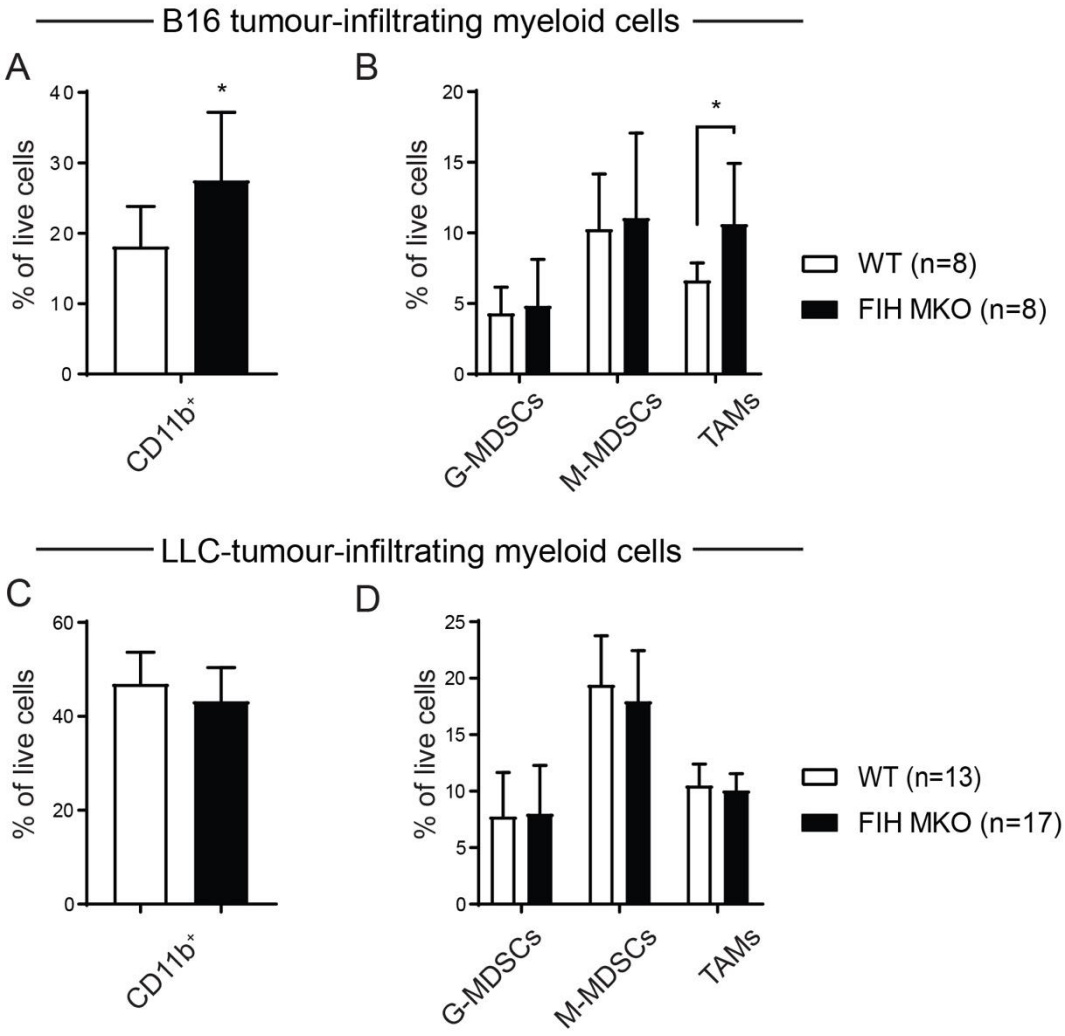

Figure 4.10 B16 tumours grown in FIH MKO mice show an increased fraction of TAMs

B16 and LLC tumour samples were stained with antibodies shown in Panel 6, Table 2.7 and analysed by flow cytometry. Myeloid cells ($CD11b^+$), G-MDSCs ($CD11b^+$ $CD11c^-$ $Ly\text{-}6G^+$ $Ly\text{-}6C^{int}$), M-MDSCs ($CD11b^+$ $CD11c^-$ $Ly\text{-}6G^-$ $Ly\text{-}6C^{hi}$), and TAMs ($CD11b^+$ $CD11c^-$ $F4/80^+$) were identified. (A) B16 tumours established in WT and FIH MKO animals were analysed. (B) LLC tumours developed in WT and FIH MKO mice were analysed. n indicates number of tumours. The graphs are plotted as mean ± SD.

Together, these data show that loss of FIH in myeloid cells leads to an increased population of TAMs in B16 but not in LLC tumours.

4.2.3.4 TAMs in mice deficient of myeloid FIH exhibit increased PD-L1 and ARG1 expression

TAMs are known to express a range of ligands that interact with T cells, including MHC class II, which mediates antigen presentation to T cells, and CD86 and PD-L1/L2, which can bind to T cell inhibitory receptors CTLA-4 and PD-1, respectively (Noy and Pollard 2014). Given the reduced population of CD4 TILs observed in FIH MKO animals, the expression of MHC class II, CD86, PD-L1, and PD-L2 on $CD11b^+$ myeloid cells and TAMs was examined (Figure 4.11A).

Among the B16-infiltrating $CD11b^+$ myeloid cells, an increased population of $CD86^+$ cells and $PD\text{-}L1^+$ cells was observed in FIH MKO animals (WT vs FIH MKO $CD86^+$: 24.89% vs 31.08%, p=0.0487; $PD\text{-}L1^+$: 26.3% vs 42.48%, p<0.0001; *t*-test Figure 4.11B), which was also recapitulated in TAMs (WT vs FIH MKO $CD86^+$: 38.35% vs 47.61%, p=0.0467; $PD\text{-}L1^+$: 44.48% vs 66.16%, p=0.0023; *t*-test; Figure 4.11C). In addition, TAMs derived from FIH MKO animals showed an increased MHC class II^+ population (WT vs FIH MKO: 45.80% vs 68.18%, p=0.0342, *t*-test; Figure 4.11C).

In the LLC model, an increased fraction of $PD\text{-}L1^+$ cells was observed in the intra-tumoural $CD11b^+$ population of FIH MKO animals (WT vs FIH MKO: 35.68% vs 41.89%, p=0.0148, *t*-test; Figure 4.11D), which was also true for the TAMs of FIH MKO mice (WT vs FIH MKO: 62.35% vs 73.06%, p=0.0015, *t*-test; Figure 4.11E).

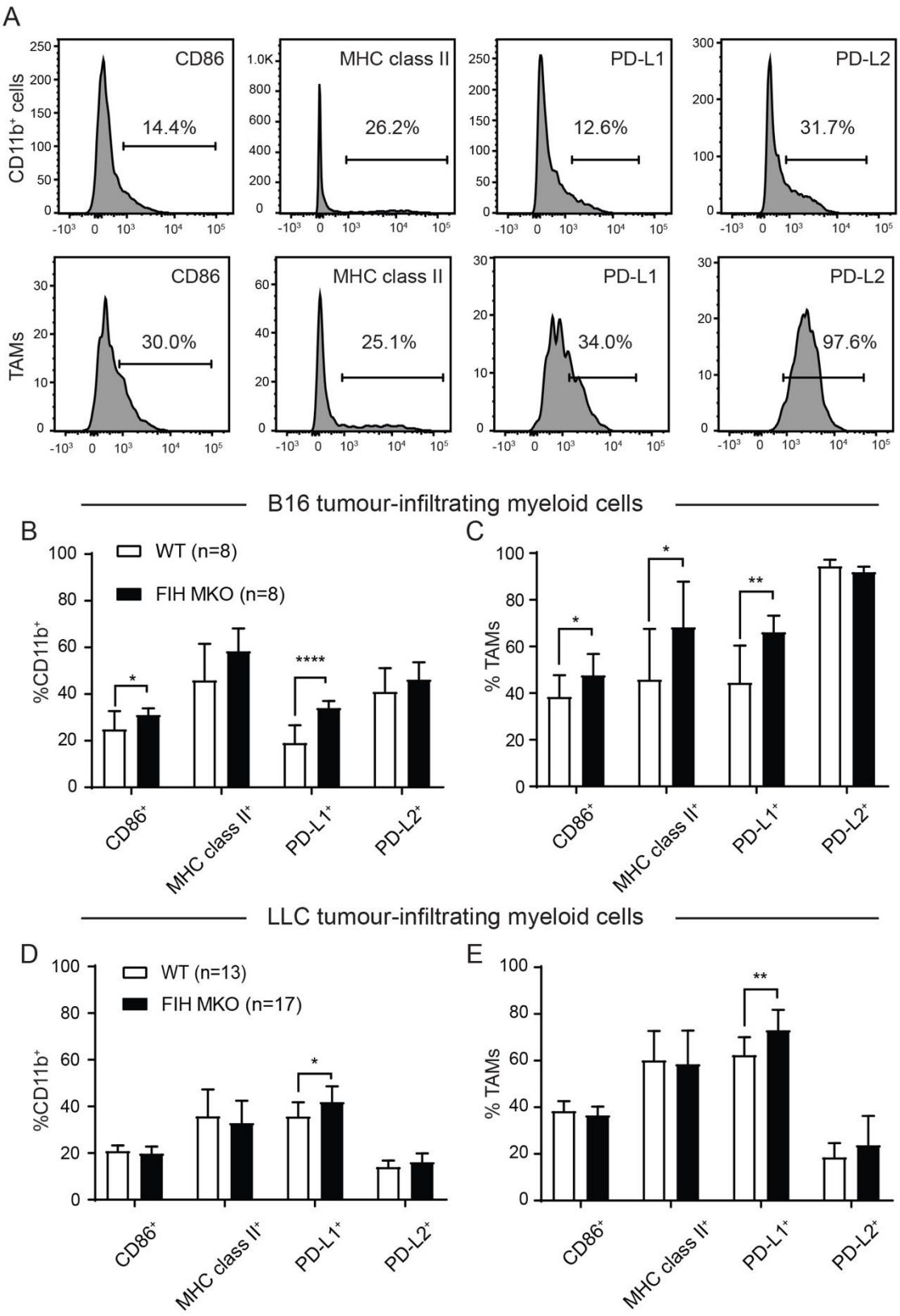
A
CD11b+ cells
CD86
14.4%
MHC class II
26.2%
PD-L1
12.6%
PD-L2
31.7%
TAMs
CD86
30.0%
MHC class II
25.1%
PD-L1
34.0%
PD-L2
97.6%
B16 tumour-infiltrating myeloid cells
B
WT (n=8)
FIH MKO (n=8)
%CD11b+
CD86+
MHC class II+
PD-L1+
PD-L2+
C
% TAMs
LLC tumour-infiltrating myeloid cells
D
WT (n=13)
FIH MKO (n=17)
E

Figure 4.11 FIH deficiency in myeloid cells results in an increased fraction of PD-L1$^+$ TAMs

B16 and LLC tumour samples were stained with antibodies shown in Panel 6, Table 2.7, followed by flow cytometry analysis. (A) Myeloid cells (CD11b$^+$) and TAMs (CD11b$^+$ CD11c$^-$ F4/80$^+$) were distinguished, and cells expressing CD86, MHC class II, PD-L1, and PD-L2 in each parental population were identified. Representative dot plots of a B16 tumour sample are shown. (B and C) B16-infiltrating CD11b$^+$ cells and TAMs were analysed. (D and E) LLC-infiltrating CD11b$^+$ cells and TAMs were analysed. n represents number of tumours. * indicates $p<0.05$, ** indicates $p<0.01$, and **** indicates $p<0.0001$ using a two-tailed, unpaired *t*-test. Data are displayed as mean ± SD.

Give that myeloid expression of FIH affected the quantity of CD4 TILs, the expression of ARG1, a functional marker of TAMs that mediates T cell proliferation arrest (Colegio et al. 2015), was examined (Figure 4.12A).

In the B16 tumour model, TAMs of FIH MKO animals showed an increased percentage of ARG1$^+$ cells (WT vs FIH MKO: 16.94% vs 21.28%, p=0.0290; *t*-test; Figure 4.12B).

In the LLC tumour model, ARG1 expression in G-MDSCs, M-MDSCs, and TAMs was examined. Among these three myeloid subsets, TAMs showed the largest ARG1$^+$ composition, followed by M-MDSCs and G-MDSCs (Figure 4.12C). An increased population of ARG1$^+$ cells was detected in the TAMs (WT vs FIH MKO: 44.04% vs 52.82%, p=0.0112; *t*-test) and G-MDSCs (WT vs FIH MKO: 2.48% vs 4.24%, p=0.0012; *t*-test) of the FIH MKO animals (Figure 4.12C).

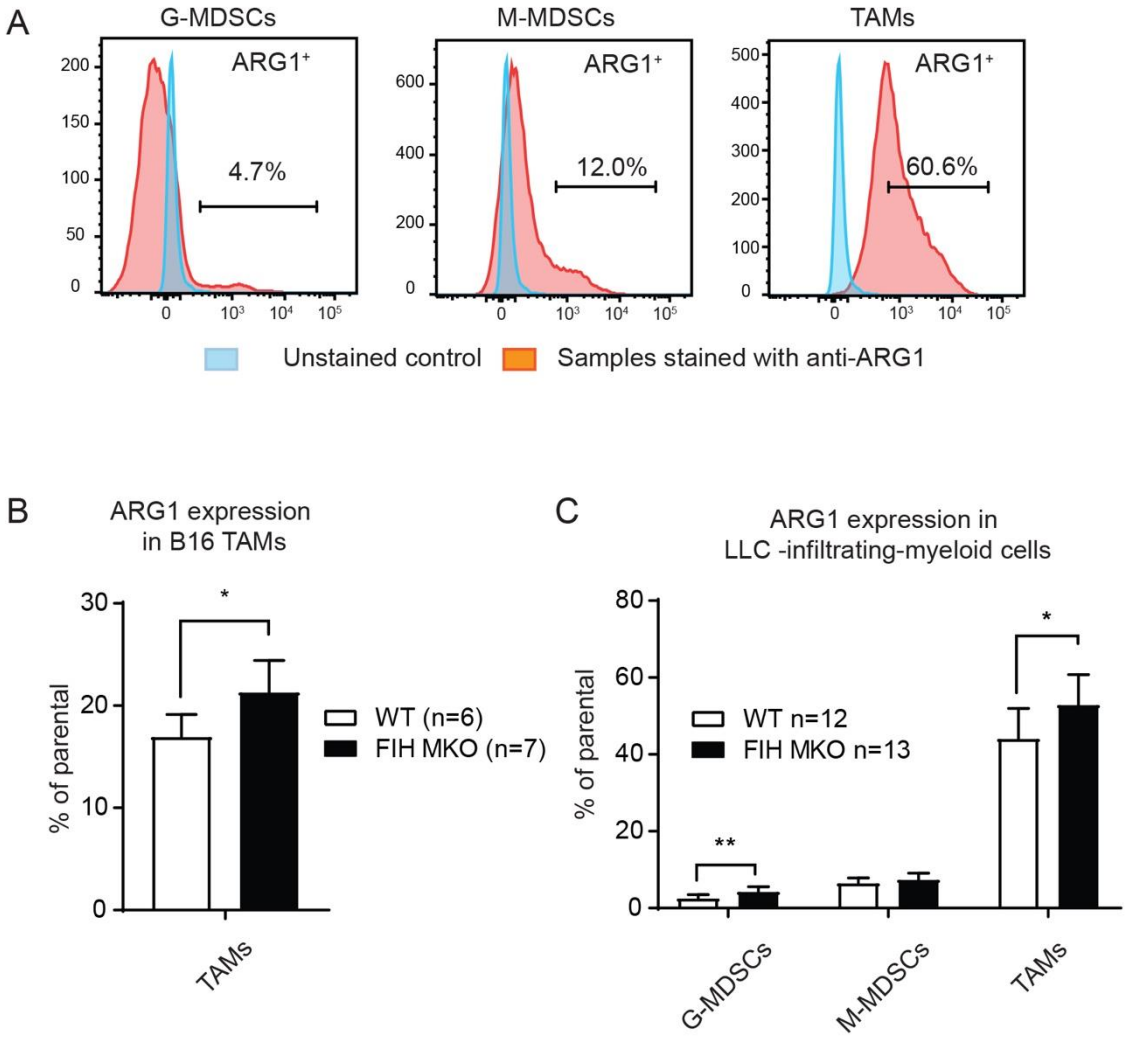

Figure 4.12 FIH MKO animals show an increased proportion of ARG1$^+$ TAMs

B16 and LLC tumour samples were stained with antibodies shown in Panel 5 and Panel 7 in Table 2.7, respectively, followed by flow cytometry analysis. (A) Demonstration of the identification of ARG1$^+$ populations in G-MDSCs, M-MDSCs, and TAMs in an LLC tumour sample is shown. (B) The percentage of ARG1$^+$ in TAMs of B16 tumour samples is shown. (C) The percentages of ARG1$^+$ cells in G-MDSCs (CD11b$^+$ CD11c$^-$ Ly-6G$^+$ Ly-6C^{int}), M-MDSCs (CD11b$^+$ CD11c$^-$ Ly-6G$^-$ Ly-6C^{hi}), and TAMs (CD11b$^+$ CD11c$^-$ F4/80$^+$) are shown. n indicates number of tumours. * indicates $p<0.05$, and ** indicates $p<0.01$ using a two-tailed, unpaired *t*-test. Data are presented as mean ± SD.

Taken together, these data show that TAMs of FIH MKO animals exhibit an increased population of PD-L1$^+$ and ARG1$^+$ cells.

4.2.3.5 Myeloid expression of FIH affects tumour immune response in the spleen of B16 tumour-bearing mice

MDSCs have been reported to be expanded in the spleens of cancer patients and tumour-bearing mice (Talmadge and Gabrilovich 2013; Jordan 2017), indicating the involvement of peripheral lymphoid organs in the tumour immune response. To examine whether FIH expression could also affect the immune response in the spleen, splenocytes from B16 and LLC tumour-bearing mice were analysed by flow cytometry techniques.

In the B16 model, the population of lymphocyte subsets (CD4 T cells, CD8 T cells, B cells, and Treg cells) and myeloid cell subsets (CD11b$^+$ CD11c$^-$, M-MDSCs, G-MDSCs, and macrophages) remained unchanged without myeloid FIH expression (Figure 4.13, A, B and E). However, the number of IFNγ-producing CD4 and CD8 T cells was significantly reduced in the spleen of FIH MKO animals (WT vs FIH MKO: % IFNγ$^+$ cells in CD4 T cells 3.19 vs 1.26, p=0.0114; % IFNγ$^+$ cells in CD8 T cells 7.82 vs 4.34, p=0.0471; *t*-test; Figure 4.13, C and D).

In the LLC model, in contrast, IFNγ expression was not detectable in CD4 T cells (Figure 4.13H). FIH expression status in myeloid cells did not affect the composition of T cell subsets and B cells (Figure 4.13, F and G), or IL-10 production by CD4 T cells (Figure 4.13H). Myeloid subsets and their expression of MHC class II, PD-L1, and PD-L2 were not altered by FIH deletion in the myeloid compartment (Figure 4.13, I–K), although an increased population of CD86$^+$ cells was observed in the macrophages of FIH MKO mice (WT vs FIH MKO: 2.43% vs 3.51%, p=0.0271; *t*-test; Figure 4.13K).

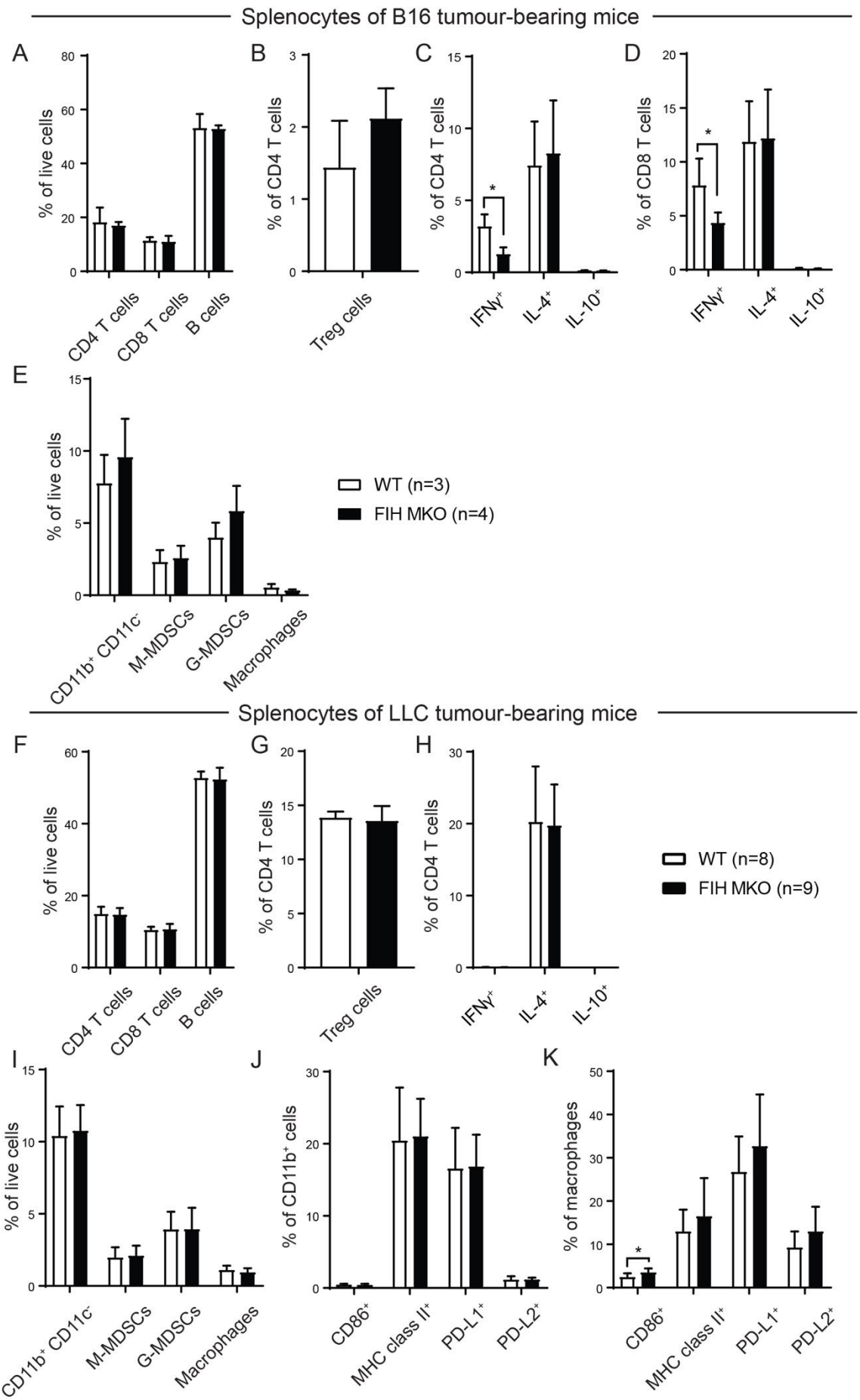
Splenocytes of B16 tumour-bearing mice
A
% of live cells
CD4 T cells
CD8 T cells
B cells
B
% of CD4 T cells
Treg cells
C
% of CD4 T cells
IFNγ+
IL-4+
IL-10+
D
% of CD8 T cells
IFNγ+
IL-4+
IL-10+
E
% of live cells
CD11b+ CD11c-
M-MDSCs
G-MDSCs
Macrophages
WT (n=3)
FIH MKO (n=4)
Splenocytes of LLC tumour-bearing mice
F
% of live cells
CD4 T cells
CD8 T cells
B cells
G
% of CD4 T cells
Treg cells
H
% of CD4 T cells
IFNγ+
IL-4+
IL-10+
WT (n=8)
FIH MKO (n=9)
I
% of live cells
CD11b+ CD11c-
M-MDSCs
G-MDSCs
Macrophages
J
% of CD11b+ cells
CD86+
MHC class II+
PD-L1+
PD-L2+
K
% of macrophages
CD86+
MHC class II+
PD-L1+
PD-L2+

Figure 4.13 Myeloid FIH expression affects tumour immune response in the spleen

Spleen samples from B16 and LLC tumour-bearing mice were analysed by flow cytometry. CD4, CD8, Treg, and B cells were identified using antibodies in Panel 1, Table 2.7; production of IFNγ, IL-10, and IL-4 by TILs was determined by using antibodies in Panel 3, Table 2.7; myeloid populations were distinguished using antibodies in Panel 2, Table 2.7; and the expression of CD86, MHC class II, PD-L1, and PD-L2 by myeloid cells was analysed using antibodies in Panel 6, Table 2.7. (A–E) Spleen samples of B16 tumour-bearing mice were analysed. (F–K) Spleen samples of LLC tumour-bearing mice were analysed. n indicates the number of animals. * Indicates $p<0.05$ using a two-tailed, unpaired *t*-test. Data are displayed as mean ± SD.

Collectively, these data show that FIH expression in myeloid cells does not profoundly affect the tumour immune response in the spleen. Nevertheless, loss of FIH results in a reduced proportion of IFNγ$^+$ T cells in B16 tumour-bearing mice and an increased fraction of CD86$^+$ macrophages in LLC tumour-bearing mice.

4.3 Discussion

In this chapter, murine syngeneic tumour models were employed to determine whether FIH could affect tumour development by modulating the functions of non-malignant cells in the TME. A lack of FIH in the host, or only in the myeloid compartment, promotes the growth of B16 and LLC tumours. Tumours established in FIH MKO animals exhibit an altered immune profile, represented by the increased expression of PD-L1 and ARG1 in TAMs, and a reduced population of CD4 TILs. Collectively, these data demonstrate that host expression of FIH is required for the control of tumour growth.

- **The link between myeloid expression of PD-L1/ARG1 and the TIL population**

When administered with tumour cells subcutaneously, reduced FIH expression results in increased tumour growth, which is observed in both FIH-total knockout animals (Figure 4.2) and myeloid-specific FIH-null animals (Figure 4.7), indicating that myeloid expression of FIH is required to control tumour growth. Further analysis of the tumour-infiltrating immune cells provides several hints regarding the underlying mechanisms.

In both B16 and LLC tumours, TAMs from FIH MKO animals show augmented expression of PD-L1 and ARG1, which may potentiate T cell suppression through the engagement of T cell inhibitory receptor PD-1 and the depletion of L-arginine, an essential amino acid for T cells (Noy and Pollard 2014). This is in line with the reduced population of CD4 TILs observed in tumours of FIH MKO animals (Figure 4.8A, E). Unlike CD4 T cells, the number of CD8 T cells is not affected by FIH status in the myeloid compartment (Figure 4.8, B and F). One explanation could be that CD8 TILs may already be sufficiently suppressed in the TME, therefore are not subjected to further inhibition imposed by FIH deficiency in myeloid cells. Indeed, both B16 and LLC tumours are categorised as 'cold tumours' due to the almost complete absence of CD8 T cells (Lechner et al. 2013), which is also confirmed in this study (Figure 4.3, B and F, Figure 4.8, B and F). Additionally, as CD8 T cells are more vulnerable to L-arginine depletion (Bronte et al. 2003), they may be less sensitive to a further reduction of L-arginine caused by FIH-deficient myeloid cells. Therefore, the increased expression of PD-L1 and ARG1 in the TAMs of FIH MKO animals may account for the reduced CD4 TIL population.

Having discussed above, the causal relationship between the immunosuppressive features of myeloid cells and the reduced T cell population needs to be determined experimentally. In the meanwhile, it should also be mentioned that T cell suppression may not result from myeloid-derived suppressor molecules such as PD-L1. Some tumours, including B16 melanoma cells, are known to be insensitive to PD-1 blockade therapy probably due to the weak immunogenicity (Kleffel et al. 2015). Additionally, PD-L1 is not only expressed on myeloid cells but also other leukocytes and tumour cells, including B16 and LLC (Okazaki and Honjo 2007; Pilon-Thomas et al. 2010; Noh et al. 2015). The relative contribution of tumour and host-derived PD-L1 appears to be context-dependent. For example, PD-L1 on highly immunogenic MC38 cells (murine colorectal adenocarcinoma cells) is dominant in the suppression of anti-tumour immunity, whereas PD-L1 on non-tumour cells is critical for inhibiting the immune surveillance to genetically modified melanoma cells (Juneja et al. 2017). Therefore, the role of host-expressed PD-L1 should be assessed separately in different tumour models.

- **The context-dependent phenotypes of FIH-deficient TAMs**

While TAMs from FIH MKO animals show upregulated expression of PD-L1 and ARG1 in both B16 and LLC tumour models, some other characteristics of TAMs are less consistent. For example, loss of FIH in myeloid cells results in an increased population of TAMs and promotes the expression of MHC class II and CD86 on TAMs in B16 tumours (Figure 4.10B and Figure 4.11C), but not in LLC tumours (Figure 4.10D and Figure 4.11E). Despite the absence of direct evidence, several lines of study provide clues for how FIH may modulate the above aspects in macrophages. For example, FIH has been demonstrated in keratinocytes to regulate cell migration (Peng et al. 2014), which could account for the altered

number of TAMs in FIH MKO mice (Figure 4.10B). In dendritic cells, HIF-1α has been shown to promote CD86 and MHC II expression (B. Kelly and O'Neill 2015), therefore FIH might regulate the expression of the two molecules in a HIF-1α-dependent manner.

However, the context-specificity of these observations indicates the involvement of B16-specific environmental factors. Compared with LLC tumours, B16 tumours in the present study exhibit two prominent features: a high percentage of dead cells (Figure 4.4A) and an abundance of CD4 TILs (Figure 4.8A), which may indicate the presence of hypoxia, hence the stabilisation of HIF-α. Additionally, the large amount of CD4 T cells may result in elevated production of cytokines such as IFNγ and IL-4, which have been reported to induce HIF-1α and HIF-2α in macrophages, respectively (Takeda, O'Dea, Doedens, and Kim 2010). The resulting augmented HIF signalling in TAMs may therefore promote the effect of FIH on HIF-α-regulated activities.

Both CD86 and MHC class II are considered as markers for M1 macrophages and can exert anti-tumour effects (Martinez and Gordon 2014). How can an increased proportion of $CD86^+$ and MHC class II^+ TAMs be reconciled with the enhanced growth of B16 tumours observed in FIH MKO animals (Figure 4.7B)? While elevated expression of MHC class II may promote antigen presentation to T cells, this may not necessarily result in T cell activation due to the presence of PD-L1, which is also upregulated in the TAMs of FIH MKO animals. Additionally, as the inhibitory receptor CTLA-4 on T cells has a higher affinity with CD86 than the costimulatory receptor CD28 (Greenwald, Latchman, and Sharpe 2002), upregulated CD86 in TAMs may convey inhibitory signal to T cells. To evaluate the

functional consequences of upregulated MHC class II and CD86, examination of PD-1, CTLA-4, and CD28 expression on TILs should give a preliminary answer.

- **The association between the aberrant immune cell composition and tumour growth**

Given that FIH MKO animals show enhanced growth of both B16 and LLC cells, and that both types of tumours from FIH MKO animals show an increased proportion of PD-L1$^+$ and ARG1$^+$ TAMs as well as a decreased population of CD4 TILs, one imminent question is whether these observations may account for the enhanced tumour growth in FIH-deficient animals.

There is a growing body of evidence that CD4 T cells may control tumour growth (Haabeth et al. 2014). In addition to helping CD8 T cells and B cells, CD4 T cells can exert cytotoxicity through various mechanisms. For example, Th1 cells secrete IFNγ, which could kill tumour cells synergistically with TNF-α; CD4 T cells can also lyse target cells in an MHC class II-restricted manner by perforin- or granzyme-mediated killing (Quezada et al. 2010). However, some CD4 T cells, especially Th2 cells and Treg cells often counteract the anti-tumour immunity. Th2 cell-derived IL-4 and IL-13 can induce macrophages to become more immune suppressive (Martinez and Gordon 2014; Noy and Pollard 2014); IL-5 produced by Th2 cells has been correlated with progressive growth of renal cell carcinoma and melanoma (Tatsumi et al. 2002). In line with above, a tumour model using IL-12-producing B16 melanoma cells revealed that depletion of CD4 T cells with anti-CD4 antibody eliminated Th2 cells and resulted in a Th1-dominant cytokine profile, which may account for the tumour regression (Nagai et al. 2000). In another study, researchers found that adoptive transfer of CD4 T and CD8 T cells depleted of Tregs into immune-deficient hosts led to rejection of B16F10 tumours expressing

specific antigen (Kline et al. 2008). The current study shows that Th1, Th2 and Treg cell populations were all reduced in the tumours of FIH-deficient animals (Figure 4.3 and Figure 4.8). Their roles in tumour immune responses can be further dissected by characterising the cytotoxic function of CD4 T cells and by neutralising corresponding signature cytokine of each T cell lineage in the tumour-bearing mice.

On the other hand, macrophages may also affect tumour growth, and this may be particularly true for LLC tumours, given their low infiltration of CD4 TILs (~1%, Figure 4.8E) and high percentage of myeloid cells (~40%, Figure 4.10C). The increased expression of ARG1 may promote the accumulation of polyamides, which can promote cell proliferation (Z. Yang and Ming 2013; Munder 2009). Meanwhile, the increased expression of ARG1 may limit the production of cytotoxic NO catalysed by NOS2, thus promoting tumour cell survival (C. I. Chang, Liao, and Kuo 2001).

In conclusion, the alterations of CD4 T cells and/or TAMs may account for tumour growth, however, the causal effect needs to be demonstrated experimentally.

- **The role of FIH in the systemic tumour immune response**

The effect of FIH on immune response to tumour may extend outside of the tumour site. In the B16 model, for example, reduced proportions of IFNγ-producing CD4 and CD8 T cells are observed in the spleens of FIH MKO tumour-bearing mice (Figure 4.13, C and D), indicating a more immunosuppressive environment in the FIH MKO mice. However, this was not observed in the TILs, which might be due to the extremely small population of T cells that expressed IFNγ in the TME (Figure 4.8D). In light of the altered immune profiles in the spleens, other tissues, such as the tumour-draining lymph node (TDLN) and peripheral blood, would be worth

characterising to evaluate the role of FIH in mediating the systemic tumour immune response.

- **Host expression of FIH and CD4 TILs**

While this study demonstrates the significant role of FIH in myeloid-mediated tumour suppression, it does not exclude the role of FIH in other cell types. For example, in the B16 model, myeloid deletion of FIH results in a reduced CD4 TIL population (Figure 4.8A), while global deletion of FIH gives rise to an expanded CD4 TIL population (Figure 4.3A). One explanation could be that FIH may intrinsically regulate CD4 T cell biology such as cell proliferation. However, as this was not observed in LLC tumours (Figure 4.3E), environmental factors may also be involved. T cell proliferation is dependent on an array of external factors, including the availability of APCs, IL-2, and co-stimulatory signals (Janeway 2005). An examination of these aspects in the tumour samples, together with the *in vitro* characterisation of FIH-null CD4 T cells, will help us better understand the discrepancies between the two models.

One limitation of the syngeneic tumour model in the present study is that the tumour cells are very aggressive: most tumour-bearing animals had to be culled due to the size of the tumour within 2 weeks post-tumour inoculation. This may not provide enough time for the adaptive immune system to act against the tumour. Another issue is that both B16 and LLC tumours are known to have weak immunogenicity with small quantities of tumour-infiltrating lymphocytes (Lechner et al. 2013). Therefore, B16 and LLC tumour models may be biased against the adaptive immune system. The employment of less aggressive, more immunogenic tumour models will allow a better understanding of the role of FIH in adaptive immunity.

Collectively, these data indicate that host expression of FIH suppresses tumour development, and that this effect could be partially, mediated by FIH expression in the myeloid cells. The enhanced tumour growth of mice lacking FIH in myeloid cells could be associated with a more immunosuppressive TME, reflected by the augmented expression of the inhibitory molecules PD-L1 and ARG1 in TAMs, and a reduced CD4 TIL population. The aberrant expression profile of PD-L1 and ARG1 in TAMs *in vivo* may result from a cell intrinsic role of FIH in gene regulation, or may be secondary to differential environmental factors in FIH-deficient animals. To investigate how FIH may relate to heightened expression of PD-L1 and ARG1, and whether FIH is required for other macrophage functions, *in vitro* characterisation of $FIH^{-/-}$ macrophages was performed and is discussed in the next chapter.

Chapter 5 The role of FIH in macrophage function

5.1 Introduction

Macrophages are essential in orchestrating immune responses to tissue injury, infection, and tumours. They are efficient in detecting and taking up pathogens, producing inflammatory mediators, and activating the adaptive immune system (Mosser and Edwards 2008; Dunster 2015) (for more information, please refer to section 1.2.1). The function of macrophages is tightly associated with the activity of HIF signalling, which has been demonstrated in a number of inflammation models including atherosclerosis, adipose tissue inflammation, sepsis, airway allergy, and cutaneous inflammation (N. Lin and Simon 2016). For example, mice deficient of myeloid HIF-1α are more protected against acute and chronic cutaneous inflammation and arthritis (Cramer et al. 2003). Similarly, mice with HIF-2α deficiency in myeloid cells show dampened inflammatory responses in models of sepsis, cutaneous inflammation, and peritonitis (Imtiyaz et al. 2010).

Some mechanisms underlying the role of HIF have been uncovered by *in vitro* studies utilising primary macrophages. HIF-1α deletion in macrophages diminishes the expression of *Glut1* and the glycolytic enzyme phosphoglyceratekinase (*Pgk1*), which may account for the impairment of glycolysis and ATP generation. This, in

consequence, results in defective energy-consuming activities such as cell motility and bacterial killing (Cramer et al. 2003; Peyssonnaux et al. 2005; B. Kelly and O'Neill 2015). HIF-2α, on the other hand, does not alter energy production but instead affects the expression of pro-inflammatory genes in M1 macrophages, among which IL-6 has been identified as a direct target (Imtiyaz et al. 2010).

While the role of HIF signalling in the regulation of macrophage activities is well established, the involvement of FIH remains elusive. In line with the notion that myeloid expression of FIH is important for the anti-tumour immune response (section 4.2.3), FIH was found to be induced at the mRNA level in macrophages by tumour cell-derived factors *in vitro*. To investigate the role of FIH in macrophage function, primary macrophages from $FIH^{-/-}$ animals were characterised in this chapter.

5.2 Results

5.2.1 FIH is induced in BMDMs transcriptionally by inflammatory stimuli

BMDMs were obtained by differentiating the committed myeloid progenitors in the bone marrow with M-CSF provided by LCM (Weischenfeldt and Porse 2008). The maturity of the macrophages was confirmed by the expression of F4/80 detected by ICC (Figure 5.1A) and flow cytometry (Figure 5.1B).

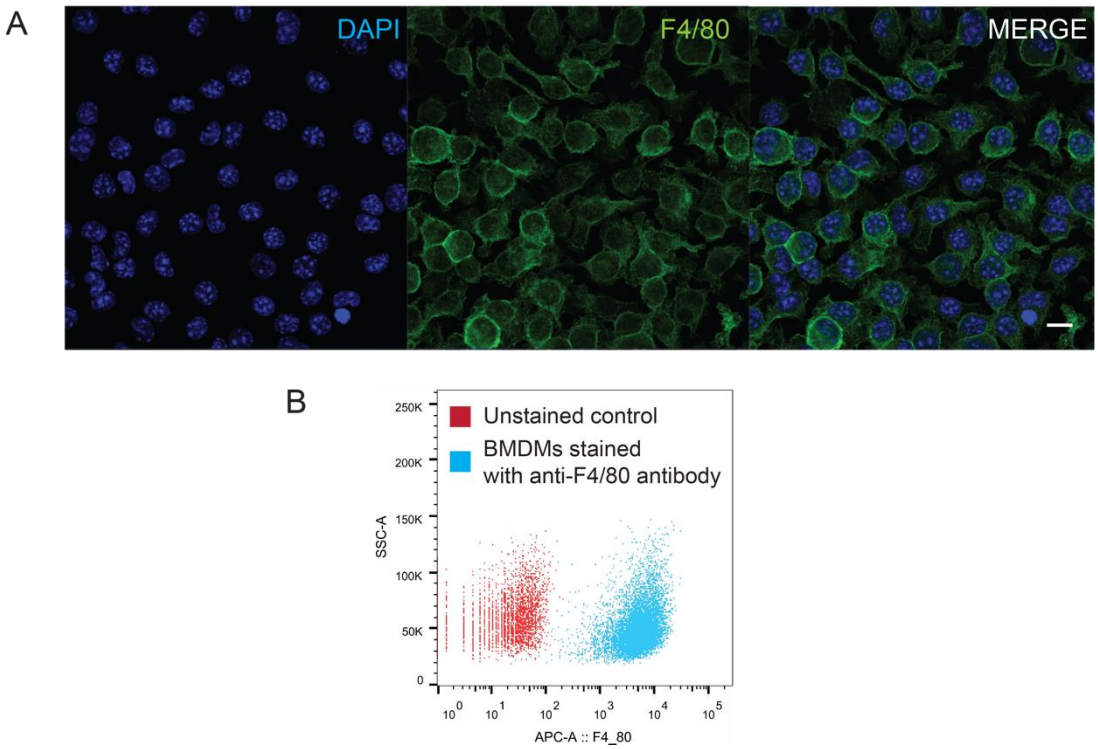

Figure 5.1 Generation of BMDMs
Bone marrow cells collected from murine tibias and femurs were allowed to differentiate to BMDMs in the presence of LCM for 7 days. (A) BMDMs were stained with anti-F4/80 antibody and nuclear dye DAPI and imaged by confocal microscopy. Scale bar, 10 μm. (B) BMDMs were stained with anti-F4/80 antibody and analysed by flow cytometry. Unstained cells were included as a negative control.

Previous studies have shown that myeloid expression of FIH affects intra-tumoural inflammation (section 4.2.3). To examine whether FIH expression could be regulated by inflammatory signals, BMDMs were exposed to various stimulants and the mRNA level of FIH was examined by RT-qPCR.

To mimic the TME, tumour-conditioned media (TCM) collected from B16 and LLC tissue culture supernatants were used to stimulate macrophages. As shown in Figure 5.2A, LLC TCM upregulated the mRNA level of FIH by ~2–fold ($p=0.0151$; *t*-test), while the effect of B16 TCM was less apparent.

To represent the inflammatory environment in a more generalised way, BMDMs were treated with LPS plus IFNγ, or IL-4 for 24 hr, to induced M1 or M2 macrophages, respectively. (This polarising method was used throughout the chapter unless otherwise stated.) Compared to the untreated cells, increased FIH expression was observed in M1 (fold change 3.37, p=0.0019; *t*-test) but not M2 macrophages (Figure 5.2B).

As M1 macrophages are commonly involved in the host defence against infection (Labonte, Tosello-Trampont, and Hahn 2014), FIH expression was also examined in macrophages infected by *M. bovis* BCG. FIH was transiently induced upon infection, with its mRNA level peaking at 2 days post-infection (fold change 6.98, p=0.0044, *t*-test; Figure 5.2C). The expression level stayed high 72 hr post-infection (fold change 5.89, p=0.0042; *t*-test) before it decreased 96 hr post-infection (Figure 5.2C).

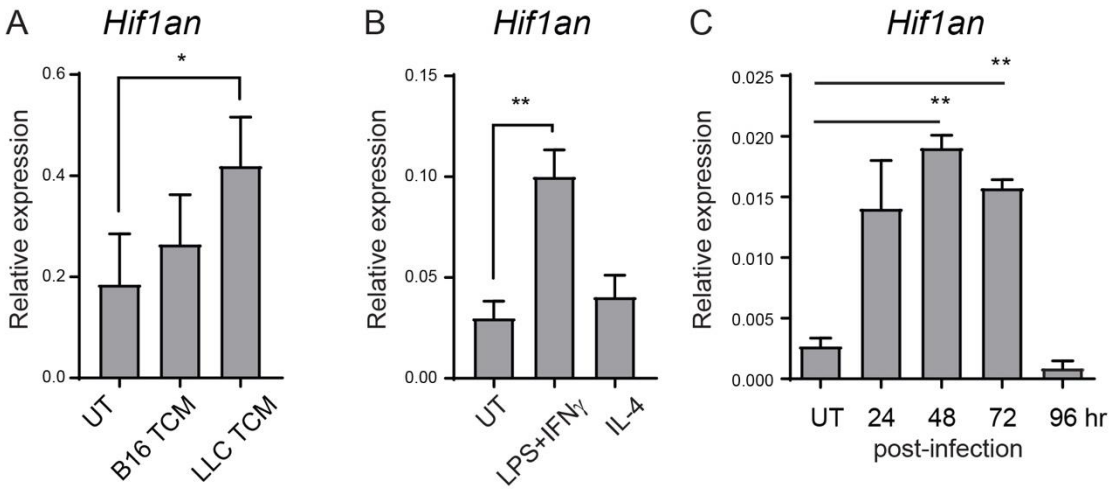

Figure 5.2 The transcription of FIH is induced by LLC TCM, LPS/IFNγ, and BCG infection in BMDMs

WT BMDMs were stimulated as indicated. FIH expression was determined by RT-qPCR and was normalised by γ-actin level. (A) BMDMs were treated with B16- or LLC-derived TCM for 24 hr. (B) WT BMDMs were induced to M1 macrophages with LPS (5 ng/ml)

and IFNγ (1 ng/ml), or M2 macrophages with IL-4 (10 ng/ml), for 24 hr. (C) BMDMs were infected with BCG at an MOI of 1 for the indicated period of time. * indicates p<0.05, ** indicates p<0.01, and *** indicates p<0.001 by a paired, two-tailed student's *t*-test. UT, untreated. The histogram bars are displayed as mean ± SD.

Together, these data show that FIH is transcriptionally upregulated by LLC TCM, LPS/IFNγ, and BCG infection.

5.2.2 FIH-null BMDMs show increased *Cd274* (PD-L1) expression

As an increased fraction of PD-L1^{+} TAMs was observed in mice deficient of myeloid FIH (Figure 4.11, C and E), it was of interest to investigate whether FIH could regulate PD-L1 expression in macrophages. To address this, WT and FIH$^{-/-}$ BMDMs were induced to M1 and M2 macrophages and PD-L1 expression was determined by flow cytometry (Figure 5.3A). The expression of other T cell-interacting molecules, such as PD-L2, MHC class II, and CD86, was analysed simultaneously (Figure 5.3, B–D).

PD-L1 was strongly induced in M1 but less so in M2 macrophages (Figure 5.3E). In contrast, PD-L2 was upregulated in M2 but suppressed in M1 macrophages (Figure 5.3F). In comparison with the WT BMDMs, loss of FIH marginally upregulated PD-L1 expression by 24% in unstimulated macrophages (p=0.0474; *t*-test) and 11% in M1 macrophages (p=0.0196; *t*-test; Figure 5.3E). PD-L2 expression was not affected by FIH status (Figure 5.3F).

Activated macrophages also serve as professional APCs by upregulating MHC class II and costimulatory molecule CD86 (Martinez and Gordon 2014). Surprisingly, induction of MHC class II was not observed in M1 but M2 macrophages (Figure 5.3G). CD86, as expected, was upregulated in M1 but not

M2 macrophages (Figure 5.3H). FIH deficiency had no effect on the expression of MHC class II and CD86 under the conditions tested (Figure 5.3, G and H).

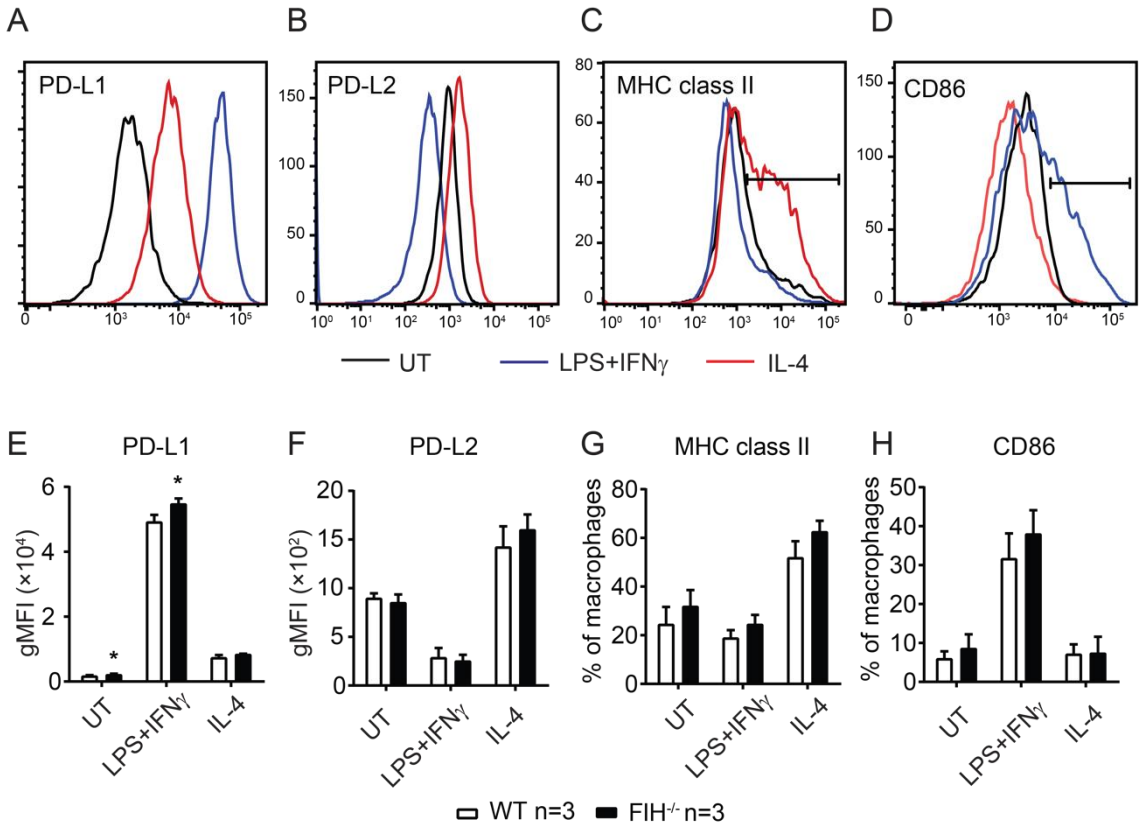

Figure 5.3 FIH$^{-/-}$ BMDMs show increased PD-L1 expression on unpolarised and M1 BMDMs

BMDMs were polarised to M1 or M2 macrophages. The surface expression of PD-L1, PD-L2, MHC class II, and CD86 on BMDMs (defined by CD11b^{+} F4/80^{+}) was analysed by flow cytometry. (A–D) Representative histogram plots of a WT, M1 macrophage sample are shown. (E and F) PD-L1 and PD-L2 expression is evaluated by geometric mean fluorescence intensity (gMFI). (G and H) MHC class II and CD86 expression is demonstrated as the percentage of the gated population (as shown in C and D) out of the total macrophage population. * indicates $p<0.05$ by an unpaired, two-tailed student's *t*-test. The histogram bars are displayed as mean ± SD.

Taken together, these data demonstrate that a loss of FIH marginally promotes PD-L1 expression on the cell surface of unstimulated and M1 BMDMs.

PD-L1 has been demonstrated to be a transcriptional target of HIF-1α in MDSCs and macrophages (Noman et al. 2014). To investigate whether FIH could regulate the transcription of PD-L1, the mRNA levels of PD-L1 were determined by RT-qPCR in WT and FIH$^{-/-}$ BMDMs in response to various stimuli. To induce the accumulation of HIF-α, a parallel set of samples was stimulated under hypoxia (1% oxygen was used throughout the chapter).

In agreement with the expression profile at the protein level (Figure 5.3E), *Cd274* (the gene that encodes PD-L1) mRNA was significantly induced in M1 macrophages and marginally upregulated in M2 macrophages under normoxia (Figure 5.4A). Loss of FIH promoted *Cd274* expression in untreated macrophages (fold change 1.28, p=0.0262; *t*-test) and M1 (fold change 1.22, p=0.0325; *t*-test) macrophages, but had no effect on M2 macrophages (Figure 5.4A). Oxygen deprivation moderately augmented PD-L1 expression in unstimulated and M2 cells, but not in M1 macrophages (Figure 5.4B). Under hypoxia, FIH deficiency enhanced *Cd274* expression only in unpolarised cells (fold change 1.66, p=0.0127; *t*-test), but not in M1 or M2 macrophages (Figure 5.4B).

To represent the TME more faithfully, BMDMs were subjected to TCM treatment. Under normoxia, both B16 and LLC TCM were able to upregulate PD-L1 expression, while LLC TCM seemed to be a more potent inducer (Figure 5.4C). FIH showed an inhibitory effect on PD-L1 expression regardless of the type of treatment that BMDMs received (untreated: fold change 1.46, p=0.0156; B16 TCM: fold change 1.69, p=0.0065; LLC TCM: fold change 1.59, p=0.0027; *t*-test; Figure 5.4C). Hypoxia further boosted PD-L1 expression in macrophages treated in all

conditions (Figure 5.4D). However, the effect of FIH was only preserved in untreated cells (fold change 1.61; p=0.0049; *t*-test) and diminished in macrophages stimulated by B16 or LLC TCM (Figure 5.4D).

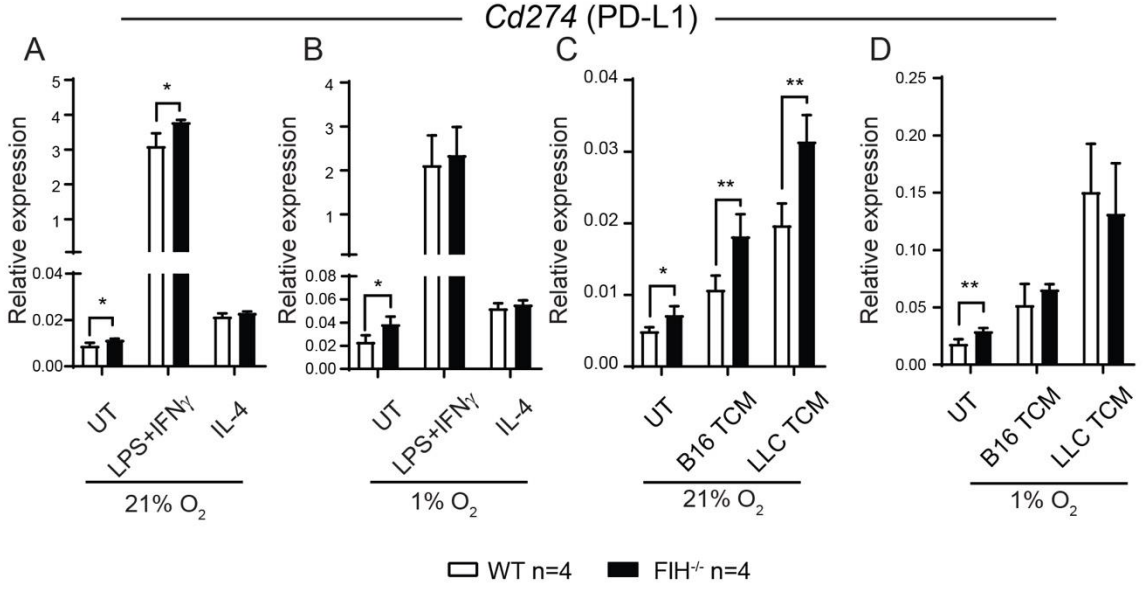

Figure 5.4 *Cd274* expression is elevated in FIH-null BMDMs
WT and FIH$^{-/-}$ BMDMs were stimulated as indicated. The expression level of PD-L1 was examined by RT-qPCR and was normalised by γ-actin level. BMDMs were induced to M1 or M2 macrophages under normoxia (A) or hypoxia (B). BMDMs were treated with B16 or LLC TCM under normoxia (C) or hypoxia (D). * indicates p<0.05 and ** indicates p<0.01 by an unpaired, two-tailed student's *t*-test. The histogram bars are displayed as mean ± SD.

Altogether, these data show that FIH suppresses the basal expression of *Cd274* under normoxia and hypoxia. FIH also inhibits *Cd274* induction by M1 stimulators and TCM under normoxia.

5.2.3 FIH-deficient macrophages show augmented *Arg1* induction in M1 and LLC TCM-treated BMDMs

In addition to PD-L1, an increased percentage of $ARG1^+$ myeloid cells was also observed in tumours derived from FIH MKO animals (Figure 4.12). To test whether FIH could intrinsically affect ARG1 expression, BMDMs from WT and $FIH^{-/-}$ animals were activated and ARG1 expression was analysed by Western blotting.

When polarised to M1 or M2 macrophages, NOS2, a marker protein for M1 macrophages (Martinez and Gordon 2014), was detectable after 6 hr of polarisation and the expression was further enhanced after 24 hr of stimulation in M1 but not M2 macrophages (Figure 5.5A). ARG was detected by a polyclonal antibody recognising both ARG1 and ARG2 isoforms, which share similar functions but are encoded by separate genes (Z. Yang and Ming 2014). ARG induction was observed in both M1 and M2 macrophages, yet it was more dramatic in M2 macrophages (Figure 5.5A). FIH appeared to suppress ARG expression in M1 rather than M2 macrophages (Figure 5.5A).

When exposed to B16 or LLC TCM, ARG expression was only detected in cells treated by LLC TCM, which was further enhanced by FIH deficiency in BMDMs (Figure 5.5B). Phosphorylated p65, an indicator of activation of the NFκB pathway (Christian, Smith, and Carmody 2016), was detectable in control samples and mildly upregulated in TCM-treated BMDMs regardless of FIH status (Figure 5.5B). Activation of the STAT3 pathway was assessed by the phosphorylation of STAT3 at Ser727 (Wen, Zhong, and Darnell 1995), which was not affected by external stimuli or FIH status (Figure 5.5B).

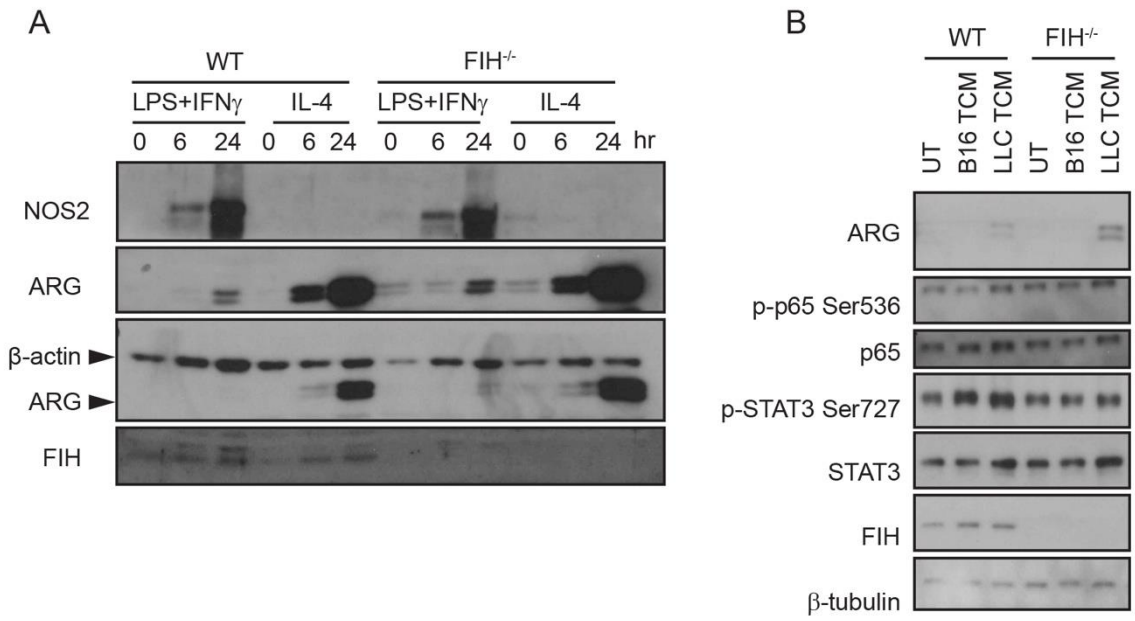

Figure 5.5 FIH$^{-/-}$ BMDMs exhibit enhanced ARG induction by LPS/IFNγ and LLC TCM

(A) BMDMs obtained from WT and FIH$^{-/-}$ animals were polarised to M1 and M2 macrophages and analysed by Western blotting. The expression of NOS2, ARG, and FIH was examined. β-actin was used as a loading control. (B) WT and FIH$^{-/-}$ BMDMs were stimulated with B16- or LLC-derived TCM for 24 hr. Expression of ARG and FIH was analysed by Western blotting. Activation of the NFκB and STAT3 signalling pathways was assessed by phosphorylation of p65 at serine 536 (Ser536) and phosphorylation of STAT3 at serine 727 (Ser727) respectively. β-tubulin was used as a loading control. Results are representative of two to three independent experiments.

To examine whether FIH could regulate *Arg1* at the transcriptional level, WT and FIH$^{-/-}$ BMDMs were exposed to various stimuli under normoxia or hypoxia, and the mRNA level of *Arg1* was determined by RT-qPCR.

Arg1 was potently induced in both M1 and M2 BMDMs under normoxia (Figure 5.6A), and the induction was augmented by hypoxia (Figure 5.6B). While LLC TCM was able to induce *Arg1*, the effect of B16 TCM was relatively mild (Figure 5.6C). *Arg1* induction by both LLC and B16 TCM was potentiated under hypoxia (Figure 5.6D). Under normoxia, loss of FIH promoted *Arg1* induction in M1 (fold change

2.92, p<0.0001; *t*-test; Figure 5.6A) and LLC TCM-stimulated BMDMs (fold change 4.21, p=0.0151; *t*-test; Figure 5.6C). However, under hypoxia, the effect of FIH was less dramatic in M1 macrophages (fold change 1.92, p=0.0087, *t*-test; Figure 5.6B) and abolished in LLC TCM-treated macrophages (Figure 5.6D).

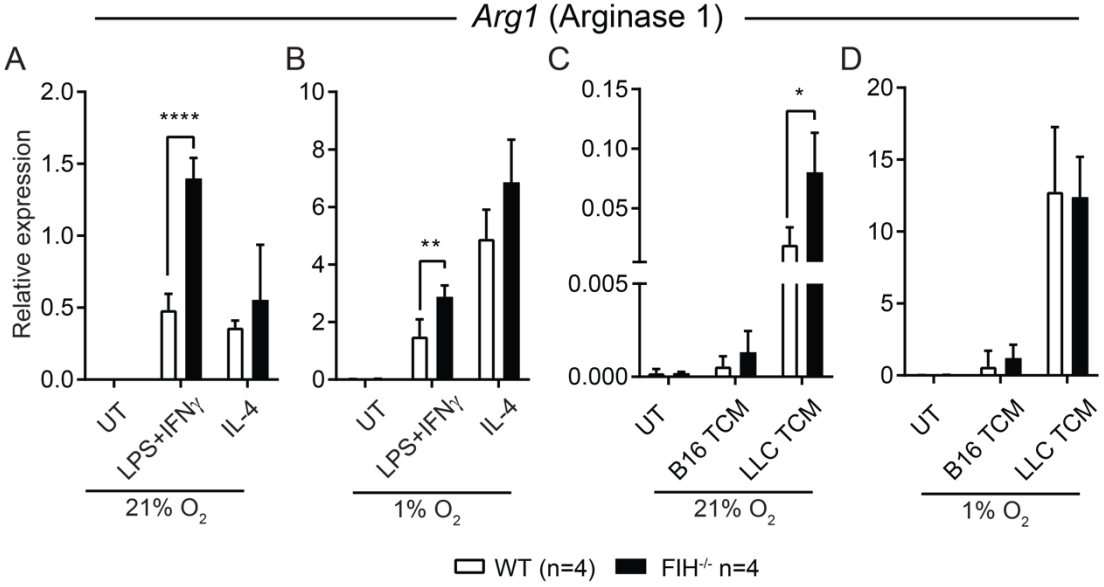

Figure 5.6 *Arg1* induction is augmented in FIH-null macrophages in response to M1 polarising reagents and LLC TCM

WT and FIH$^{-/-}$ BMDMs were stimulated as indicated for 24 hr. The expression of *Arg1* was evaluated by RT-qPCR and was normalised by γ-actin level. BMDMs were polarised to M1 or M2 macrophages under normoxia (A) or hypoxia (B). BMDMs were treated with B16- or LLC-derived TCM, under normoxia (C) or hypoxia (D). *Arg1* expression level relative to γ-actin is presented. * indicates p<0.05, ** indicates p<0.01, and **** indicates p<0.0001 by an unpaired, two-tailed student's *t*-test. The histogram bars are displayed as mean ± SD. Results are representative of two independent experiments.

In summary, these data show that FIH suppresses *Arg1* induction in M1 macrophages under normoxia and hypoxia. In LLC TCM-treated BMDMs, FIH inhibits *Arg1* induction only under normoxia.

5.2.4 BMDMs deficient of FIH show improved migration towards CCL5 and C5a

Previous experiments performed on FIH MKO mice showed an increased TAM population within B16 tumours (Figure 4.10B). TAMs mostly originate from circulating monocytes and differentiate into macrophages when they enter the tumour site (Y. Liu and Cao 2015). The enlarged TAM population could therefore result from the enhanced migration of monocytes towards the site of the tumour. Tumour cells are known to produce growth factors and chemokines to recruit macrophages (J. W. Pollard 2004). Melanoma cells have been reported to produce CXCL1-3, CXCL5-10, and CCL2-5, which are implicated in tumour growth and progression (Richmond, Yang, and Su 2009; Harlin et al. 2009). In the present study, migration towards CCL2 and CCL5 was tested, given that both chemokines have been demonstrated to be associated with an altered myeloid or T cell involvement in melanoma (Mellado et al. 2001; Gazzaniga et al. 2007; Harlin et al. 2009).

Macrophage migration was monitored with an RTCA-DP system using CIM plates (Figure 5.7A) for up to 5 hr. Unexpectedly, CCL2 did not elicit robust migration of BMDMs, as reflected by the similar migration traces of control groups and chemokine-exposed groups in both WT and FIH-null cells (Figure 5.7B). In contrast, CCL5 (10 ng/ml) appeared to be a more effective chemoattractant, as was indicated in both migration traces, as well as maximum–minimum (max–min)

and area under curve (AUC) analysis of the traces (Figure 5.7C-E). Furthermore, FIH-deficient macrophages showed increased migration towards CCL5 compared to the WT control, as shown in the max–min analysis (p=0.0035, *t*-test; Figure 5.7D) and AUC analysis (p=0.0137; *t*-test; Figure 5.7E).

Apart from in tumours, immune cells are also recruited during infection, sepsis, and chronic inflammatory diseases, where complement component 5a (C5a) acts as a strong chemoattractant (Guo and Ward 2005). To test whether FIH also affects macrophage migration to C5a, WT and $FIH^{-/-}$ BMDMs were exposed to 10 ng/ml C5a and cell migration was monitored by the RTCA-DP instrument (Figure 5.7F). Increased migration was also observed in FIH-deficient BMDMs by max–min analysis (p=0.0036, *t*-test; Figure 5.7G) and AUC analysis (p=0.0083, *t*-test; Figure 5.7H).

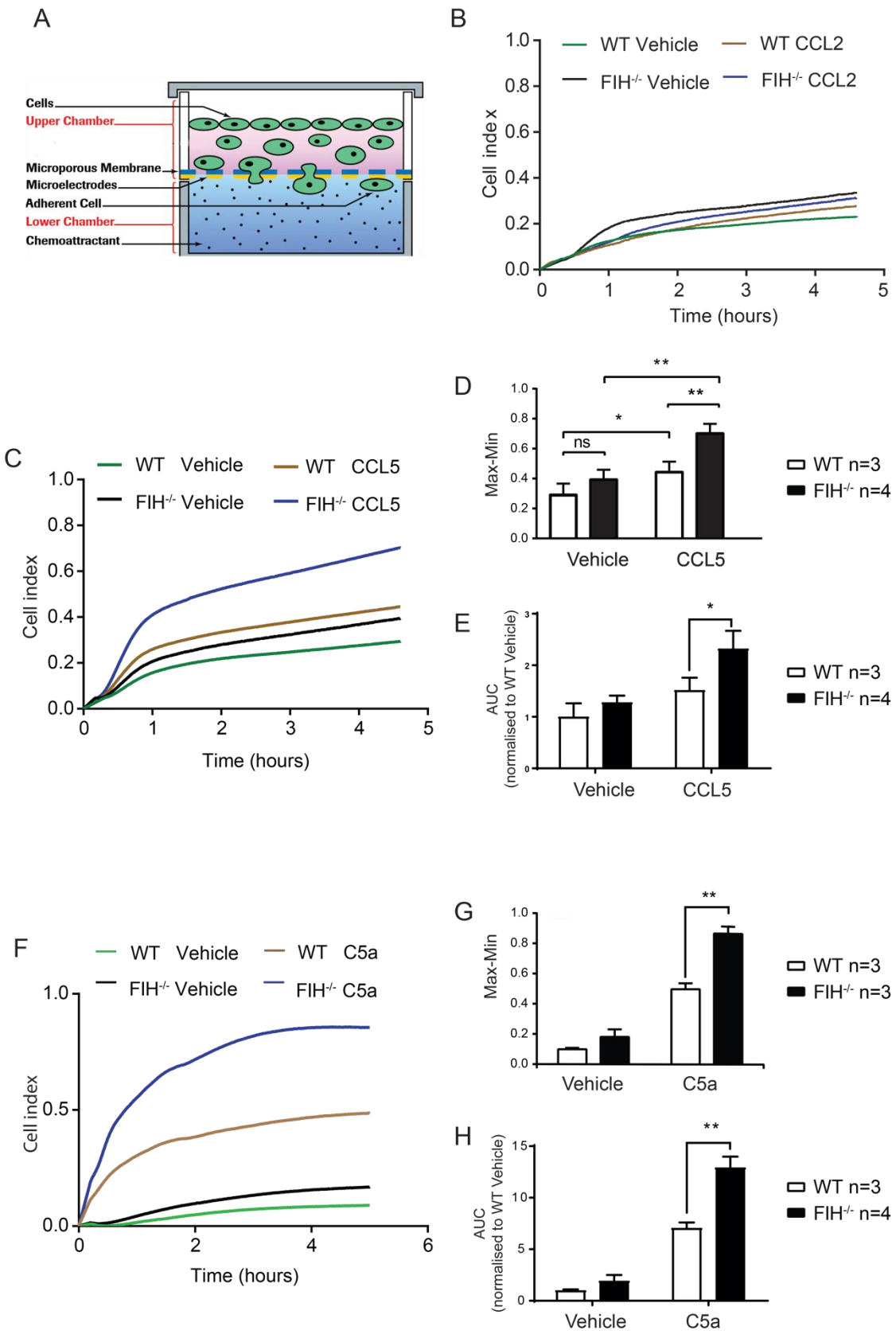
A
Cells
Upper Chamber
Microporous Membrane
Microelectrodes
Adherent Cell
Lower Chamber
Chemoattractant
B
WT Vehicle
WT CCL2
FIH-/- Vehicle
FIH-/- CCL2
Cell index
Time (hours)
C
WT Vehicle
WT CCL5
FIH-/- Vehicle
FIH-/- CCL5
Cell index
Time (hours)
D
Max-Min
ns
*
**
**
Vehicle
CCL5
WT n=3
FIH-/- n=4
E
AUC
(normalised to WT Vehicle)
*
Vehicle
CCL5
WT n=3
FIH-/- n=4
F
WT Vehicle
WT C5a
FIH-/- Vehicle
FIH-/- C5a
Cell index
Time (hours)
G
Max-Min
**
Vehicle
C5a
WT n=3
FIH-/- n=3
H
AUC
(normalised to WT Vehicle)
**
Vehicle
C5a
WT n=3
FIH-/- n=4

Figure 5.7 FIH-null macrophages show enhanced migration towards CCL5 and C5a

Cell migration was monitored by an RTCA-DP instrument using CIM plates. (A) A schematic illustration of the migration well is shown (adapted from RTCA-DP product brochure). Each well of a CIM plate is composed of an upper chamber and a lower chamber, separated by a microporous membrane. Macrophages added to the upper chamber were allowed to migrate through the membrane to the chemokine-containing lower chamber. As cells passed through the membrane they adhered to the underside of the membrane, which was embedded with electrodes. This generated a signal of electrical impedance and was reflected as an arbitrary unit (cell index) as shown in the migration trace (B, C, and F). It has been confirmed that rising cell impedance correlates with an increasing number of migrated cells (Iqbal et al. 2013). (B) Migration traces of WT and $FIH^{-/-}$ BMDMs towards CCL2 (2.5 ng/ml) and vehicle control are shown. (C–E) WT and $FIH^{-/-}$ BMDMs were allowed to migrate towards 10 ng/ml CCL5 or vehicle control. Representative migration traces (C), max–min (D), and AUC (E) analysis of the traces are shown. (F–H) WT and $FIH^{-/-}$ BMDMs were allowed to migrate to 10 ng/ml C5a or vehicle control. Representative migration traces (F), max–min (G), and AUC (H) analysis of the traces are shown. * indicates $p<0.05$ and ** indicates $p<0.01$ by an unpaired, two-tailed student's *t*-test. The histogram bars are displayed as mean ± SD.

Chemotaxis is initiated by interaction with a corresponding receptor expressed on the cell surface (Jones 2000). To test whether the enhanced migration of FIH-deficient BMDMs was due to the aberrant expression of chemokine receptors, expression of C-C chemokine receptor type 5 (CCR5) and complement component 5a receptor 1 (C5AR) in unstimulated WT and $FIH^{-/-}$ BMDMs was determined by flow cytometry. Compared with WT BMDMs, $FIH^{-/-}$ cells exhibited a marginally increased level of CCR5 (fold change 1.16, $p=0.0042$, *t*-test; Figure 5.8A) and C5AR (fold change 1.93, $p=0.0115$, *t*-test; Figure 5.8B).

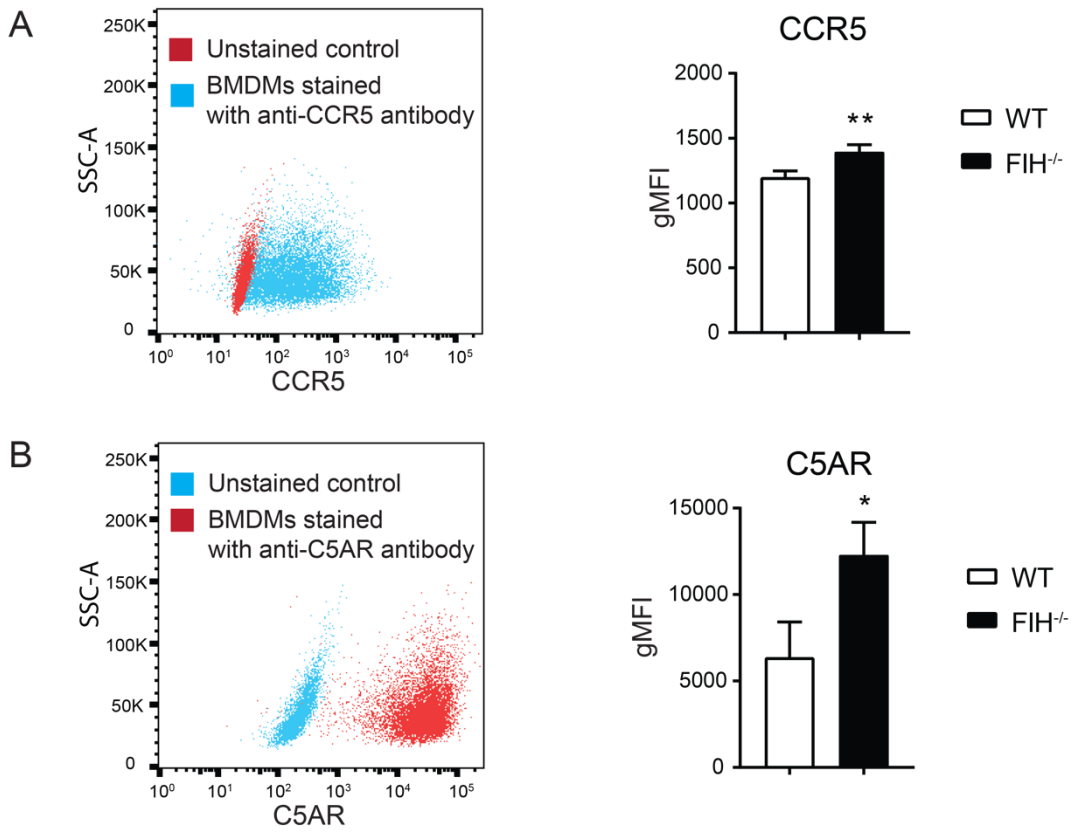

Figure 5.8 FIH$^{-/-}$ BMDMs show increased expression of receptors for CCL5 and C5a on the cell surface
WT (n=3) and FIH$^{-/-}$ (n=4) BMDMs were stained with anti-CCR5 and anti-C5AR antibodies and subjected to flow cytometry analysis. Representative dot plots of CCR5 (A) and C5AR (B) expression are shown on the left, and compiled data showing the gMFI of the corresponding staining are shown on the right. * indicates $p<0.05$ and ** indicates $p<0.01$ by an unpaired, two-tailed student's *t*-test. The histogram bars are displayed as mean ± SD.

Together, these data show that FIH$^{-/-}$ BMDMs exhibit enhanced migration towards CCL5 and C5a, accompanied by increased expression of the corresponding chemokine receptors.

5.2.5 FIH may not be required for macrophage phagocytosis

As professional phagocytes, macrophages are extremely efficient at taking up cell debris and infectious reagents. Engulfed subjects are enclosed in phagosomes, which are then fused with lysosomes to generate phagolysosomes where enzymatic degradation takes place (Aderem and Underhill 1999; Feng et al. 2015). This process demands a large supply of energy (Chandak et al. 2010). As HIF-1α is essential for energy-consuming activities by maintaining the cellular ATP level (Cramer et al. 2003), it was hypothesised that FIH could modulate phagocytic activity.

To address this, phagocytosis was assess using pH-sensitive fluorescent dye-conjugated zymosan particles (pHrodo^{TM}). The zymosan particles only emit fluorescence inside the phagosomes where the pH is low, allowing the visualisation and quantification of intracellular particles. As shown in the proof-of-concept test, the beads emitted green fluorescence when incubated in hydrochloric acid (HCl) solution (Figure 5.9A, second row) but not in the neutral phagocytosis buffer (Figure 5.9A, first row). Fluorescent particles were only detected within cells that were incubated with the beads (Figure 5.9A, fourth row). Macrophages alone displayed no apparent autofluorescence excited by the 488-nm laser under the imaging conditions (Figure 5.9A, third row).

The phagocytosis of zymosan particles by WT and FIH$^{-/-}$ BMDMs was examined under normoxia and hypoxia. During the time frame monitored, neither hypoxic conditions nor FIH expression status had a profound effect on phagocytic activity, as reflected by the relative fluorescence intensity (Figure 5.9B).

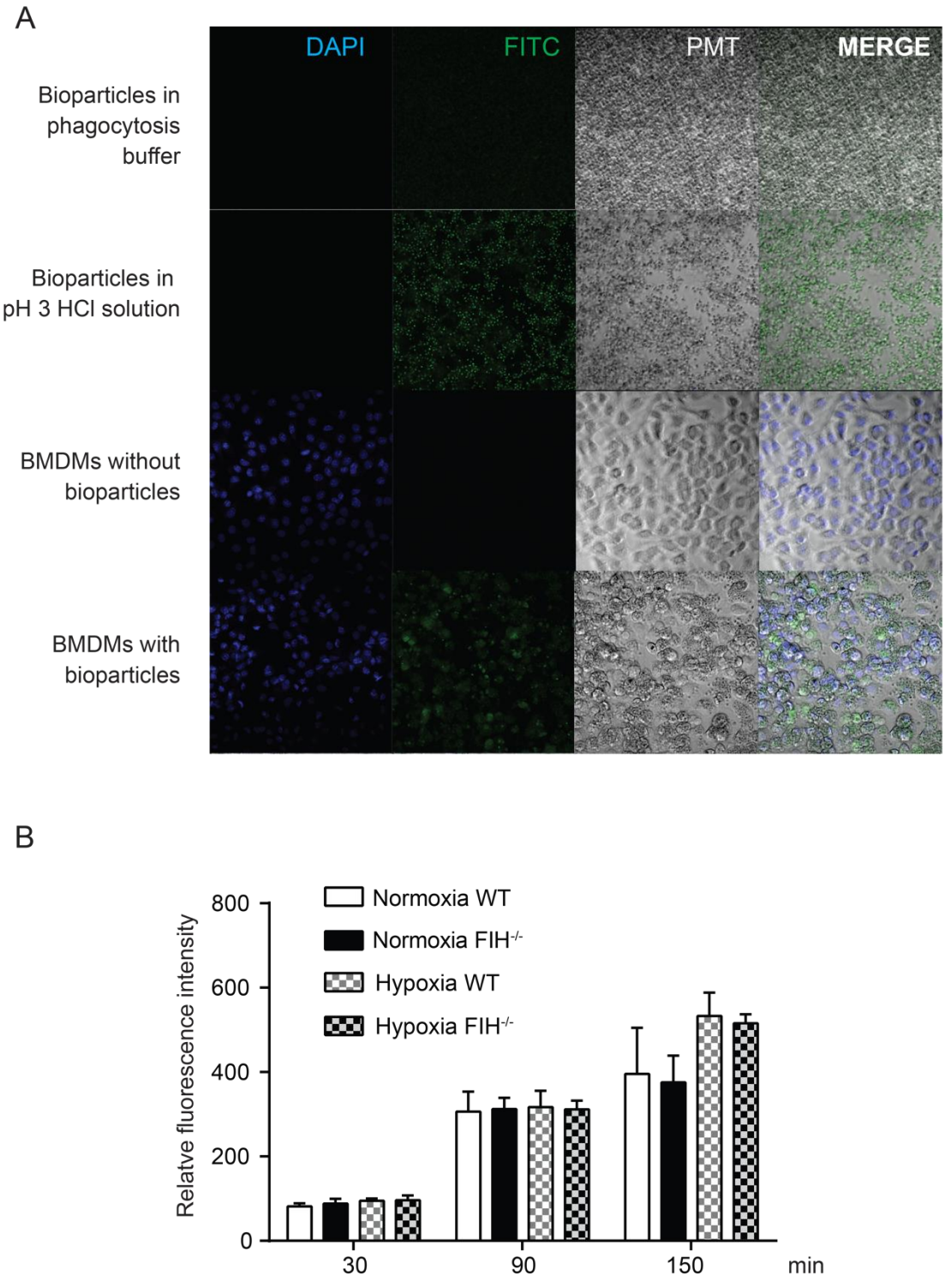

Figure 5.9 FIH is dispensable for macrophage phagocytosis
(A) The phagocytic activity of BMDMs was evaluated by the uptake of pH-sensitive fluorescent dye-conjugated zymosan particles. Microscopic images of indicated experimental settings are shown. (B) WT (n=3) and FIH$^{-/-}$ (n=3) BMDMs were seeded in 96-well plates

and incubated with zymosan particles under normoxia or hypoxia. At the indicated time point, cells were washed with PBS to remove extracellular particles and the fluorescence intensity of each well was measured by a microplate reader. The fluorescence intensity of the experimental well (cells with zymosan particles) was subtracted by that of the corresponding control well (cells without zymosan particles) to obtain the value of relative fluorescence intensity. No difference was found between WT and FIH$^{-/-}$ cells using an unpaired, two-tailed student's *t*-test. The histogram bars are displayed as mean ± SD.

5.2.6 FIH-null M1 macrophages show aberrant expression of *Egln3*, *Sell* and *Cxcl1*

It has been reported that macrophages lacking myeloid HIF-1α or HIF-2α show an aberrant expression profile of pro-inflammatory cytokines during sepsis, adipose tissue inflammation, and atherosclerosis (Peyssonnaux et al. 2007; Imtiyaz et al. 2010; Mahabeleshwar et al. 2012; Choe et al. 2014; Tawakol et al. 2015). To test whether FIH could affect the gene expression profile of activated macrophages, WT and FIH$^{-/-}$ BMDMs were induced to M1 macrophages and the expression of a panel of genes including HIF targets (*Egln3*, *Glut1*, and *Adm*) (Dengler, Galbraith, and Espinosa 2013), chemokines (*Cxcl1*, *Cxcl2*, and *Ccl2*), cytokines (*Il-6*, *Il-10*, *Il-12b*, and *Tnfa*), and other inflammatory mediators was examined by RT-qPCR.

HIF-1α targets *Glut1*, *Adm*, and *Egln3* were all upregulated by LPS and IFNγ; however, FIH only inhibited the transcription of *Egln3* (untreated: fold change 5.73, p=0.0285; M1: fold change 3.80, p=0.0136; *t*-test; Figure 5.9A) but not the other two (Figure 5.10, B and C). Among the genes involved in cell migration, loss of FIH led to a reduced expression of *Sell* (the gene that encodes L-selectin, reduced by 70% in FIH-null cells, p=0.0298, *t*-test; Figure 5.10D) and enhanced expression of

chemokine *Cxcl1* (enhanced by ~1-fold in FIH$^{-/-}$ unpolarised cells and ~1.6-fold in FIH$^{-/-}$ M1 macrophages, p=0.0230 and 0.0367, respectively, *t*-test; Figure 5.10E). The expression of *Il-6*, *Il-10*, *Il-12b*, *Tnfa*, and *Nos2* was induced by LPS/IFNγ treatment in an FIH-independent manner (Figure 5.10, H–L). In addition, *Hif-1a* was induced whereas *Hif-2a* was suppressed in M1 macrophages (Figure 5.10, N and O).

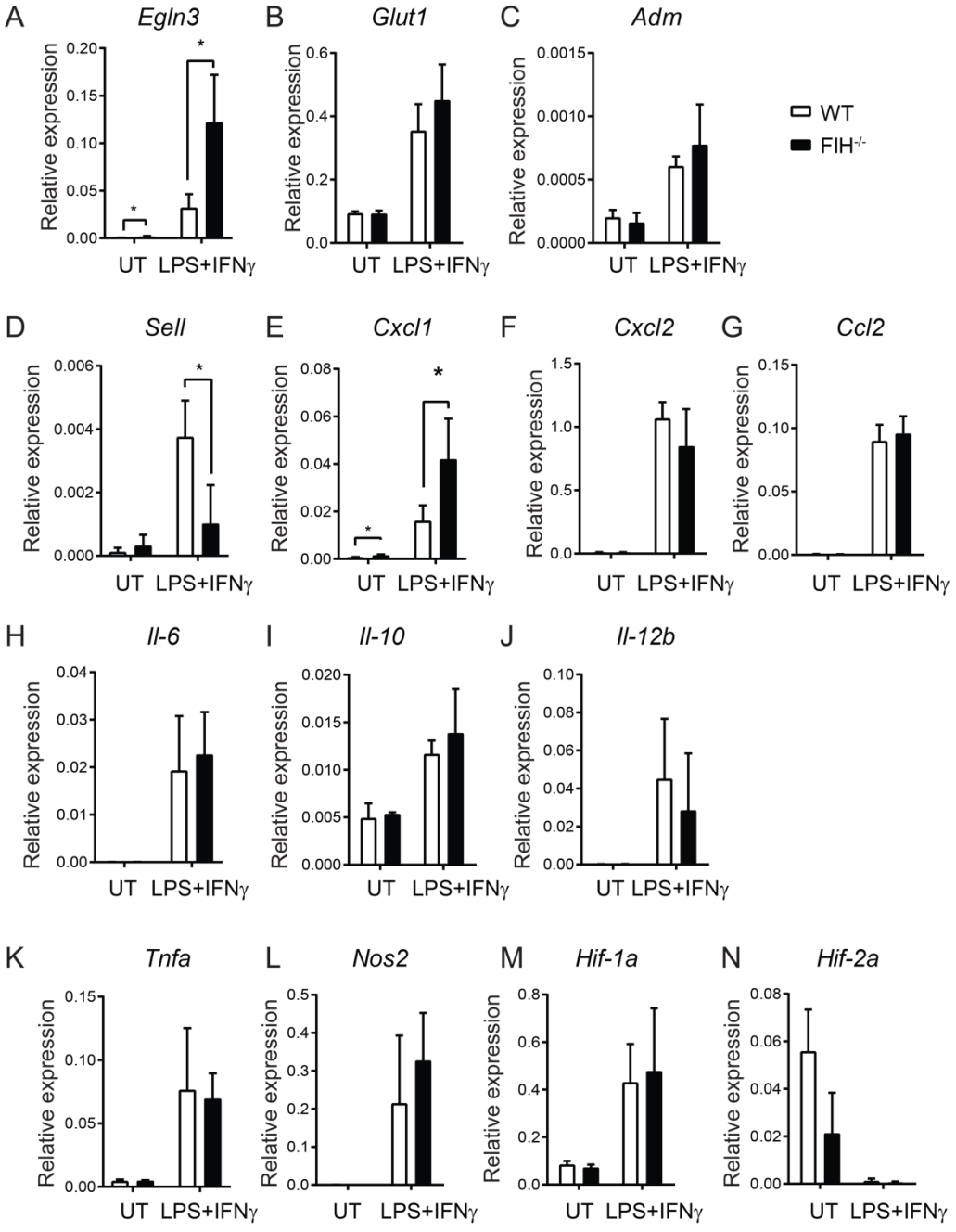

Figure 5.10 FIH-deficient M1 macrophages display altered expression of *Egln3*, *Sell,* and *Cxcl1*
WT and FIH$^{-/-}$ BMDMs were polarised to M1 macrophages and their expression of indicated genes relative to γ-actin was evaluated by RT-qPCR. BMDMs isolated from WT (n=3–4) and FIH$^{-/-}$ (n=3–4) animals were tested. * indicates $p<0.05$ by an unpaired, two-tailed student's *t*-test. Histogram bars are displayed as mean ± SD. Results are representative of two independent experiments.

Together, these data show that loss of FIH does not overly change the expression of inflammatory mediators in M1 macrophages, but does affect the expression of *Sell*, *Cxcl1*, and HIF target gene *Egln3* (PHD3).

5.2.7 FIH is required for the expression of *Mrc1* and *Retnla* in M2 macrophages

On the other side of the coin, M2 macrophages usually exhibit an immunoregulatory phenotype and are induced during tissue repair, wound healing, allergy, and parasitic infection (Rőszer 2015). To examine whether FIH could affect the phenotype of M2 macrophages, WT and FIH-null BMDMs were treated by IL-4 under normoxia or hypoxia. The expression of three M2 macrophage marker genes *Mrc1* (mannose receptor C type 1, also known as *Cd206*), *Retnla* (resistin-like molecule alpha, also known as *Fizz1*), and *Chil3* (chitinase-like 3, also known as *Ym1*) was examined by RT-qPCR (Figure 5.11, A–C). All three genes were induced upon IL-4 stimulation with various abundance (Figure 5.11, A–C). In comparison with the WT BMDMs, the expression of *Mrc1* and *Retnla* was reduced in FIH-deficient M2 macrophages (*Mrc1*: fold change 0.43, p=0.0136; *Retnla*: fold change 0.44, p=0.0248; *t*-test; Figure 5.10, A and B). *Chil3* also tended to be downregulated in the absence of FIH (Figure 5.11C). Hypoxia treatment further

boosted the induction of these genes by IL-4, yet the effect of FIH observed under normoxia was diminished under hypoxic conditions (Figure 5.11, A–C).

Given that IL-4 signalling was initiated at the IL-4 receptor (IL-4R), IL-4R expression on macrophages under normoxia was examined by flow cytometry. Loss of FIH did not affect IL-4R levels in unstimulated or IL-4-activated BMDMs (Figure 5.11D).

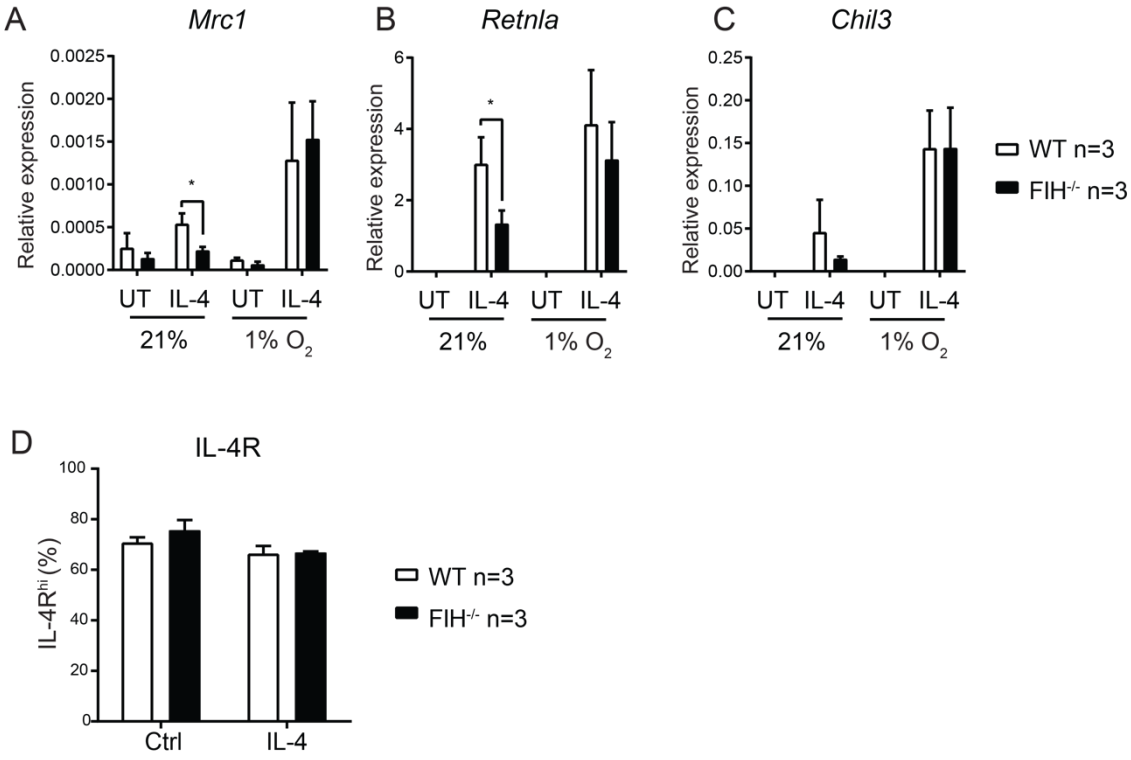

Figure 5.11 Expression of *Mrc1* and *Retnla* is aberrant in FIH$^{-/-}$ M2 BMDMs

(A) WT and FIH$^{-/-}$ BMDMs were polarised to M2 macrophages under normoxia or hypoxia for 24 hr. Expression of *Mrc1*, *Retnla*, and *Chil3* was examined by RT-qPCR and normalised by γ-actin level. (B) WT and FIH$^{-/-}$ BMDMs were polarised to M2 macrophages under normoxia for 24 hr. Surface level of IL-4R was evaluated by flow cytometry. * indicates $p<0.05$ by an unpaired, two-tailed student's *t*-test. The histogram bars are displayed as mean ± SD. Ctrl, control.

Collectively, these data suggest that FIH positively affects the expression of *Mrc1* and *Retnla* in M2 macrophages but does not affect IL-4R level.

5.3 Discussion

The development of this chapter was prompted by the recognition of the tumour suppressive effect of myeloid FIH (section 4.2.3). In agreement with the *in vivo* observations, loss of FIH promotes the expression of inhibitory molecules PD-L1 (*Cd274*) and ARG1 (*Arg1*) at both protein and mRNA level. FIH$^{-/-}$ BMDMs also exhibit enhanced migratory activity towards chemoattractants CCL5 and C5a, with concomitant upregulation of the corresponding receptors. FIH does not profoundly affect the phagocytic activity of macrophages, regardless of the oxygen level. Gene expression analysis of activated macrophages reveals that FIH deficiency does not alter the transcription profile overly but does result in an aberrant expression of *Egln3*, *Sell*, and *Cxcl1* in M1 macrophages, and reduced expression of *Mrc1* and *Retnla* in M2 macrophages. Importantly, FIH is transcriptionally induced in BMDMs by TCM, as well as other inflammatory stimulants such as LPS/IFNγ and bacterial infection. Collectively, these data suggest that FIH could be involved in the regulation of macrophage-mediated inflammatory responses.

FIH expression has been reported to be expressed at a relatively constant level in human cancer cells (Lisy and Peet 2008). Unexpectedly, this study demonstrates that FIH is transcriptionally induced in macrophages in response to inflammatory stimuli. According to the Champion ChIP Transcription Factor Search Portal (QIAGEN), several transcription factors rooted in inflammatory responses can bind to the FIH promoter region, including activator protein 1 (AP-1) and NFκB

(Medzhitov and Horng 2009). It will be necessary to investigate which pathway mediates the induction of FIH. It will be also of interest to examine the localisation of FIH in macrophages under inflammatory stress. FIH has been mostly detected in the cytoplasm (Metzen 2003; Stolze, Tian, Appelhoff, Turley, Wykoff, Gleadle, and Ratcliffe 2004a). Recently, FIH was shown to enter the nucleus when stimulated by the PHD inhibitor DMOG in a HIF-1α-dependent manner (Liang et al. 2015). Whether FIH localisation is altered by inflammatory stimuli and how the translocation may affect the function of FIH would be worth investigating.

The upregulation of FIH in macrophages may incite a series of functional changes. In the context of tumour-associated inflammation, increased expression of FIH can be associated with alleviated immunosuppression. For example, FIH may dampen T cell suppression by downregulating the expression of PD-L1 and ARG1 (Figure 5.4, C and D; Figure 5.6, C and D). In addition, FIH may suppress the recruitment of MSCs to the tumour site, given the enhanced migration to CCL5 observed in FIH-null macrophages (Figure 5.7, C–E).

In the scenario of infection, the induction of FIH may be required for the regulation of inflammatory responses. FIH may prevent the migration of monocytes to the site of inflammation, as evidenced by the enhanced migration to C5a of $FIH^{-/-}$ BMDMs (Figure 5.7, F–H). FIH may also tune down the recruitment of neutrophils, given the elevated expression of *Cxcl1,* a key chemokine for neutrophil recruitment (De Filippo et al. 2013), in FIH-deficient macrophages (Figure 5.10E). FIH may further downregulate the recruitment of monocytes due to its positive effect on *Sell* (L-selectin) expression (Figure 5.10D), which can sequester monocytes in lymphoid tissues (Xu et al. 2008). Apart from mobilising monocytes/macrophages to the site of inflammation, FIH may also enhance the

cytotoxicity of macrophages by inhibiting the expression of *Arg1* (Figure 5.5A and Figure 5.6A), which has been shown to compromise the control of intracellular pathogens (Iniesta et al. 2002; Kasmi et al. 2008). Furthermore, FIH may also affect macrophage viability by inhibiting the expression of *Egln3* (Figure 5.10A), although PHD3 has been demonstrated to have opposing effects on the survival of neutrophils and macrophages (Walmsley et al. 2011; Swain et al. 2014). Based on the above, FIH can affect multiple aspects of the inflammatory responses, and hence it is hard to conclude whether the overall effect of FIH is beneficial or detrimental. Additionally, strong inflammatory responses may effectively eliminate the assault, but may also cause excessive tissue damage. Therefore, the biological consequence of FIH induction needs to be investigated in inflammatory models and evaluated in a context-dependent manner.

Notably, a lot of these functions are associated with the altered expression of relevant genes, which echoes the role of FIH as a suppressor of the transcription factor HIF. Indeed, *Cd274*, *Ccr5*, and *Cxcl1* have all been identified as HIF-α target genes (Noman et al. 2014; Shepardson et al. 2014; Chaturvedi et al. 2014; Triner et al. 2017). The expression of *Arg1* has also been shown to be HIF-1α-dependent (Colegio et al. 2015). Nevertheless, whether the aberrant expression of these genes accounts for the corresponding phenotype of macrophages requires further investigation. Take the chemotaxis of macrophage as an example: the subtle elevation of CCR5 expression on FIH-null macrophages may not explain the enhanced migration to CCL5 (Figure 5.7 C-E, Figure 5.8A); other contributors may exist. Additionally, given that $FIH^{-/-}$ macrophages also tend to migrate more without being exposed to chemokine (Figure 5.7 C-H), it will be worthwhile to check the directionality of cell motility to refine the effect of FIH on cell migration.

Despite the link with HIF, the results also support that FIH may affect the expression of several genes not directly through HIF. For example, among the reported HIF target genes that are sensitive to FIH status shown in this study, most (*Cd274*, *Cc5r*, *Egln3*, and *Cxcl1*) are already affected by FIH in untreated macrophages, except for *Arg1*, which is not convincingly detectable without stimulation (Figure 5.6). While this does not exclude the possibility that FIH may regulate HIF activity at its basal level, it also indicates the involvement of HIF-independent mechanisms. Additionally, although FIH deficiency promotes PD-L1 upregulation in activated macrophages under normoxia, the effect is abolished under 1% O_2 (Figure 5.4). Since FIH has been reported to suppress the transcriptional activity with oxygen level as low as 0.2% (Stolze, Tian, Appelhoff, Turley, Wykoff, Gleadle, and Ratcliffe 2004b), the diminished effect of FIH may indicate the involvement of other pathways that are affected by HIF activation or hypoxia. The determination of FIH activity in macrophages in the current experimental setting would be helpful to interpret the result, however, one should take into consideration that FIH may also interact with HIF in an enzymatic activity-independent manner (Schofield and Ratcliffe 2004b). Another example is the downregulation of *Mrc1* and *Retnla in* $FIH^{-/-}$ M2 macrophages. While upregulated by hypoxia, the expression of *Mrc1* and *Retnla* is inhibited by FIH deficiency (Figure 5.11, A and B), indicating that FIH may interact with other pathways.

The FIH/HIF interaction is further complicated by the existence of other FIH-interacting partners. For example, FIH has been found to bind munc18-1-interacting protein 3 (Mint3) and membrane type 1 matrix metalloproteinase (MT1-MMP/MMP-14), the latter of which is specifically expressed in mesenchymal cells including macrophages (Sakamoto and Seiki 2009; Sakamoto and Seiki 2010).

Mint3 and MT1-MMP/MMP-14 can sequester FIH in the peri-nuclear region, therefore prevent FIH from interacting with HIF. Functionally, it has been shown that FIH suppresses GLUT1 and PGK1 expression only in the absence of Mint3 (Sakamoto and Seiki 2009). The interaction of FIH with Mint3/MT1-MMP/MMP-14, together with FIH substrates such as IκBα (Shin et al. 2009) and Notch (Coleman et al. 2007; Zheng et al. 2008), may retain FIH and restrain its contact with HIF, providing another mechanism of HIF regulation by FIH. This could be one reason why FIH deletion does not alter a wide range of HIF-dependent phenotypes.

No matter which pathways it intervenes in, the effect of FIH seems to be selective. For example, the expression of proven HIF-2α target IL-6 (Imtiyaz et al. 2010), together with other classical HIF target genes *Glut1* and *Adm*, are not affected by FIH status (Figure 5.10, B C, and H). Additionally, while the expression of proven STAT6 target genes *Mrc1* and *Retnla* in M2 macrophages requires FIH expression (Figure 5.11, A and B), *Arg1*, which is also induced by STAT6 in M2 macrophages, remains unaffected by FIH status (Figure 5.6A) (Lawrence and Natoli 2011). A genome-wide transcription study will help to uncover FIH-sensitive genes/pathways systematically and delineate how FIH regulates them in a selective way.

In conclusion, data from this chapter show that FIH is induced in macrophages in response to inflammatory stimuli, which may, as a consequence, alter the inflammatory responses of macrophages. The effect of FIH may be realised by altering expression of relevant genes in HIF-α–dependent and –independent ways.

Chapter 6 Final discussion and perspectives

6.1 Overview

This study arises from the notion that multiple aspects of tumourigenesis are regulated by HIF (Rankin and Giaccia 2008). However, given the complex and sometimes contradictory roles of HIF on malignant phenotypes and its crucial physiological functions (Semenza 2014), pan-inhibition of HIF signalling pathway could incur undesirable consequences. Instead of manipulating HIF directly, targeting the regulators of HIF signalling may be a more specific strategy. FIH has been shown to inhibit the transcription of selective HIF target genes; moreover, unlike HIF, loss of FIH has not been shown to cause developmental defects in experimental models (N. Zhang et al. 2010; Semenza 2012), rendering FIH as a potential therapeutic target.

However, our knowledge of the biological roles of FIH is still limited. On one hand, there is a lack of physiological evidence as most of the studies to date were performed *in vitro*; on the other, FIH does not only target HIF but also an array of ARD-containing proteins, the consequence of which remains poorly understood. With this in mind, the aim of the study was to interrogate the function of FIH *in vivo*, by taking advantage of genetically modified mice.

By monitoring the mice over an extended period of time, it was found that FIH suppresses spontaneous development of low-grade B cell lymphomas, particularly in the lung. Consistently, FIH also shows inhibitory effects on the growth of syngeneic tumours, which could be partially attributed to myeloid-derived FIH.

Myeloid deletion of FIH results in an altered intra-tumoural immune profile, represented by an increased proportion of the PD-L1^{+} and ARG1^{+} TAMs as well as a decreased CD4 TIL population. This effect of FIH may also extend to secondary lymphoid organs such as the spleen.

In BMDMs, FIH expression is induced by TCM, BCG infection, and the pro-inflammatory stimulators LPS/IFNγ. In line with the phenotypes of FIH$^{-/-}$ TAMs, FIH suppresses the induction of PD-L1 and ARG1 by TCM. Further, FIH may affect the transcription of a broader range of genes, evidenced by the aberrant expression of *Sell* and *Cxcl1* in M1 macrophages and downregulation of *Mrc1* and *Retnla* in M2 macrophages without FIH. Functionally, FIH negatively regulates the migration of BMDMs towards selective chemokines such as CCL5 and C5a. These observations indicate that FIH may drive phenotypic changes of macrophages to modulate inflammatory responses, which is in line with the requirement for FIH in myeloid cells in tumour suppression demonstrated *in vivo*.

6.2 FIH status in tumours and the tumour stroma

One major contribution of this study is to identify the role of FIH in tumour suppression. Remarkably, mice lacking one allele of FIH already show enhanced tumourigenesis, as demonstrated in both spontaneous (Figure 3.2) and syngeneic tumour models (Figure 4.2). While FIH expression in the heterozygous animals has not been examined in this study, others have shown that FIH$^{+/-}$ embryos (on embryonic day 12.5) expressed an intermediate level of FIH compared with WT and FIH$^{-/-}$ counterparts, using a mouse strain of which exon 2 of *Hif1an* is deleted (N. Zhang et al. 2010). This raises the hypothesis that FIH gene could be

haploinsufficient in tumour suppression. To prove this, it will be essential to examine the loss of heterozygosity of *Hif1an* in tumours derived from $FIH^{+/-}$ mice.

Nonetheless, the effect of FIH heterozygosity on tumourigenesis promotes the significance of FIH in cancer biology. Although not frequently mutated in the cancer genome (Figure 1.7), FIH has been shown to be downregulated in head and neck carcinoma (C. J. Liu et al. 2010), glioma (Yuan et al. 2014), and prostate cancer cells (Y. Li et al. 2015) by microRNAs. Additionally, the activity of FIH could be suppressed in the TME by severe hypoxia and ROS (Lando, Peet, Gorman, et al. 2002; Masson et al. 2012). In this case, reduced FIH expression or activity could be sufficient to promote oncogenesis.

In contrary to the downregulation of FIH in cancer cells, FIH expression may be upregulated in the stromal cells, given the elevated expression of FIH in BMDMs stimulated with TCM (Figure 5.11B). The upregulation of FIH in macrophages may be part of the host defence mechanisms against cancer. However, this may not be generalisable to all types of tumour. A study of human PET samples has found that FIH expression in the stroma is correlated with poorer DFS (Couvelard et al. 2008). One reason could lie in the variation in the TME components across different types of cancer. In Couvelard's study, most of the stromal cells in PET samples are fibroblasts. How FIH may regulate the function of other TME components, including cancer-associated fibroblasts, is an intriguing question to pursue.

6.3 FIH in tumour suppression: mechanism of action

Enhanced tumour growth in FIH MKO animals suggests that FIH may control tumour development by modulating the immune response. Is it also the mechanism by which FIH suppresses low-grade B lymphomagenesis?

The answer could be yes, given the association between the cause of low-grade B cell lymphomas and inflammation. A large-scale epidemiological study shows an increased risk of NHL (6.5-fold) associated with Sjögren syndrome, an autoimmune disorder affecting exocrine glands including the parotid gland. When analysing the subtypes of NHL, a 9-fold increase in the risk of DLBCL (a type of high grade lymphoma), and a dramatic 1,000-fold increase in the risk of parotid gland MALT lymphoma (a type of low-grade lymphoma), are observed in patients with Sjögren syndrome (Ekström Smedby et al. 2008). In addition to the autoimmune disorder, chronic inflammation induced by infection is another major cause of low-grade B cell lymphomas, especially MALT lymphomas. This is best exemplified by the strong association between gastroduodenitis induced by *H. pylori* infection and gastric MALT lymphoma (Sagaert et al. 2010).

Although the experimental animals in this study were not likely to experience autoimmune diseases or pathogen infection, ageing can be a trigger of chronic inflammation. In accordance with the notion that human ageing is accompanied by chronic inflammation (Franceschi and Campisi 2014), immune cell infiltration was observed in aged mice regardless of their genotype in this study (Figure 3.2). The accumulation of inflammation during ageing may foster the development of low-grade B cell lymphomas. Indeed, most of the B cell lymphomas were developed in mice that were more than 1 year old (Figure 3.2), which echoes the late onset of low-grade B cell lymphomas in patients (median age: 60 years old) (Zinzani 2012). Therefore, FIH expression may suppress age-associated inflammation, therefore inhibiting spontaneous tumourigenesis. Furthermore, ASPP2 has also been shown as a gatekeeper of inflammation, which could explain why partial deficiency of ASPP2 can further accelerate the tumourigenesis in FIH-null animals (Figure 3.5F).

Another interesting finding is that the tumour suppressive effect of FIH seems to be particularly dramatic in the lung (Figure 3.4), an organ which has constant exposure to an abundant flux of exogenous antigens. Pulmonary inflammation can potentially be exaggerated by FIH deficiency, given the downregulation of *Mrc1* and *Retnla* in FIH$^{-/-}$ macrophages (Figure 5.11, A and B), which have been shown to reduce airway inflammation (Lee et al. 2014; Kambara et al. 2015).

Follow-up studies should be performed to investigate how FIH may affect tumourigenesis by modulating the immune system. To begin with, it would be worthwhile to examine the immune profile, especially signs of chronic inflammation, in FIH-deficient mice when aged. In the present study, general characterisation of the immune system revealed no major defects in FIH$^{-/-}$ mice that were 12 weeks old (Figure 4.1), yet the picture may change with ageing. In addition, characterisation of the stromal compartment of the spontaneous tumour samples in the present study will help understand how FIH may affect the immune profile in established tumours. Furthermore, an inflammation-induced tumour model (e.g., colitis-induced colon cancer model) might be a good system to study how FIH affects tumour-initiating inflammation and the immune response to established tumours in an integrated manner.

6.4 The role of FIH as a HIF regulator

One motivation behind investigating the role of FIH is that FIH may specifically regulate HIF functions. While not yet proven experimentally, some observations of FIH-deficient animals/cells do align with the reported functions of HIF. Phenotypically, in agreement with the overall tumour-promoting effect of HIF (Rankin and Giaccia 2008), this study indicates that FIH suppresses tumour

development as suggested in a spontaneous and syngeneic tumour models. To be more specific, the tumour promoting role of myeloid expression of HIF-1α has been shown in an MMTV/PyMT breast cancer model (Doedens et al. 2010), and HIF-2α in a CAC model (Imtiyaz et al. 2010). In accordance, using the same strategy to delete FIH in the myeloid compartment of mice, this study shows that FIH suppresses the growth of B16 and LLC tumours (Figure 4.7). At the molecular level, genes/proteins that are upregulated in FIH$^{-/-}$ macrophages, including PD-L1/*Cd274* (Figure 5.3E, Figure 5.4), ARG1/*Arg1* (Figure 5.5, Figure 5.6), CCR5 (Figure 5.8A), and *Cxcl1* (Figure 5.10E), have been demonstrated to be direct HIF-α targets or be regulated by HIF-α (Chaturvedi et al. 2014; Noman et al. 2014; Shepardson et al. 2014; Colegio et al. 2015; Triner et al. 2017). These observations highlight the presumed role of FIH as a regulator of HIF activity.

Despite that FIH-deficient animals/cells exhibit several phenotypes that are opposite to those of HIF-deficient counterparts, this may not result from the interaction between the two molecules. The tumour studies of HIF- and FIH-deficient animals were performed using different models. The oxygen tensions may therefore vary, setting HIF activity at different levels. In the present study, for example, HIF-α protein is not strongly stabilised in the spontaneously formed B cell lymphomas (Figure 3.8). To determine the interaction between FIH and HIF in modulating tumourigenesis, assessment of HIF activation and FIH activity in the tumour samples is fundamentally important.

At the same time, the findings of the present study corroborate the notion that FIH regulates the transcription of HIF target genes in a selective manner (Chan et al. 2016). For example, expression of classical HIF target genes such as *Vegf*, *Glut1*, and *Adm*, which has been confirmed as being regulated by HIF-1α in

BMDMs (Cramer et al. 2003; Fang et al. 2009), is not affected by FIH status in TAMs (Figure 4.5, B and D) and BMDMs (Figure 5.10, B and C). The selectivity of the effect of FIH on HIF is also reflected functionally. For example, HIF-1α has been shown to be essential for the glycolytic pathway and loss of HIF-1α impairs energy-demanding processes in macrophages (Cramer et al. 2003); in contrast, $FIH^{-/-}$ macrophages do not show a general enhancement of ATP-dependent activities such as cell migration (Figure 5.7) and phagocytosis (Figure 5.9).

To determine the contribution of the HIF pathway in the tumour suppressive role of FIH, mice that are deficient of FIH and HIF-1α/HIF-2α should be generated and analysed with tumour models. It is essential to analyse the activation status of HIF signalling pathway in the tumour tissue. At the molecular level, RNA sequencing analyses of tissues from these mutant mice will provide clues to how FIH affects the transcriptional landscape of HIF or other signalling pathways. One should be cautious about the tissue-specificity of FIH's effect on HIF. Given the significance of FIH in myeloid biology identified in this study, macrophages could be an appropriate system to start with.

6.5 The potential role of FIH in the host response to infection

The induction of FIH in BMDMs infected with BCG (Figure 5.2C), an attenuated strain of *M. bovis* that resembles the lifestyle of Mtb, indicates the potential role of FIH in host defence against bacterial infection.

Macrophages in the alveoli are the primary target for Mtb. They phagocytose Mtb and activate the adaptive immune system to generate antigen-specific CD4 T cells, which normally come into action 18–20 days after the initial infection. During

this period of time, Mtb proliferate inside macrophages, until macrophages die or acquire killing activity (Orme, Robinson, and Cooper 2014).

The transient induction of FIH within the first 72 hr post-infection (Figure 5.11C) suggests that FIH may be critical for the initial control of BCG within macrophages. One key mechanism of Mtb killing by macrophages is the production of NO, which is regulated by ARG1 and NOS2. NOS2 metabolises $_{L}$-arginine to produce NO, whereas ARG1 regulates NOS2 activity via substrate competition (Munder et al. 1999; Rutschman et al. 2001). In accordance, myeloid expression of ARG1 has been shown to promote BCG survival, an effect that correlates with an enhanced NO response (Kasmi et al. 2008). Interestingly, the expression of both NOS2 and ARG1 can be suppressed by FIH, as demonstrated in TAMs or M1 macrophages (Figure 4.5D, 5.5). How FIH balances the expression of two genes and affects the outcome of bacterial clearance in macrophages will be intriguing to investigate.

Interestingly, HIF-1α-deficient mice have been shown to be highly susceptible to Mtb infection, which is associated with defective production of NO and inflammatory mediators by myeloid cells (Braverman et al. 2016). This implies that FIH might negatively regulate the host defence to Mtb infection, which will confer FIH inhibitors with therapeutic value. Examining the expression of NOS2 and other inflammatory mediators in FIH-deficient macrophages will help to assess how FIH may affect the HIF pathway during infection. Challenging FIH-deficient mice with Mtb will provide a more definite answer.

6.6 Conclusion

In conclusion, this study provides the first genetic evidence for a tumour suppressive effect of FIH in mice. Mechanistically, FIH may inhibit tumour

development by orchestrating the myeloid-mediated tumour immune response. Future work will aim to investigate the mechanism of FIH induction in macrophages, the involvement of HIF pathway in FIH-mediated tumour suppression, and the expression profile of FIH in the stroma of human cancers and how it may associate with clinical parameters of the patients.

Supplementary tables

Table S1. Tissue distribution of tumours

Code	Genotype	Type of tumour	Lymph node	Thymus	Spleen	Lung	Liver	Kidney	Peri-ureteral fat	Pericardial fat
M00047105	$FIH^{+/+}$ $ASPP2^{+/+}$				Fibrosis	Inflammation		Inflammation		
M00047091	$FIH^{+/+}$ $ASPP2^{+/+}$									
M00047067	$FIH^{+/+}$ $ASPP2^{+/+}$	B cell lymphoma	High		High	Inflammation	Inflammation			
XCFW5.2g	$FIH^{+/+}$ $ASPP2^{+/+}$									
XCFW5.8d	$FIH^{+/+}$ $ASPP2^{+/+}$					Inflammation	Inflammation			
M00047321	$FIH^{+/+}$ $ASPP2^{+/+}$	FDCS, B cell lymphoma			FDCS		Inflammation		High	
M00047087	$FIH^{+/+}$ $ASPP2^{+/+}$	B cell lymphoma			Low				Low	
M00047028	$FIH^{+/+}$ $ASPP2^{+/+}$									
XCFW5.3c	$FIH^{+/+}$ $ASPP2^{+/+}$									
XCFW5.3b	$FIH^{+/+}$ $ASPP2^{+/+}$	B cell lymphoma	Inflammation		High	Inflammation		High		
M00047292	$FIH^{+/+}$ $ASPP2^{+/+}$									
M00047315	$FIH^{+/+}$ $ASPP2^{+/+}$									
M00047053	$FIH^{+/+}$ $ASPP2^{+/+}$									
M00047028	$FIH^{+/+}$ $ASPP2^{+/+}$									
M00047290	$FIH^{+/-}$ $ASPP2^{+/+}$									
FIHTORP135	$FIH^{+/-}$ $ASPP2^{+/+}$									
XCGW29.2i	$FIH^{+/-}$ $ASPP2^{+/+}$									

Code	Genotype	Type of tumour	Lymph node	Thymus	Spleen	Lung	Liver	Kidney	Peri-ureteral fat	Pericardial fat
M00047032	$FIH^{+/-}$ $ASPP2^{+/+}$	B cell lymphoma	Low+high		Low+high	Low+high		Low+high		
XCGW33.1d	$FIH^{+/-}$ $ASPP2^{+/+}$	B cell lymphoma	Low		Low					
M00047018	$FIH^{+/-}$ $ASPP2^{+/+}$	Myeloid leukaemia			Myeloid leukaemia					
M00047017	$FIH^{+/-}$ $ASPP2^{+/+}$	B cell lymphoma			High	High	High	High		
M00047027	$FIH^{+/-}$ $ASPP2^{+/+}$	B cell lymphoma			Low+high	Low				Low
M00037361	$FIH^{+/-}$ $ASPP2^{+/+}$	B cell lymphoma		Low	High	High	Inflammation		Low+high	Low
M00037315	$FIH^{+/-}$ $ASPP2^{+/+}$	B cell lymphoma				Low				Low
M00047089	$FIH^{+/-}$ $ASPP2^{+/+}$	T cell lymphoma								
M00047293	$FIH^{+/-}$ $ASPP2^{+/+}$	B cell lymphoma		High			High			
M00047085	$FIH^{+/-}$ $ASPP2^{+/+}$	Myeloid leukaemia			Myeloid leukaemia	Myeloid leukaemia	Myeloid leukaemia	Myeloid leukaemia		
M00047096	$FIH^{+/-}$ $ASPP2^{+/+}$									
M00047038	$FIH^{+/-}$ $ASPP2^{+/+}$	B cell lymphoma	High		Low+high		Inflammation			
M00047016	$FIH^{+/-}$ $ASPP2^{+/+}$	B cell lymphoma, colon adenocarcinoma	Low+high		Low	Low	Sepsis /inflammation	Low		
M00047019	$FIH^{+/-}$ $ASPP2^{+/+}$	B cell lymphoma			High	Low				
M00047072	$FIH^{+/-}$ $ASPP2^{+/+}$									
M00047048	$FIH^{+/-}$ $ASPP2^{+/+}$									
M00079365	$FIH^{+/-}$ $ASPP2^{+/+}$									
XCFW4.2a	$FIH^{+/-}$ $ASPP2^{+/+}$									
M00047088	$FIH^{-/-}$ $ASPP2^{+/+}$				Inflammation					
M00037084	$FIH^{-/-}$ $ASPP2^{+/+}$	B cell lymphoma, HCC			Low+high	Low	HCC			
M00047291	$FIH^{-/-}$ $ASPP2^{+/+}$	B cell lymphoma	Low		Low	Low	Low	Low		Low
XCGW14.3c	$FIH^{-/-}$ $ASPP2^{+/+}$	B cell lymphoma			Low	Low+high				
XCGW34.5d	$FIH^{-/-}$ $ASPP2^{+/+}$	B cell lymphoma			Low	Low		Low	Low	

Code	Genotype	Type of tumour	Lymph node	Thymus	Spleen	Lung	Liver	Kidney	Peri-ureteral fat	Pericardial fat
XCGW15.1a	$FIH^{-/-}$ $ASPP2^{+/+}$	B cell lymphoma			Low	Low	Necrosis		Low	
XCGW14.3f	$FIH^{-/-}$ $ASPP2^{+/+}$									
M00037083	$FIH^{-/-}$ $ASPP2^{+/+}$	B cell lymphoma			Low	Low		Low		Low
M00047322	$FIH^{-/-}$ $ASPP2^{+/+}$	B cell lymphoma			Low+high	Low	Low	High	Inflammation (granulomas)	
XCGW15.1b	$FIH^{-/-}$ $ASPP2^{+/+}$	B cell lymphoma	High		Low+high					
XCGW14.3d	$FIH^{-/-}$ $ASPP2^{+/+}$	B cell lymphoma			Low	Low		Low		
XCFW5.1f	$FIH^{-/-}$ $ASPP2^{+/+}$	B cell lymphoma			Low					
XCGW28.2e	$FIH^{-/-}$ $ASPP2^{+/+}$	B cell lymphoma			Low+high	Low				
XCFW3.4g	$FIH^{-/-}$ $ASPP2^{+/+}$	B cell lymphoma			Low	Low				
XCFW3.3c	$FIH^{-/-}$ $ASPP2^{+/+}$	B cell lymphoma			Low+high	Low				
XCFW3.4a	$FIH^{-/-}$ $ASPP2^{+/+}$	Lung adenocarcinoma				Adeno-carcinoma				
XCFW3.4b	$FIH^{-/-}$ $ASPP2^{+/+}$	B cell lymphoma			Low	Low		Low	Low	
M00047043	$FIH^{-/-}$ $ASPP2^{+/+}$									
XCGW10.7c	$FIH^{-/-}$ $ASPP2^{+/+}$									
XCGW32.6e	$FIH^{-/-}$ $ASPP2^{+/+}$									
M00047323	$FIH^{-/-}$ $ASPP2^{+/+}$									
M00047162	$FIH^{-/-}$ $ASPP2^{+/+}$									
XTVFIH42	$FIH^{+/+}$ $ASPP2^{+/-}$	B cell lymphoma			Low		Inflammation			
XTVFIH89	$FIH^{+/+}$ $ASPP2^{+/-}$	Myeloid leukaemia				Inflammation (chronic)	Myeloid leukaemia			Inflammation
M00037099	$FIH^{+/+}$ $ASPP2^{+/-}$	B cell lymphoma			Low				Low	
XTVFIH114	$FIH^{+/+}$ $ASPP2^{+/-}$	Myeloid leukaemia			Myeloid leukaemia					
XTVFIH46	$FIH^{+/+}$ $ASPP2^{+/-}$	NETs in SI and B cell lymphoma			Low	Low				
XTVFIH52	$FIH^{+/+}$ $ASPP2^{+/-}$	B cell Lymphoma	Low		Low+high		Low			

Code	Genotype	Type of tumour	Lymph node	Thymus	Spleen	Lung	Liver	Kidney	Peri-ureteral fat	Pericardial fat
XTVFIH64	$FIH^{+/+}$ $ASPP2^{+/-}$	B cell lymphoma, HCC			Low					
XTVFIH101	$FIH^{+/+}$ $ASPP2^{+/-}$	B cell lymphoma, HCC			Low	Low	HCC	Low		
XTVFIH69	$FIH^{+/+}$ $ASPP2^{+/-}$	Myeloid leukaemia	Myeloid leukaemia		Myeloid leukaemia	Myeloid leukaemia	Myeloid leukaemia			
M00047049	$FIH^{+/+}$ $ASPP2^{+/-}$									
M00047139	$FIH^{+/+}$ $ASPP2^{+/-}$									
XCGW10.7b	$FIH^{-/-}$ $ASPP2^{+/-}$									
M00047110	$FIH^{-/-}$ $ASPP2^{+/-}$	Myeloid leukaemia			Myeloid leukaemia			Myeloid leukaemia		
XCGW25.3c	$FIH^{-/-}$ $ASPP2^{+/-}$	B cell lymphoma			Low	Low	Low	Low		
XCGW14.3e	$FIH^{-/-}$ $ASPP2^{+/-}$	B cell lymphoma			Low	Low	Low		Low	
XTVFIH82	$FIH^{-/-}$ $ASPP2^{+/-}$	B cell lymphoma			Low					
XCGW28.1b	$FIH^{-/-}$ $ASPP2^{+/-}$									
XTVFIH91	$FIH^{-/-}$ $ASPP2^{+/-}$	Myeloid leukaemia					Myeloid leukaemia			
M00084922	$FIH^{-/-}$ $ASPP2^{+/-}$	T cell lymphoma								
XCGW28.1a	$FIH^{-/-}$ $ASPP2^{+/-}$	B cell lymphoma			Low			Low		
XTVFIH75	$FIH^{-/-}$ $ASPP2^{+/-}$	B cell lymphoma			Low					
M00270644	$FIH^{-/-}$ $ASPP2^{+/-}$									
XCGW15.3d	$FIH^{-/-}$ $ASPP2^{+/-}$									
M00079364	$FIH^{-/-}$ $ASPP2^{+/-}$									

Low: low-grade B cell lymphoma; low+high: B cell lymphoma with both low-grade and high-grade components; high: high-grade B cell lymphoma.

Table S2. Number of animals and tumours in Figure 4.2B*

Time point	Number of tumours			Number of mice		
	WT	$FIH^{+/-}$	$FIH^{-/-}$	WT	$FIH^{+/-}$	$FIH^{-/-}$
Day 8	8	8	6	5	7	4
Day 9	8	8	6	5	7	4
Day 10	8	8	4	5	7	3
Day 11	8	7	4	5	6	3
Day 12	8	5	4	5	5	3
Day 14	8	5	4	5	5	3

Table S3. Number of animals and tumours in Figure 4.2D*

Time point	Number of tumours			Number of mice		
	WT	$FIH^{+/-}$	$FIH^{-/-}$	WT	$FIH^{+/-}$	$FIH^{-/-}$
Day 10	10	18	4	7	11	2
Day 12	10	18	4	7	11	2
Day 13	10	18	4	7	11	2
Day 14	10	14	4	7	9	2

Table S4. Number of animals and tumours in Figure 4.7B*

Time point	Number of tumours		Number of mice	
	WT	FIH MKO	WT	FIH MKO
Day 10	3	8	2	4
Day 12	8	8	5	4
Day 13	8	8	5	4

Table S5. Number of animals and tumours in Figure 4.7D*

Time point	Number of tumours		Number of mice	
	WT	FIH MKO	WT	FIH MKO
Day 8	9	15	7	8
Day 10	9	15	7	8
Day 11	13	15	9	8
Day 12	12	16	8	8
Day 13	12	17	8	9
Day 14	13	17	8	9

* Number of mice or tumours fluctuates because some animals had to be culled due to tumour ulceration, while some others developed tumours of measurable sizes at later time points.

Bibliography

Acker, Till, Antonio Diez-Juan, Julian Aragones, Marc Tjwa, Koen Brusselmans, Lieve Moons, Dai Fukumura, et al. 2005. “Genetic Evidence for a Tumor Suppressor Role of HIF-2α.” *Cancer Cell* 8 (2): 131–41. doi:10.1016/j.ccr.2005.07.003.

Aderem, A, and D M Underhill. 1999. “Mechanisms of Phagocytosis in Macrophages.” *Annual Review of Immunology* 17 (1): 593–623. doi:10.1146/annurev.immunol.17.1.593.

Albarosa, Ruth, Bruno M Colombo, Luca Roz, Ivana Magnani, Bianca Pollo, Nicola Cirenei, Cristiana Giani, Anna Maria Fuhrman Conti, Stefano DiDonato, and Gaetano Finocchiaro. 1996. “Deletion Mapping of Gliomas Suggests the Presence of Two Small Regionsfor Candidate Tumor-Suppressor Genes in a 17-cM Interval on Chromosome 10q.” *Am. J. Hum. Genet.*, no. 58 (February): 1260–67.

Andersen, Sigve, Tom Donnem, Helge Stenvold, Samer Al-Saad, Khalid Al-Shibli, Lill-Tove Busund, and Roy M Bremnes. 2011. “Overexpression of the HIF Hydroxylases PHD1, PHD2, PHD3 and FIH Are Individually and Collectively Unfavorable Prognosticators for NSCLC Survival.” Edited by Libing Song. *PLoS ONE* 6 (8): e23847–48. doi:10.1371/journal.pone.0023847.

Argyriou, Pinelopi, Sotirios G Papageorgiou, Varvara Panteleon, Amanda Psyrri, Vassiliki Bakou, Vassiliki Pappa, Aris Spathis, et al. 2010. “Hypoxia-Inducible Factors in Mantle Cell Lymphoma: Implication for an Activated mTORC1→HIF-1α Pathway.” *Annals of Hematology* 90 (3). Springer-Verlag: 315–22. doi:10.1007/s00277-010-1070-6.

Artavanis-Tsakonas, S, M D Rand, and R J Lake. 1999. “Notch Signaling: Cell Fate Control and Signal Integration in Development.” *Science* 284 (5415): 770–76.

Balkwill, Fran, and Alberto Mantovani. 2001. “Inflammation and Cancer: Back to Virchow?.” *The Lancet* 357 (9255): 539–45. doi:10.1016/S0140-6736(00)04046-0.

Barsoum, I B, C A Smallwood, D R Siemens, and C H Graham. 2014. “A Mechanism of Hypoxia-Mediated Escape From Adaptive Immunity in Cancer Cells.” *Cancer Research* 74 (3): 665–74. doi:10.1158/0008-5472.CAN-13-0992.

Bergamaschi, D, Y Samuels, B Jin, S Duraisingham, T Crook, and X Lu. 2004. “ASPP1 and ASPP2: Common Activators of P53 Family Members.” *Molecular and Cellular Biology* 24 (3): 1341–50. doi:10.1128/MCB.24.3.1341-1350.2004.

Bertout, Jessica A, Shetal A Patel, and M Celeste Simon. 2008. “The Impact of O_2 Availability on Human Cancer.” *Nature Reviews Cancer* 8 (12): 967–75. doi:10.1038/nrc2540.

Beutler, B. 2004. “Innate Immunity: an Overview.” *Molecular Immunology* 40 (12): 845–59. doi:10.1016/j.molimm.2003.10.005.

Biju, Mangatt P, Aaron K Neumann, Steven J Bensinger, Randall S Johnson, Laurence A Turka, and Volker H Haase. 2004. “Vhlh Gene Deletion Induces

Hif-1-Mediated Cell Death in Thymocytes." *Molecular and Cellular Biology* 24 (20). American Society for Microbiology: 9038–47. doi:10.1128/MCB.24.20.9038-9047.2004.

Bonde, Anne-Katrine, Verena Tischler, Sushil Kumar, Alex Soltermann, and Reto A Schwendener. 2012. "Intratumoral Macrophages Contribute to Epithelial-Mesenchymal Transition in Solid Tumors." *BMC Cancer* 12 (1). BioMed Central Ltd: 35. doi:10.1186/1471-2407-12-35.

Bracken, Cameron P, Anthony O Fedele, Sarah Linke, Wiltiana Balrak, Karolina Lisy, Murray L Whitelaw, and Daniel J Peet. 2006. "Cell-Specific Regulation of Hypoxia-Inducible Factor (HIF)-1alpha and HIF-2alpha Stabilization and Transactivation in a Graded Oxygen Environment.." *Journal of Biological Chemistry* 281 (32). American Society for Biochemistry and Molecular Biology: 22575–85. doi:10.1074/jbc.M600288200.

Braverman, Jonathan, Kimberly M Sogi, Daniel Benjamin, Daniel K Nomura, and Sarah A Stanley. 2016. "HIF-1α Is an Essential Mediator of IFNg-Dependent Immunity to Mycobacterium Tuberculosis." *Journal of Immunology (Baltimore, Md. : 1950)* 197 (4): 1287–97. doi:10.4049/jimmunol.1600266.

Bray, Sarah J. 2016. "Notch Signalling in Context." *Nature Publishing Group* 17 (11). Nature Publishing Group: 722–35. doi:10.1038/nrm.2016.94.

Broad, Lisa, Adrian Mogg, Elizabeth Eberle, Marcia Tolley, Dominic Li, and Kelly Knopp. 2016. "TRPV3 in Drug Development." *Pharmaceuticals* 9 (3). Multidisciplinary Digital Publishing Institute: 55–17. doi:10.3390/ph9030055.

Bronte, Vincenzo, Paolo Serafini, Alessandra Mazzoni, David M Segal, and Paola Zanovello. 2003. "L-Arginine Metabolism in Myeloid Cells Controls T-Lymphocyte Functions." *Trends in Immunology* 24 (6): 301–5. doi:10.1016/S1471-4906(03)00132-7.

Brugarolas, James B, Francisca Vazquez, Archana Reddy, William R Sellers, and William G Kaelin Jr. 2003. "TSC2 Regulates VEGF Through mTOR-Dependent and -Independent Pathways." *Cancer Cell* 4 (2): 147–58. doi:10.1016/S1535-6108(03)00187-9.

Burke, Bernard, Ngai Tang, Kevin P Corke, Dean Tazzyman, Kurosh Ameri, Michael Wells, and Claire E Lewis. 2002. "Expression of HIF-1alpha by Human Macrophages: Implications for the Use of Macrophages in Hypoxia-Regulated Cancer Gene Therapy." *The Journal of Pathology* 196 (2): 204–12. doi:10.1002/path.1029.

Cadranel, J, M Wislez, and M Antoine. 2002. "Primary Pulmonary Lymphoma." *European Respiratory Journal* 20 (3). European Respiratory Society: 750–62. doi:10.1183/09031936.02.00404102.

Carreau, Aude, Bouchra El Hafny-Rahbi, Agata Matejuk, Catherine Grillon, and Claudine Kieda. 2011. "Why Is the Partial Oxygen Pressure of Human Tissues a Crucial Parameter? Small Molecules and Hypoxia.." *Journal of Cellular and Molecular Medicine* 15 (6): 1239–53. doi:10.1111/j.1582-4934.2011.01258.x.

Chan, Mun Chiang, Nicholas E Ilott, Johannes Schödel, David Sims, Anthony Tumber, Kerstin Lippl, David R Mole, et al. 2016. "Tuning the Transcriptional Response to Hypoxia by Inhibiting Hypoxia-Inducible Factor (HIF) Prolyl and Asparaginyl Hydroxylases." *Journal of Biological Chemistry* 291 (39): 20661–73. doi:10.1074/jbc.M116.749291.

Chandak, Prakash G, Branislav Radovic, Elma Aflaki, Dagmar Kolb, Marlene Buchebner, Eleonore Fröhlich, Christoph Magnes, et al. 2010. "Efficient

Phagocytosis Requires Triacylglycerol Hydrolysis by Adipose Triglyceride Lipase." *The Journal of Biological Chemistry* 285 (26). American Society for Biochemistry and Molecular Biology: 20192–201. doi:10.1074/jbc.M110.107854.

Chang, Chih-Hao, Jing Qiu, David O'Sullivan, Michael D Buck, Takuro Noguchi, Jonathan D Curtis, Qiongyu Chen, et al. 2015. "Metabolic Competition in the Tumor Microenvironment Is a Driver of Cancer Progression." *Cell* 162 (6). Elsevier Inc.: 1229–41. doi:10.1016/j.cell.2015.08.016.

Chang, Chiung I, James C Liao, and Lih Kuo. 2001. "Macrophage Arginase Promotes Tumor Cell Growth and Suppresses Nitric Oxide-Mediated Tumor Cytotoxicity." *Cancer Research* 61 (3): 1100–1106.

Chaplin, David D. 2010. "Overview of the Immune Response." *Journal of Allergy and Clinical Immunology* 125 (2): S3–S23. doi:10.1016/j.jaci.2009.12.980.

Chaturvedi, Pallavi, Daniele M Gilkes, Naoharu Takano, and Gregg L Semenza. 2014. "Hypoxia-Inducible Factor-Dependent Signaling Between Triple-Negative Breast Cancer Cells and Mesenchymal Stem Cells Promotes Macrophage Recruitment." *Proceedings of the National Academy of Sciences of the United States of America* 111 (20). National Acad Sciences: E2120–29. doi:10.1073/pnas.1406655111.

Chen, J, C C Jiang, L Jin, and X D Zhang. 2016. "Regulation of PD-L1: a Novel Role of Pro-Survival Signalling in Cancer." *Annals of Oncology* 27 (3): 409–16. doi:10.1093/annonc/mdv615.

Chen, Lieping, and Dallas B Flies. 2013. "Molecular Mechanisms of T Cell Co-Stimulation and Co-Inhibition." *Nature Reviews Immunology* 13 (4): 227–42. doi:10.1038/nri3405.

Chen, Tao, Li-Qing Yao, Qiang Shi, Zhong Ren, Le-Chi Ye, Jian-Min Xu, Ping-Hong Zhou, and Yun-Shi Zhong. 2014. "MicroRNA-31 Contributes to Colorectal Cancer Development by Targeting Factor Inhibiting HIF-1α (FIH-1)." *Cancer Biology & Therapy* 15 (5): 516–23. doi:10.4161/cbt.28017.

Chen, Tao, Zhong Ren, Le-Chi Ye, Ping-Hong Zhou, Jian-Min Xu, Qiang Shi, Li-Qing Yao, and Yun-Shi Zhong. 2015. "Factor Inhibiting HIF1α (FIH-1) Functions as a Tumor Suppressor in Human Colorectal Cancer by Repressing HIF1α Pathway." *Cancer Biology & Therapy* 16 (2): 244–52. doi:10.1080/15384047.2014.1002346.

Choe, Sung Sik, Kyung Cheul Shin, Sojeong Ka, Yun Kyung Lee, Jang-Soo Chun, and Jae Bum Kim. 2014. "Macrophage HIF-2α Ameliorates Adipose Tissue Inflammation and Insulin Resistance in Obesity." *Diabetes* 63 (10). American Diabetes Association: 3359–71. doi:10.2337/db13-1965.

Christian, Frank, Emma Smith, and Ruaidhrí Carmody. 2016. "The Regulation of NF-κB Subunits by Phosphorylation." *Cells* 5 (1). Multidisciplinary Digital Publishing Institute: 12–19. doi:10.3390/cells5010012.

Clambey, E T, and E N McNamee. 2012. "Hypoxia-Inducible Factor-1 Alpha–Dependent Induction of FoxP3 Drives Regulatory T-Cell Abundance and Function During Inflammatory Hypoxia of the Mucosa." In. doi:10.1073/pnas.1202366109/-/DCSupplemental.

Clausen, B E, C Burkhardt, W Reith, R Renkawitz, and I Förster. 1999. "Conditional Gene Targeting in Macrophages and Granulocytes Using LysMcre Mice.." *Transgenic Research* 8 (4): 265–77.

Cockman, Matthew E, David E Lancaster, Ineke P Stolze, Kirsty S Hewitson, Michael A McDonough, Mathew L Coleman, Charlotte H Coles, et al. 2006.

"Posttranslational Hydroxylation of Ankyrin Repeats in IkappaB Proteins by the Hypoxia-Inducible Factor (HIF) Asparaginyl Hydroxylase, Factor Inhibiting HIF (FIH)." *Proceedings of the National Academy of Sciences* 103 (40): 14767–72. doi:10.1073/pnas.0606877103.

Cockman, Matthew E, James D Webb, and Peter J Ratcliffe. 2009. "FIH-Dependent Asparaginyl Hydroxylation of Ankyrin Repeat Domain-Containing Proteins." *Annals of the New York Academy of Sciences* 1177 (1). Blackwell Publishing Inc: 9–18. doi:10.1111/j.1749-6632.2009.05042.x.

Cockman, Matthew E, James D Webb, Holger B Kramer, Benedikt M Kessler, and Peter J Ratcliffe. 2009. "Proteomics-Based Identification of Novel Factor Inhibiting Hypoxia-Inducible Factor (FIH) Substrates Indicates Widespread Asparaginyl Hydroxylation of Ankyrin Repeat Domain-Containing Proteins." *Molecular & Cellular Proteomics : MCP* 8 (3). American Society for Biochemistry and Molecular Biology: 535–46. doi:10.1074/mcp.M800340-MCP200.

Colegio, Oscar R, Ngoc-Quynh Chu, Alison L Szabo, Thach Chu, Anne Marie Rhebergen, Vikram Jairam, Nika Cyrus, et al. 2015. "Functional Polarization of Tumour-Associated Macrophages by Tumour-Derived Lactic Acid" 513 (7519). Nature Publishing Group: 559–63. doi:10.1038/nature13490.

Coleman, Mathew L, Michael A McDonough, Kirsty S Hewitson, Charlotte Coles, Jasmin Mecinović, Mariola Edelmann, Kristina M Cook, et al. 2007. "Asparaginyl Hydroxylation of the Notch Ankyrin Repeat Domain by Factor Inhibiting Hypoxia-Inducible Factor." *Journal of Biological Chemistry* 282 (33): 24027–38. doi:10.1074/jbc.M704102200.

Cong, Weili, Tomonori Hirose, Yutaka Harita, Akio Yamashita, Keiko Mizuno, Hisashi Hirano, and Shigeo Ohno. 2010. "ASPP2 Regulates Epithelial Cell Polarity Through the PAR Complex." *Current Biology : CB* 20 (15): 1408–14. doi:10.1016/j.cub.2010.06.024.

Cooper, G M. 2000. *The Cell: a Molecular Approach*. ASM Press.

Corzo, Cesar A, Thomas Condamine, Lily Lu, Matthew J Cotter, Je-In Youn, Pingyan Cheng, Hyun-Il Cho, et al. 2010. "HIF-1α Regulates Function and Differentiation of Myeloid-Derived Suppressor Cells in the Tumor Microenvironment." *The Journal of Experimental Medicine* 207 (11): 2439–53. doi:10.1084/jem.20100587.

Couvelard, A, L Deschamps, V Rebours, A Sauvanet, K Gatter, F Pezzella, P Ruszniewski, and P Bedossa. 2008. "Overexpression of the Oxygen Sensors PHD-1, PHD-2, PHD-3, and FIH Is Associated with Tumor Aggressiveness in Pancreatic Endocrine Tumors." *Clinical Cancer Research* 14 (20): 6634–39. doi:10.1158/1078-0432.CCR-07-5258.

Cowey, C Lance, and W Kimryn Rathmell. 2009. "VHL Gene Mutations in Renal Cell Carcinoma: Role as a Biomarker of Disease Outcome and Drug Efficacy." *Current Oncology Reports* 11 (2). Current Science Inc.: 94–101. doi:10.1007/s11912-009-0015-5.

Cramer, Thorsten, Yuji Yamanishi, Björn E Clausen, Irmgard Förster, Rafal Pawlinski, Nigel Mackman, Volker H Haase, et al. 2003. "HIF-1alpha Is Essential for Myeloid Cell-Mediated Inflammation." *Cell* 112 (5): 645–57.

Crotty, Shane. 2015. "A Brief History of T Cell Help to B Cells." *Nature Reviews Immunology* 15 (3): 185–89. doi:10.1038/nri3803.

Curiel, Tyler J, George Coukos, Linhua Zou, Xavier Alvarez, Pui Cheng, Peter Mottram, Melina Evdemon-Hogan, et al. 2004. "Specific Recruitment of

Regulatory T Cells in Ovarian Carcinoma Fosters Immune Privilege and Predicts Reduced Survival." *Nat Med* 10 (9): 942–49. doi:10.1038/nm1093.

Dang, Eric V, Joseph Barbi, Huang-Yu Yang, Dilini Jinasena, Hong Yu, Ying Zheng, Zachary Bordman, et al. 2011. "Control of TH17/Treg Balance by Hypoxia-Inducible Factor 1." *Cell* 146 (5). Elsevier Inc.: 772–84. doi:10.1016/j.cell.2011.07.033.

Dayan, F, D Roux, M C Brahimi-Horn, J Pouyssegur, and N M Mazure. 2006. "The Oxygen Sensor Factor-Inhibiting Hypoxia-Inducible Factor-1 Controls Expression of Distinct Genes Through the Bifunctional Transcriptional Character of Hypoxia-Inducible Factor-1?." *Cancer Research* 66 (7): 3688–98. doi:10.1158/0008-5472.CAN-05-4564.

De Filippo, Katia, Anne Dudeck, Mike Hasenberg, Emma Nye, Nico van Rooijen, Karin Hartmann, Matthias Gunzer, Axel Roers, and Nancy Hogg. 2013. "Mast Cell and Macrophage Chemokines CXCL1/CXCL2 Control the Early Stage of Neutrophil Recruitment During Tissue Inflammation." *Blood* 121 (24). American Society of Hematology: 4930–37. doi:10.1182/blood-2013-02-486217.

de Silly, Romain Vuillefroy, Pierre-Yves Dietrich, and Paul R Walker. 2016. "Hypoxia and Antitumor CD8 T Cells: an Incompatible Alliance?." *OncoImmunology* 5 (12). Taylor & Francis: 1–8. doi:10.1080/2162402X.2016.1232236.

Deeb, George, Mary M Vaughan, Ian McInnis, Laurie Ann Ford, Sheila N J Sait, Petr Starostik, Meir Wetzler, Terry Mashtare, and Eunice S Wang. 2011. "Hypoxia-Inducible Factor-1alpha Protein Expression Is Associated with Poor Survival in Normal Karyotype Adult Acute Myeloid Leukemia." *Leukemia Research* 35 (5). Elsevier Ltd: 579–84. doi:10.1016/j.leukres.2010.10.020.

Dengler, Veronica L, Matthew D Galbraith, and Joaquín M Espinosa. 2013. "Transcriptional Regulation by Hypoxia Inducible Factors." *Critical Reviews in Biochemistry and Molecular Biology* 49 (1): 1–15. doi:10.3109/10409238.2013.838205.

Denko, Nicholas C. 2008. "Hypoxia, HIF1 and Glucose Metabolism in the Solid Tumour." *Nature Reviews Cancer* 8 (9): 705–13. doi:10.1038/nrc2468.

Depping, Reinhard, Wolfgang Jelkmann, and Friederike Katharina Kosyna. 2015. "Nuclear-Cytoplasmatic Shuttling of Proteins in Control of Cellular Oxygen Sensing." *Journal of Molecular Medicine* 93 (6). Springer Berlin Heidelberg: 599–608. doi:10.1007/s00109-015-1276-0.

Devries, Ingrid L, Rachel J Hampton-Smith, Melinda M Mulvihill, Vera Alverdi, Daniel J Peet, and Elizabeth A Komives. 2010. "Consequences of IkappaB Alpha Hydroxylation by the Factor Inhibiting HIF (FIH)." *FEBS Letters* 584 (23). Federation of European Biochemical Societies: 4725–30. doi:10.1016/j.febslet.2010.10.060.

Diaz-Montero, C Marcela, Jim Finke, and Alberto J Montero. 2014. "Myeloid-Derived Suppressor Cells in Cancer Therapeutic, Predictive, and Prognostic Implications." *Seminars in Oncology* 41 (2). Elsevier: 174–84. doi:10.1053/j.seminoncol.2014.02.003.

Dillon, Stacey R, Cindy Sprecher, Angela Hammond, Janine Bilsborough, Maryland Rosenfeld-Franklin, Scott R Presnell, Harald S Haugen, et al. 2004. "Interleukin 31, a Cytokine Produced by Activated T Cells, Induces Dermatitis in Mice." *Nature Immunology* 5 (7): 752–60. doi:10.1038/ni1084.

Doedens, Andrew L, Anthony T Phan, Martin H Stradner, Jessica K Fujimoto,

Jessica V Nguyen, Edward Yang, Randall S Johnson, and Ananda W Goldrath. 2013. “Hypoxia-Inducible Factors Enhance the Effector Responses of CD8+ T Cells to Persistent Antigen.” *Nature Immunology* 14 (11): 1173–82. doi:10.1038/ni.2714.

Doedens, Andrew L, C Stockmann, M P Rubinstein, D Liao, N Zhang, D G DeNardo, L M Coussens, M Karin, A W Goldrath, and R S Johnson. 2010. “Macrophage Expression of Hypoxia-Inducible Factor-1 Suppresses T-Cell Function and Promotes Tumor Progression.” *Cancer Research* 70 (19): 7465–75. doi:10.1158/0008-5472.CAN-10-1439.

Dranoff, Glenn. 2011. “Experimental Mouse Tumour Models: What Can Be Learnt About Human Cancer Immunology?.” *Nature Reviews Immunology* 12 (1). Nature Publishing Group: 61–66. doi:10.1038/nri3129.

Du, Rose, Kan V Lu, Claudia Petritsch, Patty Liu, Ruth Ganss, Emmanuelle Passegué, Hanqiu Song, et al. 2008. “HIF1α Induces the Recruitment of Bone Marrow-Derived Vascular Modulatory Cells to Regulate Tumor Angiogenesis and Invasion.” *Cancer Cell* 13 (3): 206–20. doi:10.1016/j.ccr.2008.01.034.

Dunster, Joanne L. 2015. “The Macrophage and Its Role in Inflammation and Tissue Repair: Mathematical and Systems Biology Approaches.” *Wiley Interdisciplinary Reviews: Systems Biology and Medicine* 8 (1). John Wiley & Sons, Inc.: 87–99. doi:10.1002/wsbm.1320.

Dyson, Jessica K. 2012. “Colorectal Cancer in Inflammatory Bowel Disease: What Is the Real Magnitude of the Risk?.” *World Journal of Gastroenterology* 18 (29): 3839–10. doi:10.3748/wjg.v18.i29.3839.

Egners, Antje, Merve Erdem, and Thorsten Cramer. 2016. “The Response of Macrophages and Neutrophils to Hypoxia in the Context of Cancer and Other Inflammatory Diseases..” *Mediators of Inflammation* 2016. doi:10.1155/2016/2053646.

Eibel, Hermann, Helene Kraus, Heiko Sic, Anne-Kathrin Kienzler, and Marta Rizzi. 2014. “B Cell Biology: an Overview.” *Current Allergy and Asthma Reports* 14 (5). Springer US: 480–10. doi:10.1007/s11882-014-0434-8.

Ekkens, Melinda J, Devon J Shedlock, Euihye Jung, Amy Troy, Erika L Pearce, Hao Shen, and Edward J Pearce. 2007. “Th1 and Th2 Cells Help CD8 T-Cell Responses.” *Infection and Immunity* 75 (5). American Society for Microbiology: 2291–96. doi:10.1128/IAI.01328-06.

Ekström Smedby, Karin, Claire M Vajdic, Michael Falster, Eric A Engels, Otoniel Martinez-Maza, Jennifer Turner, Henrik Hjalgrim, et al. 2008. “Autoimmune Disorders and Risk of Non-Hodgkin Lymphoma Subtypes: a Pooled Analysis Within the InterLymph Consortium.” *Blood* 111 (8). American Society of Hematology: 4029–38. doi:10.1182/blood-2007-10-119974.

Epstein, A C, J M Gleadle, L A McNeill, K S Hewitson, J O'Rourke, D R Mole, M Mukherji, et al. 2001. “C. Elegans EGL-9 and Mammalian Homologs Define a Family of Dioxygenases That Regulate HIF by Prolyl Hydroxylation.” *Cell* 107 (1): 43–54.

Esteban, Miguel A, Maxine G B Tran, Sarah K Harten, Peter Hill, María C Castellanos, Ashish Chandra, Raju Raval, Tim S O'Brien, and Patrick H Maxwell. 2006. “Regulation of E-Cadherin Expression by VHL and Hypoxia-Inducible Factor.” *Cancer Research* 66 (7). American Association for Cancer Research: 3567–75. doi:10.1158/0008-5472.CAN-05-2670.

Evans, A J, R C Russell, O Roche, T N Burry, J E Fish, V W K Chow, W Y Kim,

et al. 2006. “VHL Promotes E2 Box-Dependent E-Cadherin Transcription by HIF-Mediated Regulation of SIP1 and Snail.” *Molecular and Cellular Biology* 27 (1): 157–69. doi:10.1128/MCB.00892-06.

Evens, Andrew M, Paul T Schumacker, Irene B Helenowski, Amareshwar T K Singh, Danijela Dokic, Anjeni Keswani, Elizabeth Kordeluk, et al. 2008. “Hypoxia Inducible Factor-Alpha Activation in Lymphoma and Relationship to the Thioredoxin Family.” *British Journal of Haematology* 141 (5). Blackwell Publishing Ltd: 676–80. doi:10.1111/j.1365-2141.2008.07093.x.

Facciabene, A, G T Motz, and G Coukos. 2012. “T-Regulatory Cells: Key Players in Tumor Immune Escape and Angiogenesis.” *Cancer Research* 72 (9): 2162–71. doi:10.1158/0008-5472.CAN-11-3687.

Facciabene, Andrea, Xiaohui Peng, Ian S Hagemann, Klara Balint, Andrea Barchetti, Li-Ping Wang, Phyllis A Gimotty, et al. 2011. “Tumour Hypoxia Promotes Tolerance and Angiogenesis via CCL28 and Treg Cells.” *Nature* 475 (7355). Nature Publishing Group: 226–30. doi:10.1038/nature10169.

Fang, Hsin-Yu, Russell Hughes, Craig Murdoch, Seth B Coffelt, Subhra K Biswas, Adrian L Harris, Randall S Johnson, et al. 2009. “Hypoxia-Inducible Factors 1 and 2 Are Important Transcriptional Effectors in Primary Macrophages Experiencing Hypoxia.” *Blood* 114 (4): 844–59. doi:10.1182/blood-2008-12-195941.

Feng, Mingye, James Y Chen, Rachel Weissman-Tsukamoto, Jens-Peter Volkmer, Po Yi Ho, Kelly M McKenna, Samuel Cheshier, et al. 2015. “Macrophages Eat Cancer Cells Using Their Own Calreticulin as a Guide: Roles of TLR and Btk.” *Proceedings of the National Academy of Sciences of the United States of America* 112 (7). National Acad Sciences: 2145–50. doi:10.1073/pnas.1424907112.

Finlay, David K, Ella Rosenzweig, Linda V Sinclair, Carmen Feijoo-Carnero, Jens L Hukelmann, Julia Rolf, Andrey A Panteleyev, Klaus Okkenhaug, and Doreen A Cantrell. 2012. “PDK1 Regulation of mTOR and Hypoxia-Inducible Factor 1 Integrate Metabolism and Migration of CD8+ T Cells.” *The Journal of Experimental Medicine* 209 (13). Rockefeller University Press: 2441–53. doi:10.1084/jem.20112607.

Forristal, C E, A L Brown, F M Helwani, I G Winkler, B Nowlan, V Barbier, R J Powell, et al. 2015. “Hypoxia Inducible Factor (HIF)-2α Accelerates Disease Progression in Mouse Models of Leukemia and Lymphoma but Is Not a Poor Prognosis Factor in Human AML.” *Leukemia* 29 (10): 2075–85. doi:10.1038/leu.2015.102.

Forsythe, J A, B H Jiang, N V Iyer, F Agani, S W Leung, R D Koos, and G L Semenza. 1996. “Activation of Vascular Endothelial Growth Factor Gene Transcription by Hypoxia-Inducible Factor 1.” *Molecular and Cellular Biology* 16 (9). American Society for Microbiology (ASM): 4604–13.

Franceschi, C, and J Campisi. 2014. “Chronic Inflammation (Inflammaging) and Its Potential Contribution to Age-Associated Diseases.” *The Journals of Gerontology Series a: Biological Sciences and Medical Sciences* 69 (Suppl 1): S4–S9. doi:10.1093/gerona/glu057.

Frede, Stilla, Christian Stockmann, Patricia Freitag, and Joachim Fandrey. 2006. “Bacterial Lipopolysaccharide Induces HIF-1 Activation in Human Monocytes via P44/42 MAPK and NF-kappaB.” *The Biochemical Journal* 396 (3). Portland Press Limited: 517–27. doi:10.1042/BJ20051839.

Fridman, Wolf Herman, Franck Pagès, Catherine Sautès-Fridman, and Jérôme

Galon. 2012. “The Immune Contexture in Human Tumours: Impact on Clinical Outcome.” *Nature Reviews Cancer* 12 (4). Nature Publishing Group: 298–306. doi:10.1038/nrc3245.

Frolova, Olga, Ismael Samudio, Juliana Maria Benito, Rodrigo Jacamo, Steven M Kornblau, Ana Markovic, Wendy Schober, et al. 2014. “Regulation of HIF-1α Signaling and Chemoresistance in Acute Lymphocytic Leukemia Under Hypoxic Conditions of the Bone Marrow Microenvironment.” *Cancer Biology & Therapy* 13 (10): 858–70. doi:10.4161/cbt.20838.

Gallatin, M, TPS John, M Siegelman, and R Reichert. 1986. “Lymphocyte Homing Receptors.” *Cell* 44 (5): 673–80. doi:10.1016/0092-8674(86)90832-9.

Gazzaniga, Silvina, Alicia I Bravo, Angelo Guglielmotti, Nico van Rooijen, Fabricio Maschi, Annunciata Vecchi, Alberto Mantovani, José Mordoh, and Rosa Wainstok. 2007. “Targeting Tumor-Associated Macrophages and Inhibition of MCP-1 Reduce Angiogenesis and Tumor Growth in a Human Melanoma Xenograft.” *Journal of Investigative Dermatology* 127 (8). Elsevier Masson SAS: 2031–41. doi:10.1038/sj.jid.5700827.

Germain, Ronald N. 2002. “T-Cell Development and the CD4–CD8 Lineage Decision.” *Nature Reviews Immunology* 2 (5): 309–22. doi:10.1038/nri798.

Giatromanolaki, Alexandra, Michael I Koukourakis, Francesco Pezzella, Helen Turley, Efthimios Sivridis, Demosthenes Bouros, George Bougioukas, Adrian L Harris, and Kevin C Gatter. 2008. “Expression of Prolyl-Hydroxylases PHD-1, 2 and 3 and of the Asparagine Hydroxylase FIH in Non-Small Cell Lung Cancer Relates to an Activated HIF Pathway.” *Cancer Letters* 262 (1): 87–93. doi:10.1016/j.canlet.2007.11.041.

Gilkes, Daniele M, Gregg L Semenza, and Denis Wirtz. 2014. “Hypoxia and the Extracellular Matrix: Drivers of Tumour Metastasis.” *Nature Reviews Cancer* 14 (6). Nature Publishing Group: 430–39. doi:10.1038/nrc3726.

Goda, Nobuhito, Heather E Ryan, Bahram Khadivi, Wayne McNulty, Robert C Rickert, and Randall S Johnson. 2003. “Hypoxia-Inducible Factor 1alpha Is Essential for Cell Cycle Arrest During Hypoxia.” *Molecular and Cellular Biology* 23 (1). American Society for Microbiology: 359–69. doi:10.1128/MCB.23.1.359-369.2003.

Green, Douglas R, and Guido Kroemer. 2009. “Cytoplasmic Functions of the Tumour Suppressor P53.” *Nature* 458 (7242). Nature Publishing Group: 1127–30. doi:10.1038/nature07986.

Greenwald, Rebecca J, Yvette E Latchman, and Arlene H Sharpe. 2002. “Negative Co-Receptors on Lymphocytes.” *Current Opinion in Immunology* 14 (3): 391–96. doi:10.1016/S0952-7915(02)00341-2.

Grimshaw, M J. 2007. “Endothelins and Hypoxia-Inducible Factor in Cancer.” *Endocrine Related Cancer* 14 (2). BioScientifica: 233–44. doi:10.1677/ERC-07-0057.

Grivennikov, Sergei I, Florian R Greten, and Michael Karin. 2010. “Immunity, Inflammation, and Cancer.” *Cell* 140 (6): 883–99. doi:10.1016/j.cell.2010.01.025.

Guo, Ren-Feng, and Peter A Ward. 2005. “Role of C5a in Inflammatory Responses.” *Annual Review of Immunology* 23: 821–52. doi:10.1146/annurev.immunol.23.021704.115835.

Gupta, Gaorav P, and Joan Massagu. 2006. “Cancer Metastasis: Building a Framework.” *Cell* 127 (4): 679–95. doi:10.1016/j.cell.2006.11.001.

Haabeth, Ole Audun Werner, Anders Aune Tveita, Marte Fauskanger, Fredrik

Schjesvold, Kristina Berg Lorvik, Peter O Hofgaard, Hilde Omholt, Ludvig A Munthe, Zlatko Dembic, and Alexandre Corthay. 2014. “How Do CD4$^+$ T Cells Detect and Eliminate Tumor Cells That Either Lack or Express MHC Class II Molecules?.” *Frontiers in Immunology* 5 (April). doi:10.3389/fimmu.2014.00174/abstract.

Hagen, Thilo. 2012. “Oxygen Versus Reactive Oxygen in the Regulation of HIF-1 A: the Balance Tips.” *Biochemistry Research International* 2012 (12). Hindawi. doi:10.1155/2012/436981.

Haines, D C, S Chattopadhyay, and J M Ward. 2001. “Pathology of Aging B6;129 Mice..” *Toxicologic Pathology* 29 (6): 653–61. doi:10.1080/019262301753385988.

Hanahan, Douglas, and Robert A Weinberg. 2011. “Hallmarks of Cancer: the Next Generation.” *Cell* 144 (5). Elsevier Inc.: 646–74. doi:10.1016/j.cell.2011.02.013.

Hardy, Adam P, Ivan Prokes, Leanne Kelly, Iain D Campbell, and Christopher J Schofield. 2009. “Asparaginyl B-Hydroxylation of Proteins Containing Ankyrin Repeat Domains Influences Their Stability and Function.” *Journal of Molecular Biology* 392 (4). Elsevier Ltd: 994–1006. doi:10.1016/j.jmb.2009.07.070.

Harlin, Helena, Yuru Meng, Amy C Peterson, Yuanyuan Zha, Maria Tretiakova, Craig Slingluff, Mark McKee, and Thomas F Gajewski. 2009. “Chemokine Expression in Melanoma Metastases Associated with CD8+ T-Cell Recruitment.” *Cancer Research* 69 (7). American Association for Cancer Research: 3077–85. doi:10.1158/0008-5472.CAN-08-2281.

Hayden, Matthew S, and Sankar Ghosh. 2012. “NF-κB, the First Quarter-Century: Remarkable Progress and Outstanding Questions.” *Genes & Development* 26 (3). Cold Spring Harbor Lab: 203–34. doi:10.1101/gad.183434.111.

Hewitson, Kirsty S, Benoit M R Liénard, Michael A McDonough, Ian J Clifton, Danica Butler, Alexie S Soares, Neil J Oldham, Luke A McNeill, and Christopher J Schofield. 2007. “Structural and Mechanistic Studies on the Inhibition of the Hypoxia-Inducible Transcription Factor Hydroxylases by Tricarboxylic Acid Cycle Intermediates.” *Journal of Biological Chemistry* 282 (5): 3293–3301. doi:10.1074/jbc.M608337200.

Ho, Ping-Chih, Jessica Dauz Bihuniak, Andrew N Macintyre, Matthew Staron, Xiaojing Liu, Robert Amezquita, Yao-Chen Tsui, et al. 2015. “Phosphoenolpyruvate Is a Metabolic Checkpoint of Anti-Tumor T Cell Responses.” *Cell* 162 (6). Elsevier Inc.: 1217–28. doi:10.1016/j.cell.2015.08.012.

Höckel, M, and P Vaupel. 2001. “Tumor Hypoxia: Definitions and Current Clinical, Biologic, and Molecular Aspects..” *Journal of the National Cancer Institute* 93 (4): 266–76.

Hu, Jiangfeng, Chao Chen, Qidong Liu, Baohai Liu, Chenlin Song, Songchen Zhu, Chaoqun Wu, et al. 2015. “The Role of the miR-31/FIH1 Pathway in TGF-Beta-Induced Liver Fibrosis.” *Clinical Science* 129 (4): 305–17. doi:10.1042/CS20140012.

Huang, L Eric, Jie Gu, Maureen Schau, and H Franklin Bunn. 1998. “Regulation of Hypoxia-Inducible Factor 1α Is Mediated by an O_2-Dependent Degradation Domain via the Ubiquitin-Proteasome Pathway.” *Proceedings of the National Academy of Sciences* 95 (14). National Acad Sciences: 7987–92.

Hyseni, Agon, Petra van der Groep, Elsken van der Wall, and Paul J van Diest.

2011. “Subcellular FIH-1 Expression Patterns in Invasive Breast Cancer in Relation to HIF-1α Expression.” *Cellular Oncology* 34 (6): 565–70. doi:10.1007/s13402-011-0053-5.

Imai, Tsutomu, Akiko Horiuchi, Cuiju Wang, Kenji Oka, Satoshi Ohira, Toshio Nikaido, and Ikuo Konishi. 2003. “Hypoxia Attenuates the Expression of E-Cadherin via Up-Regulation of SNAIL in Ovarian Carcinoma Cells.” *The American Journal of Pathology* 163 (4): 1437–47. doi:10.1016/S0002-9440(10)63501-8.

Imtiyaz, Hongxia Z, Emily P Williams, Michele M Hickey, Shetal A Patel, Amy C Durham, Li-Jun Yuan, Rachel Hammond, Phyllis A Gimotty, Brian Keith, and M Celeste Simon. 2010. “Hypoxia-Inducible Factor 2alpha Regulates Macrophage Function in Mouse Models of Acute and Tumor Inflammation.” *Journal of Clinical Investigation* 120 (8). American Society for Clinical Investigation: 2699–2714. doi:10.1172/JCI39506.

Iniesta, Virginia, L Carlos Gómez-Nieto, Isabel Molano, Alicia Mohedano, Jesualdo Carcelén, Cristina Mirón, Carlos Alonso, and Inés Corraliza. 2002. “Arginase I Induction in Macrophages, Triggered by Th2-Type Cytokines, Supports the Growth of Intracellular Leishmania Parasites.” *Parasite Immunology* 24 (3): 113–18.

Iqbal, Asif J, Daniel Regan-Komito, Ivy Christou, Gemma E White, Eileen McNeill, Amy Kenyon, Lewis Taylor, et al. 2013. “A Real Time Chemotaxis Assay Unveils Unique Migratory Profiles Amongst Different Primary Murine Macrophages.” Edited by John Wallace. *PLoS ONE* 8 (3). Public Library of Science: e58744. doi:10.1371/journal.pone.0058744.

Izraeli, Shai. 2004. “Leukaemia - a Developmental Perspective.” *British Journal of Haematology* 126 (1). Blackwell Science Ltd: 3–10. doi:10.1111/j.1365-2141.2004.04986.x.

Jaakkola, P, D R Mole, Y M Tian, M I Wilson, Janine Gielbert, Simon J Gaskell, Alexander von Kriegsheim, et al. 2001. “Targeting of HIF-A to the Von Hippel-Lindau Ubiquitylation Complex by O2-Regulated Prolyl Hydroxylation.” *Science* 292: 468–72. doi:10.1126/science.1059817.

Janeway, C. 2005. *Immunobiology: the Immune System in Health and Disease*. Garland Science Taylor \& Francis Group.

Janke, K, U Brockmeier, K Kuhlmann, M Eisenacher, J Nolde, H E Meyer, H Mairbaurl, and E Metzen. 2013. “Factor Inhibiting HIF-1 (FIH-1) Modulates Protein Interactions of Apoptosis-Stimulating P53 Binding Protein 2 (ASPP2).” *Journal of Cell Science* 126 (12): 2629–40. doi:10.1242/jcs.117564.

Jiang, B H, G Jiang, J Z Zheng, Z Lu, T Hunter, and P K Vogt. 2001. “Phosphatidylinositol 3-Kinase Signaling Controls Levels of Hypoxia-Inducible Factor 1.” *Cell Growth & Differentiation : the Molecular Biology Journal of the American Association for Cancer Research* 12 (7): 363–69.

Jiang, Y, Y Li, and B Zhu. 2015. “T-Cell Exhaustion in the Tumor Microenvironment.” *Cell Death and Disease* 6 (6). Nature Publishing Group: 1792–99. doi:10.1038/cddis.2015.162.

Jones, G E. 2000. “Cellular Signaling in Macrophage Migration and Chemotaxis..” *Journal of Leukocyte Biology* 68 (5). Society for Leukocyte Biology: 593–602.

Jordan, Kimberly R. 2017. “Immunosuppressive Myeloid-Derived Suppressor Cells Are Increased in Splenocytes From Cancer Patients.” *Cancer Immunology, Immunotherapy* 66 (4). Springer Berlin Heidelberg: 503–13. doi:10.1007/s00262-016-1953-z.

Jost, Philipp J, and Jürgen Ruland. 2007. “Aberrant NF-kappaB Signaling in Lymphoma: Mechanisms, Consequences, and Therapeutic Implications.” *Blood* 109 (7). American Society of Hematology: 2700–2707. doi:10.1182/blood-2006-07-025809.

Juneja, Vikram R, Kathleen A McGuire, Robert T Manguso, Martin W LaFleur, Natalie Collins, W Nicholas Haining, Gordon J Freeman, and Arlene H Sharpe. 2017. “PD-L1 on Tumor Cells Is Sufficient for Immune Evasion in Immunogenic Tumors and Inhibits CD8 T Cell Cytotoxicity.” *The Journal of Experimental Medicine* 214 (4). Rockefeller University Press: 895–904. doi:10.1084/jem.20160801.

Jung, Yun-Jin, Jennifer S Isaacs, Sunmin Lee, Jane Trepel, and Len Neckers. 2003. “IL-1beta-Mediated Up-Regulation of HIF-1alpha via an NFkappaB/COX-2 Pathway Identifies HIF-1 as a Critical Link Between Inflammation and Oncogenesis..” *FASEB Journal : Official Publication of the Federation of American Societies for Experimental Biology* 17 (14): 2115–17. doi:10.1096/fj.03-0329fje.

Jung, YunJin, Jennifer S Isaacs, Sunmin Lee, Jane Trepel, Zheng-Gang Liu, and Len Neckers. 2003. “Hypoxia-Inducible Factor Induction by Tumour Necrosis Factor in Normoxic Cells Requires Receptor-Interacting Protein-Dependent Nuclear Factor Kappa B Activation.” *The Biochemical Journal* 370 (Pt 3): 1011–17. doi:10.1042/BJ20021279.

Kambara, Kenta, Wakana Ohashi, Kengo Tomita, Michinori Takashina, Shiho Fujisaka, Ryuji Hayashi, Hisashi Mori, Kazuyuki Tobe, and Yuichi Hattori. 2015. “In Vivo Depletion of CD206+ M2 Macrophages Exaggerates Lung Injury in Endotoxemic Mice.” *The American Journal of Pathology* 185 (1): 162–71. doi:10.1016/j.ajpath.2014.09.005.

Karttunen, S, M Duffield, N R Scrimgeour, L Squires, W L Lim, M L Dallas, J L Scragg, et al. 2015. “Oxygen-Dependent Hydroxylation by FIH Regulates the TRPV3 Ion Channel.” *Journal of Cell Science* 128 (2): 225–31. doi:10.1242/jcs.158451.

Kasmi, El, Karim C, Joseph E Qualls, John T Pesce, Amber M Smith, Robert W Thompson, Marcela Henao-Tamayo, Randall J Basaraba, et al. 2008. “Toll-Like Receptor–Induced Arginase 1 in Macrophages Thwarts Effective Immunity Against Intracellular Pathogens.” *Nature Immunology* 9 (12): 1399–1406. doi:10.1038/ni.1671.

Kawanaka, Takashi, Akiko Kubo, Hitoshi Ikushima, Toshiaki Sano, Yoshihiro Takegawa, and Hiromu Nishitani. 2008. “Prognostic Significance of HIF-2α Expression on Tumor Infiltrating Macrophages in Patients with Uterine Cervical Cancer Undergoing Radiotherapy.” *The Journal of Medical Investigation* 55 (1,2). The University of Tokushima Faculty of Medicine: 78–86. doi:10.2152/jmi.55.78.

Kees, U R, N A Heerema, R Kumar, P M Watt, D L Baker, M K La, F M Uckun, and H N Sather. 2003. “Expression of HOX11 in Childhood T-Lineage Acute Lymphoblastic Leukaemia Can Occur in the Absence of Cytogenetic Aberration at 10q24: a Study From the Children's Cancer Group (CCG).” *Leukemia* 17 (5): 887–93. doi:10.1038/sj.leu.2402892.

Kelly, Beth, and Luke AJ O'Neill. 2015. “Metabolic Reprogramming in Macrophages and Dendritic Cells in Innate Immunity.” *Cell Research* 25 (7). Nature Publishing Group: 771–84. doi:10.1038/cr.2015.68.

Kelly, Leanne, Michael A McDonough, Mathew L Coleman, Peter J Ratcliffe, and

Christopher J Schofield. 2009. “Asparagine B-Hydroxylation Stabilizes the Ankyrin Repeat Domain Fold.” *Mol. BioSyst.* 5 (1). The Royal Society of Chemistry: 52–58. doi:10.1039/B815271C.

Kim, Jung-whan, Irina Tchernyshyov, Gregg L Semenza, and Chi V Dang. 2006. “HIF-1-Mediated Expression of Pyruvate Dehydrogenase Kinase: a Metabolic Switch Required for Cellular Adaptation to Hypoxia.” *Cell Metabolism* 3 (3): 177–85. doi:10.1016/j.cmet.2006.02.002.

Kiriakidis, S, A T Henze, I Kruszynska-Ziaja, K Skobridis, V Theodorou, E M Paleolog, and M Mazzone. 2015. “Factor-Inhibiting HIF-1 (FIH-1) Is Required for Human Vascular Endothelial Cell Survival.” *The FASEB Journal* 29 (7): 2814–27. doi:10.1096/fj.14-252379.

Kleffel, Sonja, Christian Posch, Steven R Barthel, Hansgeorg Mueller, Christoph Schlapbach, Emmanuella Guenova, Christopher P Elco, et al. 2015. “Melanoma Cell-Intrinsic PD-1 Receptor Functions Promote Tumor Growth.” *Cell* 162 (6): 1242–56. doi:10.1016/j.cell.2015.08.052.

Kline, J, I E Brown, Y Y Zha, C Blank, J Strickler, H Wouters, L Zhang, and T F Gajewski. 2008. “Homeostatic Proliferation Plus Regulatory T-Cell Depletion Promotes Potent Rejection of B16 Melanoma.” *Clinical Cancer Research* 14 (10): 3156–67. doi:10.1158/1078-0432.CCR-07-4696.

Koivunen, Peppi, Maija Hirsilä, Volkmar Günzler, Kari I Kivirikko, and Johanna Myllyharju. 2004. “Catalytic Properties of the Asparaginyl Hydroxylase (FIH) in the Oxygen Sensing Pathway Are Distinct From Those of Its Prolyl 4-Hydroxylases..” *Journal of Biological Chemistry* 279 (11). American Society for Biochemistry and Molecular Biology: 9899–9904. doi:10.1074/jbc.M312254200.

Kojima, Hidefumi, Hua Gu, Saeko Nomura, Charles C Caldwell, Tetsuji Kobata, Peter Carmeliet, Gregg L Semenza, and Michail V Sitkovsky. 2002. “Abnormal B Lymphocyte Development and Autoimmunity in Hypoxia-Inducible Factor 1alpha -Deficient Chimeric Mice.” *Proceedings of the National Academy of Sciences* 99 (4). National Acad Sciences: 2170–74. doi:10.1073/pnas.052706699.

Krock, B L, N Skuli, and M C Simon. 2012. “Hypoxia-Induced Angiogenesis: Good and Evil.” *Genes & Cancer* 2 (12): 1117–33. doi:10.1177/1947601911423654.

Kroeze, Stephanie G C, Joost S Vermaat, Aram van Brussel, Harm H E van Melick, Emile E Voest, Trudy G N Jonges, Paul J van Diest, John Hinrichs, J L H Ruud Bosch, and Judith J M Jans. 2010. “Expression of Nuclear FIH Independently Predicts Overall Survival of Clear Cell Renal Cell Carcinoma Patients.” *European Journal of Cancer* 46 (18). Elsevier Ltd: 3375–82. doi:10.1016/j.ejca.2010.07.018.

Kumar, Vinit, and Dmitry I Gabrilovich. 2014. “Hypoxia-Inducible Factors in Regulation of Immune Responses in Tumour Microenvironment.” *Immunology* 143 (4): 512–19. doi:10.1111/imm.12380.

Kumar, Vinit, Sima Patel, Evgenii Tcyganov, and Dmitry I Gabrilovich. 2016. “The Nature of Myeloid-Derived Suppressor Cells in the Tumor Microenvironment.” *Trends in Immunology* 37 (3). Elsevier Ltd: 208–20. doi:10.1016/j.it.2016.01.004.

Kuzmanov, Aleksandar, Ben Wielockx, Maryam Rezaei, Antje Kettelhake, and Georg Breier. 2012. “Overexpression of Factor Inhibiting HIF-1 Enhances Vessel Maturation and Tumor Growth via Platelet-Derived Growth Factor-C.”

International Journal of Cancer 131 (5): E603–13. doi:10.1002/ijc.27360.
Labonte, Adam C, Annie-Carole Tosello-Trampont, and Young S Hahn. 2014. "The Role of Macrophage Polarization in Infectious and Inflammatory Diseases." *Molecules and Cells* 37 (4). Korean Society for Molecular and Cellular Biology: 275–85. doi:10.14348/molcells.2014.2374.
LaGory, Edward L, and Amato J Giaccia. 2016. "The Ever-Expanding Role of HIF in Tumour and Stromal Biology." *Nature Cell Biology* 18 (4): 356–65. doi:10.1038/ncb3330.
Lando, David, Daniel J Peet, Dean A Whelan, Jeffrey J Gorman, and Murray L Whitelaw. 2002. "Asparagine Hydroxylation of the HIF Transactivation Domain a Hypoxic Switch." *Science* 295 (5556): 858–61. doi:10.1126/science.1068592.
Lando, David, Daniel J Peet, Jeffrey J Gorman, Dean A Whelan, Murray L Whitelaw, and Richard K Bruick. 2002. "FIH-1 Is an Asparaginyl Hydroxylase Enzyme That Regulates the Transcriptional Activity of Hypoxia-Inducible Factor." *Genes & Development* 16 (12). Cold Spring Harbor Lab: 1466–71. doi:10.1101/gad.991402.
Lawrence, Toby. 2009. "The Nuclear Factor NF-kappaB Pathway in Inflammation." *Cold Spring Harbor Perspectives in Biology* 1 (6). Cold Spring Harbor Lab: a001651–51. doi:10.1101/cshperspect.a001651.
Lawrence, Toby, and Gioacchino Natoli. 2011. "Transcriptional Regulation of Macrophage Polarization: Enabling Diversity with Identity.." *Nature Reviews Immunology* 11 (11): 750–61. doi:10.1038/nri3088.
Lechner, Melissa G, Saman S Karimi, Keegan Barry-Holson, Trevor E Angell, Katherine A Murphy, Connor H Church, John R Ohlfest, Peisheng Hu, and Alan L Epstein. 2013. "Immunogenicity of Murine Solid Tumor Models as a Defining Feature of in Vivo Behavior and Response to Immunotherapy." *Journal of Immunotherapy (Hagerstown, Md. : 1997)* 36 (9): 477–89. doi:10.1097/01.cji.0000436722.46675.4a.
Lee, Mi-Ran, Dahee Shim, Jihye Yoon, Hyung Seok Jang, Se-Woong Oh, Suk Hyo Suh, Jae-Hoon Choi, and Goo Taeg Oh. 2014. "Retnla Overexpression Attenuates Allergic Inflammation of the Airway." *PLoS ONE* 9 (11): e112666. doi:10.1371/journal.pone.0112666.
Leek, Russell D, Kate L Talks, Francesco Pezzella, Helen Turley, Leticia Campo, Nicholas S Brown, Roy Bicknell, Marian Taylor, Kevin C Gatter, and Adrian L Harris. 2002. "Relation of Hypoxia-Inducible Factor-2 Alpha (HIF-2 Alpha) Expression in Tumor-Infiltrative Macrophages to Tumor Angiogenesis and the Oxidative Thymidine Phosphorylase Pathway in Human Breast Cancer.." *Cancer Research* 62 (5): 1326–29.
Lewis, Claire E, Michele De Palma, and Luigi Naldini. 2007. "Tie2-Expressing Monocytes and Tumor Angiogenesis: Regulation by Hypoxia and Angiopoietin-2." *Cancer Research* 67 (18). American Association for Cancer Research: 8429–32. doi:10.1158/0008-5472.CAN-07-1684.
Li, Jinping, Enfeng Wang, Shamit Dutta, Julie S Lau, Shi-Wen Jiang, Kaustubh Datta, and Debabrata Mukhopadhyay. 2007. "Protein Kinase C-Mediated Modulation of FIH-1 Expression by the Homeodomain Protein CDP/Cut/Cux." *Molecular and Cellular Biology* 27 (20). American Society for Microbiology: 7345–53. doi:10.1128/MCB.02201-06.
Li, Yan, Duo Zhang, Xiaoyun Wang, Xuan Yao, Cheng Ye, Shengjie Zhang, Hui Wang, et al. 2015. "Hypoxia-Inducible miR-182 Enhances HIF1α Signaling via

Targeting PHD2 and FIH1 in Prostate Cancer." *Scientific Reports* 5 (1): 12495. doi:10.1038/srep12495.

Liang, Ke, Xue-qin Ding, Chen Lin, and Y James Kang. 2015. "Featured Article: Hypoxia-Inducible Factor-1 Dependent Nuclear Entry of Factor Inhibiting HIF-1." *Experimental Biology and Medicine* 240 (11): 1446–51. doi:10.1177/1535370215570821.

Lin, Elaine Y, Jiu-feng Li, Gabriel Bricard, Weigang Wang, Yan Deng, Rani Sellers, Steven A Porcelli, and Jeffrey W Pollard. 2007. "Vascular Endothelial Growth Factor Restores Delayed Tumor Progression in Tumors Depleted of Macrophages." *Molecular Oncology* 1 (3): 288–302. doi:10.1016/j.molonc.2007.10.003.

Lin, Nan, and M Celeste Simon. 2016. "Hypoxia-Inducible Factors: Key Regulators of Myeloid Cells During Inflammation." *Journal of Clinical Investigation* 126 (10): 3661–71. doi:10.1172/JCI84426.

Lisy, K, and D J Peet. 2008. "Turn Me on: Regulating HIF Transcriptional Activity." *Cell Death and Differentiation* 15 (4): 642–49. doi:10.1038/sj.cdd.4402315.

Liu, C J, M M Tsai, P S Hung, S Y Kao, T Y Liu, K J Wu, S H Chiou, S C Lin, and K W Chang. 2010. "miR-31 Ablates Expression of the HIF Regulatory Factor FIH to Activate the HIF Pathway in Head and Neck Carcinoma." *Cancer Research* 70 (4): 1635–44. doi:10.1158/0008-5472.CAN-09-2291.

Liu, Jinlin, Ning Zhang, Qun Li, Weiwei Zhang, Fang Ke, Qibin Leng, Hong Wang, Jinfei Chen, and Honglin Wang. 2011. "Tumor-Associated Macrophages Recruit CCR6+ Regulatory T Cells and Promote the Development of Colorectal Cancer via Enhancing CCL20 Production in Mice." Edited by Sven G Meuth. *PLoS ONE* 6 (4): e19495–13. doi:10.1371/journal.pone.0019495.

Liu, Yang, and Xuetao Cao. 2015. "The Origin and Function of Tumor-Associated Macrophages." *Cellular and Molecular Immunology* 12 (1). Nature Publishing Group: 1–4. doi:10.1038/cmi.2014.83.

Lodish, Harvey, Arnold Berk, S Lawrence Zipursky, Paul Matsudaira, David Baltimore, and James Darnell. 2008. *Molecular Cell Biology*. W. H. Freeman.

Louvi, Angeliki, and Spyros Artavanis-Tsakonas. 2012. "Notch and Disease: a Growing Field." *Seminars in Cell & Developmental Biology* 23 (4): 473–80. doi:10.1016/j.semcdb.2012.02.005.

Lu, Huasheng, Clifton L Dalgard, Ahmed Mohyeldin, Thomas McFate, A Sasha Tait, and Ajay Verma. 2005. "Reversible Inactivation of HIF-1 Prolyl Hydroxylases Allows Cell Metabolism to Control Basal HIF-1." *Journal of Biological Chemistry* 280 (51): 41928–39. doi:10.1074/jbc.M508718200.

Ma, Mingyang, Shuyao Hua, Gang Li, Sumei Wang, Xue Cheng, Songqing He, Ping Wu, and Xiaoping Chen. 2017. "Prolyl Hydroxylase Domain Protein 3 and Asparaginyl Hydroxylase Factor Inhibiting HIF-1 Levels Are Predictive of Tumoral Behavior and Prognosis in Hepatocellular Carcinoma." *Oncotarget* 8 (8). Impact Journals: 12983–3002. doi:10.18632/oncotarget.14677.

Mahabeleshwar, Ganapati H, Muhammad Awais Qureshi, Yoichi Takami, Nikunj Sharma, Jerry B Lingrel, and Mukesh K Jain. 2012. "A Myeloid Hypoxia-Inducible Factor 1α-Krüppel-Like Factor 2 Pathway Regulates Gram-Positive Endotoxin-Mediated Sepsis." *The Journal of Biological Chemistry* 287 (2). American Society for Biochemistry and Molecular Biology: 1448–57. doi:10.1074/jbc.M111.312702.

Mahon, P C, K Hirota, and G L Semenza. 2001. “FIH-1: a Novel Protein That Interacts with HIF-1alpha and VHL to Mediate Repression of HIF-1 Transcriptional Activity.” *Genes & Development* 15 (20): 2675–86. doi:10.1101/gad.924501.

Makino, Y, R Cao, K Svensson, G Bertilsson, and M Asman. 2001. “Inhibitory PAS Domain Protein Is a Negative Regulator of Hypoxia-Inducible Gene Expression.” *Nature* 414 (6863): 550–54. doi:10.1038/35107085.

Mansfield, Kyle D, Robert D Guzy, Yi Pan, Regina M Young, Timothy P Cash, Paul T Schumacker, and M Celeste Simon. 2005. “Mitochondrial Dysfunction Resulting From Loss of Cytochrome C Impairs Cellular Oxygen Sensing and Hypoxic HIF-A Activation.” *Cell Metabolism* 1 (6): 393–99. doi:10.1016/j.cmet.2005.05.003.

Martinez, Fernando O, and Siamon Gordon. 2014. “The M1 and M2 Paradigm of Macrophage Activation: Time for Reassessment.” *F1000prime Reports* 6 (13): 13. doi:10.12703/P6-13.

Masson, N, C Willam, P H Maxwell, C W Pugh, and P J Ratcliffe. 2001. “Independent Function of Two Destruction Domains in Hypoxia-Inducible Factor-Alpha Chains Activated by Prolyl Hydroxylation.” *The EMBO Journal* 20 (18). EMBO Press: 5197–5206. doi:10.1093/emboj/20.18.5197.

Masson, Norma, and Peter J Ratcliffe. 2014. “Hypoxia Signaling Pathways in Cancer Metabolism: the Importance of Co-Selecting Interconnected Physiological Pathways.” *Cancer & Metabolism* 2 (1): 3–17. doi:10.1186/2049-3002-2-3.

Masson, Norma, Rachelle S Singleton, Rok Sekirnik, David C Trudgian, Lucy J Ambrose, Melroy X Miranda, Ya-Min Tian, Benedikt M Kessler, Christopher J Schofield, and Peter J Ratcliffe. 2012. “The FIH Hydroxylase Is a Cellular Peroxide Sensor That Modulates HIF Transcriptional Activity.” *The EMBO Journal* 13 (3). Nature Publishing Group: 251–57. doi:10.1038/embor.2012.9.

Matsuyama, Hideyasu, Yi Pan, Satoru Yoshihiro, David Kudren, Katsusuke Naito, Ulf S R Bergerheim, and Peter Ekman. 2002. “Clinical Significance of Chromosome 8p, 10q, and 16q Deletions in Prostate Cancer.” *The Prostate* 54 (2). Wiley Subscription Services, Inc., A Wiley Company: 103–11. doi:10.1002/pros.10173.

Maxwell, P H, M S Wiesener, G W Chang, S C Clifford, E C Vaux, M E Cockman, C C Wykoff, C W Pugh, E R Maher, and P J Ratcliffe. 1999. “The Tumour Suppressor Protein VHL Targets Hypoxia-Inducible Factors for Oxygen-Dependent Proteolysis.” *Nature* 399 (6733): 271–75. doi:10.1038/20459.

Mayerhofer, M. 2002. “BCR/ABL Induces Expression of Vascular Endothelial Growth Factor and Its Transcriptional Activator, Hypoxia Inducible Factor-1alpha , Through a Pathway Involving Phosphoinositide 3-Kinase and the Mammalian Target of Rapamycin.” *Blood* 100 (10): 3767–75. doi:10.1182/blood-2002-01-0109.

Mazumdar, J, M M Hickey, and D K Pant. 2010. “HIF-2α Deletion Promotes Kras-Driven Lung Tumor Development.” *Proceedings of the National Academy of Sciences*. doi:10.1073/pnas.1001296107/-/DCSupplemental.

McMahon, Stephanie, Martine Charbonneau, Sebastien Grandmont, Darren E Richard, and Claire M Dubois. 2006. “Transforming Growth Factor Beta1 Induces Hypoxia-Inducible Factor-1 Stabilization Through Selective Inhibition of PHD2 Expression.” *Journal of Biological Chemistry* 281 (34): 24171–81. doi:10.1074/jbc.M604507200.

Medzhitov, Ruslan, and Tiffany Horng. 2009. “Transcriptional Control of the Inflammatory Response.” *Nature Reviews Immunology* 9 (10). Nature Publishing Group: 692–703. doi:10.1038/nri2634.

Mellado, M, A M de Ana, M C Moreno, C Martínez, and J M Rodríguez-Frade. 2001. “A Potential Immune Escape Mechanism by Melanoma Cells Through the Activation of Chemokine-Induced T Cell Death.” *Curbio* 11 (9): 691–96.

Messmer, Michelle N, Colleen S Netherby, Debarati Banik, and Scott I Abrams. 2014. “Tumor-Induced Myeloid Dysfunction and Its Implications for Cancer Immunotherapy.” *Cancer Immunology, Immunotherapy* 64 (1). Springer Berlin Heidelberg: 1–13. doi:10.1007/s00262-014-1639-3.

Metzen, E. 2003. “Intracellular Localisation of Human HIF-1alpha Hydroxylases: Implications for Oxygen Sensing.” *Journal of Cell Science* 116 (7): 1319–26. doi:10.1242/jcs.00318.

Mosser, David M, and Justin P Edwards. 2008. “Exploring the Full Spectrum of Macrophage Activation.” *Nature Reviews Immunology* 8 (12). Nature Publishing Group: 958–69. doi:10.1038/nri2448.

Munder, M, K Eichmann, J M Morán, F Centeno, G Soler, and M Modolell. 1999. “Th1/Th2-Regulated Expression of Arginase Isoforms in Murine Macrophages and Dendritic Cells.” *The Journal of Immunology* 163 (7): 3771–77.

Munder, Markus. 2009. “Arginase: an Emerging Key Player in the Mammalian Immune System.” *British Journal of Pharmacology* 158 (3): 638–51. doi:10.1111/j.1476-5381.2009.00291.x.

Murdoch, C. 2004. “Mechanisms Regulating the Recruitment of Macrophages Into Hypoxic Areas of Tumors and Other Ischemic Tissues.” *Blood* 104 (8): 2224–34. doi:10.1182/blood-2004-03-1109.

Murphy, K M. 2011. *Janeway's Immunobiology*. Taylor \& Francis Group.

Nagai, Hiroshi, Tatsuya Horikawa, Masahiro Oka, Masamitsu Ichihashi, Isao Hara, and Sadao Kamidono. 2000. “Elimination of CD4+ T Cells Enhances Anti-Tumor Effect of Locally Secreted Interleukin-12 on B16 Mouse Melanoma and Induces Vitiligo-Like Coat Color Alteration.” *Journal of Investigative Dermatology* 115 (6). Elsevier Masson SAS: 1059–64. doi:10.1046/j.1523-1747.2000.00156.x.

Nagarsheth, Nisha, Max S Wicha, and Weiping Zou. 2017. “Chemokines in the Cancer Microenvironment and Their Relevance in Cancer Immunotherapy.” *Nature Reviews Immunology*, May. Nature Publishing Group, 1–14. doi:10.1038/nri.2017.49.

Nakamura, Hiroshi, Yuichi Makino, Kensaku Okamoto, Lorenz Poellinger, Kei Ohnuma, Chikao Morimoto, and Hirotoshi Tanaka. 2005. “TCR Engagement Increases Hypoxia-Inducible Factor-1 Alpha Protein Synthesis via Rapamycin-Sensitive Pathway Under Hypoxic Conditions in Human Peripheral T Cells..” *The Journal of Immunology* 174 (12). American Association of Immunologists: 7592–99. doi:10.4049/jimmunol.174.12.7592.

Newton, Kim, and Vishva M Dixit. 2012. “Signaling in Innate Immunity and Inflammation.” *Cold Spring Harbor Perspectives in Biology* 4 (3). Cold Spring Harbor Lab: a006049–49. doi:10.1101/cshperspect.a006049.

Nguyen, Linh T, and Pamela S Ohashi. 2015. “Clinical Blockade of PD1 and LAG3 — Potential Mechanisms of Action.” *Nature Reviews Immunology* 15 (1). Nature Publishing Group: 45–56. doi:10.1038/nri3790.

Niecknig, Helene, Suzan Tug, Buena Delos Reyes, Michael Kirsch, Joachim Fandrey, and Utta Berchner-Pfannschmidt. 2012. “Role of Reactive Oxygen

Species in the Regulation of HIF-1 by Prolyl Hydroxylase 2 Under Mild Hypoxia." *Free Radical Research* 46 (6). Taylor & Francis: 705–17. doi:10.3109/10715762.2012.669041.

Nishi, Kenichiro, Tomoyuki Oda, Satoshi Takabuchi, Seiko Oda, Kazuhiko Fukuda, Takehiko Adachi, Gregg L Semenza, Koh Shingu, and Kiichi Hirota. 2008. "LPS Induces Hypoxia-Inducible Factor 1 Activation in Macrophage-Differentiated Cells in a Reactive Oxygen Species–Dependent Manner." *Antioxidants & Redox Signaling* 10 (5): 983–96. doi:10.1089/ars.2007.1825.

Noh, Hyangsoon, Jiemiao Hu, Xiaohong Wang, Xueqing Xia, Arun Satelli, and Shulin Li. 2015. "Immune Checkpoint Regulator PD-L1 Expression on Tumor Cells by Contacting CD11b Positive Bone Marrow Derived Stromal Cells." *Cell Communication and Signaling* 13 (1): 14–12. doi:10.1186/s12964-015-0093-y.

Noman, Muhammad Zaeem, Giacomo Desantis, Bassam Janji, Meriem Hasmim, Saoussen Karray, Philippe Dessen, Vincenzo Bronte, and Salem Chouaib. 2014. "PD-L1 Is a Novel Direct Target of HIF-1α, and Its Blockade Under Hypoxia Enhanced MDSC-Mediated T Cell Activation." *The Journal of Experimental Medicine* 211 (5): 781–90. doi:10.1084/jem.20131916.

Noy, Roy, and Jeffrey W Pollard. 2014. "Tumor-Associated Macrophages: From Mechanisms to Therapy." *Immunity* 41 (1). Elsevier Inc.: 49–61. doi:10.1016/j.immuni.2014.06.010.

Okazaki, T, and T Honjo. 2007. "PD-1 and PD-1 Ligands: From Discovery to Clinical Application." *International Immunology* 19 (7): 813–24. doi:10.1093/intimm/dxm057.

Orme, Ian M, Richard T Robinson, and Andrea M Cooper. 2014. "The Balance Between Protective and Pathogenic Immune Responses in the TB-Infected Lung." *Nature Immunology* 16 (1): 57–63. doi:10.1038/ni.3048.

Ostrand-Rosenberg, Suzanne, and Pratima Sinha. 2009. "Myeloid-Derived Suppressor Cells: Linking Inflammation and Cancer." *European Journal of Immunology* 182 (8). American Association of Immunologists: 4499–4506. doi:10.4049/jimmunol.0802740.

Palazon, Asis, Ananda W Goldrath, Victor Nizet, and Randall S Johnson. 2014. "HIF Transcription Factors, Inflammation, and Immunity." *Immunity* 41 (4). Elsevier Inc.: 518–28. doi:10.1016/j.immuni.2014.09.008.

Pals, Steven T, David J J de Gorter, and Marcel Spaargaren. 2007. "Lymphoma Dissemination: the Other Face of Lymphocyte Homing." *Blood* 110 (9). American Society of Hematology: 3102–11. doi:10.1182/blood-2007-05-075176.

Pandiyan, Pushpa, Lixin Zheng, Satoru Ishihara, Jennifer Reed, and Michael J Lenardo. 2007. "CD4+CD25+Foxp3+ Regulatory T Cells Induce Cytokine Deprivation–Mediated Apoptosis of Effector CD4+ T Cells." *Nature Immunology* 8 (12): 1353–62. doi:10.1038/ni1536.

Pankov, Roumen, and Kenneth M Yamada. 2002. "Fibronectin at a Glance." *Journal of Cell Science* 115 (Pt 20). The Company of Biologists Ltd: 3861–63. doi:10.1242/jcs.00059.

Papandreou, Ioanna, Rob A Cairns, Lucrezia Fontana, Ai Lin Lim, and Nicholas C Denko. 2006. "HIF-1 Mediates Adaptation to Hypoxia by Actively Downregulating Mitochondrial Oxygen Consumption." *Cell Metabolism* 3 (3): 187–97. doi:10.1016/j.cmet.2006.01.012.

Parissis, Haralabos. 2011. "Forty Years Literature Review of Primary Lung

Lymphoma." *Journal of Cardiothoracic Surgery* 6 (1). BioMed Central: 23. doi:10.1186/1749-8090-6-23.

Park, S k, A M Dadak, V H Haase, L Fontana, A J Giaccia, and R S Johnson. 2003. "Hypoxia-Induced Gene Expression Occurs Solely Through the Action of Hypoxia-Inducible Factor 1 (HIF-1): Role of Cytoplasmic Trapping of HIF-2 ." *Molecular and Cellular Biology* 23 (14): 4959–71. doi:10.1128/MCB.23.14.4959-4971.2003.

Pattabiraman, Diwakar R, and Robert A Weinberg. 2014. "Tackling the Cancer Stem Cells — What Challenges Do They Pose?." *Nature Reviews Drug Discovery* 13 (7). Nature Publishing Group: 497–512. doi:10.1038/nrd4253.

Pelletier, J, F Dayan, J Durivault, K Ilc, E P eacute cou, J Pouyss eacute gur, and N M Mazure. 2011. "The Asparaginyl Hydroxylase Factor-Inhibiting HIF Is Essential for Tumor Growth Through Suppression of the P53-P21 Axis." *Oncogene* 31 (24). Nature Publishing Group: 2989–3001. doi:10.1038/onc.2011.471.

Peng, Han, Nihal Kaplan, Robert B Hamanaka, Julia Katsnelson, Hanz Blatt, Wending Yang, Liangliang Hao, et al. 2012. "microRNA-31/Factor-Inhibiting Hypoxia-Inducible Factor 1 Nexus Regulates Keratinocyte Differentiation." *Proceedings of the National Academy of Sciences of the United States of America* 109 (35). National Acad Sciences: 14030–34. doi:10.1073/pnas.1111292109.

Peng, Han, Nihal Kaplan, Wending Yang, Spiro Getsios, and Robert M Lavker. 2014. "FIH-1 Disrupts an LRRK1/EGFR Complex to Positively Regulate Keratinocyte Migration." *The American Journal of Pathology* 184 (12). Elsevier: 3262–71. doi:10.1016/j.ajpath.2014.08.014.

Peng, Han, Robert B Hamanaka, Julia Katsnelson, Liang-Liang Hao, Wending Yang, Navdeep S Chandel, and Robert M Lavker. 2012. "MicroRNA-31 Targets FIH-1 to Positively Regulate Corneal Epithelial Glycogen Metabolism." *FASEB Journal : Official Publication of the Federation of American Societies for Experimental Biology* 26 (8). Federation of American Societies for Experimental Biology: 3140–47. doi:10.1096/fj.11-198515.

Peyssonnaux, Carole, Pilar Cejudo-Martin, Andrew Doedens, Annelies S Zinkernagel, Randall S Johnson, and Victor Nizet. 2007. "Cutting Edge: Essential Role of Hypoxia Inducible Factor-1alpha in Development of Lipopolysaccharide-Induced Sepsis." *The Journal of Immunology* 178 (12). American Association of Immunologists: 7516–19. doi:10.4049/jimmunol.178.12.7516.

Peyssonnaux, Carole, Vivekanand Datta, Thorsten Cramer, Andrew Doedens, Emmanuel A Theodorakis, Richard L Gallo, Nancy Hurtado-Ziola, Victor Nizet, and Randall S Johnson. 2005. "HIF-1alpha Expression Regulates the Bactericidal Capacity of Phagocytes." *Journal of Clinical Investigation* 115 (7). American Society for Clinical Investigation: 1806–15. doi:10.1172/JCI23865.

Pilon-Thomas, S, A Mackay, N Vohra, and J J Mule. 2010. "Blockade of Programmed Death Ligand 1 Enhances the Therapeutic Efficacy of Combination Immunotherapy Against Melanoma." *The Journal of Immunology* 184 (7): 3442–49. doi:10.4049/jimmunol.0904114.

Pollard, Jeffrey W. 2004. "Tumour-Educated Macrophages Promote Tumour Progression and Metastasis." *Nature Reviews Cancer* 4 (1): 71–78. doi:10.1038/nrc1256.

Pollard, P J. 2005. "Accumulation of Krebs Cycle Intermediates and Over-

Expression of HIF1 in Tumours Which Result From Germline FH and SDH Mutations." *Human Molecular Genetics* 14 (15): 2231–39. doi:10.1093/hmg/ddi227.

Qian, Bin-Zhi, and Jeffrey W Pollard. 2010. "Macrophage Diversity Enhances Tumor Progression and Metastasis." *Cell* 141 (1). Elsevier: 39–51. doi:10.1016/j.cell.2010.03.014.

Quezada, Sergio A, Tyler R Simpson, Karl S Peggs, Taha Merghoub, Jelena Vider, Xiaozhou Fan, Ronald Blasberg, et al. 2010. "Tumor-Reactive CD4(+) T Cells Develop Cytotoxic Activity and Eradicate Large Established Melanoma After Transfer Into Lymphopenic Hosts." *The Journal of Experimental Medicine* 207 (3). Rockefeller University Press: 637–50. doi:10.1084/jem.20091918.

Rankin, E B, and A J Giaccia. 2008. "The Role of Hypoxia-Inducible Factors in Tumorigenesis." *Cell Death and Differentiation* 15 (4): 678–85. doi:10.1038/cdd.2008.21.

Rath, Meera, Ingrid Müller, Pascale Kropf, Ellen I Closs, and Markus Munder. 2014. "Metabolism via Arginase or Nitric Oxide Synthase: Two Competing Arginine Pathways in Macrophages." *Frontiers in Immunology* 5 (6): 532. doi:10.3389/fimmu.2014.00532.

Raval, R R, K W Lau, M G B Tran, H M Sowter, S J Mandriota, J L Li, C W Pugh, P H Maxwell, A L Harris, and P J Ratcliffe. 2005. "Contrasting Properties of Hypoxia-Inducible Factor 1 (HIF-1) and HIF-2 in Von Hippel-Lindau-Associated Renal Cell Carcinoma." *Molecular and Cellular Biology* 25 (13): 5675–86. doi:10.1128/MCB.25.13.5675-5686.2005.

Reiser, John, and Arnob Banerjee. 2016. "Effector, Memory, and Dysfunctional CD8 +T Cell Fates in the Antitumor Immune Response." *Journal of Immunology Research* 2016 (4): 1–14. doi:10.1155/2016/8941260.

Richards, David M, Jan Hettinger, and Markus Feuerer. 2012. "Monocytes and Macrophages in Cancer: Development and Functions." *Cancer Microenvironment* 6 (2): 179–91. doi:10.1007/s12307-012-0123-x.

Richmond, Ann, Jinming Yang, and Yingjun Su. 2009. "The Good and the Bad of Chemokines/Chemokine Receptors in Melanoma." *Pigment Cell & Melanoma Research* 22 (2). Blackwell Publishing Ltd: 175–86. doi:10.1111/j.1755-148X.2009.00554.x.

Rius, Jordi, Monica Guma, Christian Schachtrup, Katerina Akassoglou, Annelies S Zinkernagel, Victor Nizet, Randall S Johnson, Gabriel G Haddad, and Michael Karin. 2008. "NF-κB Links Innate Immunity to the Hypoxic Response Through Transcriptional Regulation of HIF-1α." *Nature* 453 (7196): 807–11. doi:10.1038/nature06905.

Roda, Julie M, Laura A Sumner, Randall Evans, Gary S Phillips, Clay B Marsh, and Timothy D Eubank. 2011. "Hypoxia-Inducible Factor-2α Regulates GM-CSF-Derived Soluble Vascular Endothelial Growth Factor Receptor 1 Production From Macrophages and Inhibits Tumor Growth and Angiogenesis." *Journal of Immunology (Baltimore, Md. : 1950)* 187 (4). American Association of Immunologists: 1970–76. doi:10.4049/jimmunol.1100841.

Rodriguez, P C, A H Zea, J DeSalvo, K S Culotta, J Zabaleta, D G Quiceno, J B Ochoa, and A C Ochoa. 2003. "L-Arginine Consumption by Macrophages Modulates the Expression of CD3 Chain in T Lymphocytes." *The Journal of Immunology* 171 (3): 1232–39. doi:10.4049/jimmunol.171.3.1232.

Rodriguez, Paulo C, Augusto C Ochoa, and Amir A Al-Khami. 2017. “Arginine Metabolism in Myeloid Cells Shapes Innate and Adaptive Immunity.” *Frontiers in Immunology* 8 (Pt 1): 2791S–12. doi:10.3389/fimmu.2017.00093.

Rodriguez, Paulo C, David G Quiceno, Jovanny Zabaleta, Blair Ortiz, Arnold H Zea, Maria B Piazuelo, Alberto Delgado, et al. 2004. “Arginase I Production in the Tumor Microenvironment by Mature Myeloid Cells Inhibits T-Cell Receptor Expression and Antigen-Specific T-Cell Responses.” *Cancer Research* 64 (16). American Association for Cancer Research: 5839–49. doi:10.1158/0008-5472.CAN-04-0465.

Rose, Shawn, Alexander Misharin, and Harris Perlman. 2011. “A Novel Ly6C/Ly6G-Based Strategy to Analyze the Mouse Splenic Myeloid Compartment.” *Cytometry* 81A (4). Wiley Subscription Services, Inc., A Wiley Company: 343–50. doi:10.1002/cyto.a.22012.

Rosenberger, Christian, Stefano Mandriota, Jan Steffen Jürgensen, Michael S Wiesener, Jan H Hörstrup, Ulrich Frei, Peter J Ratcliffe, Patrick H Maxwell, Sebastian Bachmann, and Kai-Uwe Eckardt. 2002. “Expression of Hypoxia-Inducible Factor-1alpha and -2alpha in Hypoxic and Ischemic Rat Kidneys..” *Journal of the American Society of Nephrology* 13 (7). American Society of Nephrology: 1721–32. doi:10.1097/01.ASN.0000017223.49823.2A.

Rőszer, Tamás. 2015. “Understanding the Mysterious M2 Macrophage Through Activation Markers and Effector Mechanisms.” *Mediators of Inflammation* 2015 (4). Hindawi: 816460–16. doi:10.1155/2015/816460.

Ruf, Melanie, Holger Moch, and Peter Schraml. 2016. “PD-L1 Expression Is Regulated by Hypoxia Inducible Factor in Clear Cell Renal Cell Carcinoma.” *International Journal of Cancer* 139 (2): 396–403. doi:10.1002/ijc.30077.

Rutschman, R, R Lang, M Hesse, J N Ihle, T A Wynn, and P J Murray. 2001. “Cutting Edge: Stat6-Dependent Substrate Depletion Regulates Nitric Oxide Production.” *The Journal of Immunology* 166 (4). American Association of Immunologists: 2173–77. doi:10.4049/jimmunol.166.4.2173.

Sagaert, Xavier, Eric Van Cutsem, Gert De Hertogh, Karel Geboes, and Thomas Tousseyn. 2010. “Gastric MALT Lymphoma: a Model of Chronic Inflammation-Induced Tumor Development.” *Nature Reviews. Gastroenterology & Hepatology* 7 (6): 336–46. doi:10.1038/nrgastro.2010.58.

Sakaguchi, Shimon, Tomoyuki Yamaguchi, Takashi Nomura, and Masahiro Ono. 2008. “Regulatory T Cells and Immune Tolerance.” *Cell* 133 (5): 775–87. doi:10.1016/j.cell.2008.05.009.

Sakamoto, Takeharu, and Motoharu Seiki. 2009. “Mint3 Enhances the Activity of Hypoxia-Inducible Factor-1 (HIF-1) in Macrophages by Suppressing the Activity of Factor Inhibiting HIF-1.” *The Journal of Biological Chemistry* 284 (44). American Society for Biochemistry and Molecular Biology: 30350–59. doi:10.1074/jbc.M109.019216.

Sakamoto, Takeharu, and Motoharu Seiki. 2010. “A Membrane Protease Regulates Energy Production in Macrophages by Activating Hypoxia-Inducible Factor-1 via a Non-Proteolytic Mechanism.” *The Journal of Biological Chemistry* 285 (39). American Society for Biochemistry and Molecular Biology: 29951–64. doi:10.1074/jbc.M110.132704.

Samuels-Lev, Yardena, Daniel J O'Connor, Daniele Bergamaschi, Giuseppe Trigiante, Jung-Kuang Hsieh, Shan Zhong, Isabelle Campargue, Louie Naumovski, Tim Crook, and Xin Lu. 2001. “ASPP Proteins Specifically Stimulate the Apoptotic Function of P53.” *Molecular Cell* 8 (4): 781–94.

doi:10.1016/S1097-2765(01)00367-7.
Sangaletti, Sabina, Emma Di Carlo, Silvia Gariboldi, Silvia Miotti, Barbara Cappetti, Mariella Parenza, Cristiano Rumio, Rolf A Brekken, Claudia Chiodoni, and Mario P Colombo. 2008. “Macrophage-Derived SPARC Bridges Tumor Cell-Extracellular Matrix Interactions Toward Metastasis.” *Cancer Research* 68 (21). American Association for Cancer Research: 9050–59. doi:10.1158/0008-5472.CAN-08-1327.
Schofield, Christopher J, and Peter J Ratcliffe. 2004a. “Oxygen Sensing by HIF Hydroxylases.” *Nature Reviews Molecular Cell Biology* 5 (5): 343–54. doi:10.1038/nrm1366.
Schofield, Christopher J, and Peter J Ratcliffe. 2004b. “Oxygen Sensing by HIF Hydroxylases.” *Nature Reviews Molecular Cell Biology* 5 (5). Nature Publishing Group: 343–54. doi:10.1038/nrm1366.
Scholz, Carsten C, Javier Rodriguez, Christina Pickel, Stephen Burr, Jacqueline-alba Fabrizio, Karen A Nolan, Patrick Spielmann, et al. 2016. “FIH Regulates Cellular Metabolism Through Hydroxylation of the Deubiquitinase OTUB1.” Edited by Celeste Simon. *PLOS Biology* 14 (1): e1002347–22. doi:10.1371/journal.pbio.1002347.
Schwartz, Ronald H. 2003. “T Cell Anergy..” *Annual Review of Immunology* 21: 305–34. doi:10.1146/annurev.immunol.21.120601.141110.
Semenza, G L, and G L Wang. 1992. “A Nuclear Factor Induced by Hypoxia via De Novo Protein Synthesis Binds to the Human Erythropoietin Gene Enhancer at a Site Required for Transcriptional Activation.” *Molecular and Cellular Biology* 12 (12): 5447–54.
Semenza, Gregg L. 2012. “Hypoxia-Inducible Factors in Physiology and Medicine.” *Cell* 148 (3). Elsevier Inc.: 399–408. doi:10.1016/j.cell.2012.01.021.
Semenza, Gregg L. 2014. “Oxygen Sensing, Hypoxia-Inducible Factors, and Disease Pathophysiology.” *Annual Review of Pathology: Mechanisms of Disease* 9 (1): 47–71. doi:10.1146/annurev-pathol-012513-104720.
Shaida, Nadeem, Peter Chan, Helen Turley, Catherine M Jones, Suresh Kanga, Robert W Ritchie, Peter R Malone, Adrian L Harris, and Stephen B Fox. 2011. “Nuclear Localization of Factor Inhibitor Hypoxia-Inducible Factor in Prostate Cancer Is Associated with Poor Prognosis.” *The Journal of Urology* 185 (4). American Urological Association Education and Research, Inc.: 1513–18. doi:10.1016/j.juro.2010.12.001.
Shankland, Kate R Shankland, James O Armitage, and Barry W Hancock. 2012. “Non-Hodgkin Lymphoma.” *The Lancet* 380 (9844). Elsevier Ltd: 848–57. doi:10.1016/S0140-6736(12)60605-9.
Sharda, D R, S Yu, M Ray, M L Squadrito, M De Palma, T A Wynn, S M Morris, and P A Hankey. 2011. “Regulation of Macrophage Arginase Expression and Tumor Growth by the Ron Receptor Tyrosine Kinase.” *The Journal of Immunology* 187 (5): 2181–92. doi:10.4049/jimmunol.1003460.
Shepardson, Kelly M, Anupam Jhingran, Alayna Caffrey, Joshua J Obar, Benjamin T Suratt, Brent L Berwin, Tobias M Hohl, and Robert A Cramer. 2014. “Myeloid Derived Hypoxia Inducible Factor 1-Alpha Is Required for Protection Against Pulmonary Aspergillus Fumigatus Infection.” Edited by Sarah Gaffen. *PLoS Pathogens* 10 (9). Public Library of Science: e1004378–16. doi:10.1371/journal.ppat.1004378.
Shi, Lewis Z, Ruoning Wang, Gonghua Huang, Peter Vogel, Geoffrey Neale,

Douglas R Green, and Hongbo Chi. 2011. “HIF1alpha-Dependent Glycolytic Pathway Orchestrates a Metabolic Checkpoint for the Differentiation of TH17 and Treg Cells.” *The Journal of Experimental Medicine* 208 (7). Rockefeller University Press: 1367–76. doi:10.1084/jem.20110278.

Shin, Dong Hoon, Shan Hua Li, Seung-Won Yang, Byung Lan Lee, Myung Kyu Lee, and Jong-Wan Park. 2009. “Inhibitor of Nuclear Factor-kappaB Alpha Derepresses Hypoxia-Inducible Factor-1 During Moderate Hypoxia by Sequestering Factor Inhibiting Hypoxia-Inducible Factor From Hypoxia-Inducible Factor 1α.” *FEBS Journal* 276 (13). Blackwell Publishing Ltd: 3470–80. doi:10.1111/j.1742-4658.2009.07069.x.

Shklovskaya, Elena, Alexandra M Terry, Thomas V Guy, Adrian Buckley, Holly A Bolton, Erhua Zhu, Jeff Holst, and Barbara Fazekas de St Groth. 2016. “Tumour-Specific CD4 T Cells Eradicate Melanoma via Indirect Recognition of Tumour-Derived Antigen” 94 (6). Nature Publishing Group: 593–603. doi:10.1038/icb.2016.14.

So, Ju-Hoon, Jun-Dae Kim, Kyeong-Won Yoo, Hyun-Taek Kim, Seung-Hyun Jung, Jung-Hwa Choi, Mi-Sun Lee, Suk-Won Jin, and Cheol-Hee Kim. 2014. “FIH-1, a Novel Interactor of Mindbomb, Functions as an Essential Anti-Angiogenic Factor During Zebrafish Vascular Development.” Edited by Ramani Ramchandran. *PLoS ONE* 9 (10). Public Library of Science: e109517–19. doi:10.1371/journal.pone.0109517.

Soilleux, E J, H Turley, Y M Tian, C W Pugh, K C Gatter, and A L Harris. 2005. “Use of Novel Monoclonal Antibodies to Determine the Expression and Distribution of the Hypoxia Regulatory Factors PHD-1, PHD-2, PHD-3 and FIH in Normal and Neoplastic Human Tissues.” *Histopathology* 47 (6). Blackwell Science Ltd: 602–10. doi:10.1111/j.1365-2559.2005.02280.x.

Sottocomola, Roberta, Christophe Royer, Virginie Vives, Luca Tordella, Shan Zhong, Yihua Wang, Indrika Ratnayaka, et al. 2010. “ASPP2 Binds Par-3 and Controls the Polarity and Proliferation of Neural Progenitors During CNS Development.” *Developmental Cell* 19 (1). Elsevier Inc.: 126–37. doi:10.1016/j.devcel.2010.06.003.

Stewart, M, K Talks, R Leek, H Turley, F Pezzella, A Harris, and K Gatter. 2002. “Expression of Angiogenic Factors and Hypoxia Inducible Factors HIF 1, HIF 2 and CA IX in Non-Hodgkin's Lymphoma.” *Histopathology* 40 (3): 253–60.

Stockmann, Christian, Andrew Doedens, Alexander Weidemann, Na Zhang, Norihiko Takeda, Joshua I Greenberg, David A Cheresh, and Randall S Johnson. 2008. “Deletion of Vascular Endothelial Growth Factor in Myeloid Cells Accelerates Tumorigenesis.” *Nature* 456 (7223): 814–18. doi:10.1038/nature07445.

Stolze, I P, Y M Tian, R J Appelhoff, H Turley, C C Wykoff, J M Gleadle, and P J Ratcliffe. 2004a. “Genetic Analysis of the Role of the Asparaginyl Hydroxylase Factor Inhibiting Hypoxia-Inducible Factor (HIF) in Regulating HIF Transcriptional Target Genes.” *Journal of Biological Chemistry* 279 (41): 42719–25. doi:10.1074/jbc.M406713200.

Stolze, Ineke P, Ya-Min Tian, Rebecca J Appelhoff, Helen Turley, Charles C Wykoff, Jonathan M Gleadle, and Peter J Ratcliffe. 2004b. “Genetic Analysis of the Role of the Asparaginyl Hydroxylase Factor Inhibiting Hypoxia-Inducible Factor (FIH) in Regulating Hypoxia-Inducible Factor (HIF) Transcriptional Target Genes.” *Journal of Biological Chemistry* 279 (41). American Society for Biochemistry and Molecular Biology: 42719–25.

doi:10.1074/jbc.M406713200.
Stratton, Michael R, Peter J Campbell, and P Andrew Futreal. 2009. “The Cancer Genome.” *Nature* 458 (7239). Nature Publishing Group: 719–24. doi:10.1038/nature07943.
Swain, L, M Wottawa, A Hillemann, A Beneke, H Odagiri, K Terada, M Endo, Y Oike, K Farhat, and D M Katschinski. 2014. “Prolyl-4-Hydroxylase Domain 3 (PHD3) Is a Critical Terminator for Cell Survival of Macrophages Under Stress Conditions.” *Journal of Leukocyte Biology* 96 (3): 365–75. doi:10.1189/jlb.2HI1013-533R.
Takahashi, T, T Tagami, S Yamazaki, T Uede, J Shimizu, N Sakaguchi, T W Mak, and S Sakaguchi. 2000. “Immunologic Self-Tolerance Maintained by CD25(+)CD4(+) Regulatory T Cells Constitutively Expressing Cytotoxic T Lymphocyte-Associated Antigen 4.” *The Journal of Experimental Medicine* 192 (2): 303–10.
Takeda, N, E L O'Dea, A Doedens, and J Kim. 2010. “Differential Activation and Antagonistic Function of HIF-A Isoforms in Macrophages Are Essential for NO Homeostasis.” *Genes & …*. doi:10.1101/gad.
Takeda, Norihiko, Ellen L O'Dea, Andrew Doedens, Jung-whan Kim, Alexander Weidemann, Christian Stockmann, Masataka Asagiri, M Celeste Simon, Alexander Hoffmann, and Randall S Johnson. 2010. “Differential Activation and Antagonistic Function of HIF-{Alpha} Isoforms in Macrophages Are Essential for NO Homeostasis.” *Genes & Development* 24 (5). Cold Spring Harbor Lab: 491–501. doi:10.1101/gad.1881410.
Talks, K L, H Turley, K C Gatter, and P H Maxwell. 2000. “The Expression and Distribution of the Hypoxia-Inducible Factors HIF-1α and HIF-2α in Normal Human Tissues, Cancers, and Tumor-Associated Macrophages.” *The American Journal of Pathology* 157 (2): 411–21. doi:10.1016/S0002-9440(10)64554-3.
Talmadge, James E, and Dmitry I Gabrilovich. 2013. “History of Myeloid-Derived Suppressor Cells.” *Nature Reviews Cancer* 13 (10). Nature Publishing Group: 739–52. doi:10.1038/nrc3581.
Tan, Ern Yu, Leticia Campo, Cheng Han, Helen Turley, Francesco Pezzella, Kevin C Gatter, Adrian L Harris, and Stephen B Fox. 2007. “Cytoplasmic Location of Factor-Inhibiting Hypoxia-Inducible Factor Is Associated with an Enhanced Hypoxic Response and a Shorter Survival in Invasive Breast Cancer.” *Breast Cancer Research*, July, 1–10. doi:10.1186/bcr1838).
Tanaka, Atsushi, and Shimon Sakaguchi. 2016. “Regulatory T Cells in Cancer Immunotherapy.” *Cell Research* 27 (1). Nature Publishing Group: 109–18. doi:10.1038/cr.2016.151.
Tatsumi, Tomohide, Lisa S Kierstead, Elena Ranieri, Loreto Gesualdo, Francesco P Schena, James H Finke, Ronald M Bukowski, et al. 2002. “Disease-Associated Bias in T Helper Type 1 (Th1)/Th2 CD4(+) T Cell Responses Against MAGE-6 in HLA-DRB10401(+) Patients with Renal Cell Carcinoma or Melanoma..” *The Journal of Experimental Medicine* 196 (5). Rockefeller University Press: 619–28. doi:10.1084/jem.20012142.
Tawakol, Ahmed, Parmanand Singh, Marina Mojena, María Pimentel-Santillana, Hamed Emami, Megan MacNabb, James H F Rudd, et al. 2015. “HIF-1α and PFKFB3 Mediate a Tight Relationship Between Proinflammatory Activation and Anerobic Metabolism in Atherosclerotic Macrophages.” *Arteriosclerosis, Thrombosis, and Vascular Biology* 35 (6). American Heart Association, Inc.:

1463–71. doi:10.1161/ATVBAHA.115.305551.
Thiery, Jean Paul. 2002. “Epithelial–Mesenchymal Transitions in Tumour Progression.” *Nature Reviews Cancer* 2 (6): 442–54. doi:10.1038/nrc822.
Tian, H, S L McKnight, and D W Russell. 1997. “Endothelial PAS Domain Protein 1 (EPAS1), a Transcription Factor Selectively Expressed in Endothelial Cells..” *Genes & Development* 11 (1): 72–82.
Triner, Daniel, Xiang Xue, Andrew J Schwartz, Inkyung Jung, Justin A Colacino, and Yatrik M Shah. 2017. “Epithelial Hypoxia-Inducible Factor 2α Facilitates the Progression of Colon Tumors Through Recruiting Neutrophils.” *Molecular and Cellular Biology* 37 (5). American Society for Microbiology: e00481–16–16. doi:10.1128/MCB.00481-16.
Umansky, Viktor, Carolin Blattner, Christoffer Gebhardt, and Jochen Utikal. 2016. “The Role of Myeloid-Derived Suppressor Cells (MDSC) in Cancer Progression.” *Vaccines* 4 (4). Multidisciplinary Digital Publishing Institute: 36–16. doi:10.3390/vaccines4040036.
Umezu, Tomohiro, Hiroko Tadokoro, Kenko Azuma, Seiichiro Yoshizawa, Kazuma Ohyashiki, and Junko H Ohyashiki. 2014. “Exosomal miR-135b Shed From Hypoxic Multiple Myeloma Cells Enhances Angiogenesis by Targeting Factor-Inhibiting HIF-1.” *Blood* 124 (25): 3748–57. doi:10.1182/blood-2014-05-576116.
Vakil, Ladan, Reza Najafipour, Nasser Rakhshani, Farhad Zamani, Arman Morakabati, and Amir Javadi. 2016. “Investigation of FIH-1 and SOCS3 Expression in KRAS Mutant and Wild-Type Patients with Colorectal Cancer.” *Tumor Biology*, August. Tumor Biology, 1–8. doi:10.1007/s13277-015-4723-1.
Valastyan, Scott, and Robert A Weinberg. 2011. “Tumor Metastasis: Molecular Insights and Evolving Paradigms.” *Cell* 147 (2): 275–92. doi:10.1016/j.cell.2011.09.024.
Vander Heiden, Matthew G, Lewis C Cantley, and Craig B Thompson. 2009. “Understanding the Warburg Effect: the Metabolic Requirements of Cell Proliferation.” *Science* 324 (42): 841–51.
Vaupel, Peter, Arnulf Mayer, and Michael Höckel. 2004. “Tumor Hypoxia and Malignant Progression.” In *Methods in Enzymology*, 381:335–54. Methods in Enzymology. Academic Press. doi:https://doi.org/10.1016/S0076-6879(04)81023-1.
Venkatachalam, Kartik, and Craig Montell. 2007. “TRP Channels.” *Annual Review of Biochemistry* 76 (1): 387–417. doi:10.1146/annurev.biochem.75.103004.142819.
Vignali, Dario A A, Lauren W Collison, and Creg J Workman. 2008. “How Regulatory T Cells Work.” *Nature Reviews Immunology* 8 (7): 523–32. doi:10.1038/nri2343.
Vives, Virginie, Jian Su, Shan Zhong, Indrika Ratnayaka, Elizabeth Slee, Robert Goldin, and Xin Lu. 2006. “ASPP2 Is a Haploinsufficient Tumor Suppressor That Cooperates with P53 to Suppress Tumor Growth.” *Genes & Development* 20 (10): 1262–67. doi:10.1101/gad.374006.
Walmsley, Sarah R, Edwin R Chilvers, Alfred A Thompson, Kathryn Vaughan, Helen M Marriott, Lisa C Parker, Gary Shaw, et al. 2011. “Prolyl Hydroxylase 3 (PHD3) Is Essential for Hypoxic Regulation of Neutrophilic Inflammation in Humans and Mice.” *Journal of Clinical Investigation* 121 (3): 1053–63. doi:10.1172/JCI43273.
Wan, Yisong Y. 2010. “Multi-Tasking of Helper T Cells.” *Immunology* 130 (2):

166–71. doi:10.1111/j.1365-2567.2010.03289.x.
Wang, G L, B H Jiang, E A Rue, and G L Semenza. 1995. “Hypoxia-Inducible Factor 1 Is a Basic-Helix-Loop-Helix-PAS Heterodimer Regulated by Cellular O2 Tension.” *Proceedings of the National Academy of Sciences* 92 (12). National Acad Sciences: 5510–14.
Wang, Jiankang, Bingling Luo, Xiaobing Li, Wenhua Lu, Jing Yang, Yumin Hu, Peng Huang, and Shijun Wen. 2017. “Inhibition of Cancer Growth in Vitro and in Vivo by a Novel ROS-Modulating Agent with Ability to Eliminate Stem-Like Cancer Cells.” *Nature Publishing Group*, June. Nature Publishing Group, 1–9. doi:10.1038/cddis.2017.272.
Wang, Yin, Yan Liu, Sami N Malek, Pan Zheng, and Yang Liu. 2011. “Targeting HIF1α Eliminates Cancer Stem Cells in Hematological Malignancies.” *Cell Stem Cell* 8 (4): 399–411. doi:10.1016/j.stem.2011.02.006.
Webb, James D, Andrea Murányi, Christopher W Pugh, Peter J Ratcliffe, and Mathew L Coleman. 2009. “MYPT1, the Targeting Subunit of Smooth-Muscle Myosin Phosphatase, Is a Substrate for the Asparaginyl Hydroxylase Factor Inhibiting Hypoxia-Inducible Factor (FIH).” *The Biochemical Journal* 420 (2). Portland Press Limited: 327–33. doi:10.1042/BJ20081905.
Weischenfeldt, Joachim, and Bo Porse. 2008. “Bone Marrow-Derived Macrophages (BMM): Isolation and Applications.” *CSH Protocols* 2008 (12). Cold Spring Harbor Laboratory Press: pdb.prot5080–80. doi:10.1101/pdb.prot5080.
Wen, Z, Z Zhong, and J E Darnell. 1995. “Maximal Activation of Transcription by Statl and Stat3 Requires Both Tyrosine and Serine Phosphorylation.” *Cell* 82 (2): 241–50. doi:10.1016/0092-8674(95)90311-9.
Wherry, E John, and Makoto Kurachi. 2015. “Molecular and Cellular Insights Into T Cell Exhaustion.” *Nature Reviews Immunology* 15 (8). Nature Publishing Group: 486–99. doi:10.1038/nri3862.
Wiesener, M S, H Turley, W E Allen, C Willam, K U Eckardt, K L Talks, S M Wood, et al. 1998. “Induction of Endothelial PAS Domain Protein-1 by Hypoxia: Characterization and Comparison with Hypoxia-Inducible Factor-1α.” *Blood* 92 (7). American Society of Hematology: 2260–68. doi:10.1073/pnas.90.6.2423.
Wilkins, Sarah E, Jaana Hyvärinen, Johana Chicher, Jeffrey J Gorman, Daniel J Peet, Rebecca L Bilton, and Peppi Koivunen. 2009. “Differences in Hydroxylation and Binding of Notch and HIF-1α Demonstrate Substrate Selectivity for Factor Inhibiting HIF-1 (FIH-1).” *The International Journal of Biochemistry & Cell Biology* 41 (7): 1563–71. doi:10.1016/j.biocel.2009.01.005.
William, Josette, Daina Variakojis, Anjana Yeldandi, and Kirtee Raparia. 2013. “Lymphoproliferative Neoplasms of the Lung: a Review.” *Archives of Pathology & Laboratory Medicine* 137 (3): 382–91. doi:10.5858/arpa.2012-0202-RA.
Williams, Carly Bess, Elizabeth S Yeh, and Adam C Soloff. 2016. “Tumor-Associated Macrophages: Unwitting Accomplices in Breast Cancer Malignancy.” *Npj Breast Cancer*, January. Nature Publishing Group, 1–12. doi:10.1038/npjbcancer.2015.25.
Wroblewski, Lydia E, Richard M Peek, and Keith T Wilson. 2010. “Helicobacter Pylori and Gastric Cancer: Factors That Modulate Disease Risk.” *Clinical Microbiology Reviews* 23 (4). American Society for Microbiology: 713–39.

doi:10.1128/CMR.00011-10.

Wyckoff, Jeffrey, Weigang Wang, Elaine Y Lin, Yarong Wang, Fiona Pixley, E Richard Stanley, Thomas Graf, Jeffrey W Pollard, Jeffrey Segall, and John Condeelis. 2004. “A Paracrine Loop Between Tumor Cells and Macrophages Is Required for Tumor Cell Migration in Mammary Tumors.” *Cancer Research* 64 (19). American Association for Cancer Research: 7022–29. doi:10.1158/0008-5472.CAN-04-1449.

Xu, Heping, Ayyakkannu Manivannan, Isabel Crane, Rosemary Dawson, and Janet Liversidge. 2008. “Critical but Divergent Roles for CD62L and CD44 in Directing Blood Monocyte Trafficking in Vivo During Inflammation.” *Blood* 112 (4). American Society of Hematology: 1166–74. doi:10.1182/blood-2007-06-098327.

Yang, Li, and Yi Zhang. 2017. “Tumor-Associated Macrophages: From Basic Research to Clinical Application.” *Journal of Hematology and Onocology*, February. Journal of Hematology & Oncology, 1–12. doi:10.1186/s13045-017-0430-2.

Yang, Ming, Rasheduzzaman Chowdhury, Wei Ge, Refaat B Hamed, Michael A McDonough, Timothy D W Claridge, Benedikt M Kessler, Matthew E Cockman, Peter J Ratcliffe, and Christopher J Schofield. 2011. “Factor-Inhibiting Hypoxia-Inducible Factor (FIH) Catalyses the Post-Translational Hydroxylation of Histidinyl Residues Within Ankyrin Repeat Domains.” *FEBS Journal* 278 (7): 1086–97. doi:10.1111/j.1742-4658.2011.08022.x.

Yang, Muh-Hwa, Min-Zu Wu, Shih-Hwa Chiou, Po-Min Chen, Shyue-Yih Chang, Chung-Ji Liu, Shu-Chun Teng, and Kou-Juey Wu. 2008. “Direct Regulation of TWIST by HIF-1α Promotes Metastasis.” *Nature Cell Biology* 10 (3): 295–305. doi:10.1038/ncb1691.

Yang, Zhihong, and Xiu-Fen Ming. 2013. “Arginase: the Emerging Therapeutic Target for Vascular Oxidative Stress and Inflammation.” *Frontiers in Immunology*, June, 1–11. doi:10.3389/fimmu.2013.00149/abstract.

Yang, Zhihong, and Xiu-Fen Ming. 2014. “Functions of Arginase Isoforms in Macrophage Inflammatory Responses: Impact on Cardiovascular Diseases and Metabolic Disorders.” *Frontiers in Immunology* 5 (6 Suppl 2): 533. doi:10.3389/fimmu.2014.00533.

Yarchoan, Mark, Burles A Johnson, Eric R Lutz, Daniel A Laheru, and Elizabeth M Jaffee. 2017. “Targeting Neoantigens to Augment Antitumour Immunity.” *Nature Reviews Cancer* 17 (4). Nature Publishing Group: 209–22. doi:10.1038/nrc.2016.154.

Youn, Je-In, and Dmitry I Gabrilovich. 2010. “The Biology of Myeloid-Derived Suppressor Cells: the Blessing and the Curse of Morphological and Functional Heterogeneity.” *European Journal of Immunology* 40 (11): 2969–75. doi:10.1002/eji.201040895.

Yuan, Qinghua, Weida Gao, Bo Liu, and Wei Ye. 2014. “Upregulation of miR-184 Enhances the Malignant Biological Behavior of Human Glioma Cell Line A172 by Targeting FIH-1.” *Cellular Physiology and Biochemistry* 34 (4). Karger Publishers: 1125–36. doi:10.1159/000366326.

Zhang, Na, Zhenxing Fu, Sarah Linke, Johana Chicher, Jeffrey J Gorman, DeeAnn Visk, Gabriel G Haddad, et al. 2010. “The Asparaginyl Hydroxylase Factor Inhibiting HIF-1Α Is an Essential Regulator of Metabolism.” *Cell Metabolism* 11 (5). Elsevier Ltd: 364–78. doi:10.1016/j.cmet.2010.03.001.

Zhang, Wenjing, Xinpeng Shi, Ying Peng, Meiyan Wu, Pei Zhang, Ruyi Xie, Yao

Wu, Qingqing Yan, Side Liu, and Jide Wang. 2015. “HIF-1α Promotes Epithelial-Mesenchymal Transition and Metastasis Through Direct Regulation of ZEB1 in Colorectal Cancer.” Edited by Masaru Katoh. *PLoS ONE* 10 (6). Public Library of Science: e0129603. doi:10.1371/journal.pone.0129603.

Zheng, Xiaofeng, Sarah Linke, José M Dias, Xiaowei Zheng, Katarina Gradin, Tristan P Wallis, Brett R Hamilton, et al. 2008. “Interaction with Factor Inhibiting HIF-1 Defines an Additional Mode of Cross-Coupling Between the Notch and Hypoxia Signaling Pathways.” *Proceedings of the National Academy of Sciences of the United States of America* 105 (9). National Acad Sciences: 3368–73. doi:10.1073/pnas.0711591105.

Zhong, Hua, Angelo M De Marzo, Erik Laughner, Michael Lim, David A Hilton, David Zagzag, Peter Buechler, William B Isaacs, Gregg L Semenza, and Jonathan W Simons. 1999. “Overexpression of Hypoxia-Inducible Factor 1α in Common Human Cancers and Their Metastases.” *Cancer Research* 59 (22). American Association for Cancer Research: 5830–35. doi:10.1016/S0968-0004(98)01344-9.

Zhou, Jie, Tobias Schmid, and Bernhard Brüne. 2003. “Tumor Necrosis Factor-Alpha Causes Accumulation of a Ubiquitinated Form of Hypoxia Inducible Factor-1alpha Through a Nuclear Factor-kappaB-Dependent Pathway.” *Molecular Biology of the Cell* 14 (6): 2216–25. doi:10.1091/mbc.E02-09-0598.

Zhu, Jinfang, and William E Paul. 2008. “CD4 T Cells: Fates, Functions, and Faults.” *Blood* 112 (5). American Society of Hematology: 1557–69. doi:10.1182/blood-2008-05-078154.

Zilio, Serena, and Paolo Serafini. 2016. “Neutrophils and Granulocytic MDSC: the Janus God of Cancer Immunotherapy.” *Vaccines* 4 (3). Multidisciplinary Digital Publishing Institute: 31–21. doi:10.3390/vaccines4030031.

Zinzani, Pier Luigi. 2012. “The Many Faces of Marginal Zone Lymphoma.” *Hematology. American Society of Hematology. Education Program* 2012: 426–32. doi:10.1182/asheducation-2012.1.426.